Modeling, Design, and Optimization of Permanent Magnet Synchronous Machines

by

Matthew G. Angle

B.S., Massachusetts Institute of Technology (2007)
M.Eng, Massachusetts Institute of Technology (2011)

Submitted to the Department of Electrical Engineering and Computer Science
in partial fulfillment of the requirements for the degree of

Doctor of Philosophy in Electrical Engineering

at the

MASSACHUSETTS INSTITUTE OF TECHNOLOGY

February 2016

Author .....
Department of Electrical Engineering and Computer Science
December 4, 2015

Certified by .....
James L. Kirtley, Jr.
Professor
Thesis Supervisor

Certified by .....
Jeffrey H. Lang
Professor
Thesis Supervisor

Accepted by .....
Leslie A. Kolodziejski
Chairman, Department Committee on Graduate Theses

Modeling, Design, and Optimization of Permanent Magnet Synchronous Machines

by

Matthew G. Angle

Submitted to the Department of Electrical Engineering and Computer Science
on December 4, 2015, in partial fulfillment of the
requirements for the degree of
Doctor of Philosophy in Electrical Engineering

Abstract

Improvement of performance of robots has necessitated technological advances in control algorithms, mechanical structures, and electric machines. Running, legged robots have presented challenges in the area of electric machinery in particular. In addition to the low-speed, high-torque, low-mass requirements on the machines, the act of running results in an unconventional drive cycle that consists of brief periods of high torque followed by long stretches of minimal torque requirement, a performance envelope that is not matched by commercially-available machines. An optimized motor would dissipate the minimum possible power over the given drive cycle, lowering temperatures and potentially reducing required battery mass or extending range. These performance requirements have motivated faster modeling techniques to enable optimization of designs for these unconventional applications.

This thesis presents a novel, fast modeling method for permanent magnet synchronous machines consisting of a hybrid model comprising an explicit Maxwell solution and a Flux Tube solution. The Maxwell solution is performed for the rotor and airgap of the machine, where geometries are simple and materials are homogeneous. The stator, with its geometric complexities and non-linear materials, is modeled with a lumped-parameter model based on flux tubes. The two models are then stitched together, forced to be self-consistent with boundary conditions, and allowed to converge. This captures effects such as cogging torque as well as saturation of the core materials. The method is approximately four orders of magnitude faster than a reference finite element program (0.01 s versus 100 s) for the same accuracy. The modeling method is implemented for two topologies of surface-mount permanent-magnet machines, an internal-rotor machine and an external-rotor machine. It is then used to optimize machine design to a given drive cycle, including effects of core loss. A machine is built to demonstrate the validity of the model and optimization method and test results match predictions of instantaneous torque to within 5% at the worst point.

Cogging torque is another aspect of performance that is important to machines for robotics and other applications. These pulsations in torque caused by magnet alignment with geometric features in the stator result in undesired vibrations and

issues with control. One method, based on skew, for reducing or eliminating cogging torque is explored, and a simple analytical technique to predict the effect of skew is presented. Based on the machine optimized for the Cheetah, two additional machines were built to explore the effects of cogging: a skewed-rotor machine, and a skewed-stator machine. Each demonstrated reduction of a particular cogging harmonic or all of the cogging. The skewed machines reduced cogging by approximately 85%. Novel magnet shapes which further reduce cogging are presented and finite element modeling suggests that they can further reduce cogging by 60% over a straight skew.

The design and optimization tools developed herein and described above were used to optimize a motor for the MIT Cheetah Robot. The resulting motor showed nearly an order of magnitude increase in torque density when compared to commercial, off-the-shelf machines (1.3 kg vs 820 g and 10 Nm vs 28 Nm) with simultaneous improvements to efficiency.

Thesis Supervisor: James L. Kirtley, Jr.
Title: Professor

Thesis Supervisor: Jeffrey H. Lang
Title: Professor

Acknowledgments

This thesis was supported by the Defense Advanced Research Projects Agency (DARPA) Maximum Mobility and Manipulation (M3) Program under DTD 7/26/11.

Experiments were performed in the Laboratory for Electromagnetic and Electronic Systems (LEES) within the Research Laboratory of Electronics (RLE) at MIT. Dave Otten performed most of the experimental evaluation of the electric machines presented in this thesis. His expertise and test/drive electronics produced beautiful data I would have never been able to do on my own. His office's proximity to mine made him immediately accessible (perhaps more so than he would like, though he would never admit it), and he has always been willing to offer assistance, bounce around ideas, and keep me from straying too far from practicality.

The machines presented in this thesis were built at Walco in Providence, Rhode Island. Thanks to Marc Amato for considering such a project and to Paul Boisse for taking on the challenge of winding these machines and showing me how to design a machine with winding in mind. Somehow, he found some 4500 wire-slot placements inside a 4.5" diameter space in the 8-phase machine to be a possible task.

Professor Sangbae Kim provided a fantastically interesting optimization problem and a far more exciting and technically interesting platform for demonstration of a motor than I could have ever imagined. Merely mentioning the robotic cheetah in conversation has always given me an instantly-captivated crowd. I'm not sure if anyone scores theses based on youtube hits, but the robotic cheetah would certainly place this one in the running.

Professor Luca Daniel has kept me honest about comparisons of performance with Finite Element Programs and has read and commented on drafts of this thesis from its early, crude stages.

Professor Lang has been my co-supervisor for this project over the last two and a half years. I credit him with nudging me in the direction of the hybrid model upon which this work is based. He has also spend far more time than I could have asked for helping me edit this document. Thanks for your patience and for entertaining some

rather far-fetched ideas.

And finally, Professor Kirtley has been my advisor and mentor from day one at MIT. He has kept me around for ten years now and has provided much needed guidance, support, and the occasional kick or two. Thank you for all of the opportunities, the patience you've shown, and for directing me down the path of electric machinery.

Thanks to all of my friends and family for their support over the last many years.

Contents

List of Figures

List of Tables

Chapter 1

Introduction

1.1 Problem Statement

The DARPA Maximum Mobility and Manipulation (M3) program sought to improve performance of running robots through technological advances in design tools, fabrication methods, and control algorithms. As part of the program, Professor Sangbae Kim's Biomimetics Lab at MIT created a robotic Cheetah as a testbed for such technologies. Specifically, their goal was to increase the efficiency of running robots. This goal has led to advances in limb design and construction, stability algorithms, and motor design.

Professor Kim's group identified four primary ways of increasing efficiency in their robots [1]: increased torque density in motors, energy regeneration in limbs and motors, low impedance transmission, and low-inertia limbs. The first three of these are directly related to, or place unique demands upon, the motors in the Cheetah. Improvements in these areas are the motivation for this thesis.

Increased torque density, or specific torque in this case (referring to torque per unit mass instead of torque per unit volume), is directly related to efficiency in that the motors comprise a substantial portion of the mass of the robot. Decreased mass leads directly to decreased energy required for locomotion. Energy regeneration requires electric machinery with bi-directional energy converters (as opposed to hydraulic machinery) to recover kinetic energy when the robot is absorbing impact, such as limb

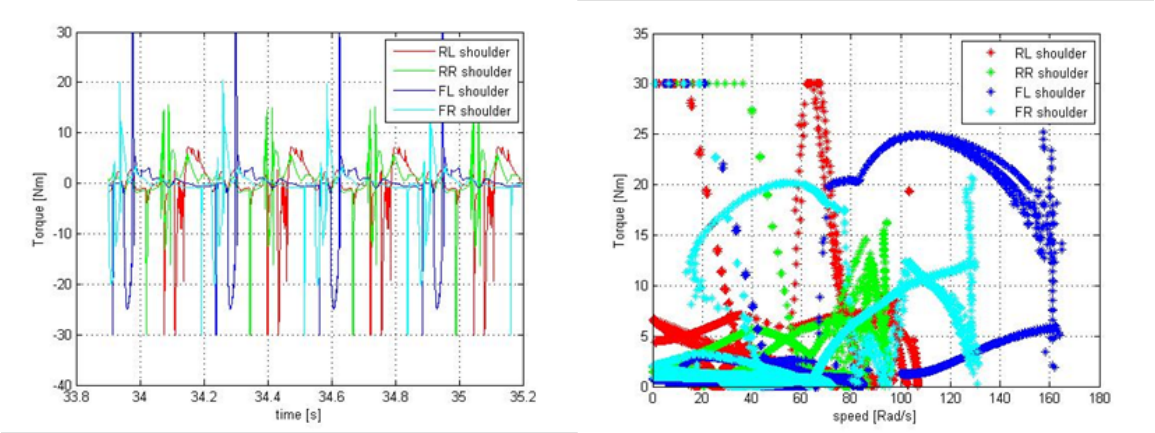

Figure 1-1: Simulated drive cycle for cheetah motors [1]

ground strikes while running.

Low impedance transmission refers to the mechanisms that translate rotary motion in the motors to complex limb motions. Currently, this consists of a planetary gearbox and pushrod linkages to actuate the knee and shoulder joints in each leg. The desire for efficiency drives the gearbox selection to low-ratio planetary gearsets and has the side effect of requiring much higher torque at low speeds from the motor. This allows the motor to be back-driveable, permitting energy regeneration. Other benefits include the ability to sense torque on the limb from the electrical terminals of the motor, obviating the need for contact sensors, which are prone to failure.

In addition to the low-speed, high-torque, low-mass requirements, the act of running results in an unconventional drive cycle that consists of brief periods of high torque followed by long stretches of minimal torque requirement. Pictured in Figure 1-1 is an example of the running drive cycle for each of the shoulder motors. The knees are similar, but have slightly different drive cycle requirements. In addition to differences between the front and back limbs, notice that the drive cycles are not symmetric side-to-side as a consequence of the preferred running gait of the animal, which is replicated by the robot. Such drive cycle differences suggest an optimized motor for each joint, but practicality dictates the same design for each motor. These optimized motors will dissipate the minimum possible power over the given drive cycle, lowering temperatures and potentially reducing required battery mass or extending range.

The first generation of the Cheetah used commercially-available Emoteq HT-05001 motors that are the standard for robotics research and the robotics industry. They are optimized for very broad use and utilize materials that are readily available and economical. Most importantly, they are built to run under load continuously. In an application like the Cheetah, there is much room for improvement, especially when freed from thermal constraints of continuous loads. The Cheetah presents several interesting design challenges and requires optimization to a use case that is not common in industry. This necessitates a fresh motor design, and potentially a different modeling and design methodology.

1.2 History of Motor Synthesis, Design, Analysis

Past modeling efforts have taken various forms, but are primarily categorized as Finite Element Modeling (FEM) [3], flux tube modeling [4], and explicit solutions of Maxwell's equations [5]. Figure 1-2 shows a history of motor development and the modeling and materials advances advances that drove their evolution.

Much of the work on permanent magnet synchronous machine modeling has been in the form of flux tube models, which are lumped-parameter magnetic circuit models. These methods often use FEM techniques to visualize flux paths and form flux tube models. In these magnetic equivalent circuits, flux passes through each element on only a single axis, thereby creating a sort of macro-FEM model. Such models are easily used to calculate iron losses and other performance parameters [6]. An example is shown in Figure 1-3. This figure shows a complicated flux tube model expanded to the point where it is able to capture relevant performance.

Other efforts have used FEM to calculate lumped parameter values at each rotor position and load condition [7] [8]. By examining the FEM results, the lumped parameters may be calculated. A diagram showing various lumped parameters is shown in Figure 1-4. Each segment in the airgap of the machine, represented by the crossed lines, is a parameter backed out form the finite element modeling that varies with rotor position. Nonlinear aspects of materials may be considered in this manner

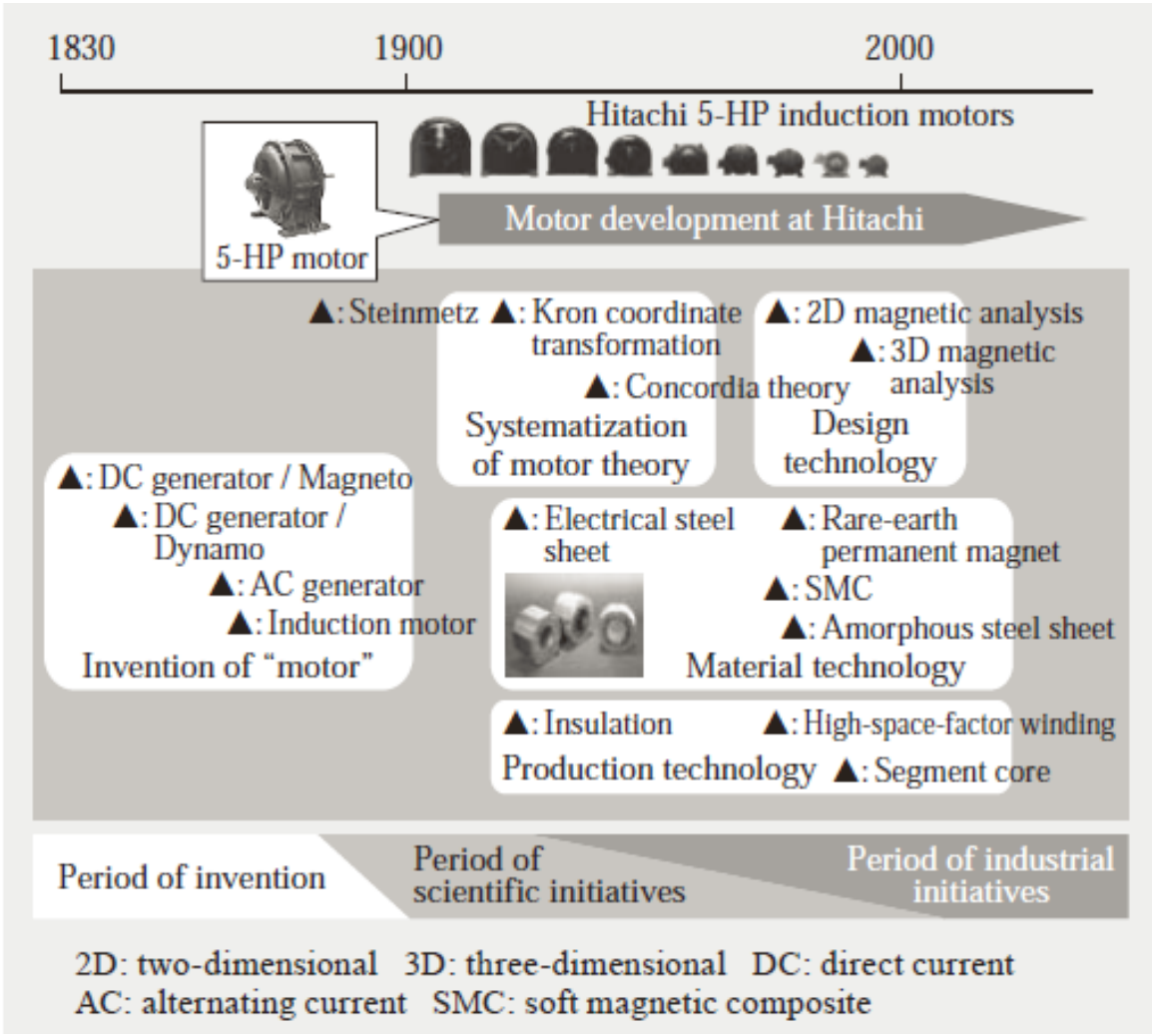

Figure 1-2: History of motor development at hitachi [2]

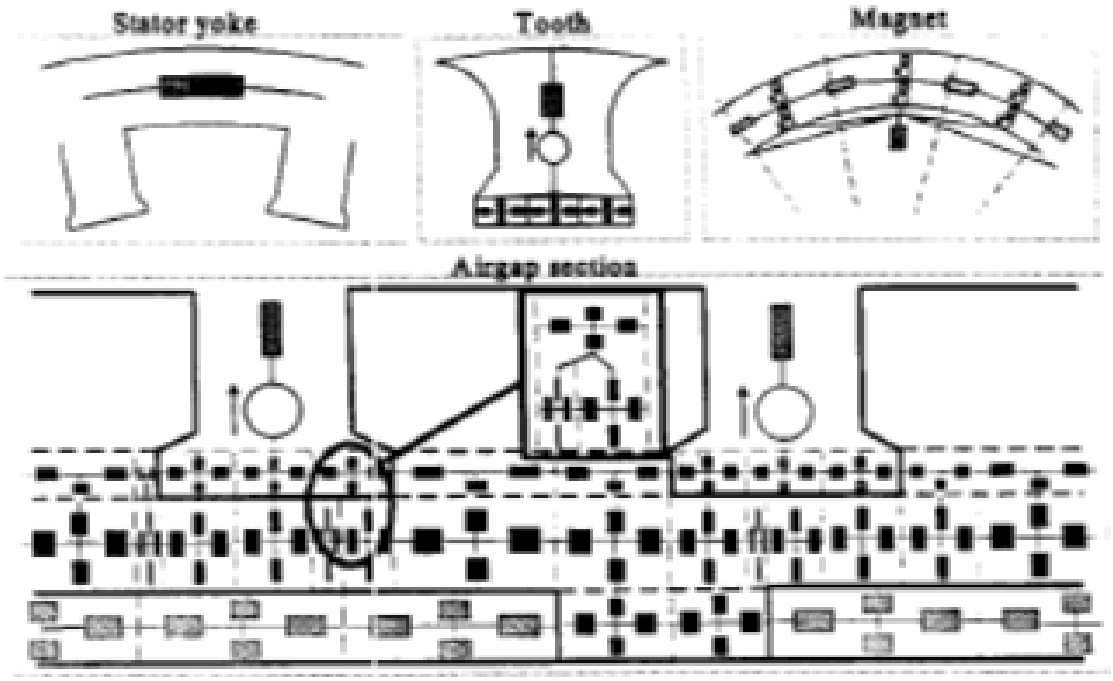

Figure 1-3: Example flux tube approximation [6]

as well.

FEM or explicit calculations may also be used to create simplified electical lumped-parameter circuit models, which typically involve calculations of inductance on the d- and q-axes and then calculating motor performance [9]. Parameter variation and loss components may be easily integrated into such models [10] [11].

Several authors have analytically calculated field solutions in the interior of the machine. This involves solving vector potential solutions in the air gap. Magnets may either be modeled as current sheets [12], or as a Poisson equation in the layer containing the magnets [13]. One author went as far as calculating eddy currents everywhere in the interior of the machine to calculate eddy current losses [14]. This generally involves modeling the permanent magnets as equivalent current sheets and solving vector potentials. Infinitely permeable steel is assumed in all of these examples, and the materials in the explicit solution are assumed to be linear.

Analytical field solutions have been used to calculate cogging torque. Dubas and Espanet [13] and [15] have calculated the vector potential in the motor gap as well as

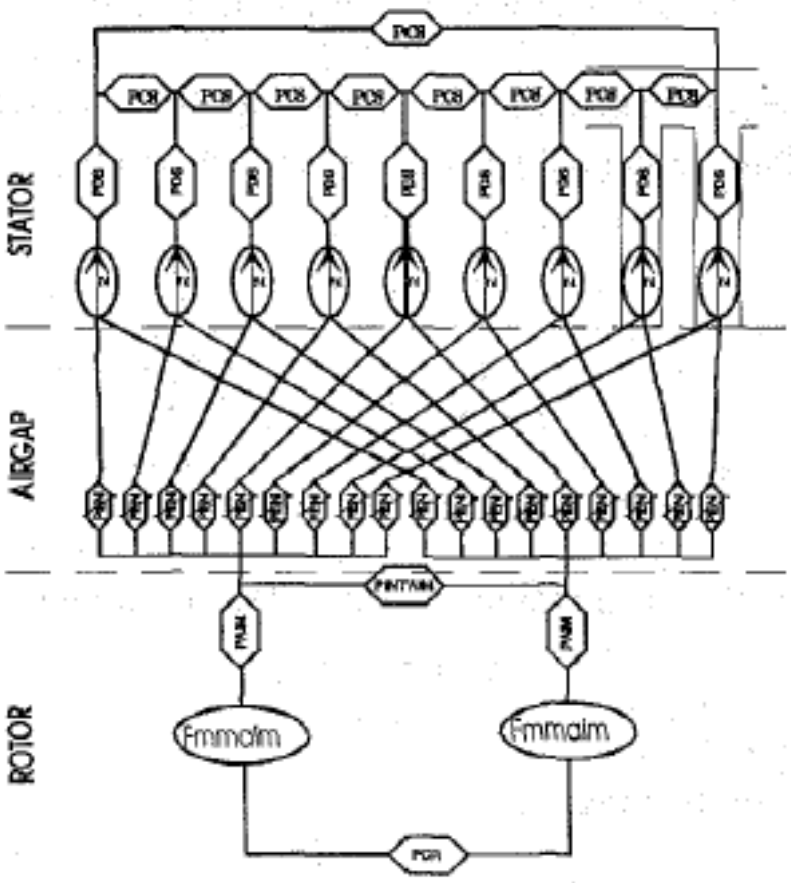

Figure 1-4: Alternate flux tube approximation [8]

in the slots of the stator and produced near-exact analytical solutions for simplified geometries assuming infinitely-permeable steel and linear materials. The difficulty in this method involves matching boundary conditions at the opening of each slot. The field solution is continuous across a complicated geometry. These solutions have produced near exact cogging torque values to simulated machines.

Another technique used to analytically calculate field solutions and calculate cogging torque is conformal transformation [16] and [17]. With this technique, an air-gap permeance is derived from the conformal transformation of slot geometry. The permeability of the slots and air gap is transformed to a smooth surface by using the Schwartz-Christoffel transformation, allowing greatly simplified field solutions. Any function defined by a potential (satisfying Laplaces equation) may be transformed in such a manner. This enables the calculation of radial and tangential fields in the machine, allowing for torque calculation from the integral of the Maxwell Stress Tensor. Again, this solution assumes linear materials in the explicit solution of Maxwell's Equations.

The conformal mapping technique results in remarkably good agreement with field distributions and captures the features of cogging torque in the machine, resulting in a technique that allows for evaluation of several different cogging torque reduction schemes with greatly reduced computation time from FEM, again with the limitation that only linear materials are considered. Results are shown in Figures 1-5 and 1-6.

These techniques each capture different performance metrics of an electric machine. They are each useful in certain ranges of operation, but all lack the ability to form a solution that matches physical hardware across the performance envelope of the machine. Those that do include magnetic saturation in the steel of the machine rely heavily upon FEM methods to do so, drastically increasing run time. Our new approach, described in Chapters 2 through 4 should combine the best aspects, or the speed of flux tube approaches and accuracy of finite element codes, resulting in reduced simulation time and maintaining most of the accuracy of FEA.

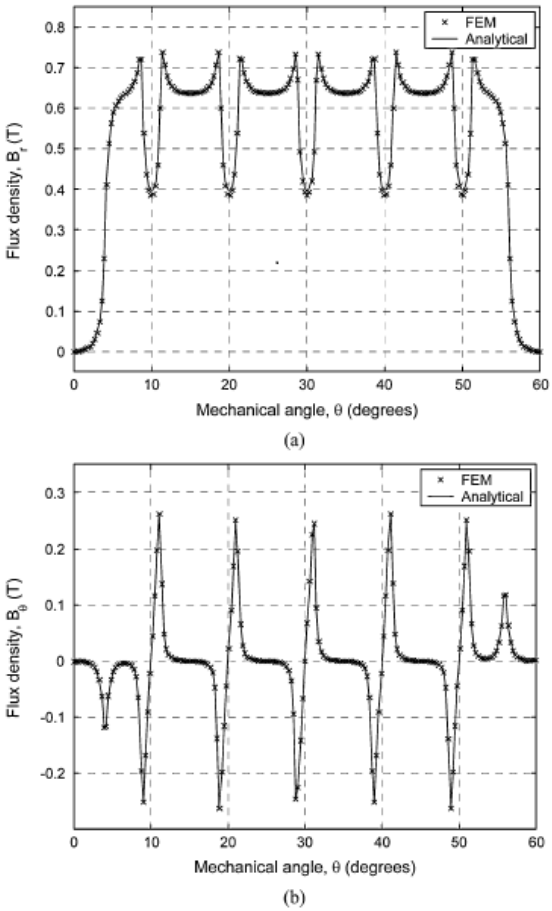

Figure 1-5: Analytical vs. finite element solution for flux densities in a notional machine by contormal mapping techinque [17]

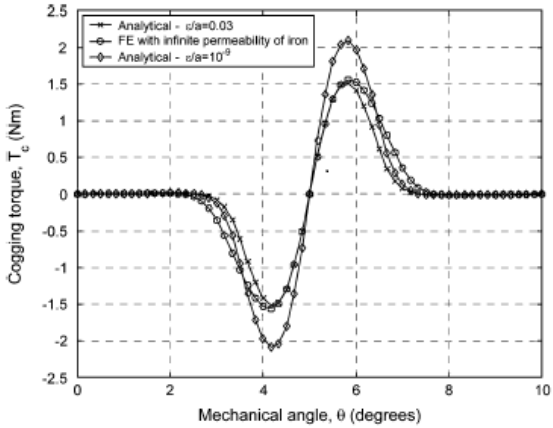

Figure 1-6: Cogging torque calculated by FEA and conformal mapping technique [17]

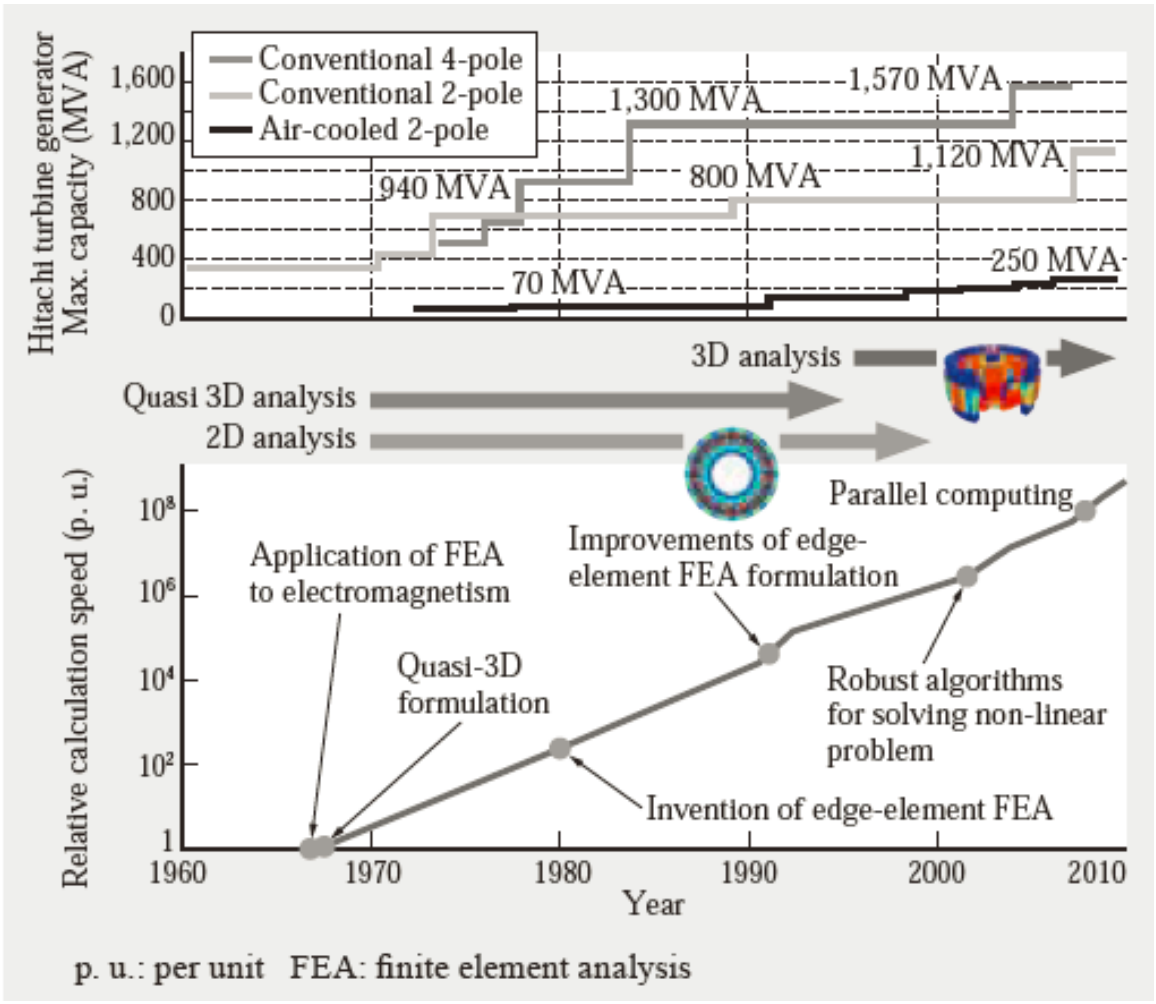

Figure 1-7: History of FEA use and development at hitachi [2]

1.3 FEA Advancement

Starting in the 1960s, Finite Element Analysis became useful for designing electric machines. Computers allowed a greater number of iterations of design without having to build prototypes. Increases in computational speed, as well as improvements in the finite element process itself allowed for design of better machines. Figure 1-7 shows the timeline of FEA/Computational advancement next to increases in capacity in turbine generators at Hitachi [2]. FEA has become the standard for checking nearly all theoretical work and represents the last hurdle before a design is constructed. It is used in this work to spot-check designs, but its run time prevents its use for broad sweeps of the design space.

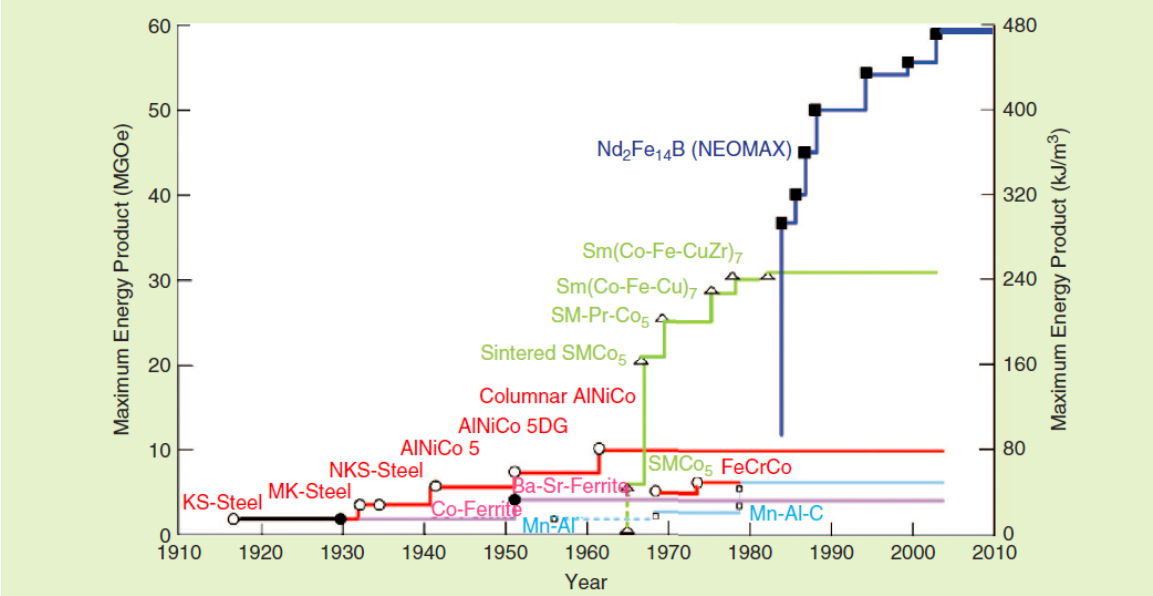

Figure 1-8: History of magnetic materials [18]

1.4 Materials Advancement

In addition to the expansion of understanding of electric machines and an increase in computational power and sophistication of FEA methods, materials advancement has driven the development of permanent magnet machines in the last century. Figure 1-8 shows the energy product of a magnetic material by year. This measure is the maximum product of the magnetic field and the remnant flux flux density in a material. There are two large advances, the first in the 1960s with the introduction of Samarium-Cobalt magnets, and the second in the 1980s with Neodymium-Iron-Boron. Such advances necessitate new design methods to take advantage of increased performance characteristics. These characteristics enable the torque density numbers needed for the cheetah, and open alternate design spaces not previously considered with lower-performance magnets.

1.5 Previous MIT Efforts

The Cheetah project began with commercially-available machines. Their limitations were soon apparent, in that they produced less than 10 Nm of torque at saturation

while dissipating significant power. This sparked interest in motor design, culminating in a second-generation machine designed and built in-house [19].

The second generation of Cheetah motors were designed in the Laboratory for Electromagnetic and Electronic Systems within the Research Laboratory for Electronics at MIT. In this work, simple relationships between the magnet geometry, air gap geometry, remnant flux density, and fields in the machine were developed. The analysis assumed a surface current on the stator to create torque. The motor was then optimized assuming good magnetic steel and rotor backiron and stator geometries sufficient to carry the flux predicted in the earlier analysis [19].

This work resulted in motors that were nearly 20% lighter and produced more than double the magnetic-saturation-limited torque of the commercially available Emoteq HT-05001s used in the first generation of the Cheetah. These machines begin to saturate teeth before reaching the design torque of 30 Nm, resulting in non-linear torque production with current. They also produce approximately 1 Nm amplitude cogging torque, which must be compensated in motor controls. Better models should allow prediction and elimination of undesirable performance characteristics.

The next effort to maximize torque density in motors for the Cheetah project [20] involved looking at torque produced by higher spatial harmonics of the rotor and stator flux interactions and effectively re-derived the rectangular or trapezoidally-driven DC machine as producing maximum torque density. This concept is illustrated in Figure 1-9. This change in motor drive, and design of the machine to support it, results in a torque density approximately 24% higher than an equivalent sinusoidally-driven machine. This solution incentivizes individual control of each slot in the machine, a prospect made more palatable by the development of GaN devices [20]. Figure 1-10 illustrates the advantages offered by Gallium Nitride transistors, showing that their on-state resistance is much lower than common devices when they are required to stand off the same voltage. This potentially allows control of current in individual slots in a multi-phase machine. Figure 1-11 shows the evolution of control algorithms and devices on motor design at Hitachi. The Gallium Nitride transistors and square-current-drive control strategy extend these performance gains.

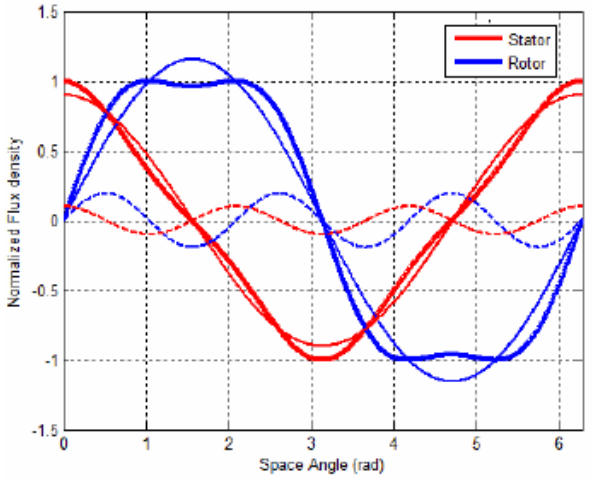

Figure 1-9: Summation of two spatial harmonics of stator and rotor flux in consonance [20]

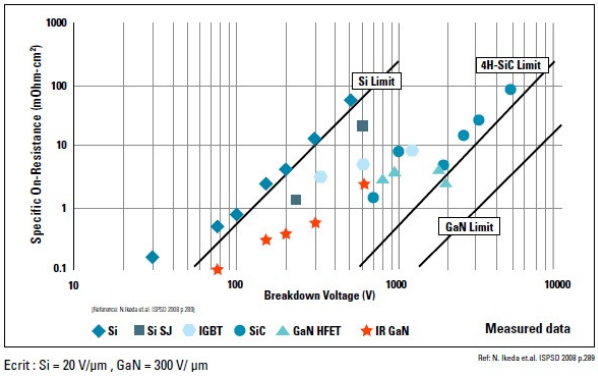

Figure 1-10: On-state resistance vs breakdown voltage for transistor materials [20]

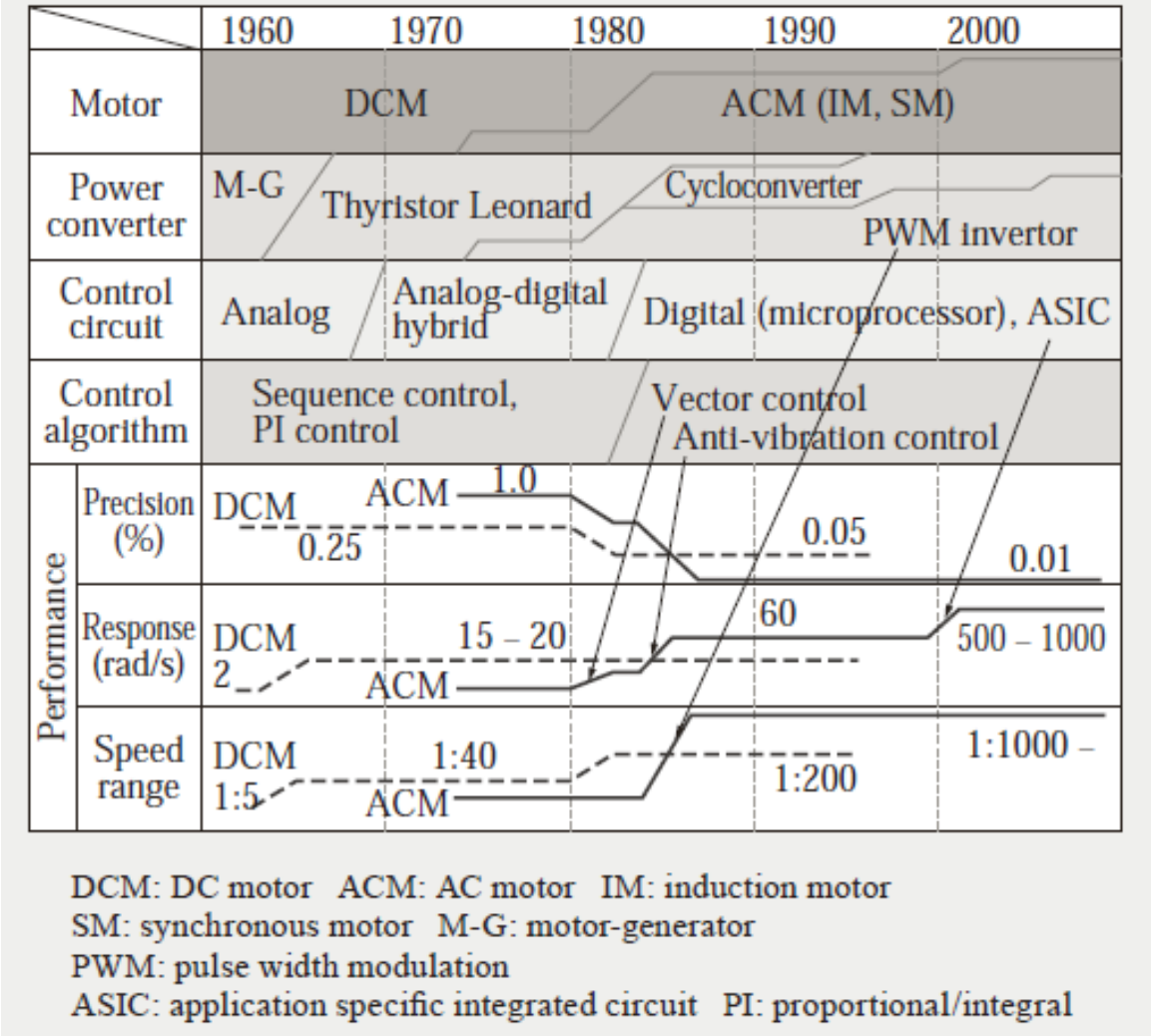

Figure 1-11: History of control development at Hitach [2]

EXEMPLARY DESIGN: COMPARISON OF THREE MACHINE DIMENSIONS

Design parameter	Sinusoidal machine		Triangular-Square wave machine with individual slot control
	High torque BLDC (Emoteq HT05001-X0X)	In-house design of high torque BLDC motor	
Pole	12	26	16
No. of slots	45	78	128
Core Material	-	Supermendur	Supermendur
Stator OD	127 mm	127 mm	127 mm
Stator ID	75.18 mm	97.6 mm	94.2 mm
Stack length	16.51 mm	15 mm	11 mm
Rotor OD	74.42 mm	96.8 mm	93 mm
Rotor ID	63.51 mm	71.6 mm	69 mm
Weight	1.23 Kg	1.02 Kg	0.81 Kg
Shear stress	-	108 kPa	160 kPa

Figure 1-12: Comparison of commercial motor with LEES-designed machines [20]. Emoteq HT05001 is generation 1 [21], In-house design is generation 2 [19], and triangular-square wave machine is the paper design [20].

Using the square-current-drive concept, a motor was designed and simulated in Comsol [20]. It demonstrated performance increases commensurate with theoretical prediction, but lacked detailed modeling of magnetic saturation and windings. For example, winding packing factor did not account for slot liners, which can comprise a large fraction of the slot area given these geometries. This effort suggested a motor further 20% lighter at the same dissipation and design torque and introduced the concept of high-phase-count machines. Specifically, the optimum, defined as minimum mass while holding maximum dissipation constant, presented was an 8-phase machine. A comparison is shown in Table 1-12.

Both of these efforts, [19] and [20] were based on simplified magnetic models of the machines that did not capture certain performance characteristics, such as cogging and magnetic saturation. They both excluded several factors that would affect performance in a physical machine. This thesis captures nonlinearities and other performance factors, such as cogging, while retaining as much computation speed as possible.

1.6 Tour of Thesis

This thesis presents a novel modeling methodology for surface-mounted permanent magnet machines that computes much faster than equivalent finite element analysis (FEA). This technique is then used to optimize machines for two specific applications, the Cheetah and a bicycle wheel motor, by Monte Carlo methods. It may also be extended to other machine topologies. The technique captures saturation effects in the core and may be used to compute cogging torque as well as motive torque, a capability that does not currently exist outside of cumbersome FEA methods.

Robotics applications, specifically running quadrupeds, present exotic drive cycles for electric machinery. Design criteria and constraints are vastly different from traditional applications. While intuition may be able to tweak existing designs to find local optima in a vast design space for these machines, global optima remain elusive. Monte Carlo methods, used to sweep possible parameters in the machine design space, should capture these global optima.

Motors are traditionally three-phase devices, designed to operate when connected to the power grid. Optimal motor design points to N-phase machines [20], where N may be much greater than three. Optimal excitation for different electric machinery has been proposed and examined with more basic models [20], but the enhanced modeling capability of this thesis should enable more accurate results. Additionally, techniques to predict cogging torque in skewed machines are presented.

This thesis will make several contributions to the state of the art for electric machinery as follows

- Fast, accurate permanent-magnet machine modeling - Chapters 2, 3, and 4 detail the modeling method and present results showing a four-order-of-magnitude increase in computation speed.

- Optimization of electric machines in global parameter space - Chapter 7 details design efforts, resulting in a machine that has approximately seven times the torque density of the commercial solution, while decreasing dissipation in a given drive cycle.

- Ability to optimize for exotic drive cycles - Chapter 7 considers the Cheetah drive cycle, consisting of large spikes of torque for short periods of time. Commerically-available motors are generally optimized for continuous torque.

- Optimization of electrical drive of machine - Chapter 9 demonstrates an application of the fast modeling technique, where current is optimally-distributed in windings to make the most torque for a given dissipation.

- Magnet skew optimization to reduce cogging torque - Chapter 5 demonstrates that magnet shapes may be used to eliminate cogging torque to different degrees.

These contributions are based on a hybrid model of an electric machine, comprising two models appropriate for their respective regions that are then joined together. A surface-mounted permanent-magnet synchronous machine has two distinct regions. One is the rotor and air gap, and the other is the stator. The rotor and gap are uniform in their construction, and one can solve Maxwell's Equations to derive an essentially exact analysis of their magnetic behaviors, minus saturation in the rotor core, which is usually inconsequential in the machines considered. The stator is much more intricate with teeth, slots, and wedges that stick into the slots from the teeth at the air gap. The stator also tends to saturate, whereas the rotor does not. It is not feasible to quickly analyze the stator by analytically solving Maxwell's Equations due to both geometric complexity and nonlinearity.

One approach to analyzing the machine is Finite Element Analysis (FEA) which carries the expense of computation time. It requires a fine mesh at least in the stator to capture its geometrical intricacies. FEA is inappropriate for the rotor since the rotor can be effectively analyzed by an explicit solution of Maxell's Equations. One could also analyze the stator using a nonlinear flux tube analysis. This is an approximation, but not a bad one if attention is paid to geometric details.

Our approach is to analytically solve Maxwell's Equations for each space harmonic in the rotor and airgap and to use a flux tube analysis for the stator. Each analysis is appropriate for its own region, and quite fast compared to FEA. The two analyses are stitched together at the boundary between the stator steel and the air gap, and

forced to be self consistent by use of boundary conditions. The analysis iterates between the two models until the solution converges. This approach is illustrated in Figure 1-13. The figure shows a finite element solution of the magnetic fields in a permanent-magnet machine. The flux-tube model is represented by the lumped parameters overlaid on the stator. The current sources are the fluxes calculated by the continuum rotor, magnets, and airgap model; resistors are reluctances associated with each segment; and voltage sources represent the magnetomotive force imparted by each winding.

The following chapters, 2, 3, and 4, present the model. The reasoning associated with the boundary conditions and inputs and outputs to each model is coupled, so there is not a linear way of presenting their evolution. They will be each presented in part with the hope that their interconnections will be understood after reading the three chapters. The selection of inputs and outputs from each model is necessary for their mutual convergence.

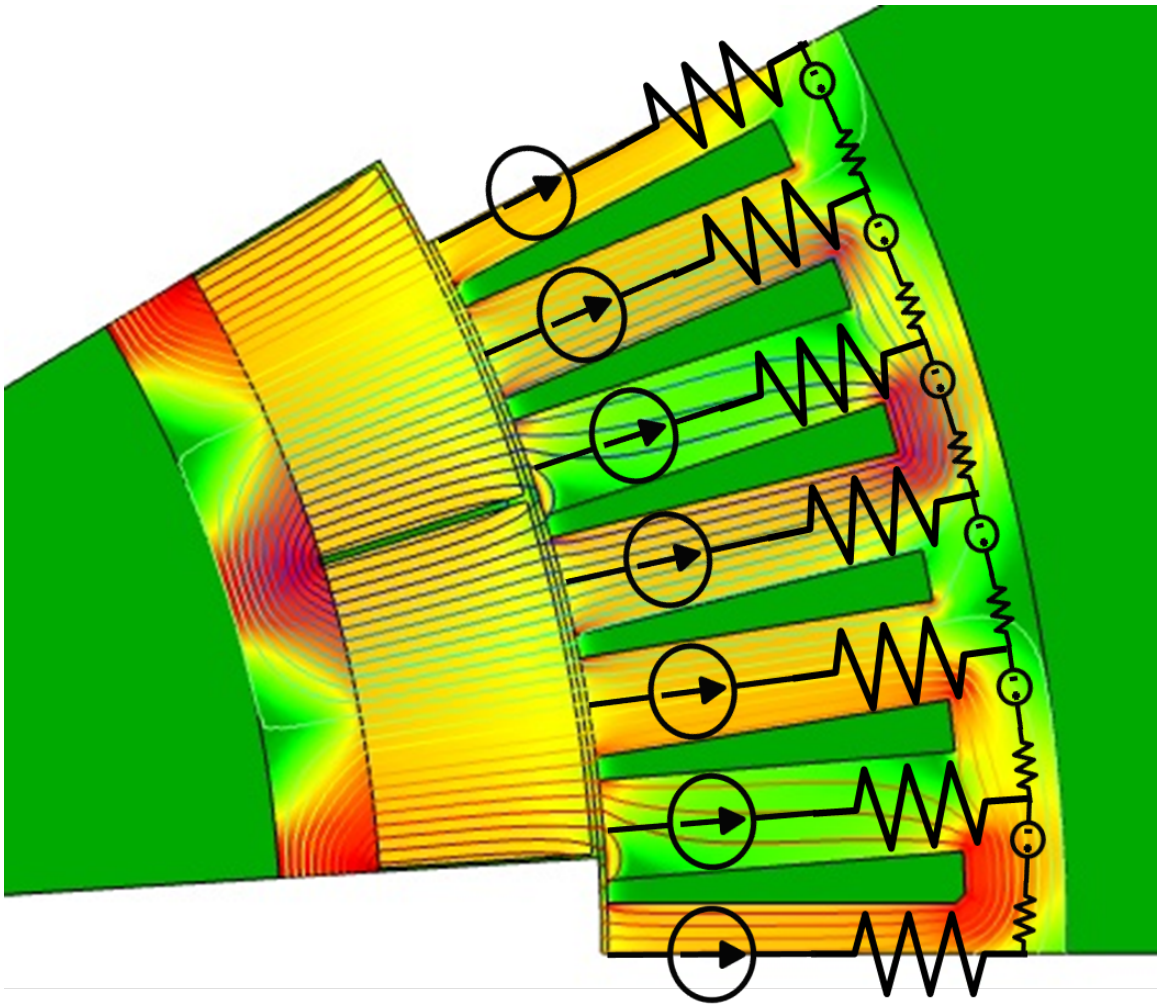

Figure 1-13: Illustration of modeling approach showing flux tubes overlaid on the stator of a finite-element solution of Maxwell's Equations

Chapter 2

Solutions to Maxwell's Equations

Maxwell's Equations form the basis of any sort of analysis of Electric or Magnetic Fields. Electric machines are concerned with the Magnetoquasistatic approximation to Maxwell's equations, as the frequencies contained in and scale of the machines in question render time delay associated with the propagation of electromagnetic fields unimportant [22] [23].

This chapter details the scalar and vector potential solutions of the fields inside the rotor core, magnets, and airgap of the machine. Figure 2-1 shows the machine and relevant parameters.

2.1 Explicit Maxwell Solution - Scalar Potential

The explicit solutions to Maxwell's equations are solved in the motor gap, magnets, and rotor core, as it is quick, easy, and accurate in these regions. This is accomplished by solving for the Scalar Potential in these three regions as a function of the fields at the boundaries. Arbitrary but periodic fields are assumed at the boundary between the stator and the rest of the machine, and it is assumed that fields do not exist in the center of the machine inside the rotor backiron, meaning that the rotor backiorn is assumed to not saturate.

The scalar potential, Ψ, is defined by Laplace's Equation for a conservative field, $H = -\nabla\Psi$ and $\nabla^2\Psi = 0$. It is allowed in this case due to the lack of currents in the

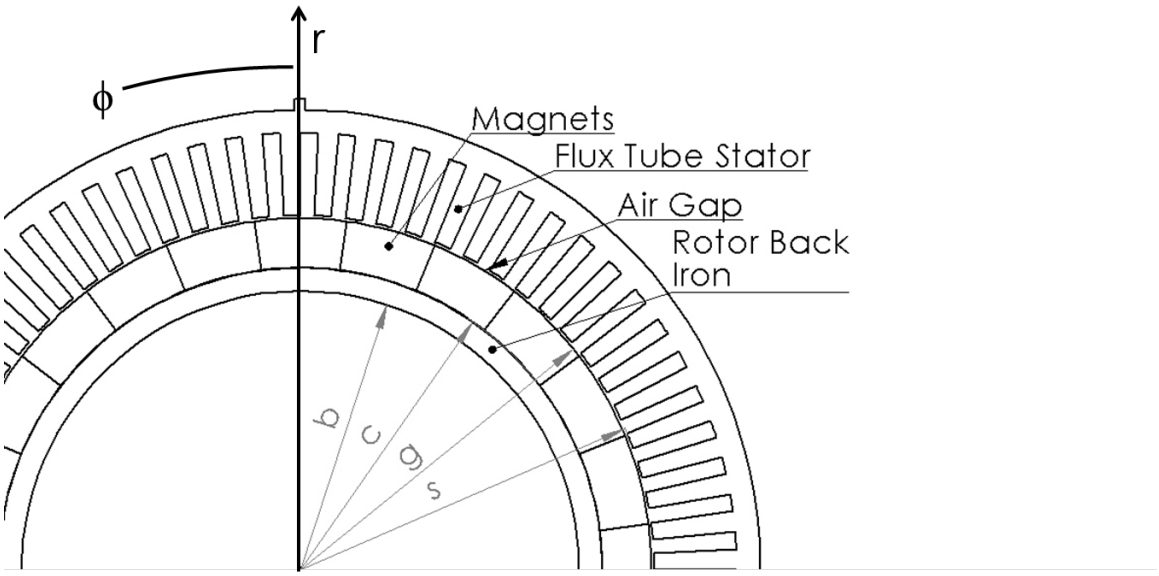

Figure 2-1: Diagram of motor showing definition of parameters

regions of interest. The solution for Laplace's Equation in cylindrical coordinates is known to be

$$\Psi(r,\phi) = \sum_{m=1}^{\infty} \left(A_m \cos\left(mp\phi\right) + B_m \sin\left(mp\phi\right)\right) \cdot \left(C_m r^{mp} + D_m r^{-mp}\right) \tag{2.1}$$

Where m is the harmonic and p is the number of pole pairs in the machine. The scalar potential is then a sum of Fourier components, with A, B, C, and D parameters that are determined for each harmonic. For practical reasons, only the first few harmonics

are considered. The magnetic field components of H are then

$$H_r = -\frac{\partial}{\partial r}\Psi \tag{2.2}$$

$$= \sum_{m=1}^{\infty} \left(-A_m C_m mpr^{mp-1} + A_m D_m mpr^{-mp-1}\right) \cos\left(mp\phi\right)$$

$$+ \left(-B_m C_m mpr^{mp-1} + B_m D_m mpr^{mp-1}\right) \sin\left(mp\phi\right) \tag{2.3}$$

$$H_\phi = -\frac{1}{r}\frac{\partial}{\partial \phi}\Psi \tag{2.4}$$

$$= \sum_{m=1}^{\infty} \left(A_m C_m mpr^{mp-1} + A_m D_m mpr^{-mp-1}\right) \sin\left(mp\phi\right)$$

$$+ \left(-B_m C_m mpr^{mp-1} - B_m D_m mpr^{mp-1}\right) \cos\left(mp\phi\right) \tag{2.5}$$

Simplifying substitutions are made, such that $W_m = A_m C_m mp$, $X_m = A_m D_m mp$, $Y_m = B_m C_m mp$, $Z_m = B_m D_m mp$. Later, the subscript, n $(n + 1, 2, 3)$ will be added to denote different regions.

$$H_r = \sum_{m=1}^{\infty} \left(-W_m r^{mp-1} + X_m r^{-mp-1}\right) \cos\left(mp\phi\right)$$

$$+ \left(-Y_m r^{mp-1} + Z_m r^{mp-1}\right) \sin\left(mp\phi\right) \tag{2.6}$$

$$H_\phi = \sum_{m=1}^{\infty} \left(W_m r^{mp-1} + X_m r^{-mp-1}\right) \sin\left(mp\phi\right)$$

$$+ \left(-Y_m r^{mp-1} - Z_m r^{mp-1}\right) \cos\left(mp\phi\right) \tag{2.7}$$

Magnetic flux densities (B) may then be calculated from the magnetic fields (H), according to

$$\text{Region 1 (Motor Gap) :} \qquad B = \mu_0 H \tag{2.8}$$

$$\text{Region 2 (Magnets) :} \qquad B = \mu_0 \left(H + M\right) \tag{2.9}$$

$$\text{Region 3 (Rotor Core) :} \qquad B = \mu_c H \tag{2.10}$$

Arbitrary but periodic fields are assumed at the stator surface. This results in

$$B_{rs} = \sum_{m=1}^{\infty} A_{mrs} \cos(mp\phi) + B_{mrs} \sin(mp\phi) \tag{2.11}$$

$$B_{\phi s} = \sum_{m=1}^{\infty} A_{m\phi s}\ cos(mp\phi) + B_{m\phi s} \sin(mp\phi) \tag{2.12}$$

The subscript, s, denotes that A and B are the Fourier components corresponding to the as-of-now arbitrary fields at the boundary between the stator and Region 1, the Motor Gap.

The magnetization of the magnets, $\vec{M}_r$, is also assumed to be periodic, radially-directed, and square, such that

$$\vec{M}_r = \sum_{m=0}^{\infty} \frac{c}{r} \left(A_m \cos(mp\phi) + B_m \sin(mp\phi)\right) \tag{2.13}$$

$$A_m = \frac{p}{\pi} \int_{\frac{-\pi}{P}}^{\frac{\pi}{P}} M \cos(mp(\phi + \theta)) d\phi \tag{2.14}$$

$$B_m = \frac{p}{\pi} \int_{\frac{-\pi}{P}}^{\frac{\pi}{P}} M \sin(mp(\phi + \theta)) d\phi \tag{2.15}$$

$$A_m = \frac{M}{m\pi} \left(2 \sin(mp\theta)(\cos(m\pi) - 1)\right) \tag{2.16}$$

$$B_m = \frac{M}{m\pi} \left(-2 \sin(mp\theta)(\cos(m\pi) - 1)\right) \tag{2.17}$$

where θ is the rotation of the rotor.

Note that $\nabla \cdot \vec{M} = 0$ (the divergence of the magnetization must be zero except at the surface of the magnets), so A_m and B_m must be scaled by the ratio of the radii of the inner and outer surfaces in the equation corresponding to the boundary at the outer surface of the magnet (radial magnetization), i.e., if $\vec{M}$ at radius $R = c$ is $\sum_{m=0}^{\infty} A_m \cos(mp\phi) + B_m \sin(mp\phi)$, but $\vec{M}$ at radius $R = g$ is $\frac{c}{g} \sum_{m=0}^{\infty} A_m \cos(mp\phi) + B_m \sin(mp\phi)$.

Boundary conditions are then matched at the boundary of each region, from stator to motor gap, motor gap to magnets, magnets to rotor backiron, and rotor backiron to inner space. See figure 2-1 for geometric details. At the stator, $r = s$, $B_r = B_\perp$ (B normal to stator teeth), $H_\phi = H_\parallel$ (H parallel to stator surface). $H_\parallel$ is set by the

flux tube model in the stator and $B_\perp$ becomes an output of the model in this chapter that is input to the flux tube model. The continuity expressions are

$$\begin{aligned}
H_{mr} =&(-W_{m1}s^{mp-1} + X_{m1}s^{-mp-1})\cos(mp\phi) \\
&+ (-Y_{m1}s^{mp-1} + Z_{m1}s^{-mp-1})\sin(mp\phi) \\
=&\frac{B_{\perp stator}}{\mu_o} \\
=&\frac{1}{\mu_0}(A_{mrs}\cos(mp\phi) + B_{mrs}\sin(mp\phi) \qquad (2.18) \\
H_{m\phi} =&(W_{m1}s^{mp-1} + X_{m1}s^{-mp-1})\sin(mp\phi) \\
&+ (-Y_{m1}s^{mp-1} - Z_{m1}s^{-mp-1})\cos(mp\phi) \\
=&A_{m\phi s}\cos(mp\phi) + B_{m\phi s}\sin(mp\phi) \qquad (2.19)
\end{aligned}$$

At the surface of the magnets, $r = g$ and B_r is continuous, as is H_ϕ. The magnetization is included on the magnet side of the boundary. The continuity expressions are

$$\begin{aligned}
B_{mr} =&(-W_{m1}g^{mp-1} + X_{m1}g^{-mp-1})\cos(mp\phi) \\
&+ (-Y_{m1}g^{mp-1} + Z_{m1}g^{-mp-1})\sin(mp\phi) \\
=&(-W_{m2}g^{mp-1} + X_{m2}g^{-mp-1})\cos(mp\phi) \\
&+ (-Y_{m2}g^{mp-1} + Z_{m2}g^{-mp-1})\sin(mp\phi) \\
&+ A_m\cos(mp\phi) + B_m\sin(mp\phi) \qquad (2.20) \\
H_{m\phi} =&(W_{m1}g^{mp-1} + X_{m1}g^{-mp-1})\sin(mp\phi) \\
&+ (-Y_{m1}g^{mp-1} - Z_{m1}g^{-mp-1})\cos(mp\phi) \\
=&(W_{m2}g^{mp-1} + X_{m2}g^{-mp-1})\sin(mp\phi) \\
&+ (-Y_{m2}g^{mp-1} - Z_{m2}g^{-mp-1})\cos(mp\phi) \qquad (2.21)
\end{aligned}$$

At the rotor backiron, $r = c$ and B_r is continuous, as is H_ϕ. Magnetization is again

included on the magnet side of the interaction. The continuity expressions are

$$\begin{aligned} B_{mr} =& \mu_0((-W_{m2}c^{mp-1} + X_{m2}c^{-mp-1})\cos(mp\phi) \\ &+ (-Y_{m2}c^{mp-1} + Z_{m2}c^{-mp-1})\sin(mp\phi)) \\ &+ A_m\cos(mp\phi) + B_m\sin(mp\phi) \\ =& \mu_c((-W_{m3}c^{mp-1} + X_{m3}c^{-mp-1})\cos(mp\phi) \\ &+ (-Y_{m3}c^{mp-1} + Z_{m3}c^{-mp-1})\sin(mp\phi)) \end{aligned} \tag{2.22}$$

$$\begin{aligned} H_{m\phi} =& (W_{m2}c^{mp-1} + X_{m2}c^{-mp-1})\sin(mp\phi) \\ &+ (-Y_{m2}c^{mp-1} - Z_{m2}c{-}mp - 1)\cos(mp\phi) \\ =& (W_{m3}c^{mp-1} + X_{m3}c^{-mp-1})\sin(mp\phi) \\ &+ (-Y_{m3}c^{mp-1} - Z_{m3}c{-}mp - 1)\cos(mp\phi) \end{aligned} \tag{2.23}$$

At the inside surface of the rotor backiron, $r = b$, $B_r = 0$. It is assumed that flux does not travel in to the inner space inside the rotor backiron, so that

$$\begin{aligned} B_{mr} =& (-W_{m3}b^{mp-1} + X_{m3}b^{-mp-1})\cos(mp\phi) \\ &+ (-Y_{m3}b^{mp-1} + Z_{m3}b^{-mp-1})\sin(mp\phi) \\ =& 0 \end{aligned} \tag{2.24}$$

Putting Equations2.8 to 2.10 and 2.19 to 2.24 together results in equation 2.25. Note that this equation must be solved for each harmonic. Also note that the equations corresponding to the radial fields at the stator surface and the tangential fields at the rotor backiron inner surface have been omitted. The system is overconstrained, so several equations may be eliminated, as the field quantities are model outputs. The tangential fields at the stator and radial fields at the rotor surface are chosen, as this results in the convergent spiral that will be discussed in Chapter 4. The square matrix is defined by the geometry and materials in their respective regions. It is divided in to groups of four columns to show interactions between each of the three regions. The first column matrix contains the parameters (W, X, Y, Z) that define the fields

in each region. The Second column matrix contains the inputs. The first two rows are associated with the boundary conditions imposed by the flux tube model, and the rest are determined by the magnet and steel properties. Solving the system is accomplished by inverting the square matrix to solve for the parameters that define the fields. Once the fields are calculated, B_r is integrated to determine flux in to each tooth.

$$
\begin{bmatrix}
s^{mp-1}s^{-mp-1} & 0 & 0 & 0 & 0 & 0 & 0 & 0 & 0 & 0 & 0 & 0 \\
0 & 0 & -s^{mp-1} & -s^{-mp-1} & 0 & 0 & 0 & 0 & 0 & 0 & 0 & 0 \\
-g^{mp-1} & g^{-mp-1} & 0 & 0 & g^{mp-1} & -g^{-mp-1} & 0 & 0 & 0 & 0 & 0 & 0 \\
0 & 0 & -g^{mp-1} & g^{-mp-1} & 0 & 0 & g^{mp-1} & -g^{-mp-1} & 0 & 0 & 0 & 0 \\
g^{mp-1} & g^{-mp-1} & 0 & 0 & -g^{mp-1} & -g^{-mp-1} & 0 & 0 & 0 & 0 & 0 & 0 \\
0 & 0 & g^{mp-1} & g^{-mp-1} & 0 & 0 & -g^{mp-1} & -g^{-mp-1} & 0 & 0 & 0 & 0 \\
0 & 0 & 0 & 0 & -\mu_0 c^{mp-1} & \mu_0 c^{-mp-1} & 0 & 0 & \mu_c c^{mp-1} & -\mu_c c^{-mp-1} & 0 & 0 \\
0 & 0 & 0 & 0 & 0 & 0 & -\mu_0 c^{mp-1} & \mu_0 c^{-mp-1} & 0 & 0 & \mu_c c^{mp-1} & -\mu_c c^{-mp-1} \\
0 & 0 & 0 & 0 & c^{mp} & c^{-mp} & 0 & 0 & -c^{mp} & -c^{-mp} & 0 & 0 \\
0 & 0 & 0 & 0 & 0 & 0 & c^{mp} & c^{-mp} & 0 & 0 & -c^{mp} & -c^{-mp} \\
0 & 0 & 0 & 0 & 0 & 0 & 0 & 0 & -b^{mp-1} & b^{-mp-1} & 0 & 0 \\
0 & 0 & 0 & 0 & 0 & 0 & 0 & 0 & 0 & 0 & -b^{mp-1} & b^{-mp-1}
\end{bmatrix}
$$

$$
\begin{bmatrix} W_{1m} \\ X_{1m} \\ Y_{1m} \\ Z_{1m} \\ W_{2m} \\ X_{2m} \\ Y_{2m} \\ Z_{2m} \\ W_{3m} \\ X_{3m} \\ Y_{3m} \\ Z_{3m} \end{bmatrix}
=
\begin{bmatrix} B_{m\phi s} \\ A_{m\phi s} \\ \frac{c}{g}A_m \\ \frac{c}{g}B_m \\ 0 \\ 0 \\ -A_m \\ -B_m \\ 0 \\ 0 \\ 0 \\ 0 \end{bmatrix}
\tag{2.25}
$$

To summarize, Equation 2.25 is the primary result of this chapter. The input to this model is $H_{\|}$ at $r = s$ which enter through $A_{m\phi s}$ and $B_{m\phi s}$ as defined by 2.12. This comes from the flux tube model of Chapter 3. The output from this model is $B_{\perp} = B_{rs}$, defined in 2.11.

2.2 Solutions to Maxwell's Equations - Vector Potential

A 2-dimensional magnetic field may also be defined by a single component of the vector potential, A_z, which is defined by $\mu H = \nabla \times A$. The solution for Laplace's Equation in cylindrical coordinates is known to be

$$A(r,\phi) = \sum_{m=0}^{\infty} \left(A_m cos\left(mp\phi\right) + B_m sin\left(mp\phi\right)\right) \cdot \left(C_m r^{mp} + D_m r^{-mp}\right) \tag{2.26}$$

where m is the harmonic and p is the number of pole pairs in the machine. Note that A, B, C, and D as used here are not the same as those used earlier in this chapter. The magnetic field components of H are then

$$\begin{aligned} H_r &= \sum_{m=0}^{\infty} \frac{1}{r}\frac{\partial}{\partial r} A_z && (2.27)\\ &= \sum_{m=0}^{\infty} -\frac{1}{r}\left(A_m C_m mpr^{mp} + A_m D_m mpr^{-mp}\right)\sin\left(mp\phi\right) \\ &\quad -\frac{1}{r}\left(-B_m C_m mpr^{mp-1} + B_m D_m mpr^{mp-1}\right)\cos\left(mp\phi\right) && (2.28)\\ H_\phi &= \sum_{m=0}^{\infty} \frac{\partial}{\partial \phi} A_z && (2.29)\\ &= \sum_{m=0}^{\infty} \left(-A_m C_m mpr^{mp-1} + A_m D_m mpr^{-mp-1}\right)\cos\left(mp\phi\right) \\ &\quad + \left(-B_m C_m mpr^{mp-1} + B_m D_m mpr^{mp-1}\right)\sin\left(mp\phi\right) && (2.30) \end{aligned}$$

Simplifying substitutions are made, such that $W_m = A_m C_m mp, X_m = A_m D_m mp, Y_m = B_m C_m mp, Z_m = B_m D_m mp$.

$$\begin{aligned} H_r &= \sum_{m=0}^{\infty} \left(W_m r^{mp-1} + X_m r^{-mp-1}\right)\sin\left(mp\phi\right) \\ &\quad + \left(Y_m r^{mp-1} + Z_m r^{mp-1}\right)\cos\left(mp\phi\right) && (2.31)\\ H_\phi &= \sum_{m=0}^{\infty} \left(-W_m r^{mp-1} + X_m r^{-mp-1}\right)\cos\left(mp\phi\right) \\ &\quad + \left(-Y_m r^{mp-1} + Z_m r^{mp-1}\right)\sin\left(mp\phi\right) && (2.32) \end{aligned}$$

Following the same process as the scalar potential and matching H_ϕ and B_r at the boundary between each region results in

$$\begin{bmatrix}
-s^{mp-1}s^{-mp-1} & 0 & 0 & 0 & 0 & 0 & 0 & 0 & 0 & 0 \\
0 & 0 & -s^{mp-1} & s^{-mp-1} & 0 & 0 & 0 & 0 & 0 & 0 \\
-g^{mp-1} & -g^{-mp-1} & 0 & 0 & g^{mp-1} & -g^{-mp-1} & 0 & 0 & 0 & 0 \\
0 & 0 & g^{mp-1} & g^{-mp-1} & 0 & 0 & -g^{mp-1} & -g^{-mp-1} & 0 & 0 \\
-g^{mp-1} & g^{-mp-1} & 0 & 0 & g^{mp-1} & -g^{-mp-1} & 0 & 0 & 0 & 0 \\
0 & 0 & -g^{mp-1} & g^{-mp-1} & 0 & 0 & g^{mp-1} & -g^{-mp-1} & 0 & 0 \\
0 & 0 & 0 & 0 & -\mu_0 c^{mp-1} & \mu_0 c^{-mp-1} & 0 & 0 & \mu_c c^{mp-1} & \mu_c c^{-mp-1} \\
0 & 0 & 0 & 0 & 0 & 0 & -\mu_0 c^{mp-1} & \mu_0 c^{-mp-1} & -\mu_c c^{mp-1} & -\mu_c c^{-mp-1} \\
0 & 0 & 0 & 0 & -c^{mp} & c^{-mp} & 0 & 0 & c^{mp} & -c^{-mp} \\
0 & 0 & 0 & 0 & 0 & 0 & -c^{mp} & c^{-mp} & 0 & 0 \\
0 & 0 & 0 & 0 & 0 & 0 & 0 & 0 & b^{mp-1} & b^{-mp-1} \\
0 & 0 & 0 & 0 & 0 & 0 & 0 & 0 & 0 & 0
\end{bmatrix}$$

$$\begin{bmatrix} W_{1m} \\ X_{1m} \\ Y_{1m} \\ Z_{1m} \\ W_{2m} \\ X_{2m} \\ Y_{2m} \\ Z_{2m} \\ W_{3m} \\ X_{3m} \\ Y_{3m} \\ Z_{3m} \end{bmatrix} = \begin{bmatrix} \frac{1}{\mu_0} A_{m\phi s} \\ \frac{1}{\mu_0} B_{m\phi s} \\ \frac{c}{g} B_m \\ \frac{c}{g} A_m \\ 0 \\ 0 \\ -\mu_0 B_m \\ -\mu_0 A_m \\ 0 \\ 0 \\ 0 \\ 0 \end{bmatrix} \tag{2.33}$$

This implementation may be seen in lines 260-271 of Appendix A.

While the scalar potential and vector potential result in substantially similar math

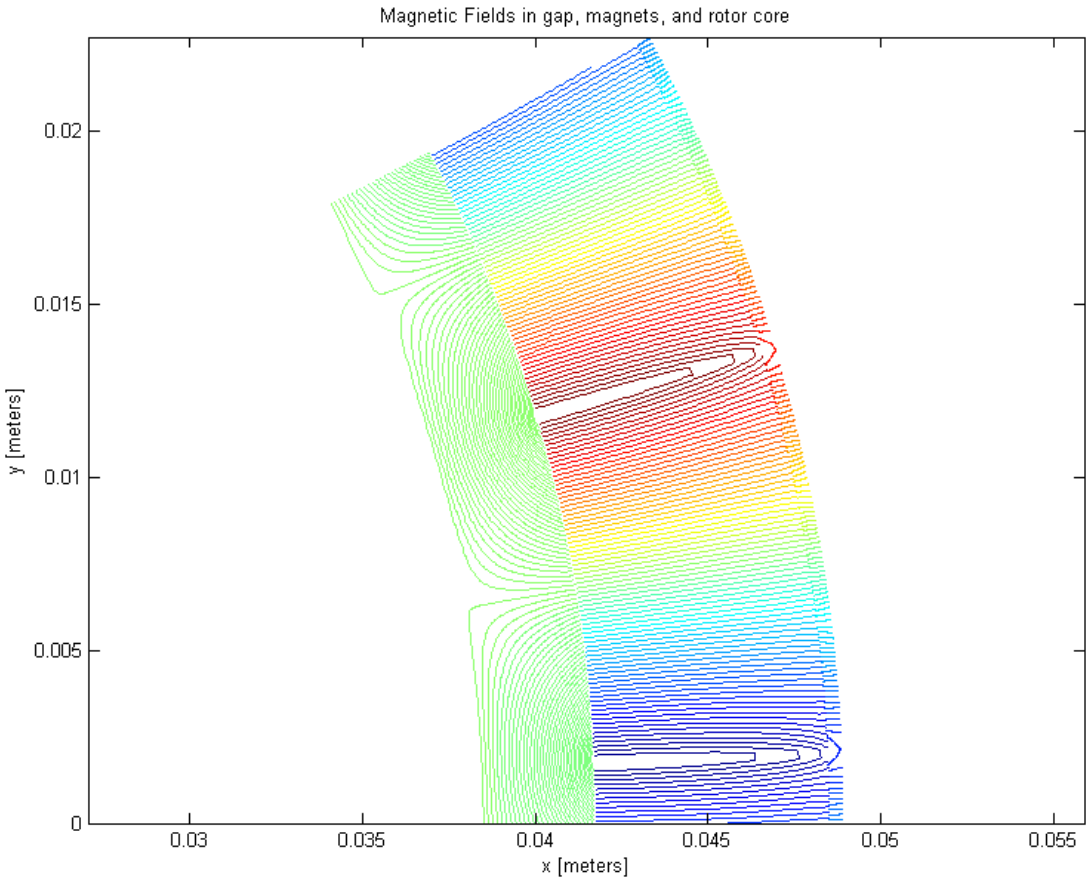

Figure 2-2: Field lines in a notional electric machine, plotted as contour lines of vector potential

and both uniquely determine the fields in the stator, the vector potential allows for easy visualization of the field lines in the material. The contour lines of the vector potential solution correspond to flux lines in the machine, allowing for simple plotting in programs such as MATLAB. An example is shown in Figure 6-12.

2.3 Torque Calculation

The Maxwell Stress Tensor is a method for calculating electromagnetic forces on an object when fields outside the object are known [24] [25]. In this application, magnetic fields are solved in the continuum region of the machine, or in the airgap, magnets, and rotor core. Torque may be calculated with the Maxwell Stress Tensor anywhere

the continuum field solution exists. The maxwell stress tensor is used to calculate force on an object with knowledge of only the fields outside of it. In this case, we may use the fields in the airgap of the machine to calculate shear stress on the rotor, which then gives the torque as

$$\tau_\phi = \mu_0 H_r H_\phi \tag{2.34}$$

$$\text{Torque} = 2\pi r^2 L_{motor} \int_0^{2\pi} \tau_\phi d\phi \tag{2.35}$$

where H_r is radial Magnetic Field Strength, H_ϕ is tangential Magnetic Field Strength, L_{motor} is motor stack length, and τ_ϕ is shear stress. The implementation is shown on lines 318-330 of Appendix A.

2.4 Modification to capture cogging effects

At the surface of the stator, our approach assumes that the surface of each tooth sits at the same magnetic potential (MMF). This means that tangential H exists only in the spaces between the teeth. It also assumes that the field lines are normal to the surface of the tooth. This approximation ignores the divergence of the field lines between the teeth and captures only the integrated value of H between them. The fourier coefficients are built up from each tooth. These equations take the output from the flux-tube model and convert them to fourier components of fields that are used as inputs in the Equations 2.25 and 2.33 according to

$$H = \frac{\Delta\Psi}{\Delta l} \tag{2.36}$$

$$A_{H_\parallel} = \frac{1}{\pi}\int H_\parallel \cos\left(np\phi\right) r d\theta \tag{2.37}$$

$$B_{H_\parallel} = \frac{1}{\pi}\int H_\parallel \sin\left(np\phi\right) r d\theta \tag{2.38}$$

$$A_{H_\parallel} = \frac{r}{\pi}\sum_{tooth}\frac{1}{nP} H_\parallel \sin np\phi \tag{2.39}$$

$$B_{H_\parallel} = \frac{r}{\pi}\sum_{tooth}\frac{-1}{nP} H_\parallel \cos np\phi \tag{2.40}$$

This is shown on lines 177-182 of Appendix A.

The integrated value of H between each tooth is sufficient to calculate the fundamental torque, but it ignores the fringing fields between the teeth that cause cogging. To capture this important performance parameter, the fringing fields must be approximated.

Their absence has little effect on motive torque calculation, as the missing reluctance multiplied by the flux (to get the integral of H between teeth) is small next to the tangential H produced by the windings, and their contribution to the total reluctance of the stator is small due to flux preferentially traveling though the teeth.

To capture cogging torque, the reluctance of each tooth must be augmented by the reluctance of the empty space where the fringing fields reside. A simple approach is to approximate the reluctance seen by the fringing fields and add it to each individual tooth in the flux tube model. This may be done by calculating the reluctance of the air gap assuming the teeth span the whole tooth pitch (gap between the teeth is nonexistant), as seen in Figure 2-4, calculating the reluctance assuming the fields follow a trapezoidal path to the teeth as in Figure 2-5, and subtracting the two. This reluctance may then be added to the teeth in the flux tube model. While this method captures the missing piece that contributes to cogging, it is highly dependent on geometry in a way that is not expected to scale.

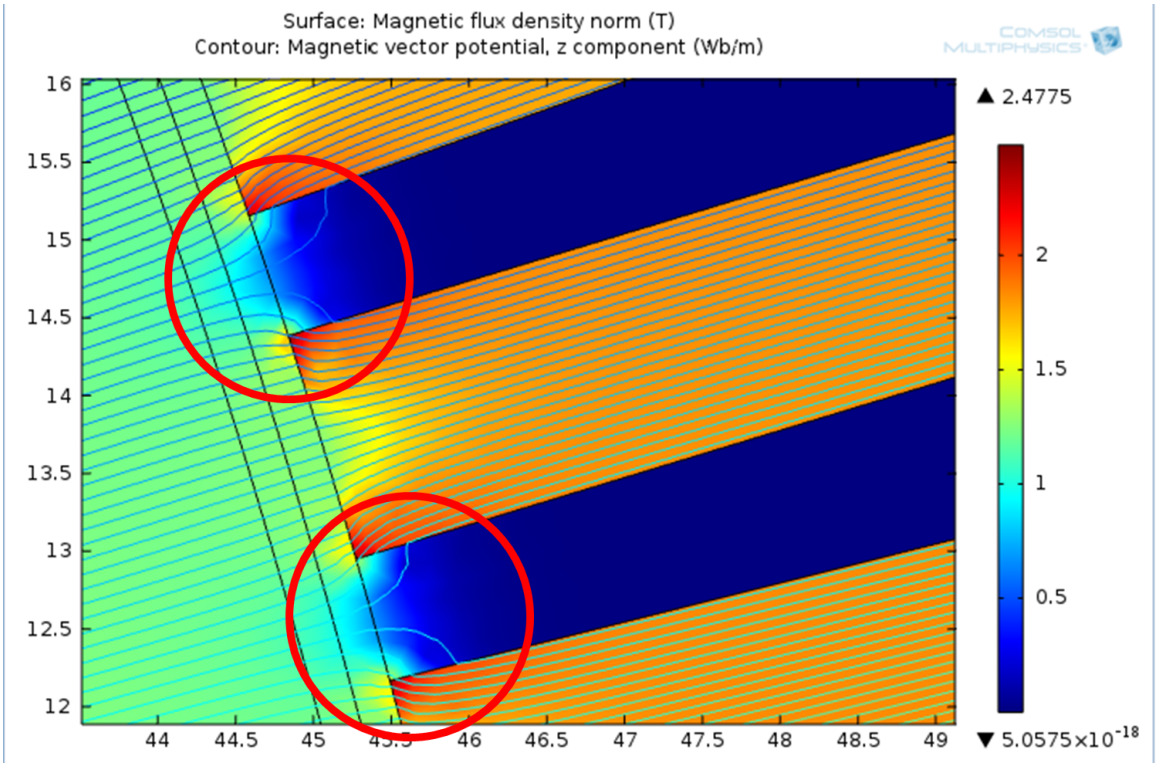

Figure 2-3: Fringing fields in an example motor

$$R \approx \left(\frac{g}{\mu_0 W \theta \left(1 - \frac{\delta}{2}\right) r_s} - \frac{g}{\mu_0 W \theta r_s} \right) \tag{2.41}$$

$$\approx \frac{g\delta}{W\theta 2 r_s \mu_0} \tag{2.42}$$

2.5 A Better Way to Capture Cogging Effects

The previous method allowed the cogging effects to be seen more clearly, but is expected to break down as geometry changes. H_ϕ was then approximated by a linear ramp, knowing that only the low-frequency spatial components of the ramp are important to cogging torque.

An illustration of the following paragraph is shown in Figure 2-6. We must first approximate the height of the ramp. Radial flux density at the edge of tooth is

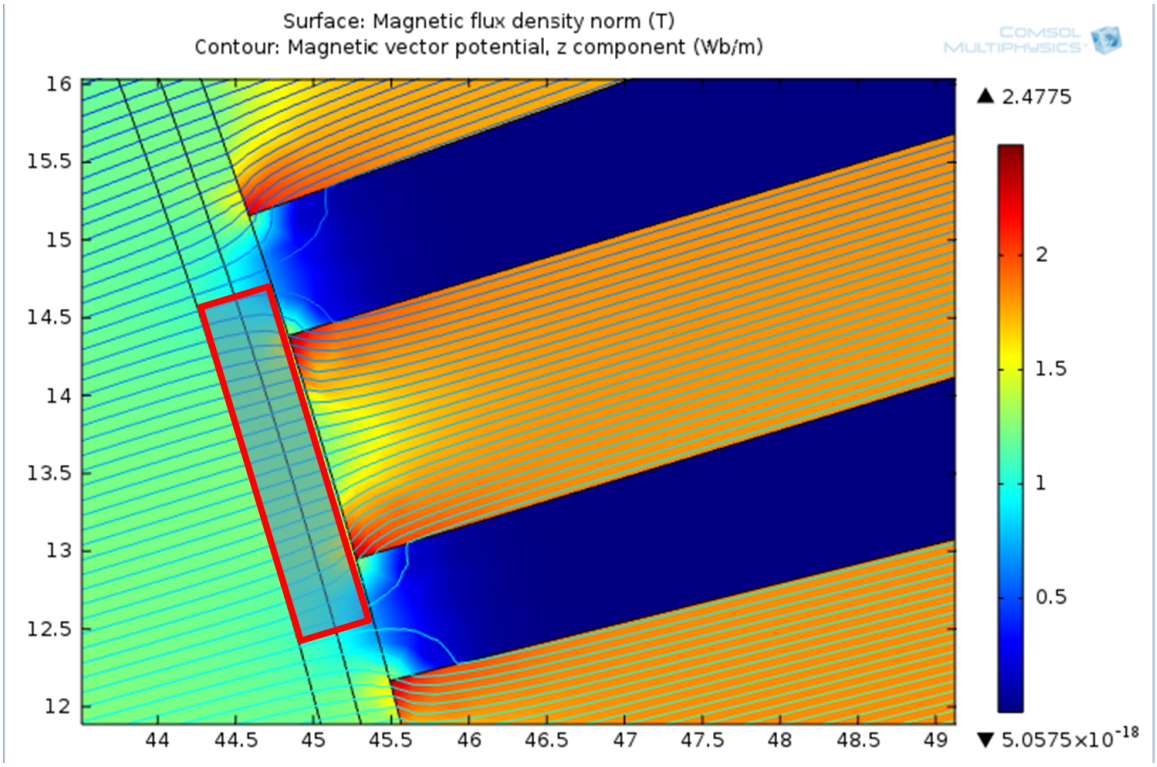

Figure 2-4: Rectangular reluctance approximation

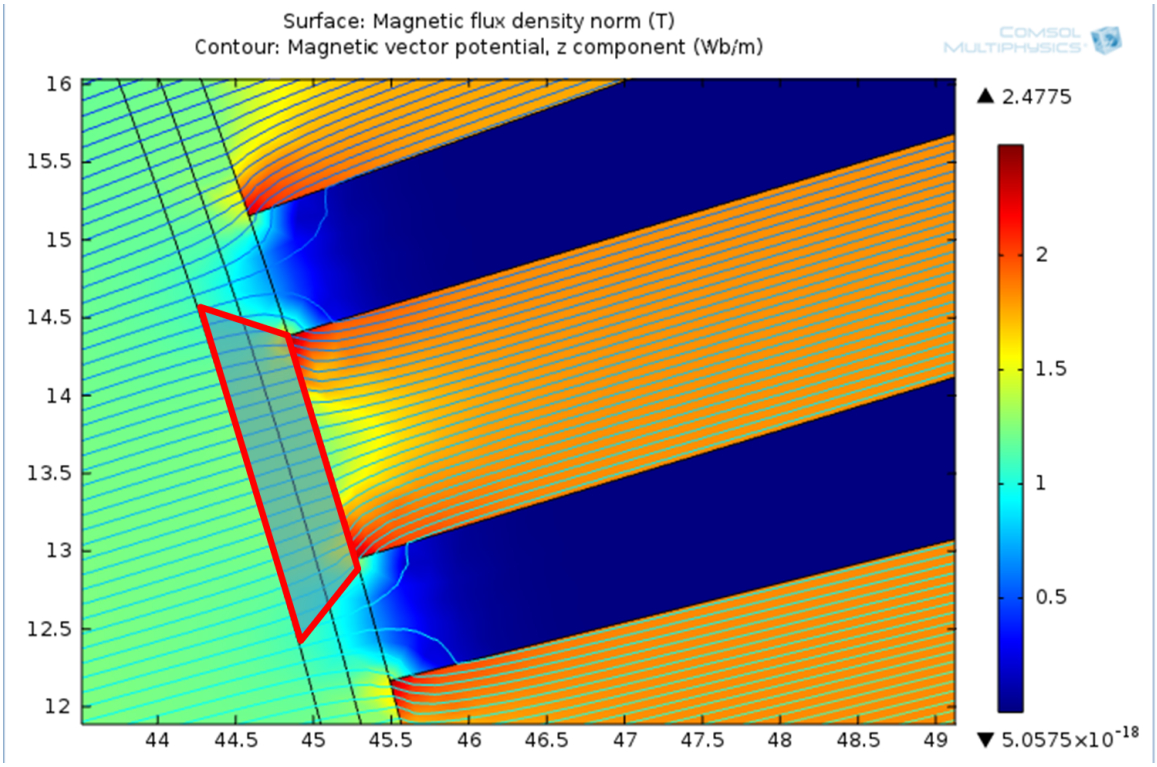

Figure 2-5: Trapezoidal reluctance approximation

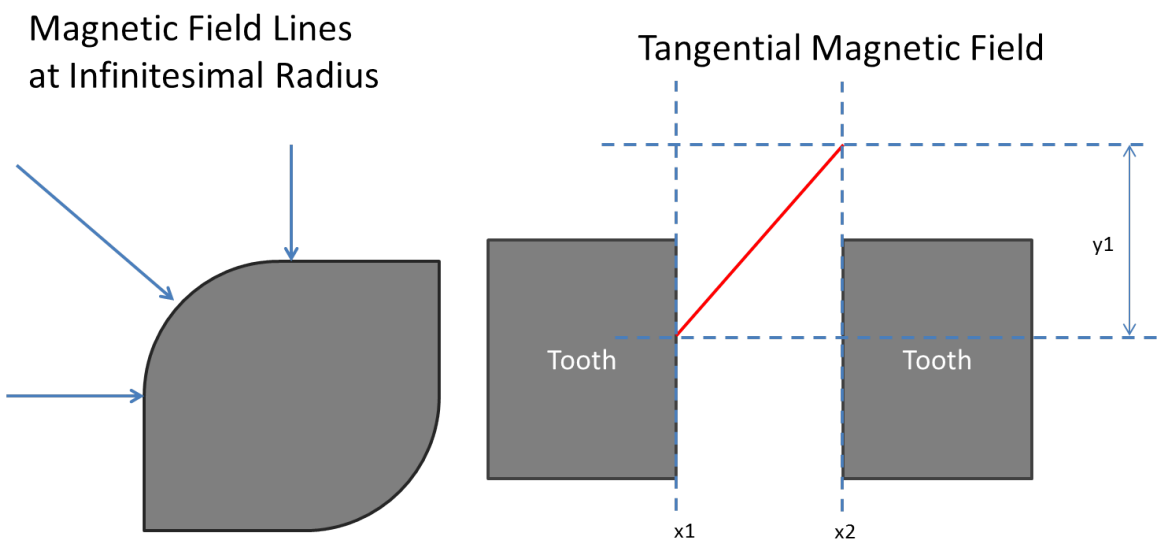

Figure 2-6: Magnetic field approximation between teeth

assumed to be equal to tangential flux density at the edge of tooth. Flux is, by definition, perpendicular to the surface of an infinitely permeable material. In this case, the edge of the tooth is an arc with an arbitrarily small radius. Lines of flux must be normal to this arc, resulting in flux lines at 45° and setting the two flux densities equal. Fundamentally, in a field governed by a potential, flux lines follow the gradient of the field. On a boundary where the potential is equal to a constant (the stator steel), the gradient will be, by definition, equal in the radial and tangential directions at a corner. In the case where the boundary between two magnets sits between teeth in the stator, it is assumed that two ramps occupy the gap with the boundary between aligned with the boundary between magnets. The fourier coefficients from the ramp are then added to the coefficients calculated from the difference in MMF on the surface of each tooth and are calculated as

$$a_n = \frac{1}{x_2 - x_1} \int_{x_1}^{x_2} \frac{y_1}{x_2 - x_1} (x - x_2) \cos(n\pi x)\, dx \tag{2.43}$$

$$a_n = \frac{y_1}{(x_2 - x_1)^2} \left(\frac{\pi n \left((x_2 - x_1) \sin(n\pi x_1) - \cos(n\pi x_1) + \cos(n\pi x_2) \right)}{n^2 \pi^2} \right) \tag{2.44}$$

$$b_n = \frac{1}{x_2 - x_1} \int_{x_1}^{x_2} \frac{y_1}{x_2 - x_1} (x - x_2) \sin(n\pi x)\, dx \tag{2.45}$$

$$b_n = \frac{y_1}{(x_2 - x_1)^2} \left(\frac{\pi n \left((x_1 - x_2) \cos(n\pi x_1) - \sin(n\pi x_1) + \sin(n\pi x_2) \right)}{n^2 \pi^2} \right) \tag{2.46}$$

These equations may be seen on lines 190-242 in Appendix A.

To calculate flux into each tooth, the flux density is integrated over the tooth and half way in to each gap between the teeth. B at the stator surface is first calculated from the coefficients solved in the Maxwell model, then this is integrated

$$B_r = \mu_0 \left(-W_1 s^{mp-1} + X_1 s^{-mp-1} \right) \cos mp\phi + \mu_0 \left(-Y_1 s^{mp-1} + Z_1 s^{-mp-1} \right) \sin mp\phi \tag{2.47}$$

$$U = \mu_0 \left(-W_1 s^{mp-1} + X_1 s^{-mp-1} \right) \tag{2.48}$$

$$V = \mu_0 \left(-Y_1 s^{mp-1} + Z_1 s^{-mp-1} \right) \tag{2.49}$$

$$Br = U \cos mp\phi + V \sin mp\phi \tag{2.50}$$

$$\Phi = \int B_r r \mathrm{d}\phi \mathrm{d}z \tag{2.51}$$

$$\Phi = sL_{motor} \int (U \cos mp\phi + V \sin mp\phi)\, d\phi \tag{2.52}$$

$$\Phi = sL_{motor} \left(\frac{U}{mp} \sin mp\phi \Big|_{low}^{high} - \frac{V}{mp} \cos mp\phi \Big|_{low}^{high} \right) \tag{2.53}$$

The implementation of this equation can be seen on lines 292-294 in Appendix A.

One can justify this choice of boundary conditions by considering the scalar potential distribution at the tips of the teeth. The tangential H is assumed to be zero across

a tooth tip, meaning that there is no gradient in the scalar potential in this direction. The gradient in the radial direction counteracts the magnetization of the magnets, providing a means of weakening flux produced by the magnets as the permeability in the steel drops or as the winding currents produce more MMF.

2.6 Summary and Alternate Forms

This chapter has presented a method for solving the fields in three regions composed of the rotor core, magnets, and airgap of the machine using both scalar and vector potentials. Some knowledge of requirements for convergence with the flux tube model of Chapter 3 has been assumed in selection of inputs and outputs. These have been derived with the idea of modeling fields in a radial-flux electric machine that is uniform along its axial dimension, hence the cylindrical 2D coordinate frame. Similar solutions exist over other frames where the solution to the Laplace equation is known. These include the cartesian (2D and 3D), the cylindrical 3D, and the spherical 3D frames. Of note for motor design are the cartesian frame for linear machines, the 3D cylindrical frame for axial flux machines, and the spherical frame for spherical motors.

Chapter 3

Flux-Tube Analysis of Stator

This chapter derives the flux-tube model that is used to model the stator of the machine. Its inputs come from the fluxes through each tooth calculated from the radial fields solved by the continuum model in Chapter 2. The flux-tube model then calculates the tangential fields at the boundary between the two models used as inputs to the continuum model.

3.1 Jusification of Flux Tubes

A flux tube is based on the notion that a magnetic material will confine lines of flux. Figure 3-1 shows the magnetic field lines of a dipole when contained inside spheres of different permeabilities. The solid lines are magnetic flux, while the dotted lines are contours of magnetic scalar potential. The first sphere has a relative permeability of one, meaning that the permeability is equal to μ_0, or the permeability of free space. The field lines are unaffected. The second sphere has a relative permeability of three. In this example, the field lines are highly distorted, being confined mostly to the sphere. In the third sphere, relative permeability is one hundred. Nearly all of the flux is confined to the sphere [22]. Figure 1-3 shows an example of a flux tube model implementation, while Figures 1-13, 2-3, 2-4, and 2-5 show examples of this confinement of magnetic fields inside electric machines. Typical steels have permeabilities well in excess of one thousand, meaning that they very effectively

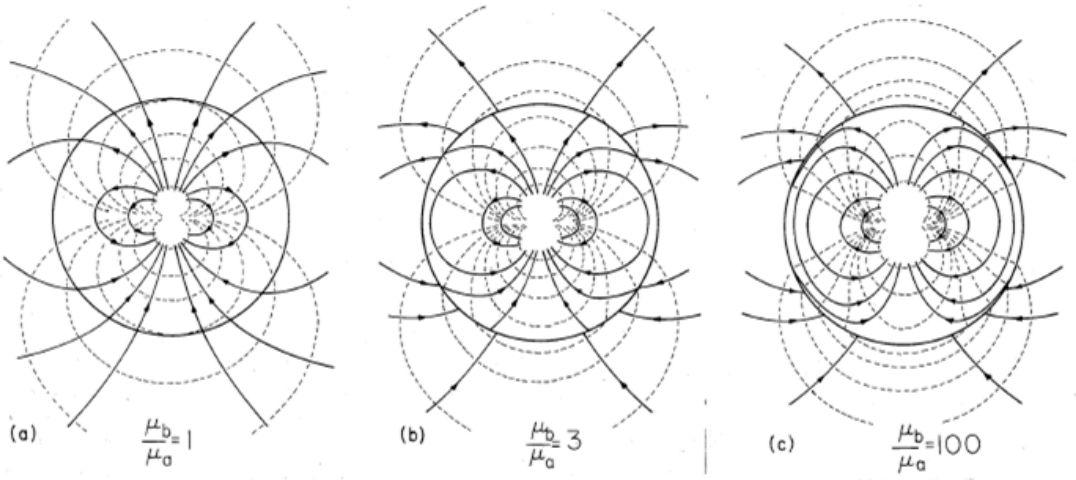

Fig. 9.6.2 Magnetic potential and lines of field intensity in and around the magnetizable sphere of Fig. 9.6.1. (a) With the ratio of permeabilities equal to 1, the dipole field extends into the surrounding free space region without modification. (b) With $\mu_b/\mu_a = 3$, field lines tend to be more confined to the sphere. (c) With $\mu_b/\mu_a = 100$, the field lines (and hence the flux lines) tend to remain inside the sphere.

Figure 3-1: Flux tube justification [22]

confine magnetic flux.

In an electric machine, steel is used for the purpose of confining and guiding flux. As a constant, for linear materials, the permeability, μ, is the relationship of the Magnetic Field Strength, or H, to Magnetic Flux Density B. Figure 3-2 shows the relationship of B to H for several materials commonly used in magnetic applications. Permeability of the material is defined as the slope of this line. Relative permeability is the slope of the line from the origin to a point on the BH curve, and incremental permeability is the local slope of the curve. Relative permeabilities will be used to calculate segment reluctances in this model. Note that most of the curves are highly non-linear, exhibiting saturation at a certain value for each material. A good magnetic steel, such as Hyperco50, may have a relative permeability around 20000. Such a material may be expected to effectively confine flux well beyond saturation, defined as the point where the incremental permeability drops to that of free space, or μ_0.

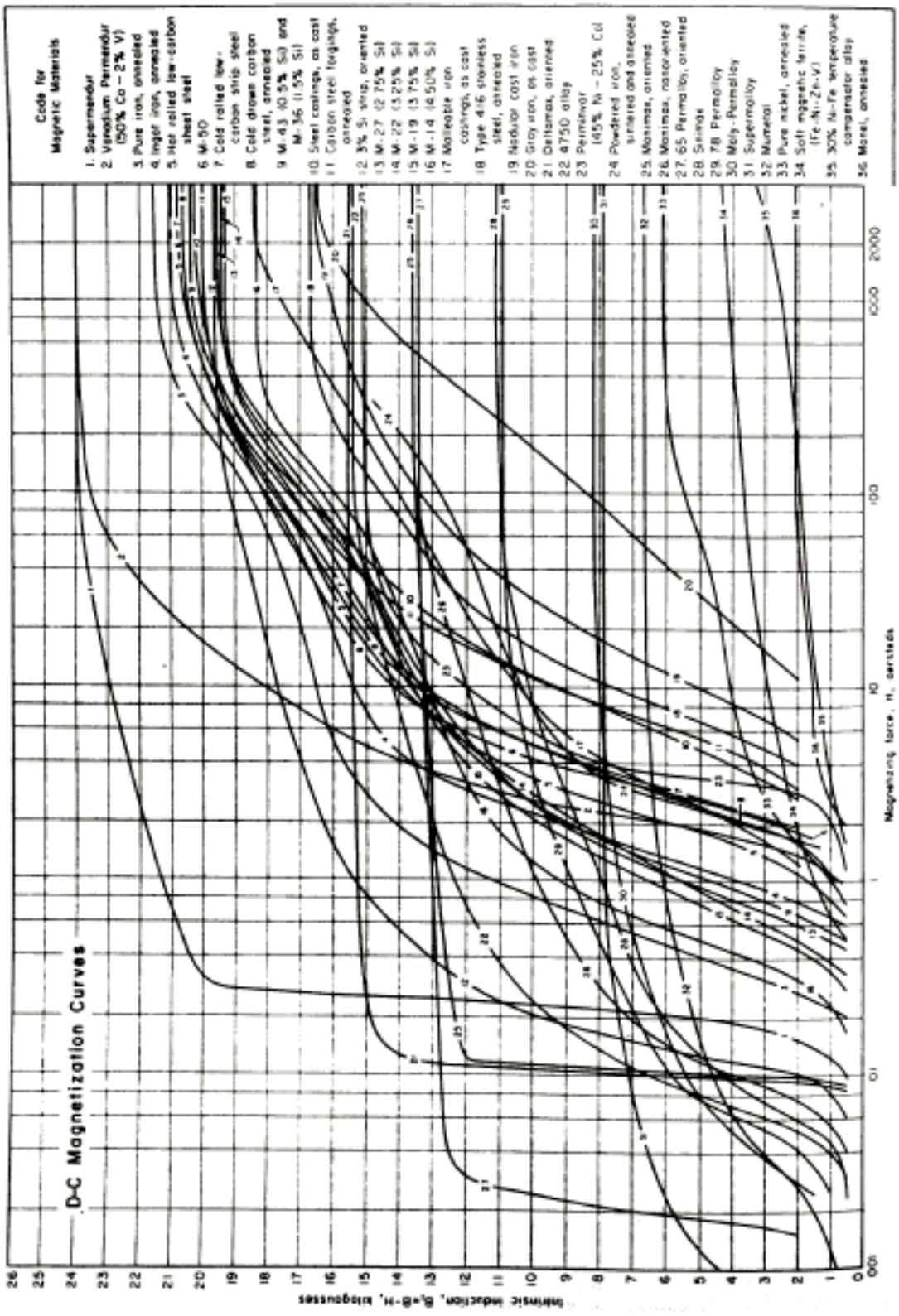

Fig. 17. Direct-current magnetization curves for various magnetic materials

Figure 3-2: BH Curves of various magnetic materials [26]

3.2 Derivation of Flux Tubes

A magnetic system in which flux is driven by magnetomotive force (MMF) and guided by material tubes may be evaluated in the same way as an electric circuit in which current is driven by electromotive force (EMF) and guided by material tubes by reducing each segment to a lumped parameter analogous to a resistor [25]. This lumped parameter is known as a reluctance, $\Re$. The behavior of these materials may be seen directly from Maxwell's equations. Ampere's law in magnetoquasistatic form states that $\int H \cdot \delta l = \iint J \cdot \delta s$, which relates the Magnetic Field Strength around a loop to the current contained in the area enclosed by the loop (J is current density), and is the equivalent of Kirchoff's Voltage Law. Gauss' Law for magnetic flux states that $\int B \cdot \delta s = 0$, meaning that magnetic monopoles are not known to exist in our universe, and so that field lines must be closed, which is the equivalent of Kirchoff's Current Law. Following Figure 3-3, the two equations may be manipulated to yield Figure 3-4, which is the equivalent circuit model.

We start with Ampere's Law. Applying it to Figure 3-3 around the dashed contour yields

$$\int H \cdot \delta l = \iint J \cdot \delta s \tag{3.1}$$

$$H_c l_c + H_g l_g = Ni \tag{3.2}$$

$$\frac{B_c l_c}{\mu_c} + \frac{B_g l_g}{\mu_0} = Ni \tag{3.3}$$

Here, l_g is illustrated in the figure, and l_c is the path length through the core. Ni refers to a coil wrapped around the core with N turns and i current through each.

Then, assuming $\int B \cdot \delta s = 0$, or that flux is conserved around the loop,

$$\Phi = B_c A_c = B_g A_g \tag{3.4}$$

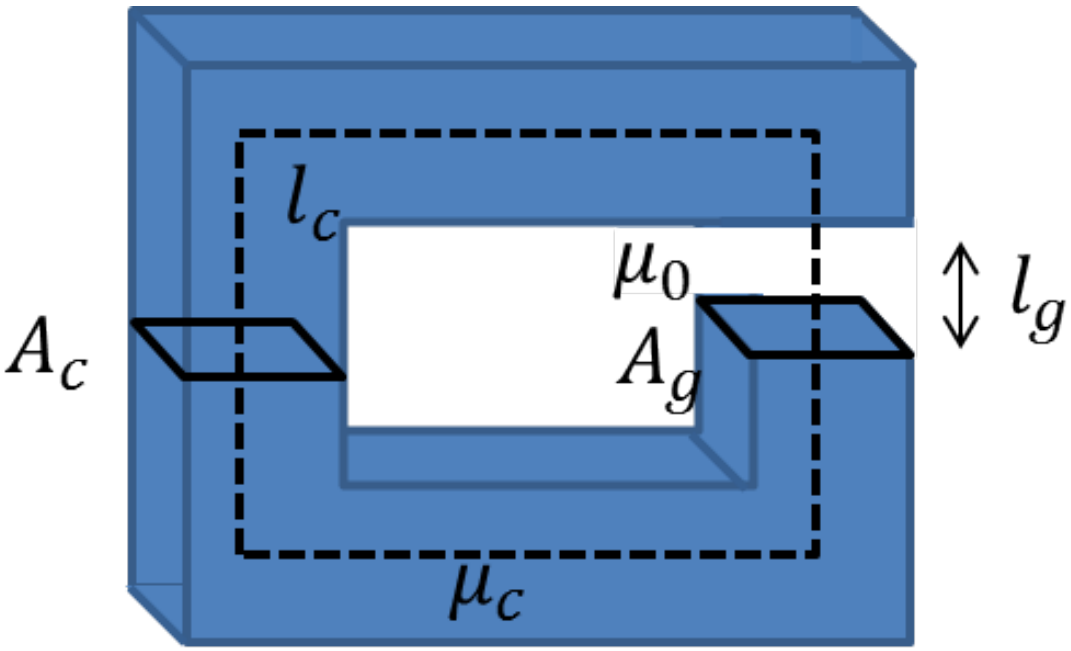

Figure 3-3: Flux tube model

Substituting Equation 3.3 in to Equation 3.4,

$$\Phi = \frac{Ni}{\frac{l_c}{\mu_c A_c} + \frac{l_g}{\mu_0 A_g}} \tag{3.5}$$

$$\Re_c = \frac{l_c}{\mu_c A_c} \tag{3.6}$$

$$\Re_g = \frac{l_g}{\mu_g A_g} \tag{3.7}$$

$$\Phi = \frac{Ni}{\Re_c + \Re_g} \tag{3.8}$$

This results in a quantity called reluctance that allows any segment of magnetic material to be treated as a resistor in a circuit model where current is analogous to magnetic flux and voltage is analogous to magnetomotive force. Equation 3.8 expresses the flux tube analysis as an electric circuit analog in which the magnetic flux Φ is analagous to current, the MMF drive Ni is analogous to voltage, and the reluctances $\Re$ are analogous to resistance. This curcuit analogy is further emphasized in Figure 3-4. A complicated structure of magnetic steel may then be analyzed as a network of resistors, each corresponding to a flux tube, or segment of steel that

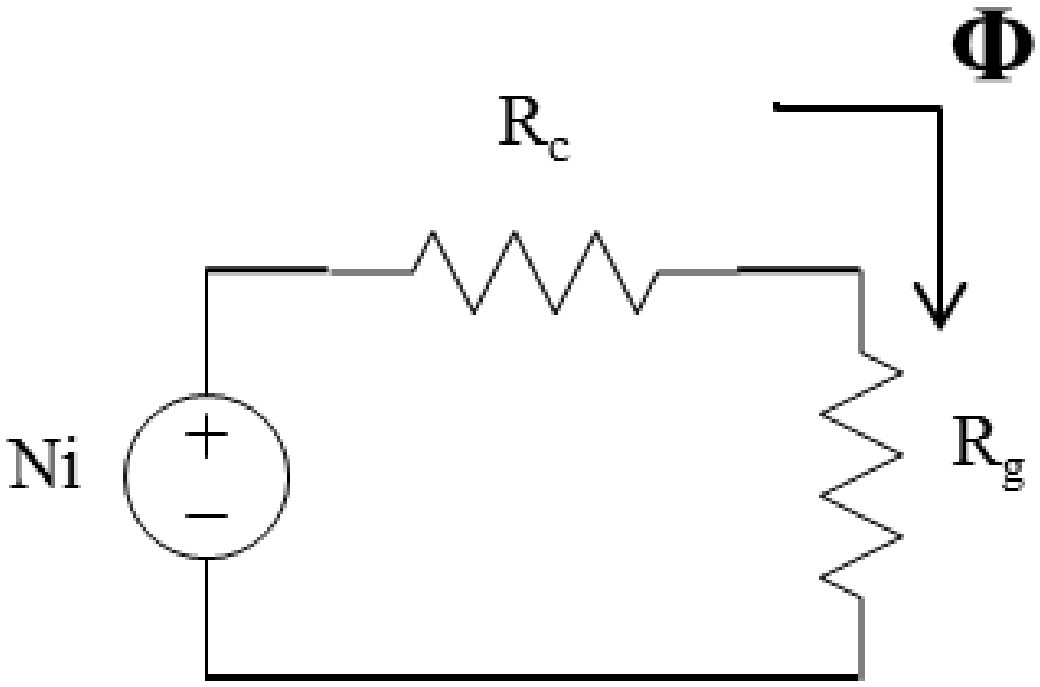

Figure 3-4: Flux tube model: circuit equivalent

confines flux. In the case of nonlinear materials, $\Re$ may be extended to become $\Re(\Phi)$ via a $\mu(H)$.

3.3 Materials and Issues

The materials used in an electric machine are often highly nonlinear, meaning that they saturate. Material data from a manufacturer is commonly given to the point where the incremental permeability drops to that of free space, μ_0. To use this data in a simulation, it may be extended in to the saturation region.

Given the importance of torque density to the robotic Cheetah, a steel with high permittivity is important. Hyperco 50, a trade name for Vanadium Permendur (material 2 in Figure 3-2) is commonly used for this purpose. The B-H curve for Hyperco 50 was obtained from Carpenter, a manufacturer of magnetic materials, and is included in Appendix C. It consists simply of B and H values for the steel of a specific lamination and annealing process of interest. This supplied data was given up to the

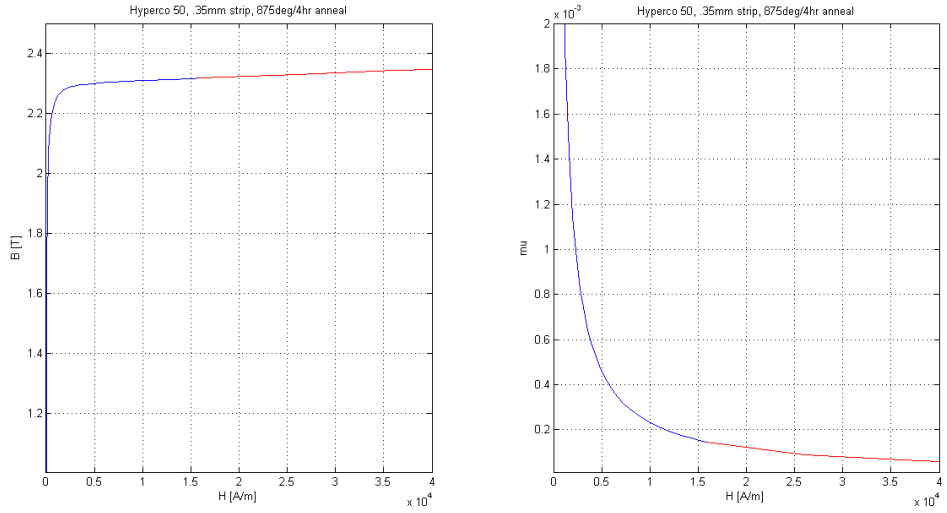

Figure 3-5: Extended B-H and absolute permeability curves. Blue is manufacturer data, and red is extended data assuming an incremental permeability of μ_0.

point of saturation, defined as the point where the incremental permittivity drops to μ_0. To allow a simulation to operate in the saturation region, this data was extended by assuming that the incremental permeability would remain at μ_0 indefinitely. Figure 3-5 shows the results of the extension of this data. It is important for convergence that these curves have a continuous first derivative in the transition region. Since the incremental permeability of the steel has dropped to that of free space at saturation, this line may be simply extended with a permeability of μ_0.

The alloy in question, Vanadium Permendur, is composed of approximately 48.75% Cobalt, 2% Vanadium, .4% Carbon, small quantities of Manganese and Silicon, and the balance Iron. Different alloying elements have various effects on the properties of the steel. Vanadium is often added to increase workability of the metal, as well as to increase its resistivity, thereby reducing eddy current losses. Figure 3-6 shows the effect of different alloying elements on the resistivity of the steel. Cobalt is added primarily to increase the saturation flux density of the material. Figure 3-7 shows this effect. The material is further processed into strips which are then machined and laminated, minimizing the cross section of any one strip, which minimizes eddy current losses. The material is then annealed to eliminate internal stresses, maximize the grain size, and eliminate impurities [27].

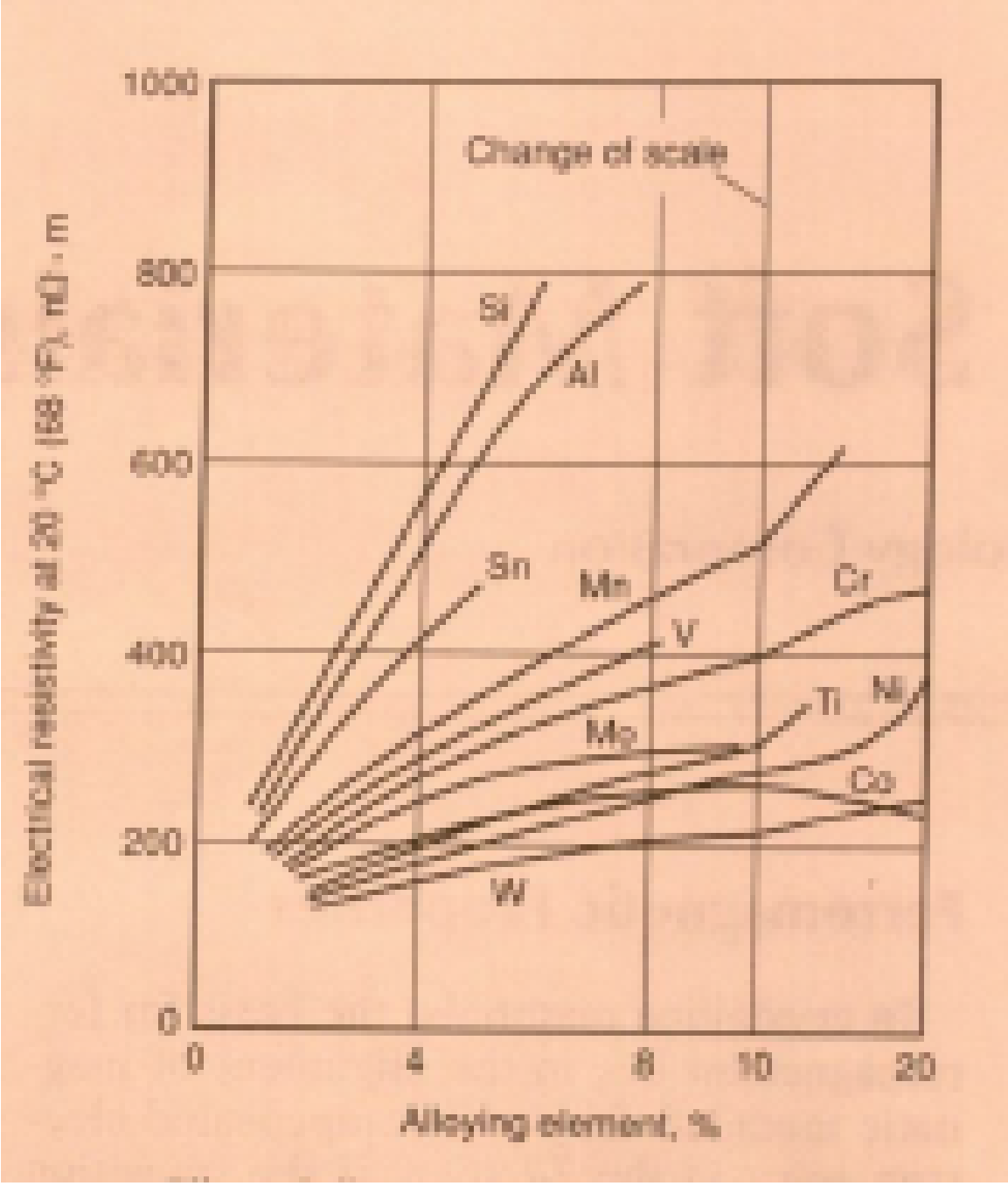

Figure 3-6: Effect of alloying elements on resistivity of steel [27]

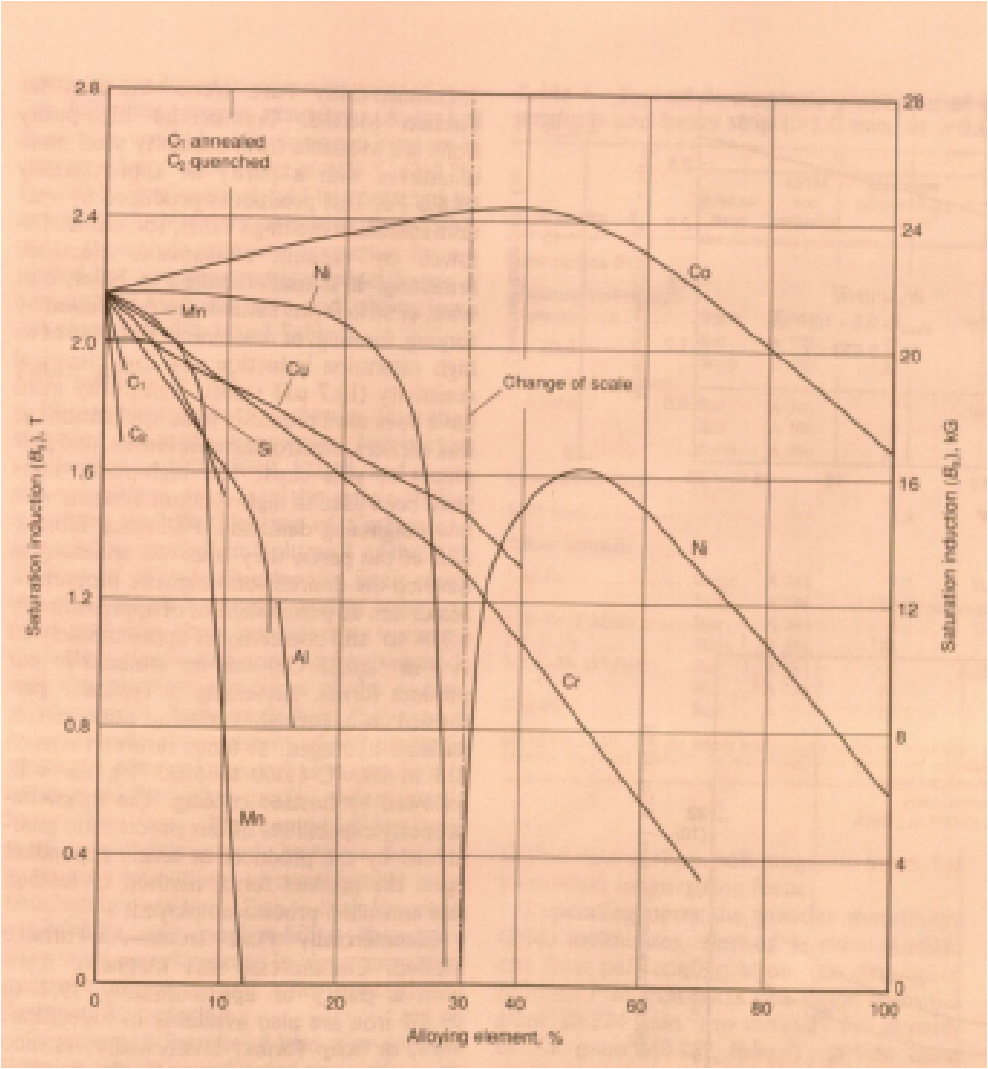

Figure 3-7: Effect of alloying elements on saturation flux density of steel [27]

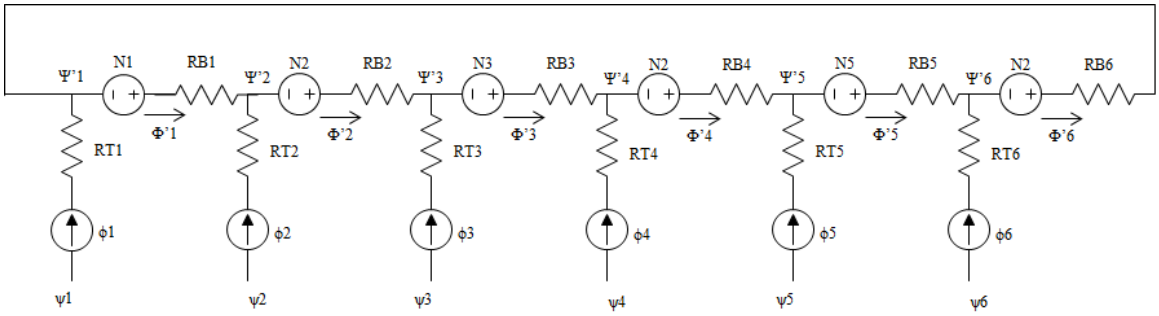

Figure 3-8: Flux tube model: circuit equivalent

The performance data (B-H curve) is used to determine the non-linear reluctances in the stator model. In the case of this particular simulation, a piecewise-linear interpolation is used. Each segment has a relationship, $MMF = \Re(\Phi) \times \Phi$, where $\Re = \frac{l}{\mu A}$ where l is the length of the segment and A is the cross-sectional area. The reluctances in the rest of this section are similarly nonlinear, but are not specifically written as such for simplicity.

3.4 Reluctance Models of an Electric Machine

In this section, the equations that govern the stator model are presented assuming a balanced 3-phase machine (3 teeth per pole, 6 per pole pair). Figure 3-8 shows the circuit model for the stator. ϕ_i is flux in stator tooth i. ϕ'_i is flux through backiron segment i. ψ_i is MMF at the surface of tooth i that faces the air gap, ψ'_i is MMF at the node at tooth-backiron intersection i, and N_i is the MMF contributed by slot winding i. Here, ϕ_i are the inputs from the model of Chapter 2 and ψ_i are outputs to the model of Chapter 2. Figure 3-9 shows an electric machine stator overlaid with the equivalent flux tube model.

It is assumed that each pole pair in the machine is identical, therefore there is a common node before the first tooth and after the sixth tooth in a 3ϕ machine. Equations 3.9 to 3.14 below govern the model's behavior. Following Figure 3-8, the node equations may be written. For simplicity, the equations for teeth 2-5 are omitted.

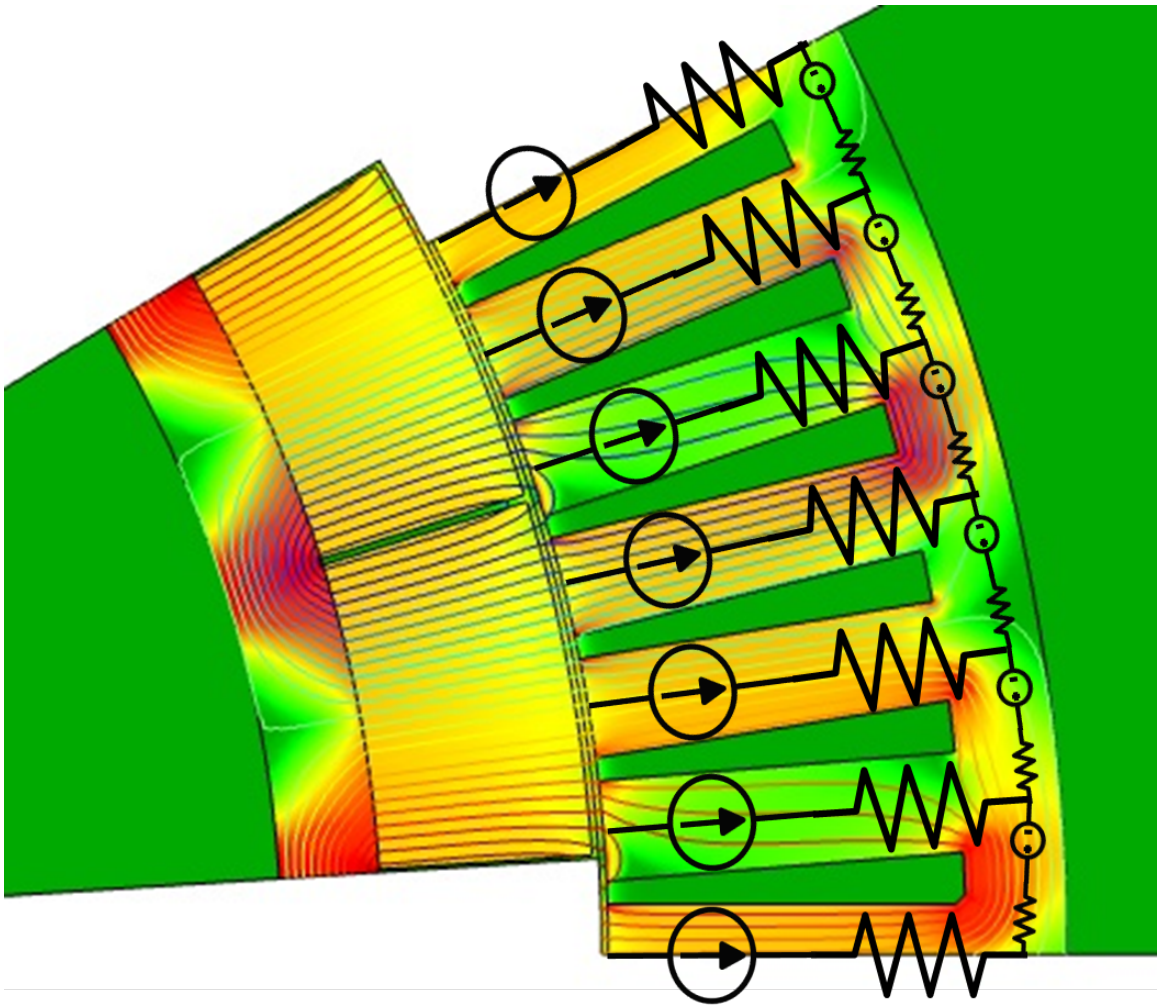

Figure 3-9: Electric machine stator overlaid with flux tube equivalent

$$\psi_1' = \psi_1 - R_{T1}\phi_1 \tag{3.9}$$

$$\psi_6' = \psi_6 - R_{T6}\phi_6 \tag{3.10}$$

$$\phi_1' = \frac{\psi_1' + N_1 - \psi_2'}{R_{B1}} \tag{3.11}$$

$$\phi_6' = \frac{\psi_6' + N_6 - \psi_1'}{R_{B6}} \tag{3.12}$$

$$\phi_1 = -\phi_6' + \phi_1' \tag{3.13}$$

$$\phi_6 = -\phi_5' + \phi_6' \tag{3.14}$$

where ψ is MMF, R is the non-linear reluctance associated with each segment (calculated from the piecewise-linear interpolation of the B-H curve discussed earlier), and ϕ is the flux in each segment.

Combining terms from Equations 3.9 to 3.14 and separating variables results in

$$\begin{aligned}
&\phi_1(1 + \frac{R_{T1}}{R_{B1}} + \frac{R_{T1}}{R_{B6}}) + \phi_2(-\frac{R_{T2}}{R_{B1}}) + \phi_6(-\frac{R_{T6}}{R_{B6}}) \\
&\quad + N_1(-\frac{1}{R_{B1}}) + N_6(\frac{1}{R_{B6}}) \\
&\quad = \psi_1(\frac{1}{R_{B1}} + \frac{1}{R_{B6}}) + \psi_2(-\frac{1}{R_{B1}}) + \psi_6(-\frac{1}{R_{B6}})
\end{aligned} \tag{3.15}$$

$$\begin{aligned}
&\phi_6(1 + \frac{R_{T6}}{R_{B6}} + \frac{R_{T6}}{R_{B5}}) + \phi_1(-\frac{R_{T1}}{R_{B6}}) + \phi_5(-\frac{R_{T5}}{R_{B5}}) \\
&\quad + N_5(\frac{1}{R_{B5}}) + N_6(-\frac{1}{R_{B6}}) \\
&\quad = \psi_6(\frac{1}{R_{B6}} + \frac{1}{R_{B5}}) + \psi_1(-\frac{1}{R_{B6}}) + \psi_5(-\frac{1}{R_{B5}})
\end{aligned} \tag{3.16}$$

Combining 3.15 and 3.16, as well as the omitted equations of the same form for the other teeth, results in matrix equation 3.17, which is, in symbolic form

$$
\begin{bmatrix}
(1+\frac{R_{T1}}{R_{B1}}+\frac{R_{T1}}{R_{B6}})-\frac{R_{T2}}{R_{B1}} & 0 & 0 & 0 & -\frac{R_{T6}}{R_{B6}} & \\
-\frac{R_{T1}}{R_{B1}} & (1+\frac{R_{T2}}{R_{B2}}+\frac{R_{T2}}{R_{B1}}) & -\frac{R_{T3}}{R_{B2}} & 0 & 0 & 0 \\
0 & -\frac{R_{T2}}{R_{B2}} & (1+\frac{R_{T3}}{R_{B3}}+\frac{R_{T3}}{R_{B2}}) & -\frac{R_{T4}}{R_{B3}} & 0 & 0 \\
0 & 0 & -\frac{R_{T3}}{R_{B3}} & (1+\frac{R_{T4}}{R_{B4}}+\frac{R_{T4}}{R_{B3}}) & -\frac{R_{T5}}{R_{B4}} & 0 \\
0 & 0 & 0 & -\frac{R_{T4}}{R_{B4}} & (1+\frac{R_{T5}}{R_{B5}}+\frac{R_{T5}}{R_{B4}}) & -\frac{R_{T6}}{R_{B5}} \\
-\frac{R_{T1}}{R_{B6}} & 0 & 0 & 0 & -\frac{R_{T5}}{R_{B5}} & (1+\frac{R_{T6}}{R_{B6}}+\frac{R_{T6}}{R_{B5}})
\end{bmatrix}
\begin{bmatrix}\phi_1\\ \phi_2\\ \phi_3\\ \phi_4\\ \phi_5\\ \phi_6\end{bmatrix}
$$

$$
+\begin{bmatrix}
-\frac{1}{R_{B1}} & 0 & 0 & 0 & 0 & \frac{1}{R_{B6}} \\
\frac{1}{R_{B1}} & -\frac{1}{R_{B2}} & 0 & 0 & 0 & 0 \\
0 & \frac{1}{R_{B1}} & -\frac{1}{R_{B2}} & 0 & 0 & 0 \\
0 & 0 & \frac{1}{R_{B1}} & -\frac{1}{R_{B2}} & 0 & 0 \\
0 & 0 & 0 & \frac{1}{R_{B1}} & -\frac{1}{R_{B2}} & 0 \\
0 & 0 & 0 & 0 & \frac{1}{R_{B1}} & -\frac{1}{R_{B2}}
\end{bmatrix}
\begin{bmatrix}N_1\\ N_2\\ N_3\\ N_4\\ N_5\\ N_6\end{bmatrix}
$$

$$
=\begin{bmatrix}
(\frac{1}{R_{B1}}+\frac{1}{R_{B6}})-\frac{1}{R_{B1}} & 0 & 0 & 0 & 0 & -\frac{1}{R_{B6}} \\
-\frac{1}{R_{B1}} & (\frac{1}{R_{B2}}+\frac{1}{R_{B1}}) & -\frac{1}{R_{B2}} & 0 & 0 & 0 \\
0 & -\frac{1}{R_{B2}} & (\frac{1}{R_{B3}}+\frac{1}{R_{B2}}) & -\frac{1}{R_{B3}} & 0 & 0 \\
0 & 0 & -\frac{1}{R_{B3}} & (\frac{1}{R_{B4}}+\frac{1}{R_{B3}}) & -\frac{1}{R_{B4}} & 0 \\
0 & 0 & 0 & -\frac{1}{R_{B4}} & (\frac{1}{R_{B5}}+\frac{1}{R_{B4}}) & -\frac{1}{R_{B5}} \\
-\frac{1}{R_{B6}} & 0 & 0 & 0 & -\frac{1}{R_{B5}} & (\frac{1}{R_{B6}}+\frac{1}{R_{B5}})
\end{bmatrix}
\begin{bmatrix}\psi_1\\ \psi_2\\ \psi_3\\ \psi_4\\ \psi_5\\ \psi_6\end{bmatrix}
\tag{3.17}
$$

$$A_{flux}(\phi)\phi + A_{source}(\phi)N = A_{mmf}(\phi)\psi \tag{3.18}$$

This equation relates the tooth tip MMFs (ψ) to the contributions from the windings (N_i) and the fluxes (ϕ_i) from the continuum model. The equation is solved for the tooth tip MMFs, and that solution is used as an input to the continuum model discussed in Chapter 2. Specifically, these MMFs are used to determine the fields at the boundary between the stator and airgap or the flux-tube and continuum models, which are defined by coefficients A_m and B_m in Chapter 2 and are seen on lines 273-274 in the code in Appendix A, where they are called $A_{sf}(mm)$ and $B_{sf}(mm)$.

As written, the matrices are singular, as the MMFs (ψ) may have an arbitrary offset. The system is ungrounded, so it needs a reference to have a unique solution. To allow the system to be solved, it is assumed that the average of the MMFs is 0. Since only the relative values of MMF at the face of each tooth are important, the reference may be arbitrarily set. This involves setting the first row of A_{mmf} to ones and the first row of A_{source} and A_{flux} to zeros. This result is implemented on lines 148-174 in Appendix A.

Additionally, the reluctances in the model are nonlinear, displaying saturation behavior as shown in Figure 3-5. For this reason, a model as presented in this section must be solved iteratively. After each iteration, a new reluctance for each segment may be calculated based on the flux, ϕ through it. The solution is iterated until the values of flux in each segment converge.

3.5 Simplifications to Flux-Tube Stator Model Based on Convergence Direction

The equations governing the flux tube stator, and that relate fluxes and magnetomotive forces through and on each segment, may be solved iteratively. This results in a model that contains an iteration inside an iteration, as 3.17 is not a linear equation

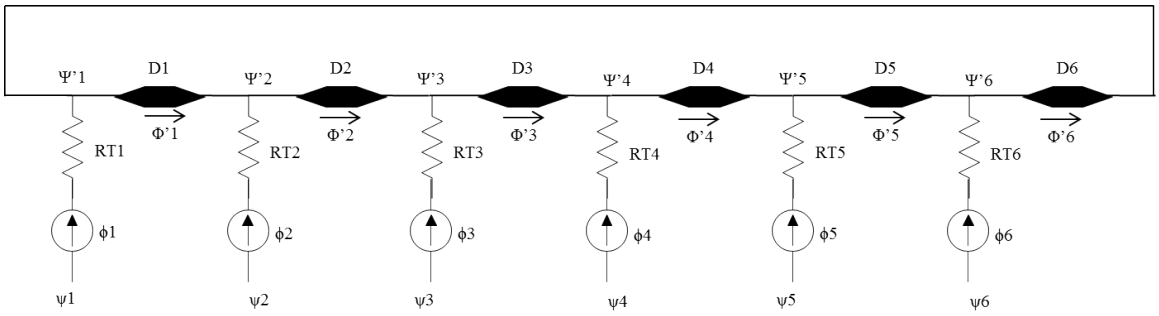

Figure 3-10: Flux tube model: circuit equivalent with backiron simplification

(all of the reluctances are nonlinear), resulting in a longer run time.

As will be explained in Chapter 4, the flux-tube model takes fluxes into each tooth as an input and outputs MMF on each tooth tip. Combining this with the spatial periodicity of the field solution and the physical structure, useful simplifications can be made, resulting in an explicit solution without iteration.

For the moment, we will consider Figure 3-10. The reluctance and MMF contribution of each element of the backiron have been replaced with a generalized parameter, D_i. D_i relates $(\Psi'_{i+1} - \Psi'_i)$ to ϕ'_i

Given the fluxes in each tooth (each input to the flux-tube model) and assuming symmetry in the rotor backiron elements, D_i, the fluxes are defined without having to iterate to solve the flux tube model. In this section, again, calculations are performed for a 3-phase machine.

When imposing a flux value upon each tooth (the input to the flux-tube model), the reluctances of each tooth may be immediately solved. Because of the assumed periodicity of the field solution in the motor gap region, one may assume that the fluxes are symmetric, such that

$$\phi_1 = -\phi_4 \tag{3.19}$$

$$\phi_2 = -\phi_5 \tag{3.20}$$

$$\phi_3 = -\phi_6 \tag{3.21}$$

Further, assuming symmetry in the backiron fluxes, ϕ'_1 to ϕ'_6,

$$\phi'_1 = -\phi'_4 \tag{3.22}$$

$$\phi'_2 = -\phi'_5 \tag{3.23}$$

$$\phi'_3 = -\phi'_6 \tag{3.24}$$

Note that this symmetry assumes that there is no circulating flux in the rotor backiron segments (D_1 to D_6).

Then, calculate fluxes in the backiron, ϕ'_i

$$\phi'_1 = \phi'_6 + \phi_1 \tag{3.25}$$

$$\phi'_2 = \phi'_1 + \phi_2 \tag{3.26}$$

$$\phi'_3 = \phi'_2 + \phi_3 \tag{3.27}$$

Substitute 3.22 to 3.24, and we obtain ϕ' without the need to iterate. The backiron fluxes are then uniquely determined by tooth fluxes when they are symmetric.

$$\phi'_1 = \frac{1}{2}(\phi_1 - \phi_2 - \phi_3) \tag{3.28}$$

$$\phi'_2 = \frac{1}{2}(\phi_1 + \phi_2 - \phi_3) \tag{3.29}$$

$$\phi'_3 = \frac{1}{2}(\phi_1 + \phi_2 + \phi_3) \tag{3.30}$$

This result is implemented as shown on lines 128-133 in Appendix A.

The MMF sources, or stator windings must then be examined. The previous calculations showed that in the absence of a loop current, backiron fluxes, ϕ'_i, are uniquely determined by tooth fluxes, ϕ_i. Now, assume D_i is equal to $R_{Bi}(\phi'_i) + N_i$. Figure 3-10 becomes 3-8. Figure 3-11 shows the contributions of MMF sources to loop flux, as this is the only component of backiron flux, ϕ'_i undefined by the tooth

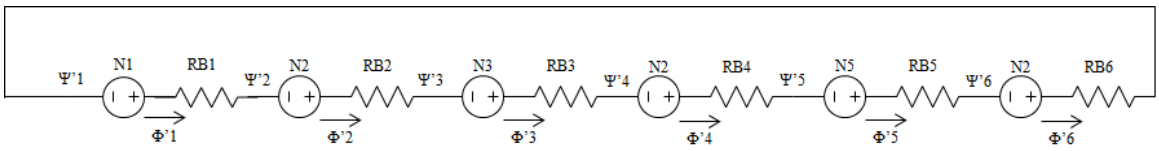

Figure 3-11: Flux tube model with current sources neglected

fluxes, ϕ_i. Loop flux is then simple to calculate. $\phi = \frac{\sum N_i}{\sum R_{Bi}}$, or the sum of the MMFs from the windings divided by the sum of the reluctances in the backiron. When the windings are balanced, $N_4 = -N_1$, $N_5 = -N_2$, $N_6 = -N_3$. Therefore $\sum N = 0$ and $\phi'_i = 0$. The windings may only drive flux in a loop around the stator backiron, but their balanced nature makes this impossible.

Periodicity of the fields in the motor gap obviates the need for iteration in the flux tube model. Additionally it means that only half of the flux tube model need be solved to form the complete solution.

Since the fluxes are solved immediately due to the single path through the network of reluctances, the value of the reluctances may be interpolated from the material data. The tooth MMFs may then be solved with Equation 3.17.

This result is implemented on lines 148-174 in Appendix A, though the code has not been rewritten to fully take advantage of the simplified calculation of tooth MMFs beyond not iterating.

3.6 Core Loss

Core loss may be easily calculated from the flux tube model. Core loss for a given material depends on both the maximum flux density value seen in a cycle and the frequency of the excitation. It is normally modeled as an imaginary component to the reluctance of each segment, but in this case, where core losses are small compared to electrical losses, it may be calculated afterwards, knowing the flux densities in each segment and their frequency.

The fluxes in the machine move around each pole pair with a frequency corresponding to the electrical frequency of the drive. This results in a periodic flux

distribution that repeats in time and space during each commutation period. After the fields are solved for a single commutation window, all of the information needed to calculate core loss in the machine is known. Since each segment will cycle through the values computed in one step, the maximum seen in each type of segment (tooth or backiron segment) may be assumed to be the maximum in a commutation window, thereby defining core loss.

Core loss may be interpolated from a manufacturer's data sheet or calculated from a curve fit to this data. For silicon iron, an exponential fit of the form, $P \approx P_0 \left(\frac{B}{B_0}\right)^{\epsilon_B} \left(\frac{f}{f_0}\right)^{\epsilon_F}$ has been shown [25].

Both the core loss and B-H data for Hyperco 50 may be found in Appendix D.

3.7 Summary

This chapter has derived the equations used for solving the flux tube model that represents the stator. The flux tube model takes radial fluxes from the continuum model as an input and outputs MMFs at each tooth tip. The reluctances in the flux tube model are nonlinear, but an assumption about the symmetry of the fluxes in the teeth and balanced windings, coupled with the preferred direction of iteration discussed in Chapter 4 allows this nonlinear problem to be solved without iteration.

Chapter 4

Solvers

4.1 Operation

An iterative solver is required due to the non-linear nature of the steel in the machine. In both the stator and the rotor core, the permeability of the steel changes with changes in flux.

To begin, the motor physical parameters are used to determine the sizes of each of the segments of the stator flux tube model. The magnet parameters are used to set the parameters that go in to the Maxwell continuum model. The model is started by assuming an input to the flux tube model. Given the magnetic materials in question, a 1T flux density that follows the placement of the magnets is assumed, meaning that 1T is assumed in the proper direction in each tooth, unless the boundary between oppositely-polarized magnets sits on a tooth, in which case, zero flux is assumed. The flux tube model is then run with the integral of the flux densities across each tooth. Implementation may be seen on lines 88-89 and 94-99 of Appendix A.

The output of the flux tube model is the integral of the magnetic field across the gap between teeth, or the magnetomotive force on each tooth. The continuum solution of Maxwell's equations shown in Chapter 2 is fed with these values Through coefficients $A_{sf}(mm)$ and $B_{sf}(mm)$ on lines 273-274 of Appendix A. The tangential field at the surface of the stator is decomposed into its Fourier components, and each harmonic is used to solve for 12 parameters that determine the field solution for that

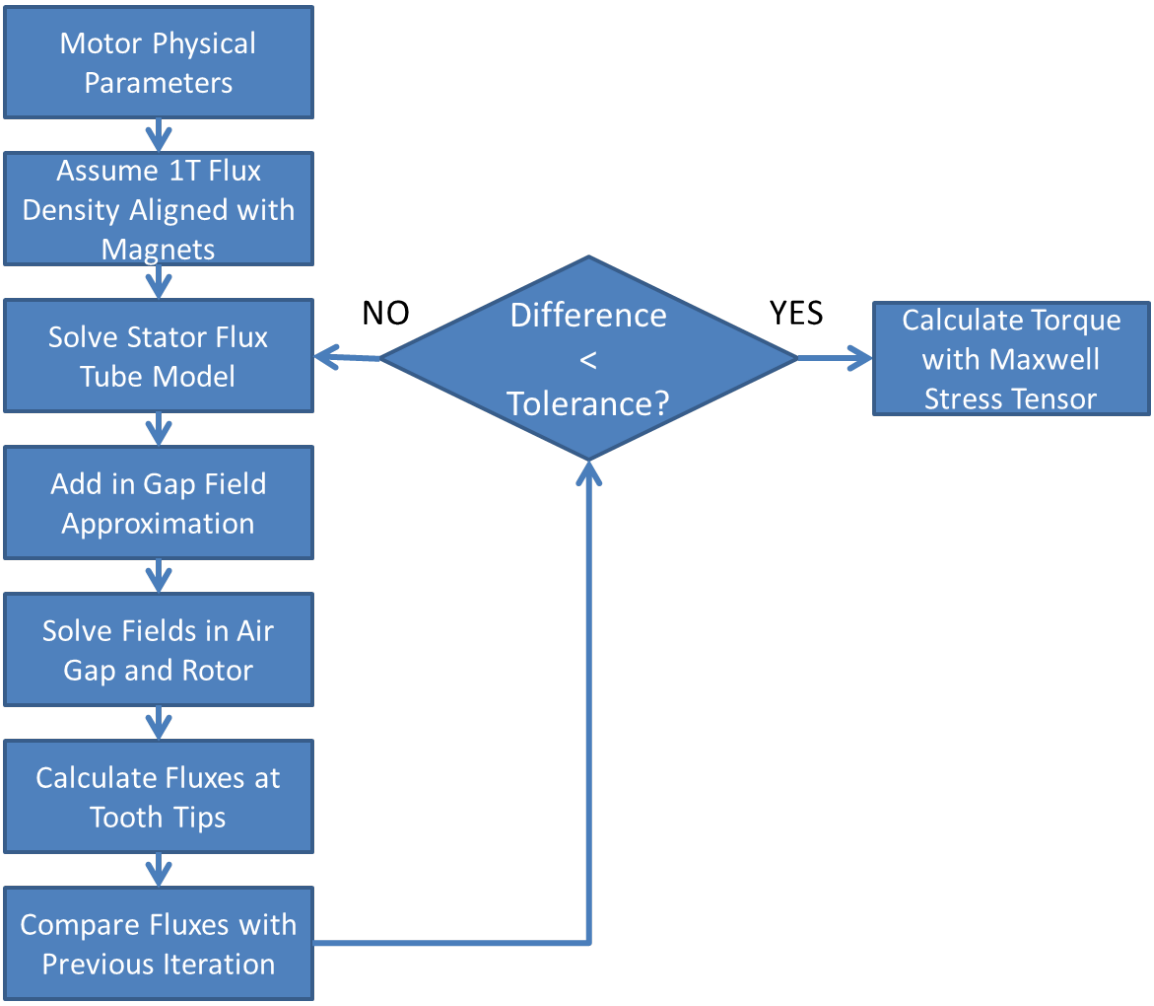

Figure 4-1: Flowchart showing iteration process

harmonic (lines 256 to 287). Once each harmonic of interest is solved, the radial fields are integrated over each tooth to find the fluxes in each tooth (lines 291-294) . These values are compared to the previous fluxes(lines 306-307), and once the difference is smaller than a pre-set value, the simulation is considered to have converged. Torque is then calculated with the Maxwell Stress Tensor (lines 317-329). Figure 4-1 shows the operation of the simulation.

4.2 Convergence

Iteration between the flux-tube and continuum models is effectively equivalent to matching a linear source with a nonlinear load. Figure 4-2 illustrates this process.

The source line, representing the magnets, is shown by the line with the negative slope. Its slope is increased to more easily illustrate the process. The stator, rotor backiron, and air gap, are represented by the nonlinear line. A solution is found by picking either an H or B value for one of the two models, tracing it to its intersection on one of the lines, then tracing it to the opposite line in a direction perpendicular to the first trace. This process continues until the point at which the two curves intersect. In this situation, picking B or H as a starting point on one of the two lines will cause the solution to either converge or diverge, resulting in an inward or outward spiral.

This analogy is a bit simplistic in that it does not address the fact that this solution exists on a spatial continuum. The solution exists between two models that are pinned together at six discrete points, and magnetic flux moves as the solution at each point converges.

In Figure 4-2, the line denoted by the green dashed line shows an example of convergence and the red dotted line an example of divergence when the operating point is solved iteratively. The dashed line begins with a value of B, traces it horizontally to the load line, obtains a value of H and traces it vertically to the source line, and continues until it converges on the intersection point. This may be explained by the fact that the load line has a negative second derivative in the region of interest. Because of the magnetic properties of the steel in the stator, the load line will not have a slope approaching that of the load line until the steel has heavily saturated. Given that the two models may take tangential H or radial B as an input or output, his observation suggests that the flux tube model should have radial B (integrated to form flux in each tooth) as an input and tangential H as an output.

4.3 Core μ

The core is the only piece of the continuum solution that may not be modeled as a linear material. For this reason, it is treated the same as the different segments in the stator. Unfortunately, the flux paths are not as spatially defined, so a continuum

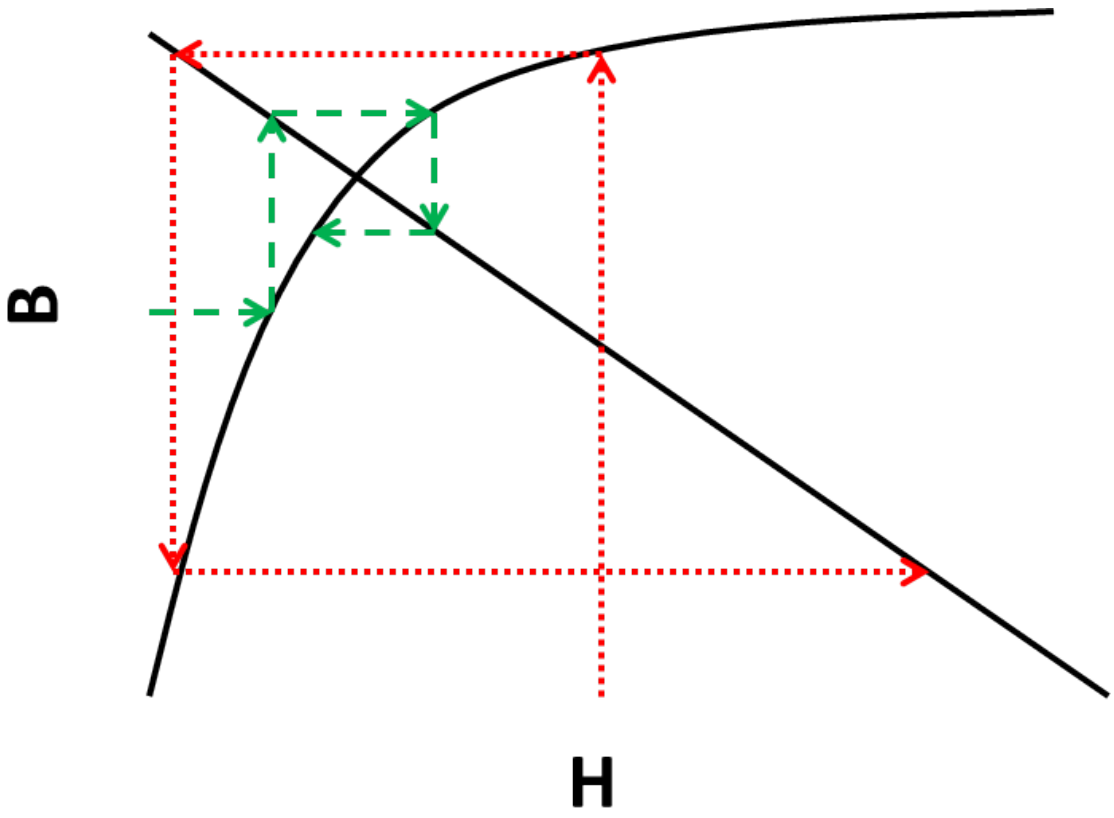

Figure 4-2: Illustration of convergence as linear source and nonlinear load

solution is still appropriate. To consider nonlinearity in the material, the maximum flux density at the centerline of the rotor is calculated, and the permeability is calculated based on this value. To aid the simulation in converging, the solutions are weighted according to:

$$\mu_c = \alpha\mu_{ck} + (1-\alpha)\,\mu_{ck-1}$$

So long as care is taken to appropriately size the core for the flux through the magnets, its permeability has relatively little effect on the performance of the machine. Even at the point where incremental permeability of the steel approaches μ_0, the total permeability is still approximately $92\mu_0$. Given that the magnets have an effective permeability of μ_0, the reluctance of the airgap and magnets dominates the reluctance of the total flux path in the continuum model. Rotor core flux must be checked for reasonable values.

4.4 Saturation

As described, the model does not, and cannot converge in areas of heavy saturation. The reason may be most easily seen graphically. In Figure 4-3, Figure 4-2 has been modified to show a solution in a place where the nonlinear load line has a slope matching that of the linear source line. In this case, the solution will not converge, as it will indefinitely follow the same rectangle.

There are several ways of dealing with this phenomenon, the simplest being an accelerating factor. The solver then takes the form

$$A_n = \alpha A_{n-1} + (1-\alpha)\,A_{n-2}$$

where A is the solution, and alpha is a value close to 1. By doing this, the solutions are artificially forced inward on a spiral to convergence.

Alternately, a 'method of relaxation' [28] may be used. With this method, the permeability of the stator core is scaled. To begin, it is scaled by a large factor, the

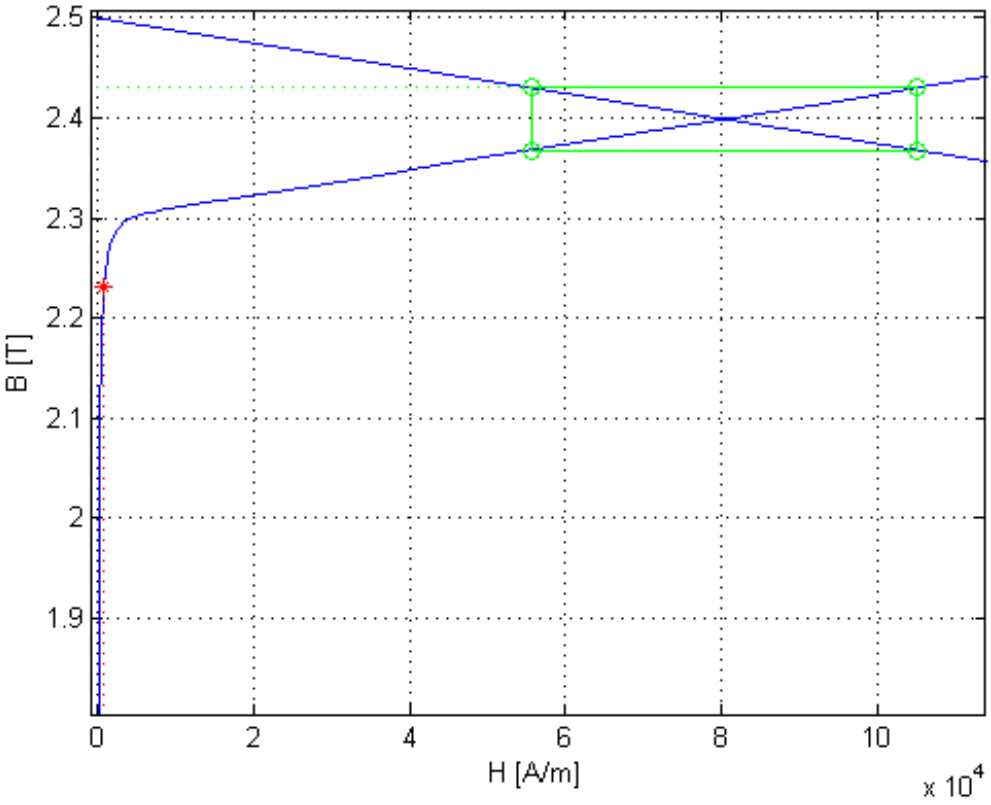

Figure 4-3: Illustration of convergence process in the case of saturation

model is allowed to converge, the factor is reduced, and the model is run again. In this manner, combined with the accelerating factor, the solution is walked down the source line to its eventual convergence.

Unfortunately, in this case, the basic premise of the flux tube model is broken. In areas of heavy saturation, the steel no longer effectively confines the flux. The model will produce a solution in these cases, but it will assume that flux is still confined to the stator, and results in greater torque than would otherwise be produced.

4.5 Performance

Figure 4-4 shows the computation performance of the simulation. In this example, which is one run of the drive current optimizer detailed in 9, the simulation is called 390639 times in 3568 seconds, for a run time of 0.009 seconds per point. In this run, interp1, a native MATLAB interpolation function, which is called twice per run, is called 5924758 times, meaning that the simulation is converging in an average of 7.58 iterations. Since this particular test is run on a machine that is not forced into heavy saturation, the method of relaxation is not used, allowing a faster computation time. The method of relaxation would be used to force convergence in a region of heavy saturation.

To compare with Comsol, the same simulation was run, but the program was commanded to stop at certain numbers of iterations. The results of these tests may be seen in Appendix E. To converge, Comsol required an average of 77-100 iterations for a total of 80-112 seconds. The solution is not within 10% of the eventual solution until approximately 85 iterations and 70-80 seconds.

4.6 Summary

When the models are combined in an iterative solver, they reliably converge in most cases. The solutions (fluxes in each stator tooth) spiral in to an operating point very quickly, usually in 6-8 iterations. When the machine is forced in to operating

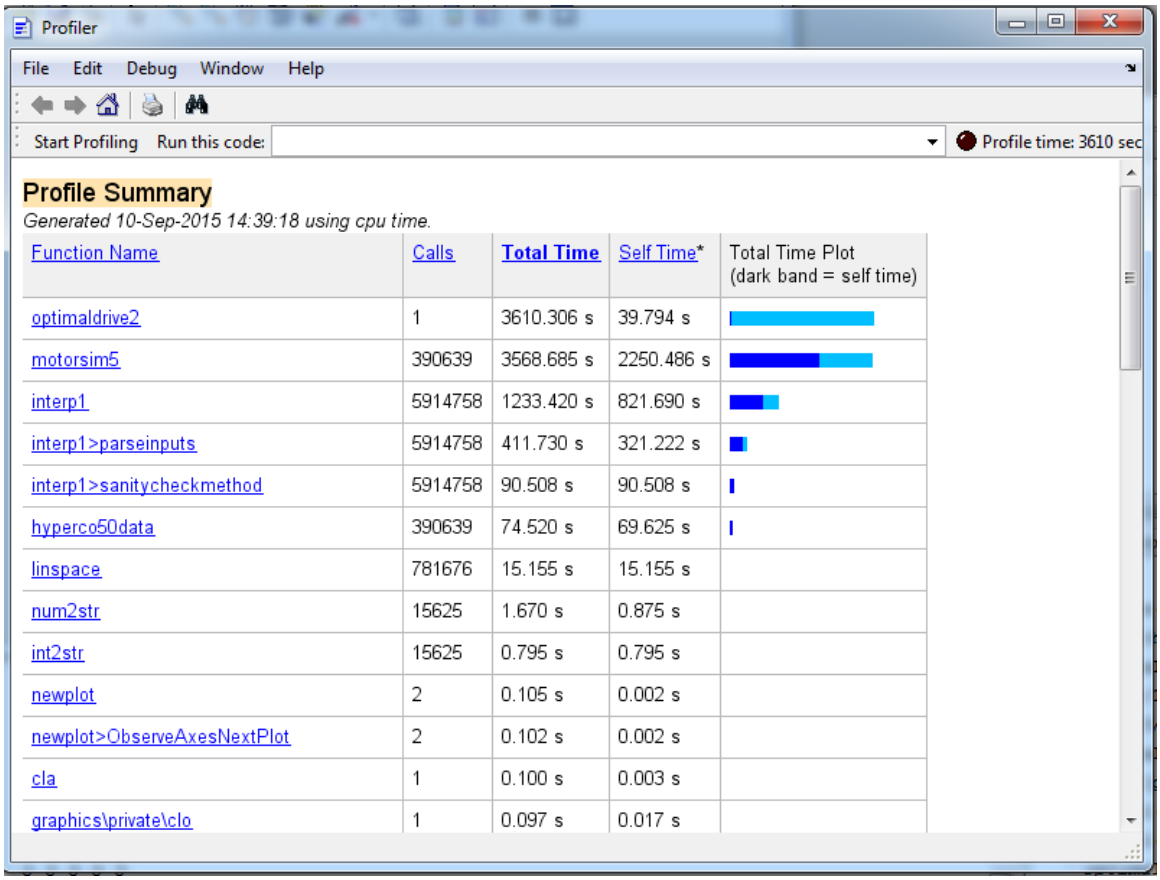

Figure 4-4: MATLAB's profiler result showing simulation time

regions where much of the machine is saturated, iterative factors or more intensive techniques may be used to force the simulation to converge, though some fundamental assumptions about the flux-tube model are no longer valid. In reasonable (not heavily saturated) regions of operation, the simulation can be expected to converge four orders of magnitude faster than an equivalent Comsol 2-D finite element simulation on the same computer hardware.

Chapter 5

Cogging Torque and Reduction Techniques

Reducing cogging torque is a primary goal in research into permanent-magnet synchronous machines. Cogging torque refers to the tendency for the rotor to preferentially align with the stator in certain positions due to slots in the stator in the absence of winding excitation. When the windings are driven, it contributes to torque ripple. These slots create paths of varying reluctance as a function of position, resulting in differing energy stored as a function of position. The derivative of this stored energy is torque. In most applications, this torque is undesirable, as it makes position control difficult, introduces mechanical vibrations, and in some cases, causes audible noise.

This may be reduced in many different ways. Magnets may be spaced, or dithered, in such a manner that they cancel harmonics of cogging [29]. They may also be short-pitched or the corners may be rounded. Each of these techniques will have some adverse effect on motive torque [30].

5.1 Non-commensurate poles

A common technique used to eliminate cogging torque is to design a machine with a different number of magnets and teeth in the stator. To do this, windings must be distributed in a way that allows fluxes to be driven at the spatial frequency of the

rotor. This type of machine may also be modeled with a model similar to the one presented in Chapters 2, 3, and 4. This would involve modeling the machine as a single pole pair and changing the fourier components associated with the magnetization.

5.2 Skew

Skew is the act of twisting either the rotor or stator of the machine. The idea is that the interaction between the rotor and stator will averaged about lamination-like slices of the machine.

For a first pass, imagine a rotor split in the radial plain, consisting of two sets of magnets. Each of these rotors, if installed in the stator, would produce a cogging torque waveform of the same form as the complete rotor, with approximately half the amplitude. If the two rotors were installed, but rotated slightly, it stands to reason that one could calculate the cogging torque waveform by superimposing the two cogging waveforms from each half. By varying the rotation between the two sets of magnets, the fundamental, or any individual harmonic of the cogging torque waveform could be eliminated.

The same process could be repeated for two, three, or infinitely many slices of the rotor. In the limit as the number of slices approaches infinity, all of the harmonics of the torque waveform may be eliminated. This process is fundamentally a convolution in space with a box corresponding to the extent of the skew. This box in angular space becomes a sinc in spatial frequency.

The effects of a full-pitch skew may be seen in figure 5-1. For a 3-phase machine with one slot per phase, the fundamental cogging harmonic is the 6^{th} harmonic. Note that a full-pitch skew (one tooth width) puts the first zero of the sinc at the 6th harmonic. It will cancel the 6^{th}, 12^{th}, 18^{th} and so on. Notice that it also affects the motive torque production, or the fundamental frequency corresponding to a pole pair. In the case of the full-pitch skew on a three-phase machine, this causes a 4.5% reduction in the torque production of the machine.

Skew may be accomplished with either a skewed stator or a skewed magnet. The

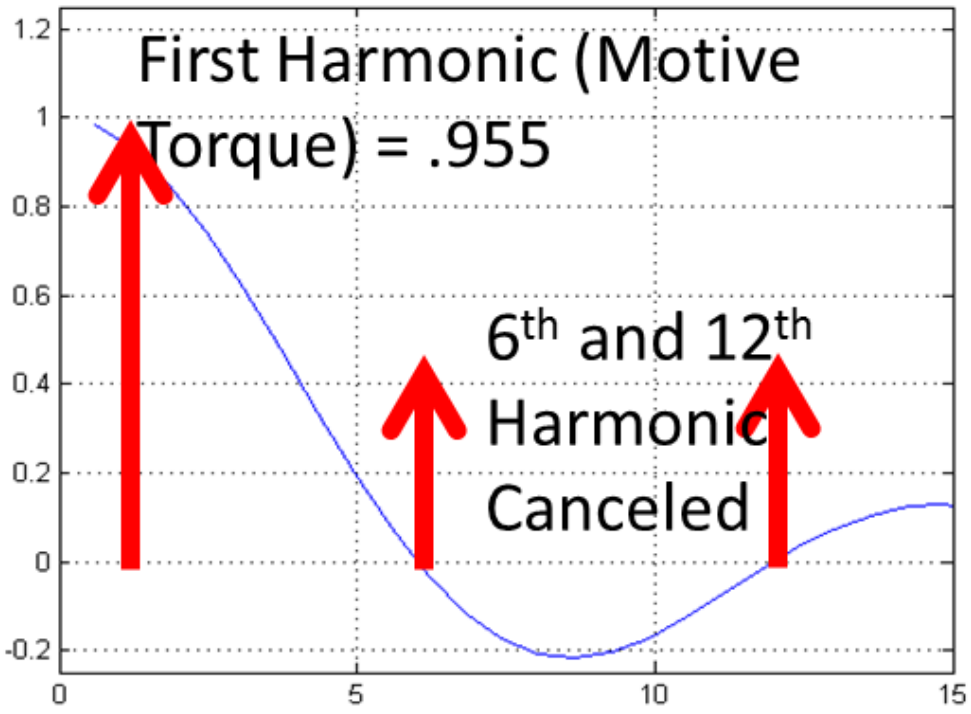

Figure 5-1: Sinc function in spatial harmonics as a result of skew

convolution process is unaffected by the choice.

Skewing of the stator is theoretically simple in terms of construction, as the stator is made of thin laminations of steel. These laminations may simply be twisted before being stacked and glued. In practice, this is difficult. Laminations have other features cut in them, such as keyways or other alignment features. This strategy would then require unique laminations, and would require keeping track of them during the stacking process. Additionally, skewing the stator reduces the cross-sectional area of the slot by the cosine of the angle of the skew and lengthens the wire in the slot by the inverse of the cosine of the angle. These increase losses.

Magnets may also be skewed. In a surface-mounted permanent magnet machine, this means that the magnets will be helically-cut, resulting in complicated geometries. Ne-Fe-B magnets are sintered, so odd shapes are not an issue once the mold is built, and it does not further complicate construction. Spacing the magnets is, however, difficult, as spacers must be precisely cut to hold proper alignment. Figure 5-2 shows the completed rotor with skewed magnets.

5.2.1 Experiments

Several skewed stators and one skewed rotor were built to test these concepts and reduce cogging torque in the Cheetah machines. Both the rotor and stator were skewed one full tooth pitch, meaning that they should eliminate all harmonics of the cogging waveforms. In practice, fringing fields around the outside of the machine and axial misalignment of the rotor result in residual cogging torque. Figure 5-3 shows the results of these efforts, compared to the original straight rotor/stator machines. Cogging torque was reduced to approximately 10% of the original cogging amplitude.

Additionally, Motive torque measurements were made on the skewed stator machines, as they needed to be calibrated for use on the robot. Figure 5-4 shows the comparison of measured data between the two machines. As expected, cogging torque is drastically reduced. Motive torque is expected to be reduced by 4.5%, and this test shows approximately a 3% reduction in amplitude.

The data also allows a comparison with the convolution explanation. Figures 5-5

Figure 5-2: Skewed magnets in rotor

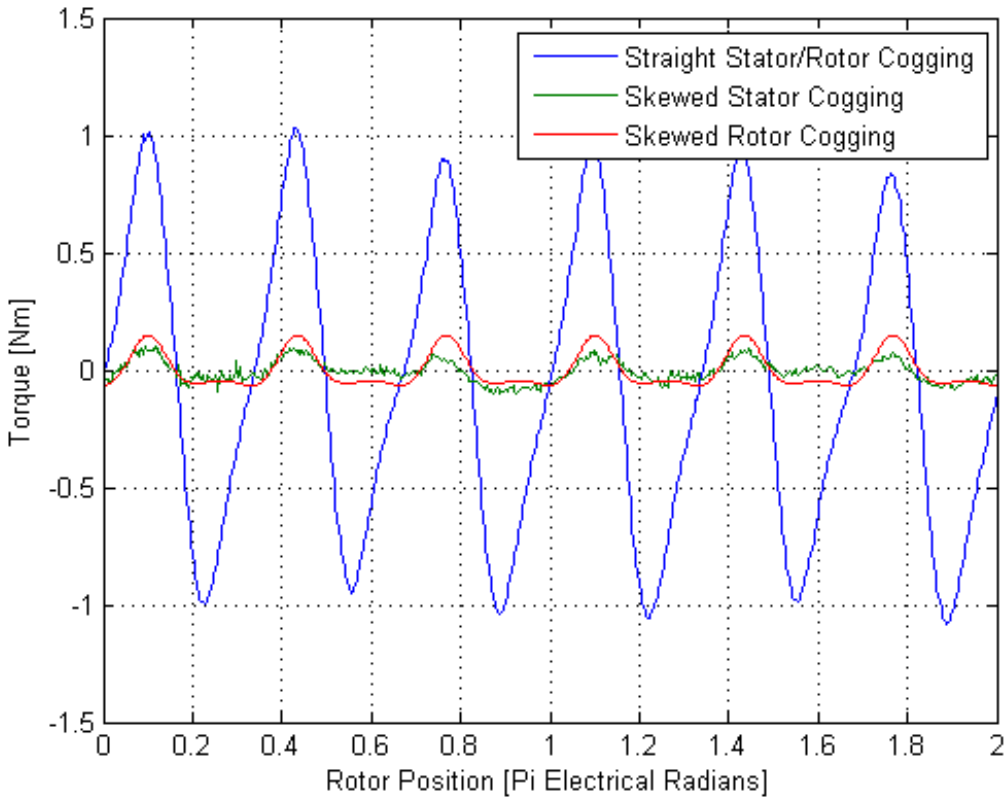

Figure 5-3: Comparison of cogging torque in a straight rotor/stator, a skewed rotor, and a skewed stator

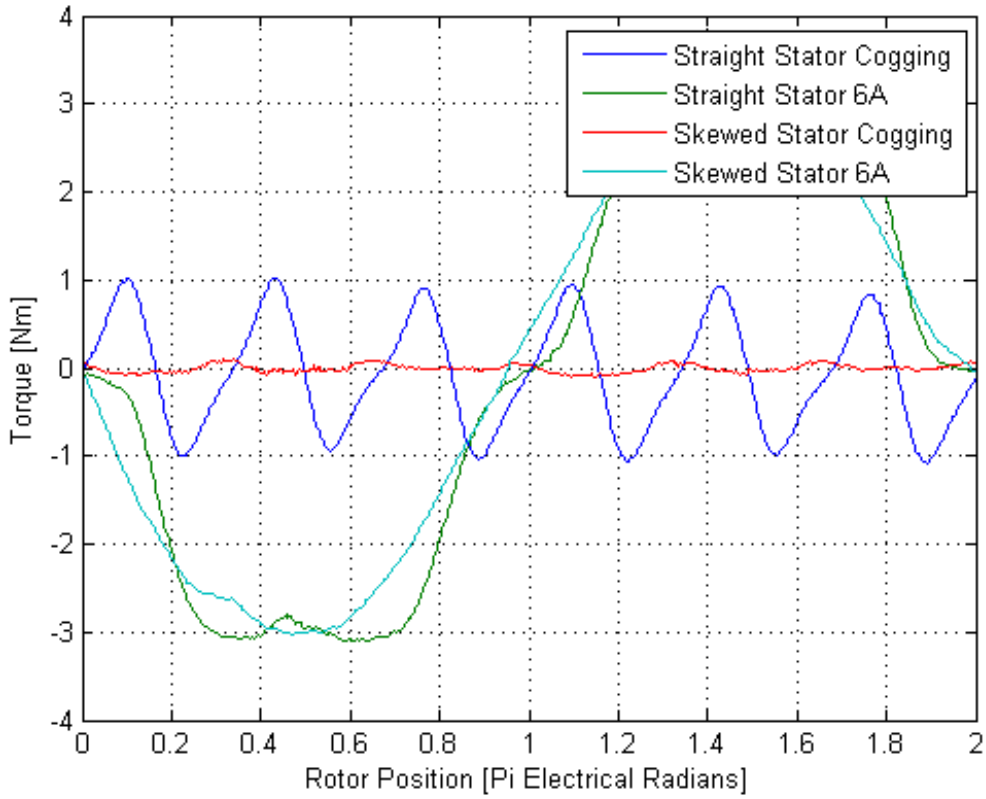

Figure 5-4: Skewed stator compared with straight rotor/stator

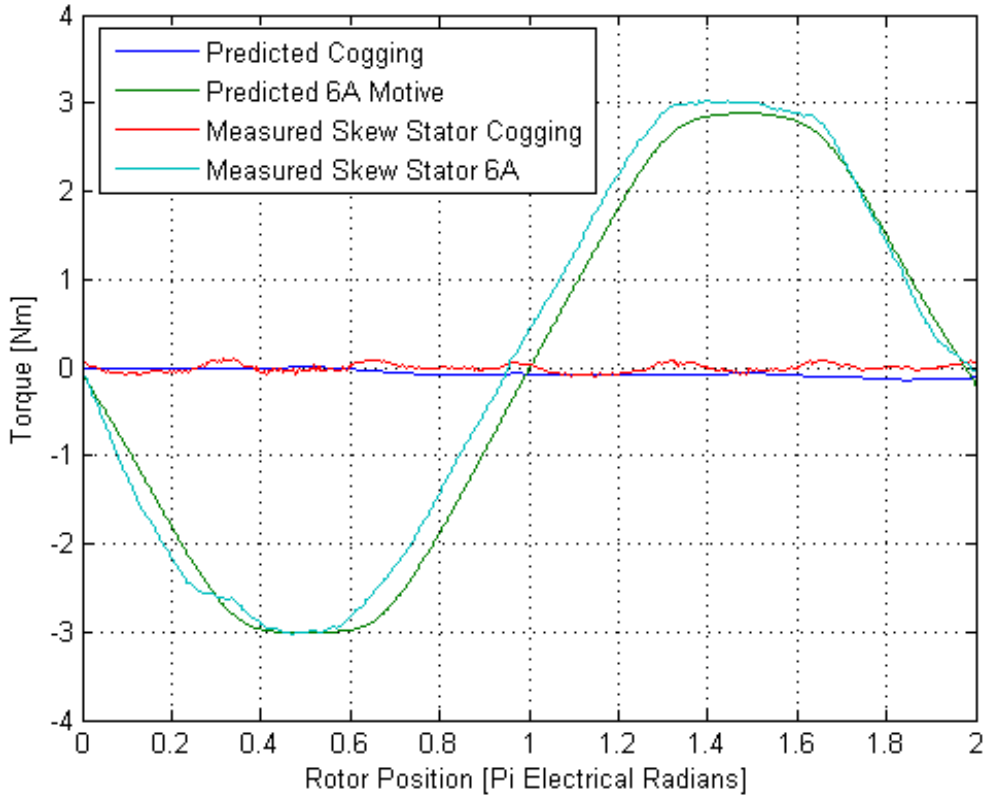

Figure 5-5: Skewed stator measurement compared with prediction

and 5-6 show measured data plotted with the convolution of a box and the original torque measurements on the straight rotor/stator machine.

In both machines, the magnets are slightly wider than the stators. In the skewed stator machine, this means that we expect to see a slight contribution from the fringing fields.

In the skewed rotor machine, a wider rotor than stator means that the effective skew is shorter than a full tooth pitch. To match the data in Figure 5-6, a $\frac{14}{16}$ tooth pitch skew is assumed, along with a contribution from the fringing fields. The asymmetric torque waveform seen here is a consequence of the axial misalignment and the differing interactions of the fringing fields at the edges of the machines. This was recreated by placing a dirac delta in the convolution waveform to represent the interaction of the fringing fields. Effectively, the original torque data is convolved with a box and a dirac delta function on one end corresponding to approximately 20% of

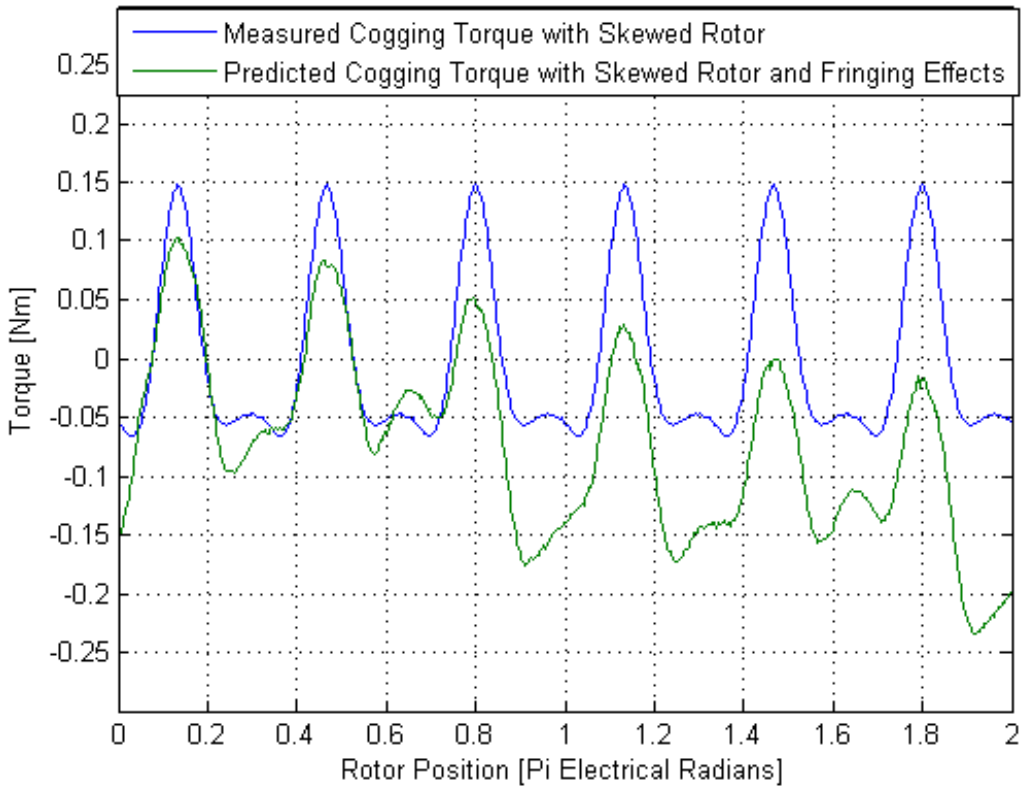

Figure 5-6: Skewed rotor measurement compared with prediction

the area under the box. To obtain these numbers, it would require an axial rotor misalignment of approximately 1.5 mm, which was not measured before the machine was disassembled.

5.2.2 Fringing fields and alternately-shaped magnets

Building on the work in the previous sections, specifically the explanation of skew as a spatial convolution, one can do interesting things with the shape of the magnet. With care in designing the magnet shape, one can make the magnet insensitive to axial misalignment and fringing fields. Fringing fields are shown in Figure 5-7. In the same manner as the split rotor described in a previous section, one harmonic of the cogging waveform may be canceled with control of the two endpoints. If the edges of the magnet are spaced a half-tooth-pitch apart, as in the case of the split rotor, the

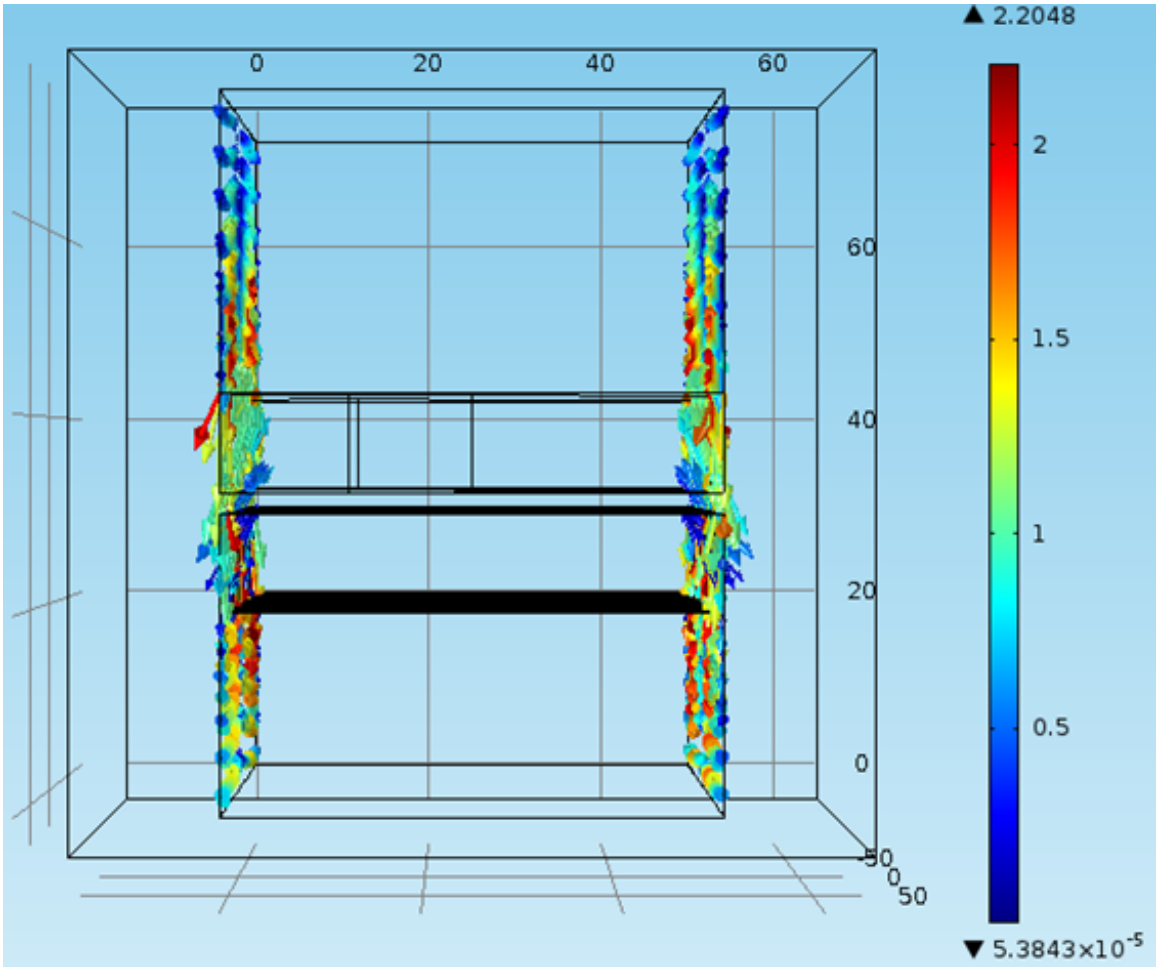

Figure 5-7: FEA analysis showing fringing fields at edge of machine

fundamental cogging harmonic produced by the fringing fields should be canceled.

It is possible to design a magnet, by rearranging the infinitesimal slices of a skewed magnet, that retains the properties of convolving the box in space, but leaves the edges a half-pitch apart. Two such arrangements are shown in figure 5-8.

These magnet shapes were evaluated in a 3-D FEA simulation of a cartoon stator. The straight magnets, skewed magnets, and the shape shown on the right in Figure 5-8 were evaluated with the magnet edges placed at the edge of a tooth. The force in the three cases was 700 N, 70 N, and 20 N, respectively. A full-pitch skew eliminates 90% of cogging torque in this geometry. Intelligently rearranging the magnet reduces this residual cogging by a further 60%, or to 3% of the original cogging torque.

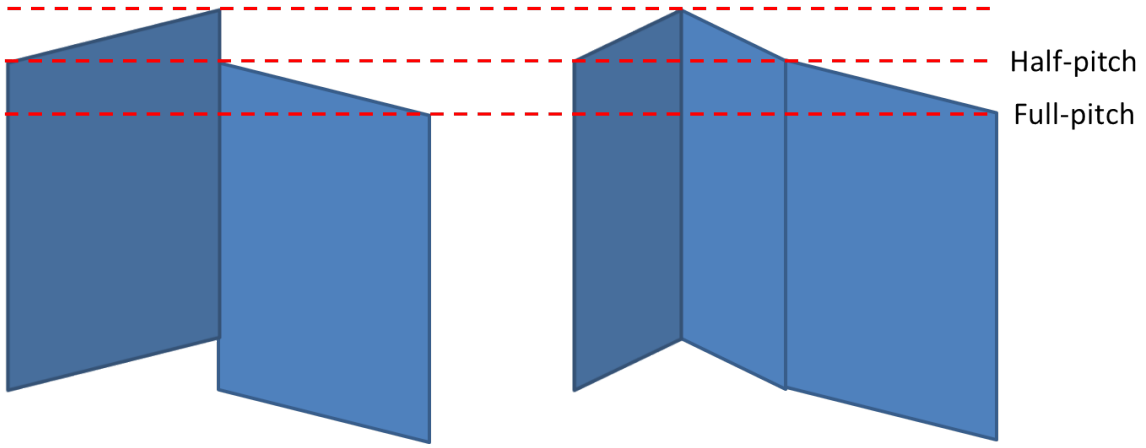

Figure 5-8: Proposed magnet shapes for eliminating cogging torque as a result of fringing fields and axial misalignment

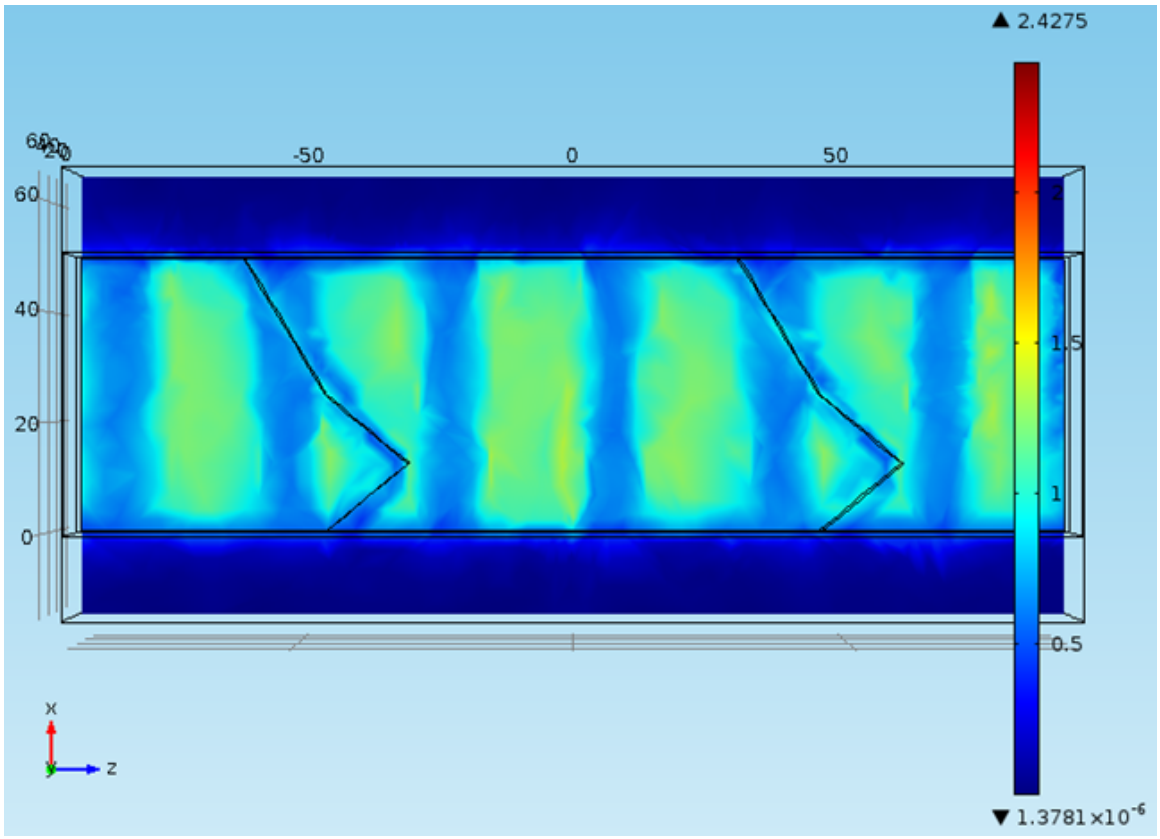

Figure 5-9: Flux density in airgap of shaped magnet linear machine

5.3 Summary

This chapter has introduced the concept of skewing both the rotor and stator of a machine. Stators are commonly skewed in production machines, and rotors are often skewed in AC machines. Skewed magnets are less common. Both techniques were constructed and resulted in machines with negligible cogging torque. The spatial filter concept was extended to magnet shapes that controlled fringing fields in meaningful ways to further eliminate cogging, and was demonstrated in FEA analysis.

In the Cheetah, decreased cogging torque allows for more precise control of the position of the limbs. At speed, cogging torque is not as noticeable. Removing it does, however, reduce mechanical vibration. Skewed magnets are clearly easier from a construction point of view and have less effect on performance, as they do not affect the area or length of the windings.

Chapter 6

Experimental Verification of Materials and Previous Machines

6.1 Hyperco50 Characterization

To anchor the modeling efforts, the assumption of the material characteristics required verification. For this purpose, a transformer was constructed with a spare rotor core. In such an arrangement, a primary winding is used to drive flux in the core, and the voltage is measured on an open secondary winding. Flux is then the integral of this voltage. Magnetic field, or H, is determined by the number of turns in the primary, the current flowing through them, and the dimensions of the core. With knowledge of both the flux, BA_c (magnetic flux density times the area of the core), and these other dimensions, μ, or the permeability of the material may be determined. The resulting plot of B and H should match that given by the manufacturer. Calculations performed to determine the required current and number of windings may be see in Table 6.1.

For the second attempt, the edges of the core were first wrapped in kapton tape. This is shown in Figure 6-1. All four edges were completely covered in two layers of tape before being again wrapped with electrical tape. This was then covered with insulation stripped from a large, multi-conductor cable, which was then affixed to the core with electrical tape. This is shown in Figure 6-2. The primary winding was

Bmax	T	2.32	
Hmax	A/m	20000	
mu at saturation	-	1.169E-4	
relative mu	-	92.31	
ID	mm	72.4	
OD	mm	83.8	
thickness	mm	11.3	
circumference	mm	45.4	
core length	mm	245.358	
-	m	0.245358	
core area	mm$\hat{2}$	64.44	
-	m$\hat{2}$	6.44E-5	
N1	160		
N2	39		
flux	Wb	1.49-4	
reluctance	-	32838976.90	
energy	J	0.3666	
Inductance	H	7.801E-4	
Current	A	30.67	
primary wire length	mm	7264	
frequency	hz	59.88	
-	rad/s	376.237	
Volts/turn	V	5.62E-2	
Vout	-	2.19	

Table 6.1: Design of transformer used to characterize core material. Experiment is designed to hit the B-H point shown in the first two lines of the table.

Figure 6-1: Kapton

wrapped around the core in two layers, separated by another layer of electrical tape. Figure 6-3 shows the core before the addition of the second layer of windings.

To drive the primary of the transformer with 30 A requires a drastic stepdown from line voltage. A variable autotransformer, shown in Figure 6-4 is used to do this. The transformer was placed between two phases of the variac. To measure current, a current sense resistor of 0.1Ω was placed in series with the transformer. A floating voltage probe was used to measure voltage on either side of the resistor to obtain current. Another voltage probe was used to measure voltage on the secondary winding. These connections may be seen in figure 6-5.

To trigger the oscilloscope, the trigger was set to 3.5V on a rising edge on channel 1, which corresponds to a current of 35A through the 0.1Ω resistor, and the scope was places in 'single sequence' mode to record a set amount of time after the it is triggered. Figure 6-6 shows the waveforms recorded on the oscilloscope. The yellow

Figure 6-2: Rubber insulation taken from large 4-conductor cable

Figure 6-3: Wire wrapped around protected core

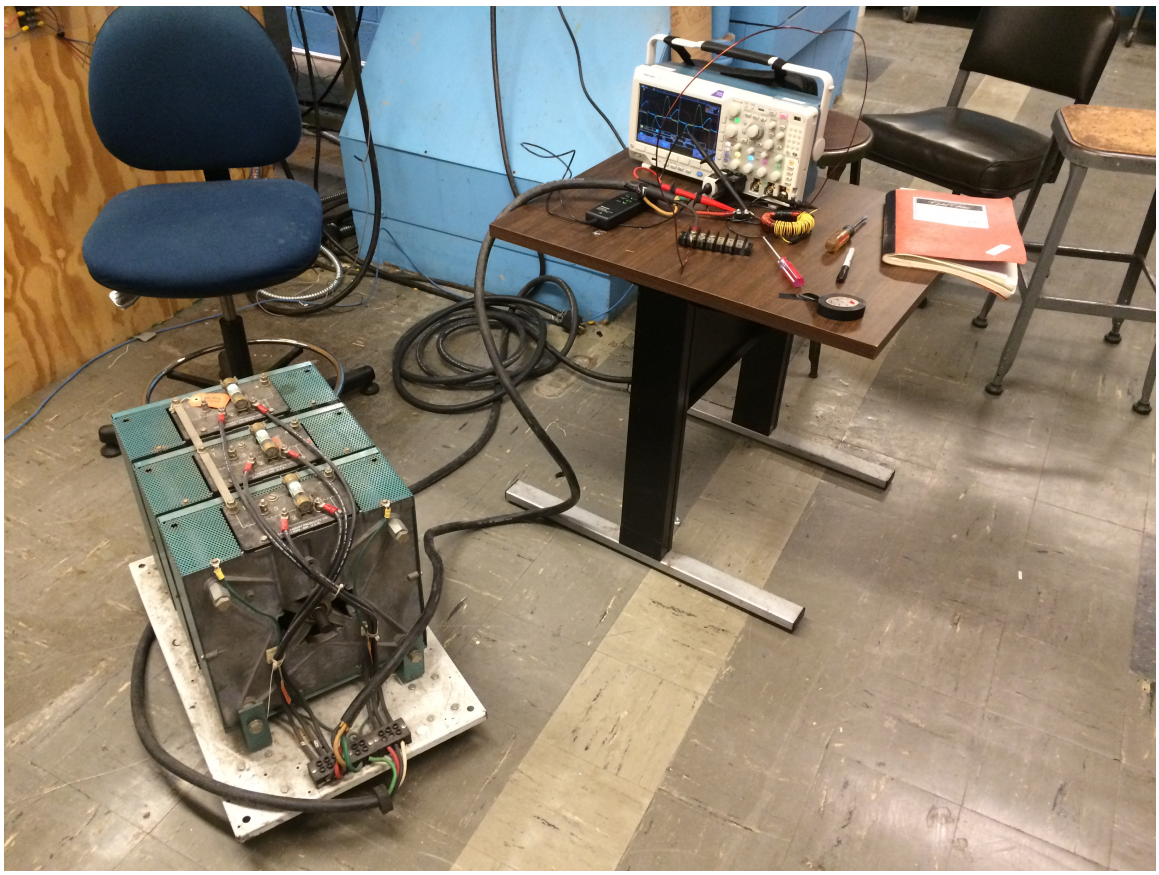

Figure 6-4: Variac used to drive experimental setup

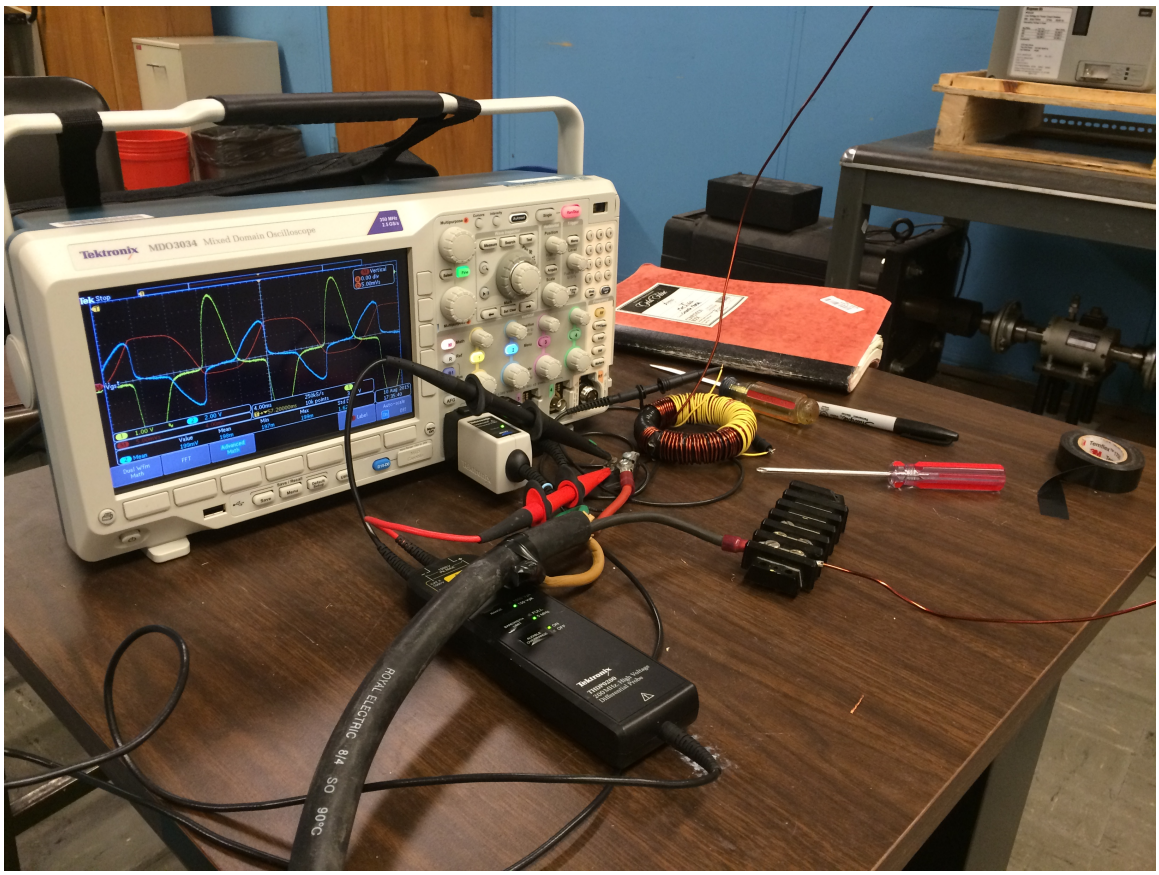

Figure 6-5: Materials characterization setup

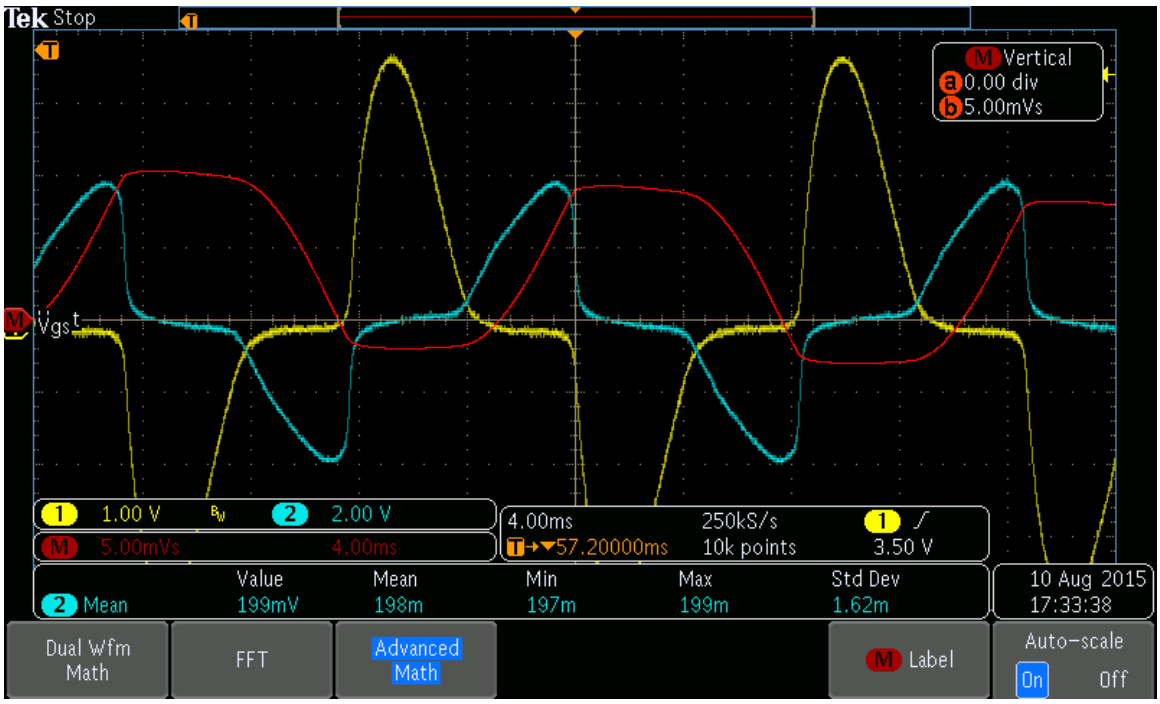

Figure 6-6: Scope trace showing primary current (yellow), secondary voltage (blue), and the integral of secondary voltage, or flux (red)

trace is the current in the primary (scaled by the 0.1Ω resistor), and the blue trace is the voltage on the secondary. The red waveform is the integral of the secondary voltage, or flux, plus an offset determined by where the integration was started in the cycle. Figure 6-7 shows an x-y plot of primary current and secondary voltage over several cycles.

When this data was processed, it resulted in Figure 6-8. The material in question matches the manufacturers data well into the saturation region, but has lower permeability in the region before heavy saturation. Practically, this will result in less flux in the machine in areas that are not driven hard, but the regions that are driven hard should be modeled appropriately.

For the design and optimization of the machine shown in Chapter 7, the manufacturer's data was used. The spare rotor core used for this testing was unavailable prior to the delivery of the machine designed around the data.

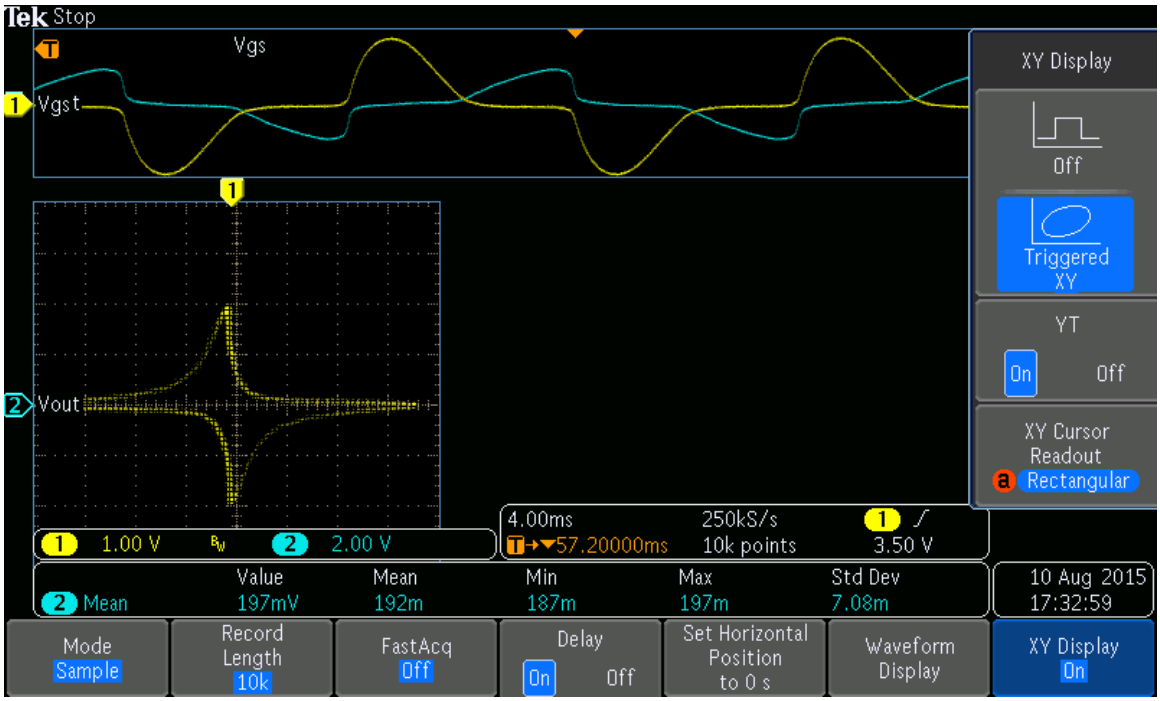

Figure 6-7: Scope trace showing primary current (yellow), secondary voltage (blue), and the 2-D trace of primary current vs secondary voltage

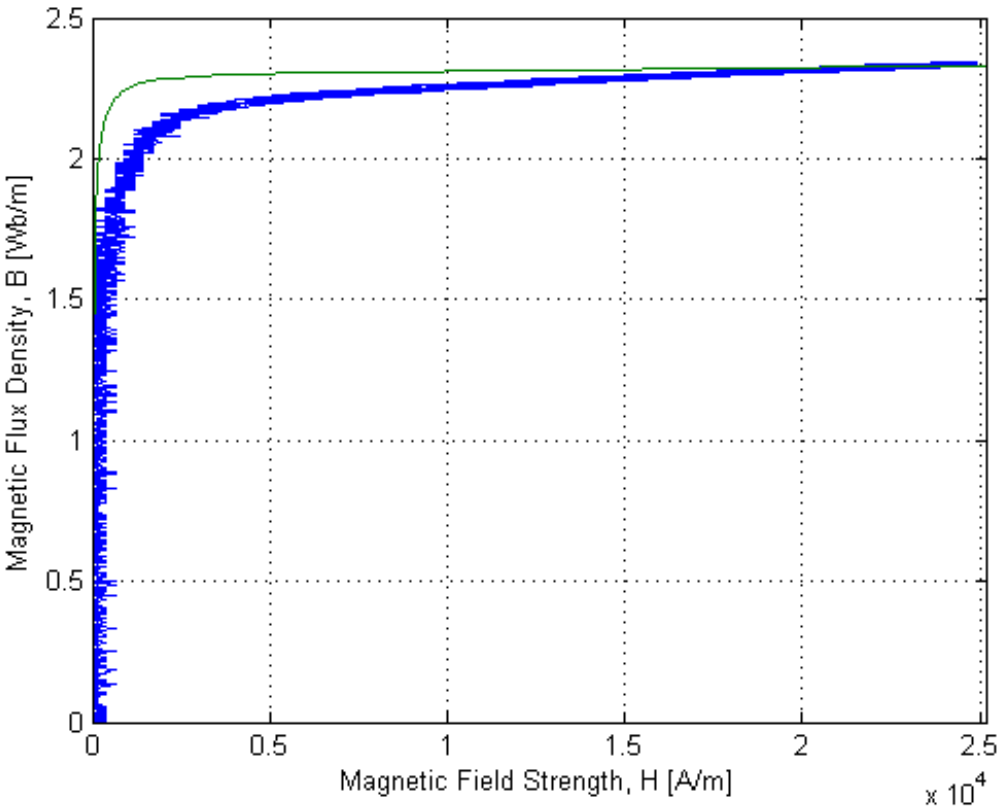

Figure 6-8: BH Curve. Green line shows manufacturer data, blue line shows measured data.

6.2 Validation of Model with Generation 2 Cheetah Motor

Simulation data was compared with a motor that has been previously built for the cheetah. Figure 6-9 shows the match between the model (asterisks) and the measured data (solid lines). For this experiment, the machine was driven with current into phase A and out of phase C with 6 A and 15 A. At 15 A, the machine has begun to heavily saturate individual teeth. The machine was rotated through the angular displacement corresponding to a single pole, and force at the end of a lever arm was recorded. This force was translated to torque by multiplying by the length of the lever arm. This setup is more fully described in Chapter 8.

The result is as near of a match as can be expected. To obtain the plot, the gap width of the teeth has been modified slightly. In the physical motor, the slots get narrower at the very tip of the teeth (the tooth gets wider). Local saturation changes the torque characteristic slightly in these regions. To account for this difference, half of the width of the slot closure is assumed to saturate, and is removed. This has the effect of increasing the magnitude of the cogging waveform slightly. Given that a tooth makes up a large fraction of the tooth pitch, adjusting the width of the pieces that close the slots has a minimal effect on performance.

The measured motor was designed and built to power the MIT Biomimetics Lab's robotic Cheetah. The machine uses a 13-pole-pair, 3-phase architecture and takes advantage of high permeability, high flux density steel [19]. A picture is shown in Figure 6-10. There are 8 such motors on the robot, powering the shoulder and knee joints. Specific torque, torque density, and efficiency are important design parameters [1]. To properly drive the motor, its torque characteristics have been extensively analyzed.

Figure 6-11 shows the radial and tangential fields corresponding to the first sixteen spatial harmonics. This captures the 6th and 12th harmonic corresponding to the first two harmonics of the cogging torque. Figure 6-12 shows the simulated field lines in the areas of the machine represented by the explicit maxwell solutions. This figure

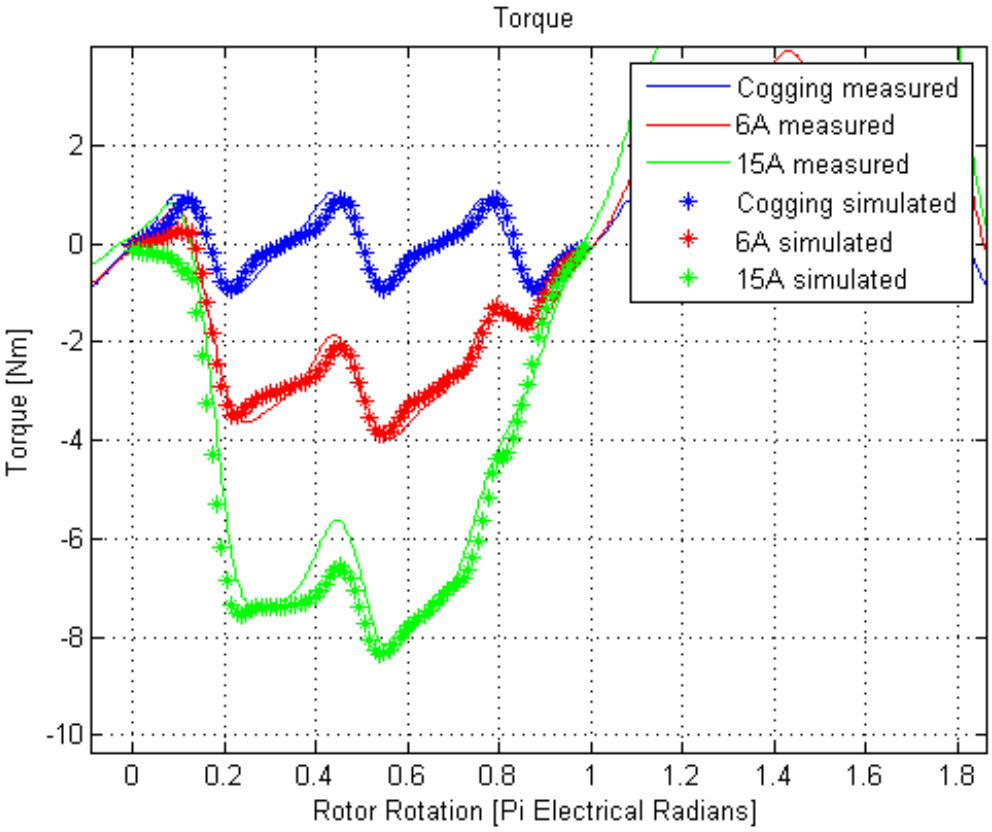

Figure 6-9: Cogging and excited torque: measured and simulated

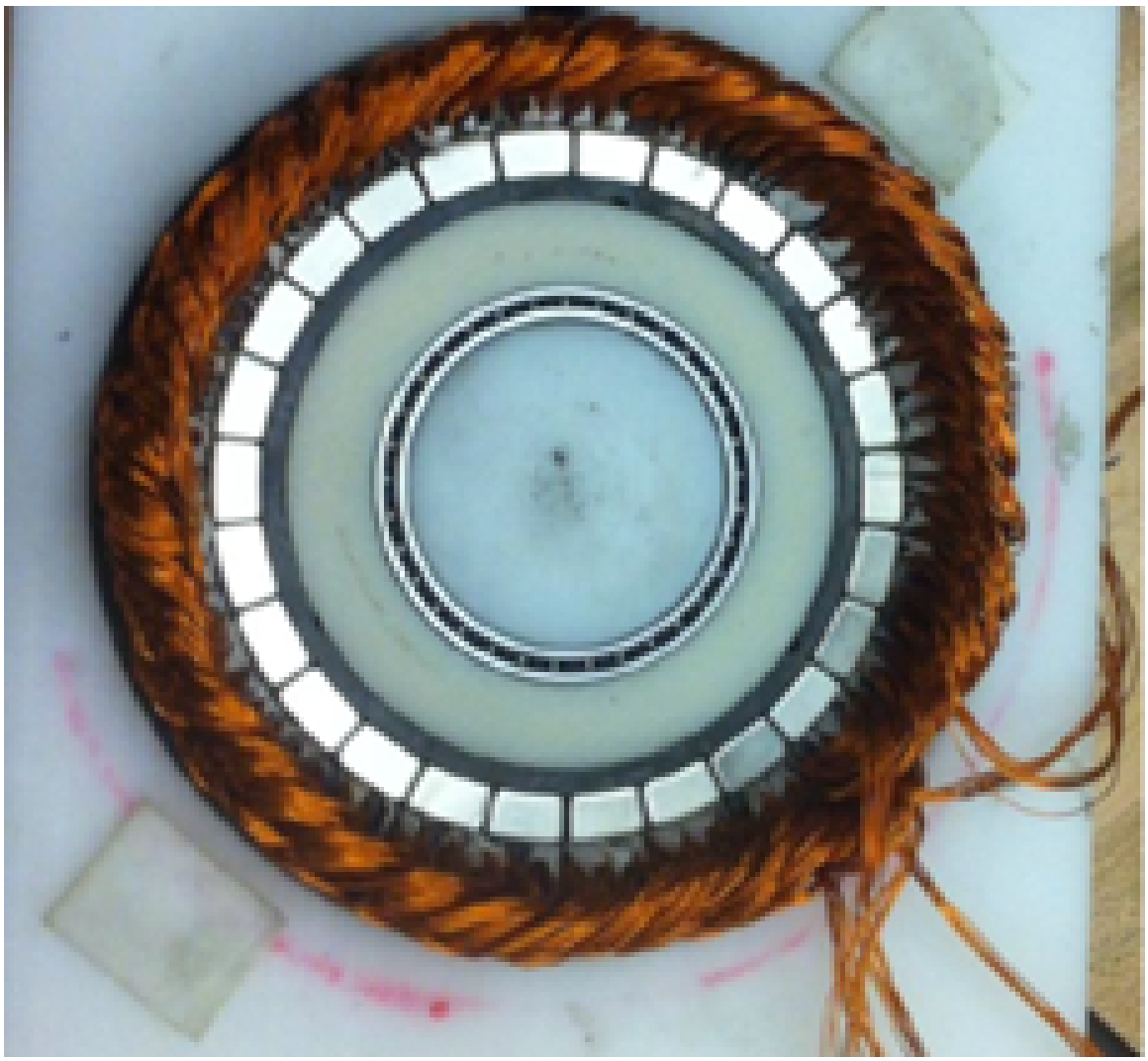

Figure 6-10: Current robotic cheetah motor used to test modeling method

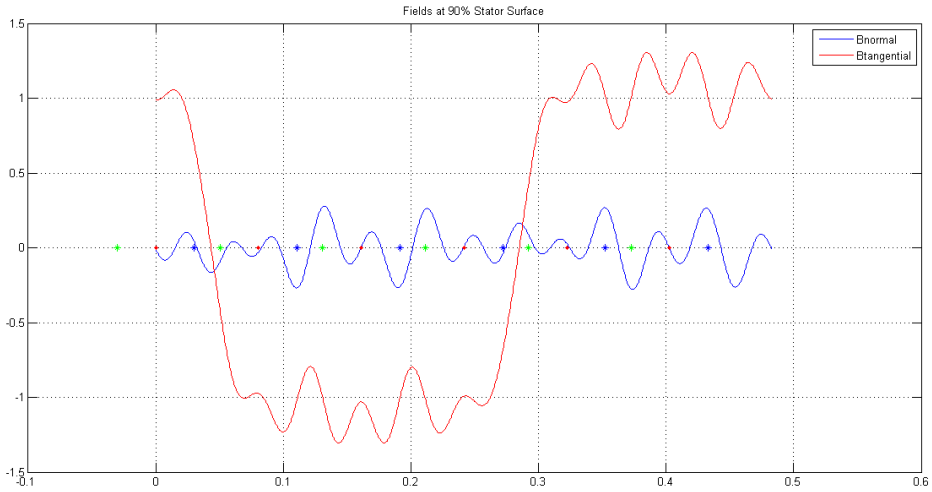

Figure 6-11: Magnetic fields at stator surface

tells us that the higher-order harmonics (that become numerically problematic within the simulation) are unimportant for capturing the behavior of the machine.

6.3 Summary

The material used for construction of the machine was characterized and closely matches the data provided by the manufacturer. The model described in Chapters 2 to 4 was used to predict performance characteristics of an existing machine in the lab, resulting in a spectacularly close match with measured data. Figure 6-9 is remarkable in that the model captures the cogging, saturation, and motive torque behavior of a physical machine measured on the test stand.

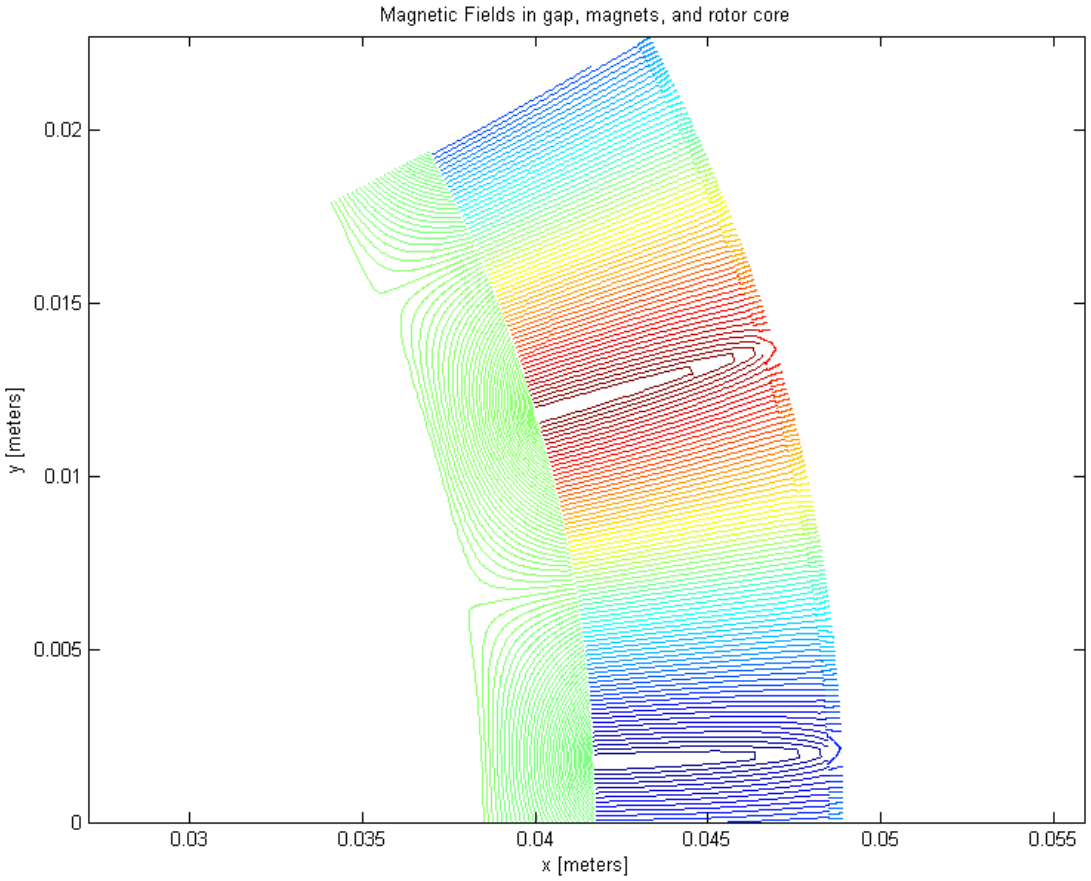

Figure 6-12: Field lines in machine

Chapter 7

Design

The performance of an electric machine is dependent on the geometric details of the flux-carrying elements. In a machine such as the cheetah motor, shown in Figure 7-1, details comprise five radii, three width fractions (tooth, tooth tip, magnet), two layout parameters (number of phases and poles), and a stack length which define the design. These eleven parameters are mapped onto a two-dimensional performance space spanning mass and power dissipation. This mapping exposes the trade off between power dissipation and mass, and ultimately the selection of an optimal machine. Power dissipation, in this case, is calculated based on the drive cycles of the eight motors in the cheetah. Other parameters may be included in the output space, but mass and power dissipation are chosen for the cheetah design.

While intuition may guide changes to a known configuration to change its characteristics, this method of design, shown in Figure 7-2, is useful only for finding a local optimum. With a fast method of analyzing motor performance, like the hybrid model presented in Chapters 2 to 4, the design space may be analyzed by brute-force methods, or alternately, by considering a wide grid and then analyzing interesting areas with a finer grid. In this case, design parameters may be swept and each potential design scored against an example drive cycle. This design process is shown in Figure 7-2, and is less likely to get stuck in a local optimum.

This chapter will illustrate the design process with two examples: a cheetah motor and a bicycle motor. The design methodology is the same for both, but the require-

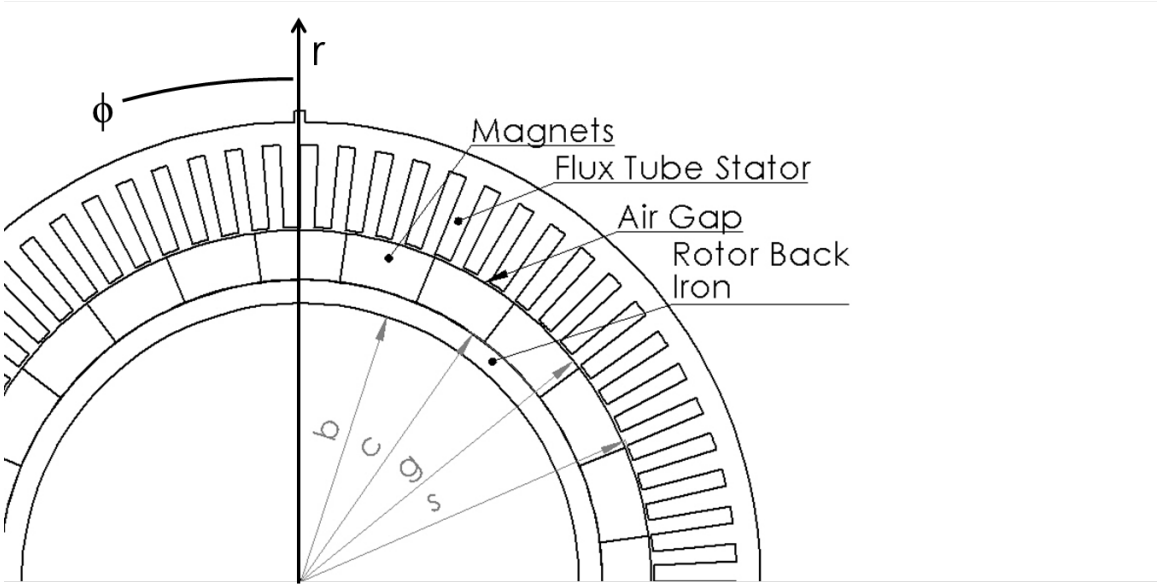

Figure 7-1: Diagram of motor showing definition of parameters

ments and the output are dramatically different. Code for the cheetah motor desing and evaluation is included in Appendices B and C.

7.1 Cheetah (Internal Rotor)

7.1.1 Design challenge

The demands on the motor for the cheetah are unique in that they have temporally brief spikes of very high torque but make a small fraction of that torque for the majority of operation. Additionally, each machine in the robot sees a different drive cycle; see Figures 7-3 through 7-6. The knees and shoulders have different requirements, as do front and back and left and right motors, as quadruped gaits are asymmetric. While an optimum machine could be built for each position, practical constraints prohibit this. Instead, all of the different drive cycles are appended to each other, and a single optimum motor design is produced.

Figure 7-3 shows the drive requirements for the knees, while figure 7-4 shows drive requirements for the shoulders. The spikes of torque are readily visible, as is the difference between left and right and front and back. This data is taken from

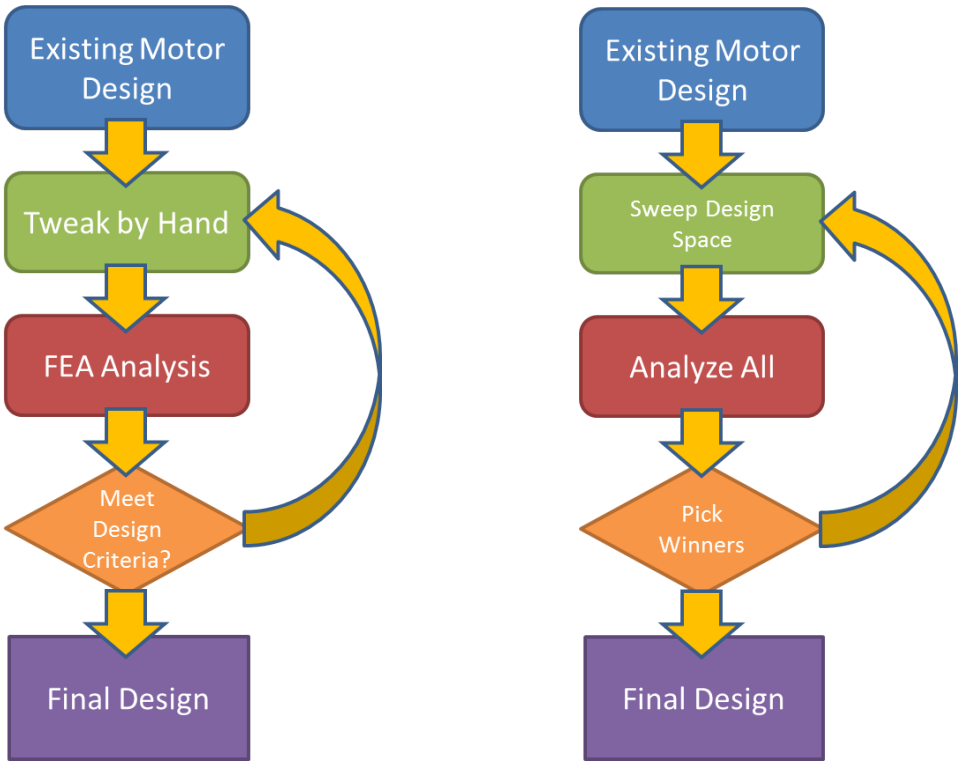

(a) Traditional motor design process

(b) New motor design process

Figure 7-2: Traditional vs. new design process

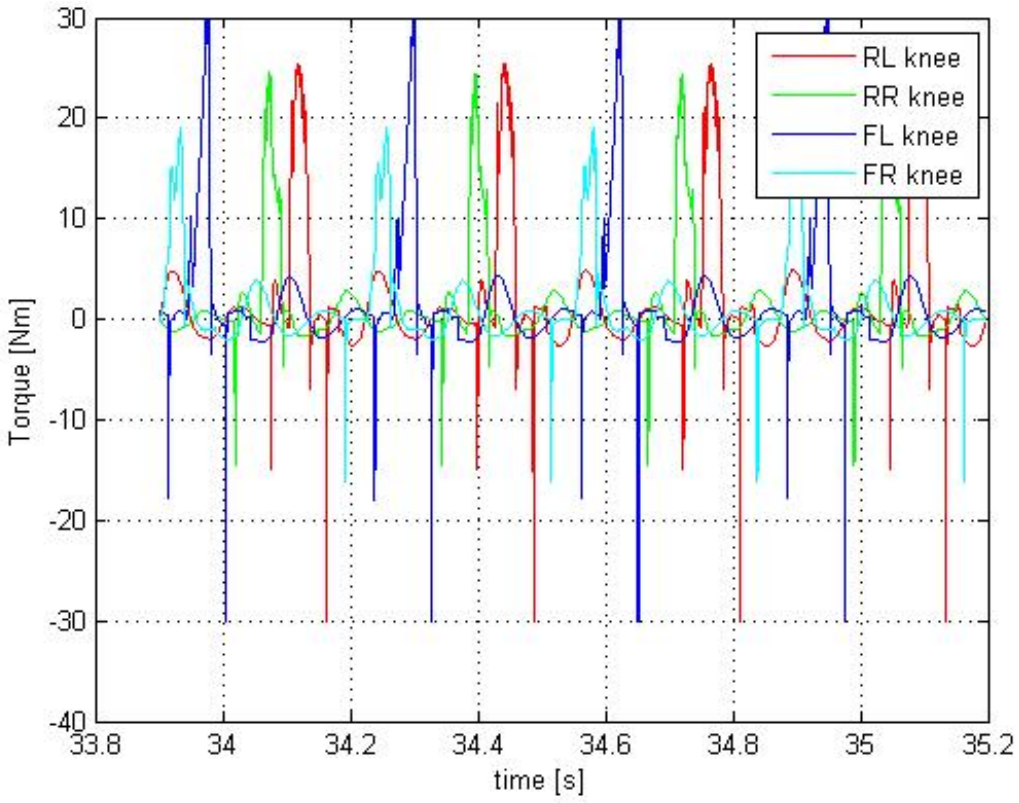

Figure 7-3: Torque vs time for knee joints

simulations of a running cheetah provided by Professor Kim's group.

Figures 7-5 and 7-6 show the torque information plotted against speed. The differences in requirements for each joint are more apparent here. The front left knee and shoulder require the most power of any of the joints.

7.1.2 Design Process

The parameters defined in Figure 7-1, as well as parameters defining the width of the teeth, are swept over a fixed grid. To reduce computation time, reasonable assumptions about sizing may be made, and parameters dithered around these points. A simple assumption is that steel structures are sized to carry the remnant flux density of the magnets used. This will place the design in the proper neighborhood, allowing for exploration around this point.

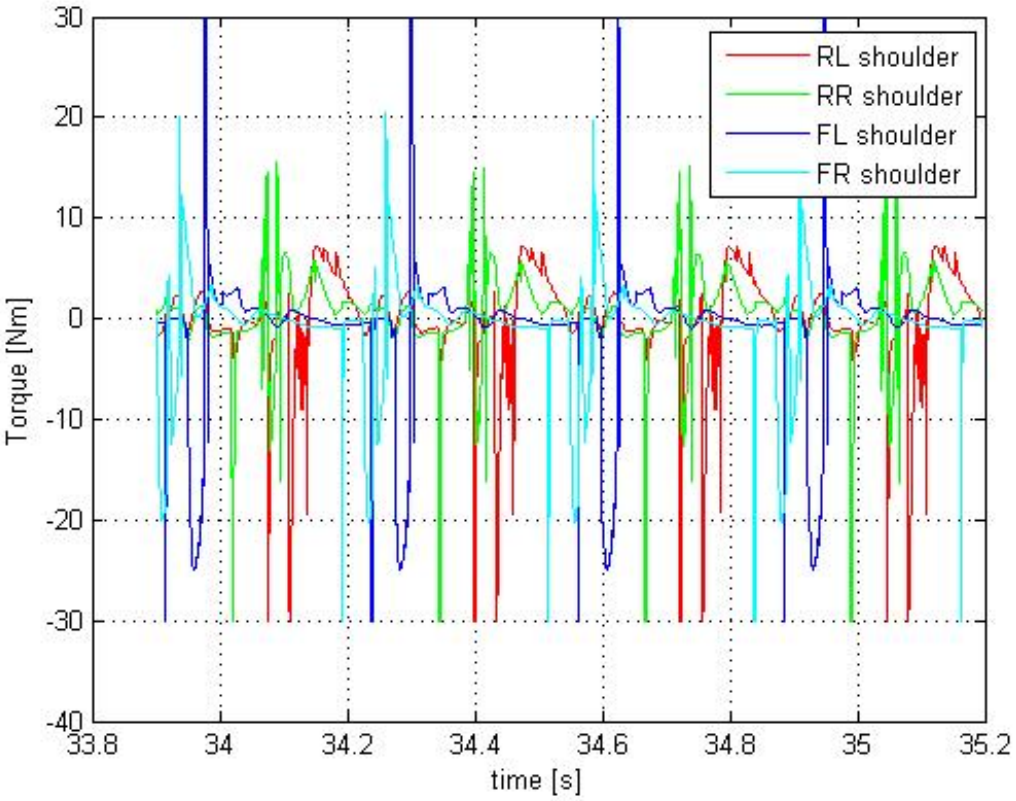

Figure 7-4: Torque vs time for shoulder joints

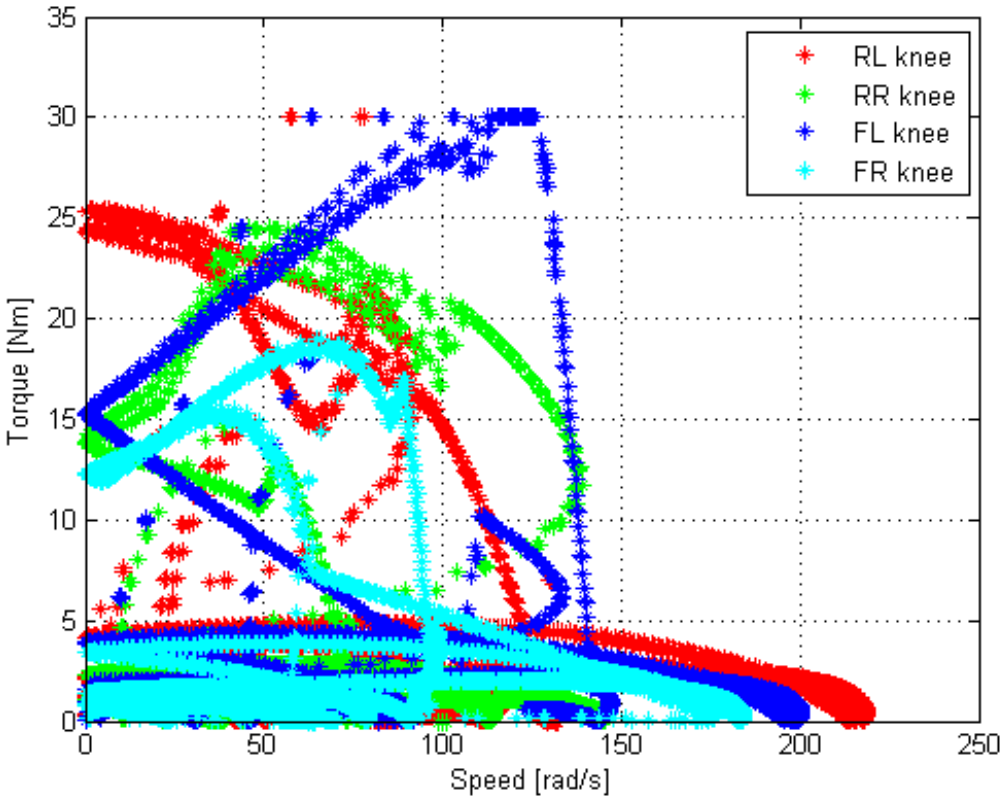

Figure 7-5: Torque vs speed for knee joints

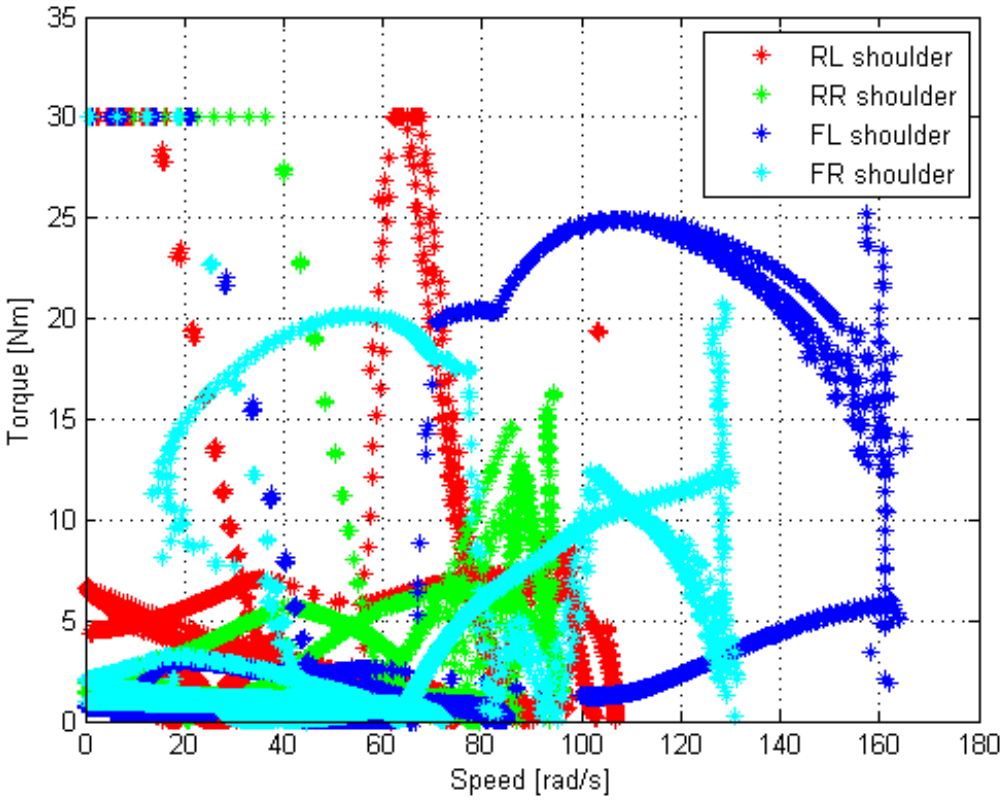

Figure 7-6: Torque vs speed for shoulder joints

For each design, relevant parameters are calculated, and the torque produced is evaluated at a rotor angle inside the commutation window. This point may be one side of the commutation window, and may be chosen to be the worst-case scenario in terms of saturation. The best case point for torque production is the very center. This process is shown in figure 7-7. For the cheetah machine, the worst-case point, the one at the edge of the commutation window, is chosen.

Since torque is proportional to current and winding loss proportional to the square of current, it is assumed that heavy saturation is not a desired operating region, as it will necessarily lower the torque constant of the machine. Therefore, we want to know at what point in the current excitation saturation occurs so max current may be limited to that value. Determining maximum current for the rectangular drive from [20] is accomplished with a binary search. Rectangular current drive is assumed, and the maximum current that does not push the machine into heavy saturation is found with a binary search, as shown in Figure 7-8.

With this maximum current value, torque per unit stack length (width of the motor) is calculated. Stack length is then set such that the motor produces the maximum specified torque. From the maximum torque and the current required to reach it, a torque constant is calculated. This information, combined with the motor mass and phase resistance calculated from physical parameters of the design, is used to calculate the electrical dissipation throughout the given drive cycle.

7.1.3 Windings

Packing factor is the defining characteristic of a winding scheme. Wires are usually round, forced to occupy a rectangular or trapezoidal slot, and must nest with each other. They also must be electrically isolated by means of conformal insulation. Because of this, only a fraction of the slot may be filled with wire. The packing factor numbers are taken from machines that have been built in the past for this project. The liner is assumed to occupy the three walls of the slot, and the packing factor is determined by taking the area of wire in the slot divided by the total area not occupied by the liner. For the previous machines, this number comes to 47%, and is

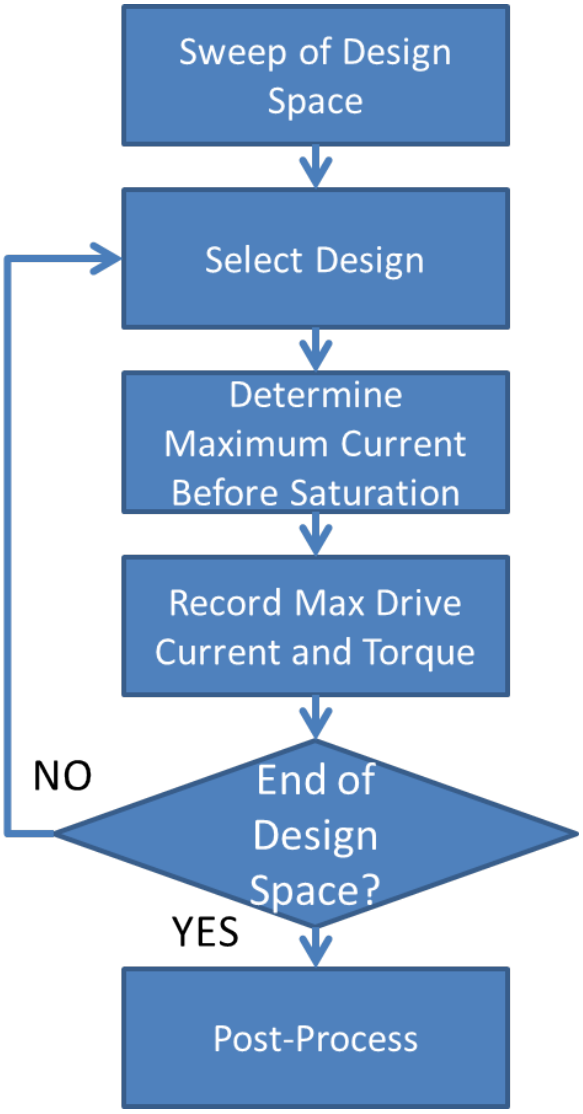

Figure 7-7: Design flowchart

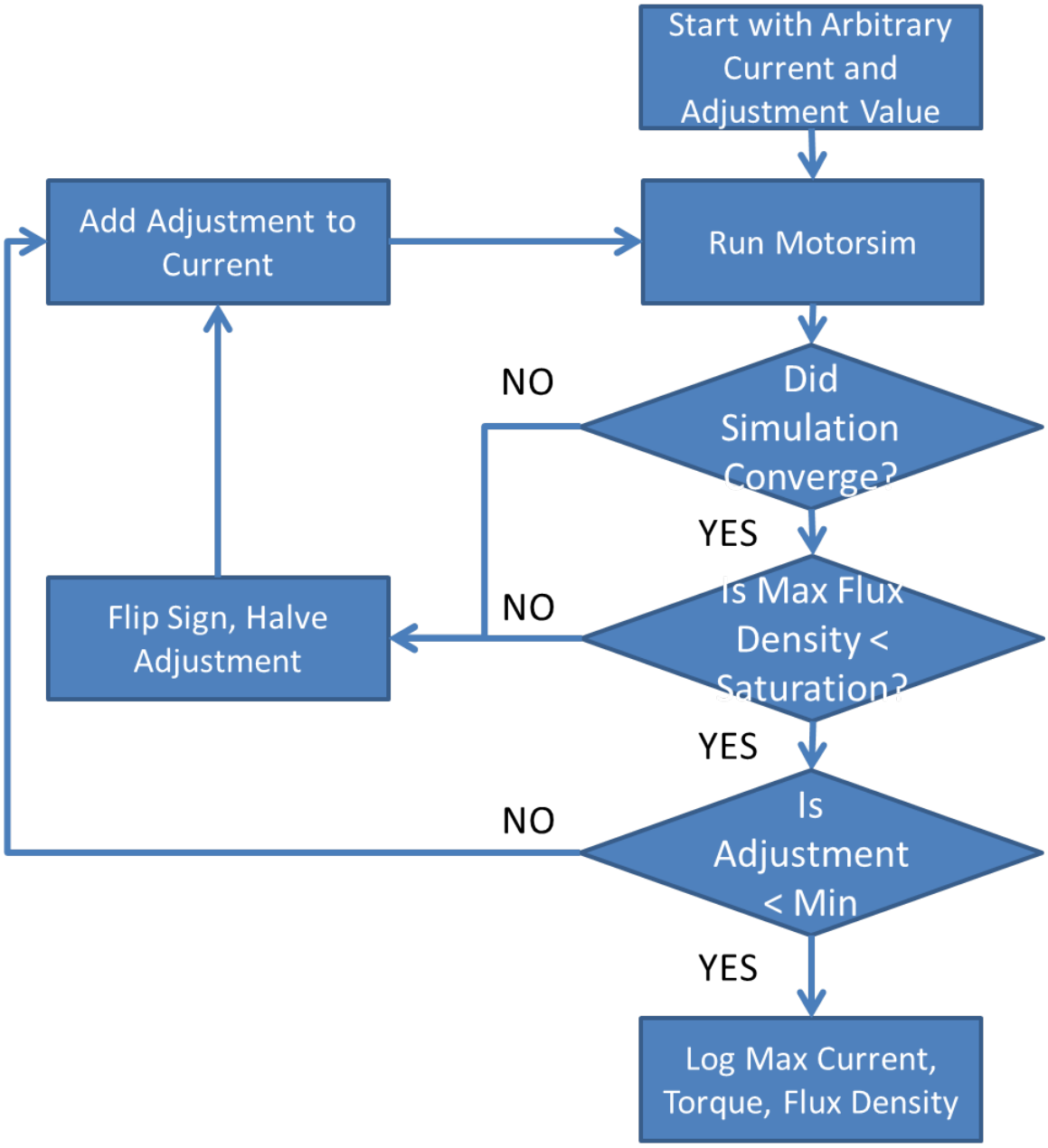

Figure 7-8: Maximum current flowchart

dependent on wire size, slot size, method of winding, and other factors. It is assumed that subsequent machines would be geometrically similar and wound by the same people and processes.

The end turn length is another parameter that is dependent on the winding method and the geometry of the machine. The immediate thought is to model end turns as a semi-circle, but in practice, they are much shorter. In the previous machines, this length is closer to the arc length between slots corresponding to the same phase in adjacent poles.

7.1.4 Output

Figure 7-9 shows the output from the optimizer. Stack lengths other than the minimum (in terms of magnetic saturation) are shown. These additional stack lengths effectively scale the torque capacity of the design relative to that required by the application. An increased torque capacity allows the current to be reduced. Running the machine light also reduces core loss. In the figure, the asterisks correspond to the minimum stack length, while the circles and plusses correspond to 12.5% and 25% increases in stack length. Since torque scales linearly with current and stack length, and dissipation scales with the square of current, dissipation numbers are reduced when stack length is increased. This has the effect of moving the designs up (increased mass) and left (decreased dissipation) in the output space.

The hyperbola on the plot represents the line where $\frac{dP}{P} = \frac{dM}{M}$. While a cost function for a motor is dependent on a particular application, this line serves as a useful reference for a machine where mass and dissipation are important. In this scheme, points lying on the hyperbola closest to the origin are assumed to be the best solutions, as the shape approximates the Pareto front that naturally results from displaying designs produced with a sweep of the design space.

This figure is an example of a small subset of the potential design space and takes approximately two minutes to produce on a consumer-grade laptop. More computation time and more powerful computers will allow greater exploration of the design space. The final cheetah motor design is taken from this plot, as it represents

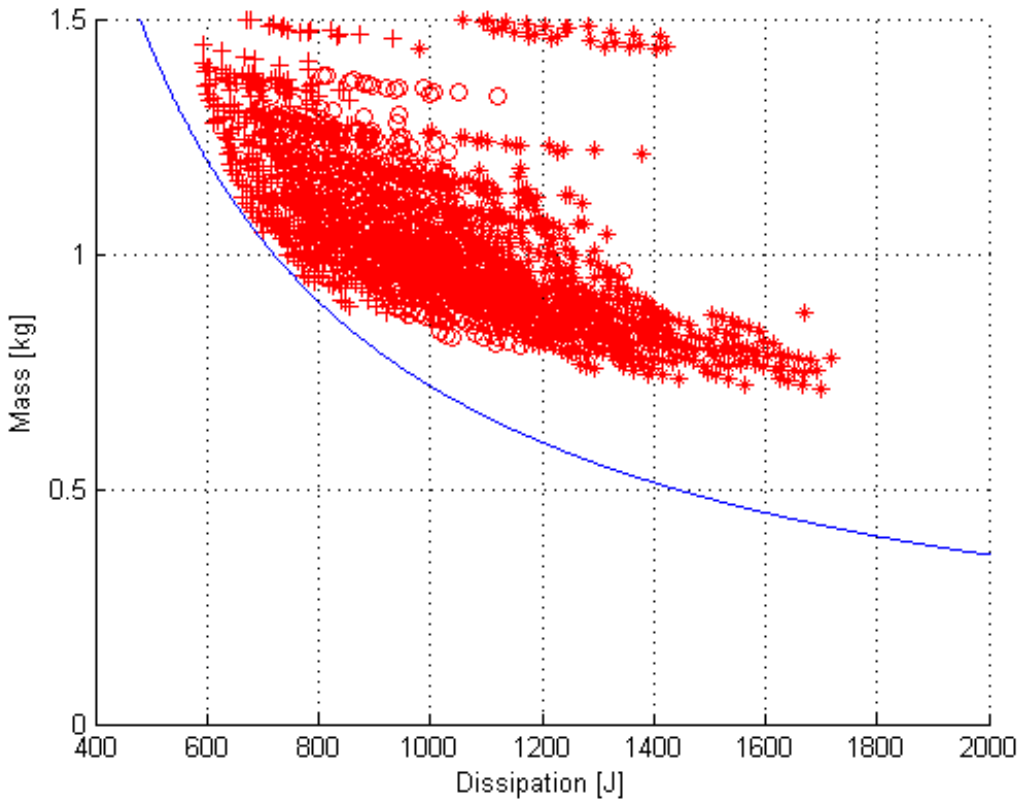

Figure 7-9: Cheetah motor design comparison. The hyperbola is the line where $\frac{dP}{P} = \frac{dM}{M}$.

an interesting space that is expected to adequately anchor the model.

Figures 7-10 and 7-11 display design tradeoffs in numbers of poles and phases. Different colors denote different numbers of poles and phases, while asterisks correspond to the minimum stack length, and circles and plusses correspond to 12.5% and 25% increases in stack length.

Table 7.1 shows the dimensions of the chosen design for the Cheetah machine, and Figure 7-12 shows the labeled dimensions. Detailed drawings may be found in Appendix F.

7.1.5 Thoughts on Design

The cheetah machine is optimized for relatively little steady-state torque with short temporal spikes of high torque. The magnets are comparatively large, making up the

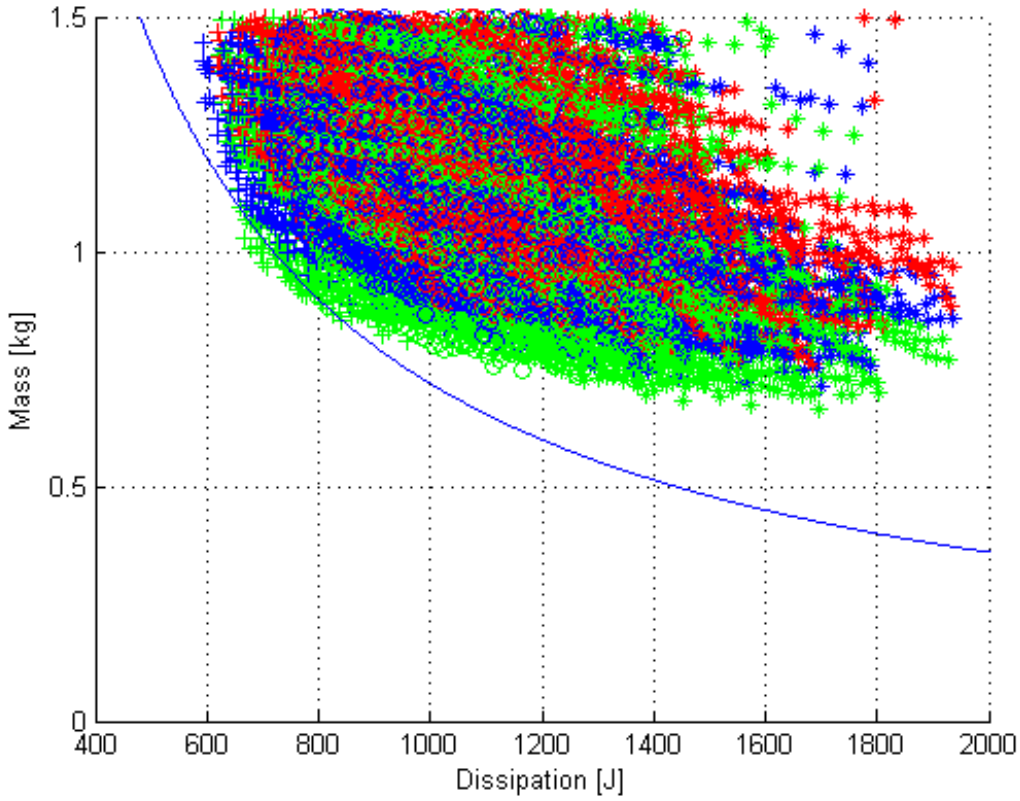

Figure 7-10: Cheetah motor design comparison. Red is 7 phases, blue is 8, and green is 9. The hyperbola is the line where $\frac{dP}{P} = \frac{dM}{M}$.

Parameter	Value	Units
Pole Pairs	9	-
Phases	8	-
R1	36.2	mm
R2	41.4	mm
R3	48.9	mm
R4	59.1	mm
R5	63.5	mm
Airgap	0.4	mm
Stack Length	11.7	mm
Slot Fraction	0.33	-
Total Mass	0.8345	kg
Rphase	0.1668	Ohms

Table 7.1: Cheetah motor selected design parameters

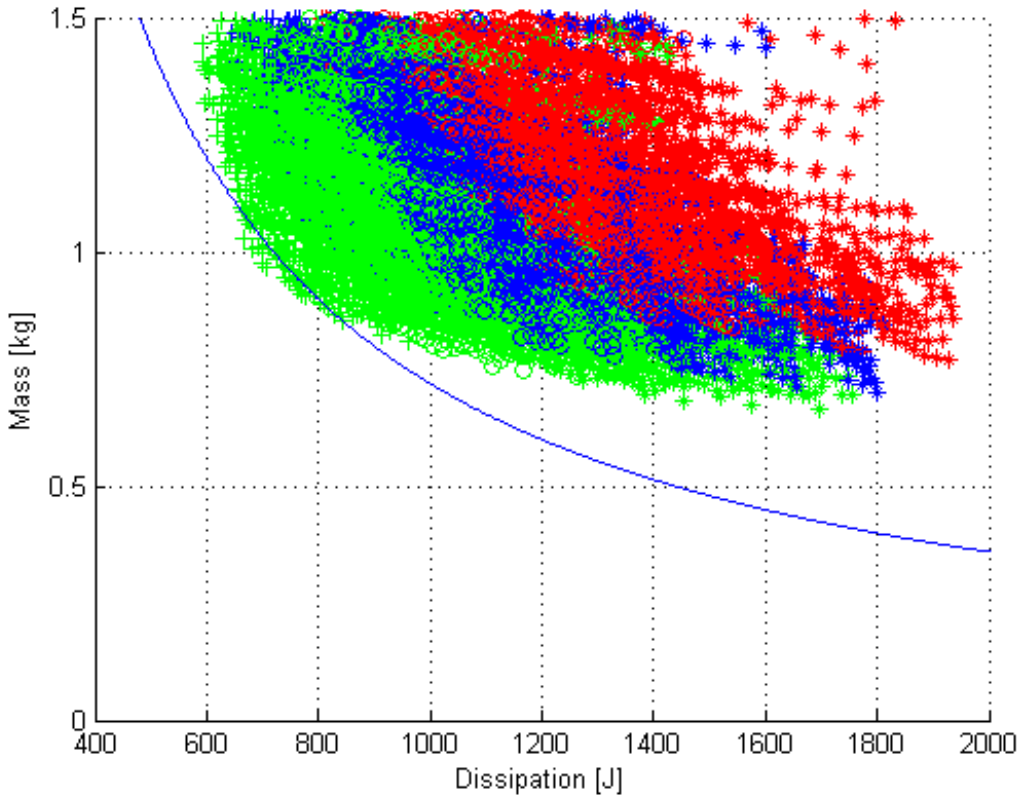

Figure 7-11: Cheetah motor design comparison. Red is 7 pole pairs, blue is 8, and green is 9. The hyperbola is the line where $\frac{dP}{P} = \frac{dM}{M}$.

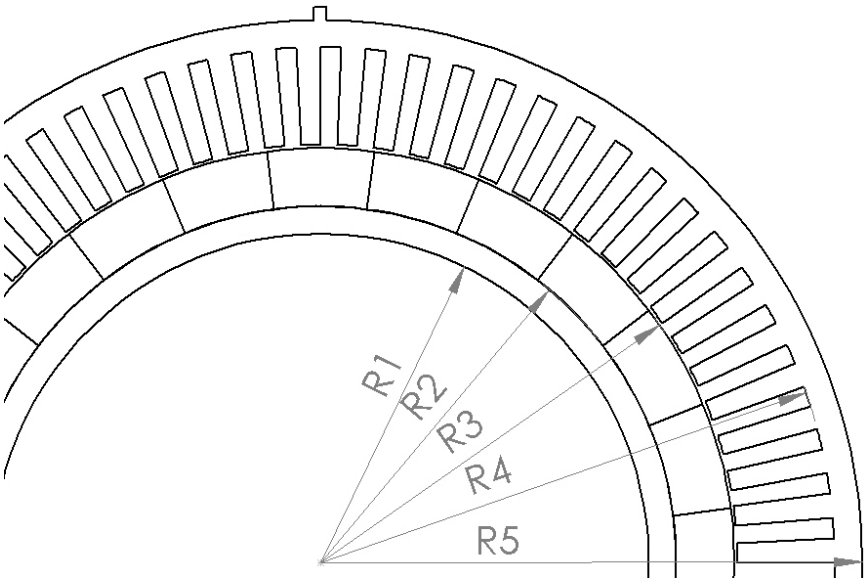

Figure 7-12: Diagram of motor

majority of the flux in the machine. This results in a machine that is heavily biased towards magnetic structure with small windings. In this way, iron, and flux carrying capacity of the teeth is traded with winding area, or current carrying capability.

Larger numbers of teeth generally improve all aspects of performance until the slot liners become a significant fraction of the slot area. Numbers of poles and phases are traded, with an increasing number of phases allowing greater harmonic content in the flux waveform, while greater numbers of poles make the backiron on both the rotor and stator smaller (the amount of flux contained in a pole, and therefore required to be carried by the backiron, is proportionally reduced). Greater numbers of poles increases the ratio between electrical and mechanical frequency, increasing core losses.

The 8-phase design removes approximately 40% of the mass of the commercial solution and produces approximately three times as much torque before saturation. It improves upon the second-generation machine by approximately 30% of mass, and makes 20% more torque before saturation.

7.2 Traction (external rotor)

In this section, the same methodology is applied to the design of a machine for a traction application, specifically an electrically-assisted bicycle. The machine in Figure 7-13 has been commercially produced and optimized for a propulsion application, meaning that efficiency is far more important than mass. The black dot in the Figures, 7-16 to 7-26 represents this motor, the starting point for new designs. A first pass shows that a mass reduction of approximately 30% is possible without decreasing efficiency or changing the physical envelope when using materials and design methodology as used for the cheetah. This served as a baseline, which suggested improvement was possible.

7.2.1 Design challenge

Figures 7-14 and 7-15 show a representative drive cycle of the machine in the bicycle. Note the differences in the time scale between the cheetah and the bicycle. The spikes

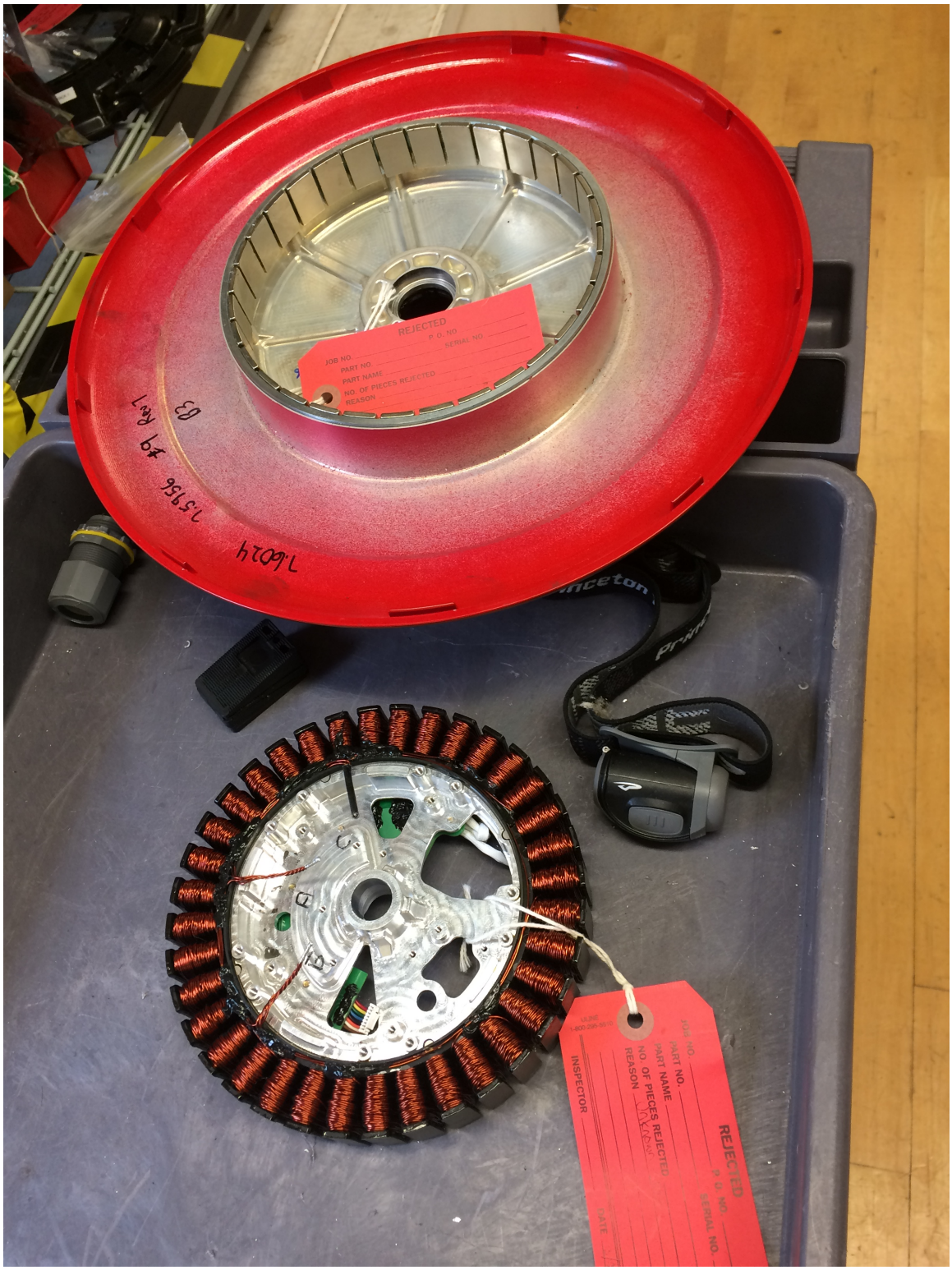

Figure 7-13: Traction motor example

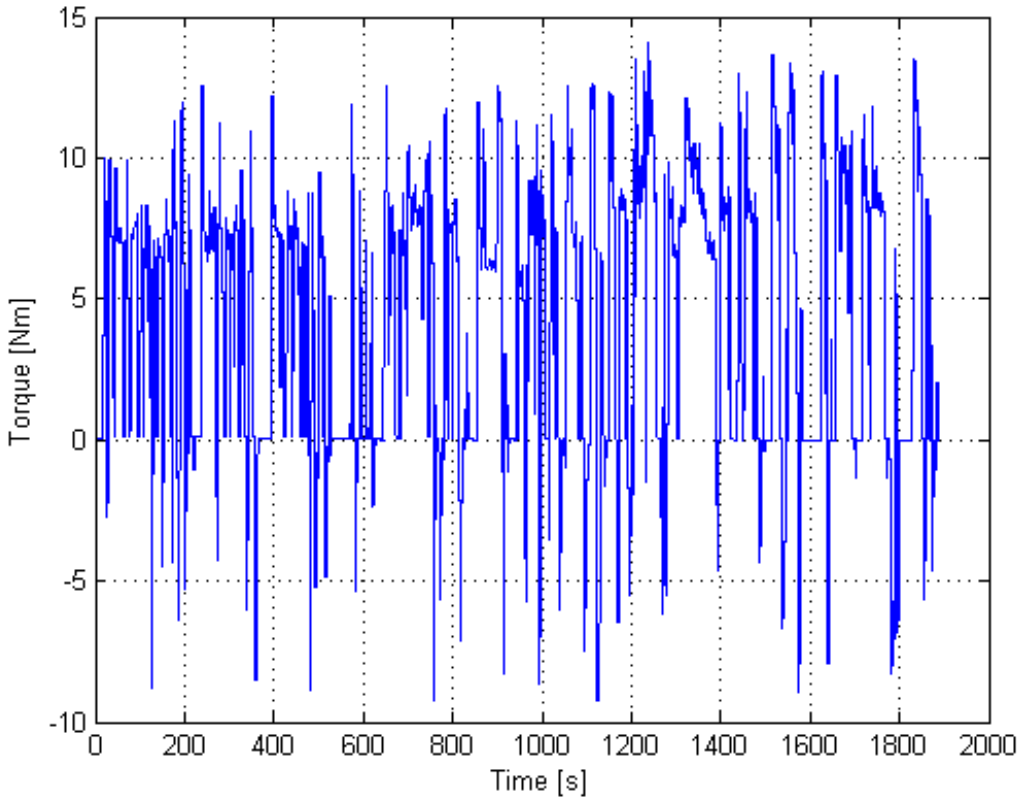

Figure 7-14: Traction motor example torque vs. time

of torque last minutes, meaning that the machine must operate near maximum torque for extended periods of time. Drastic mass reduction may not be accomplished at the expense of thermal capacity as in the case of the cheetah.

Initially, the optimization was run so as to match the materials and operating style of the commercial motor. Magnets were reduced to having a 1 Tesla remnant flux density, and Hyperco 50 was used. A sinusoidal drive was assumed, and the optimizer was run with torque values calculated with the rotor in the center of a pole to best compare with known motor data. Packing factor was a conservative 35%. Figure 7-16 shows the initial result. While a 30% reduction in mass is possible, financial constraints preclude the use of an exotic material such as Hyperco 50, the steel used in the cheetah machine. The magnets and packing factor are significant handicaps, suggesting that a dramatic increase in performance may be possible even with a more reasonable material for the stator and rotor core. Thus a clean sheet

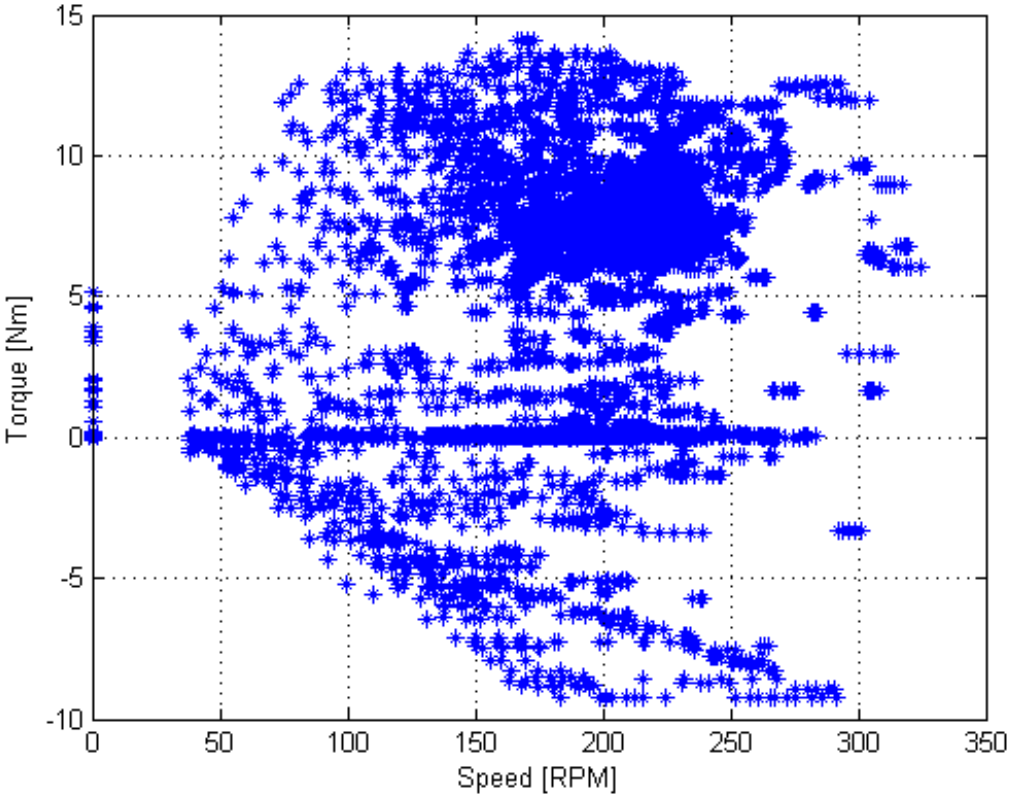

Figure 7-15: Traction motor example torque vs. speed

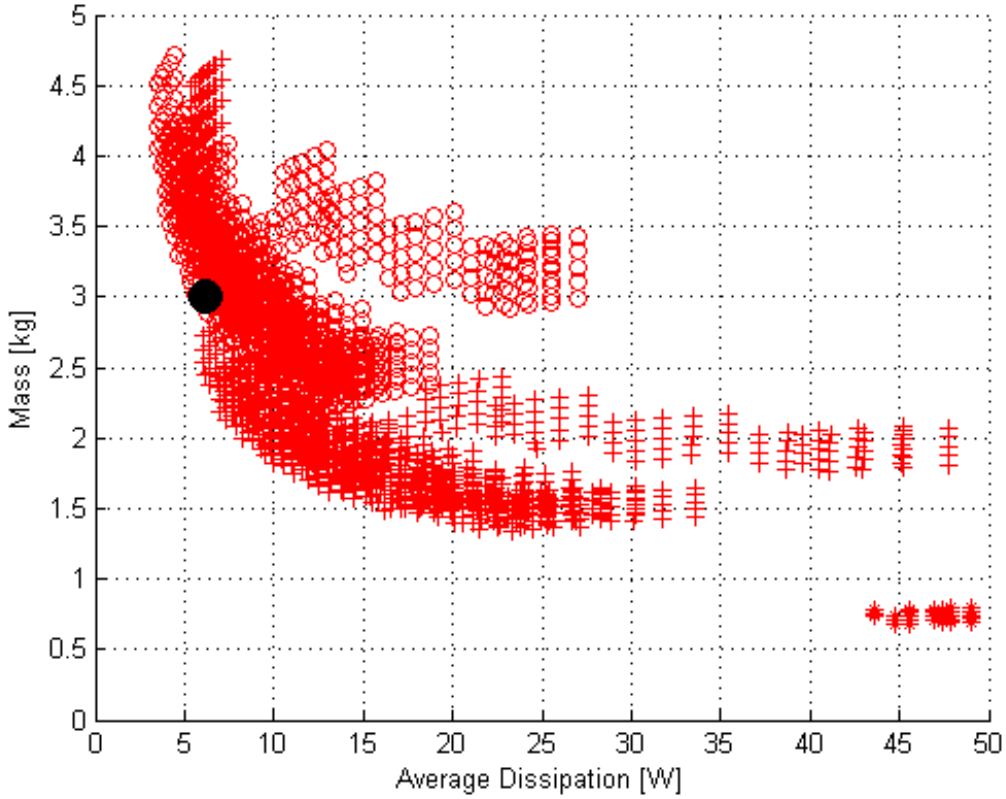

Figure 7-16: Initial results with Hyperco50 and weak magnets. The black dot represents the commercial solution. Asterisks are minimal stack length. Plusses and circles are 6 and 10 times minimal stack length.

design was undertaken.

The diameter of the machine is variable in a clean-sheet design. Increasing the diameter of the airgap produces more torque for the same shear, so it stands to reason that this could result in a lighter machine. As the airgap is increased, the stack length of the machine decreases to make the same amount of torque. As the stack length decreases, the end turns of the machine become more significant, as their length does not change with stack length, eventually negating the advantage of moving the airgap outward. Figure 7-17 shows this result (when compared to Figure 7-16), showing that a further reduction in mass or increase in efficiency is possible with a larger outer diameter.

Hyperco50 is an expensive alloy, consisting of almost half Cobalt. Such materials

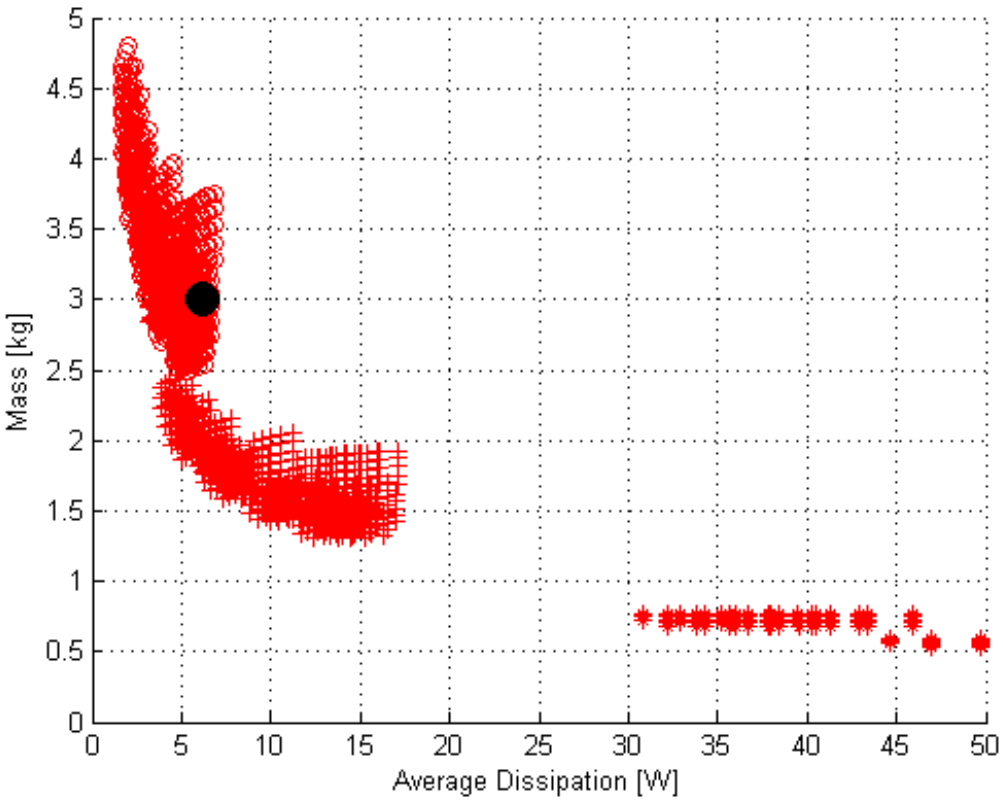

Figure 7-17: Initial results with Hyperco50 and weak magnets at 1.5x diameter. The black dot represents the commercial solution. Asterisks are minimal stack length. Plusses and circles are 6 and 10 times minimal stack length.

are not suitable for mass-produced, cheap machines. M-19 is a silicon steel alloy that retains much of the performance of Hyperco50, but is cheaper. Figure 7-18 shows the B-H curves of selected materials. M-19 has a saturation flux density of around 1.95 Tesla, while Hyperco50, a trade name for Vanadium Permendur, saturates around 2.4 Tesla. The saturation flux density of M-19 is common among many similar materials, but differs in core loss. For this reason, it is assumed to be comparable to the material in the commercial machine in terms of flux density, but not necessarily core loss.

Figure 7-19 shows the same analysis in machines with M-19 and 1 Tesla remnant flux density magnets. In the figure, the red corresponds to a 3-phase, sinusoidally-driven machine. The blue is 4 phases, the green is 5 phases, the cyan is 6 phases, and the magenta is 7 phases. All of the machines with more than three phases assume rectangular current drive, which is a far more effective use of the steel in the stator, resulting in a lighter machine. In this case, the commercial solution lies near the Pareto front resulting from the analysis, so it appears to be well optimized for an application, but perhaps not this application, to the limit that it is assumed to use the same materials considered by this analysis. The analysis produces a 4-phase machine that will slightly reduce the mass compared to the reference machine. Packing factor is still very conservative at 35%. A more reasonable number would move the curve to the left and slightly upward, due to increasing the mass of the windings and decreasing their resistance.

Figure 7-20 includes core loss. The maximum flux density in each type of segment in the stator, along with the speed is used in a curve-fit equation to calculate core loss. This is then added to the copper loss to form a more accurate picture of the losses in the machine. The commercial machine is not included on plots that include core loss, as the information needed to make a proper comparison (the material in the stator and its core loss characteristics) is unknown.

Figures 7-21, 7-22, 7-23, and 7-24 show the results when the outer diameters are 1.2 and 2 times the diameter of the reference machine. The mass or dissipation may be steadily decreased, effectively decreasing mass by up to 33% with respect to the reference machine. These plots still assume a very conservative winding packing factor

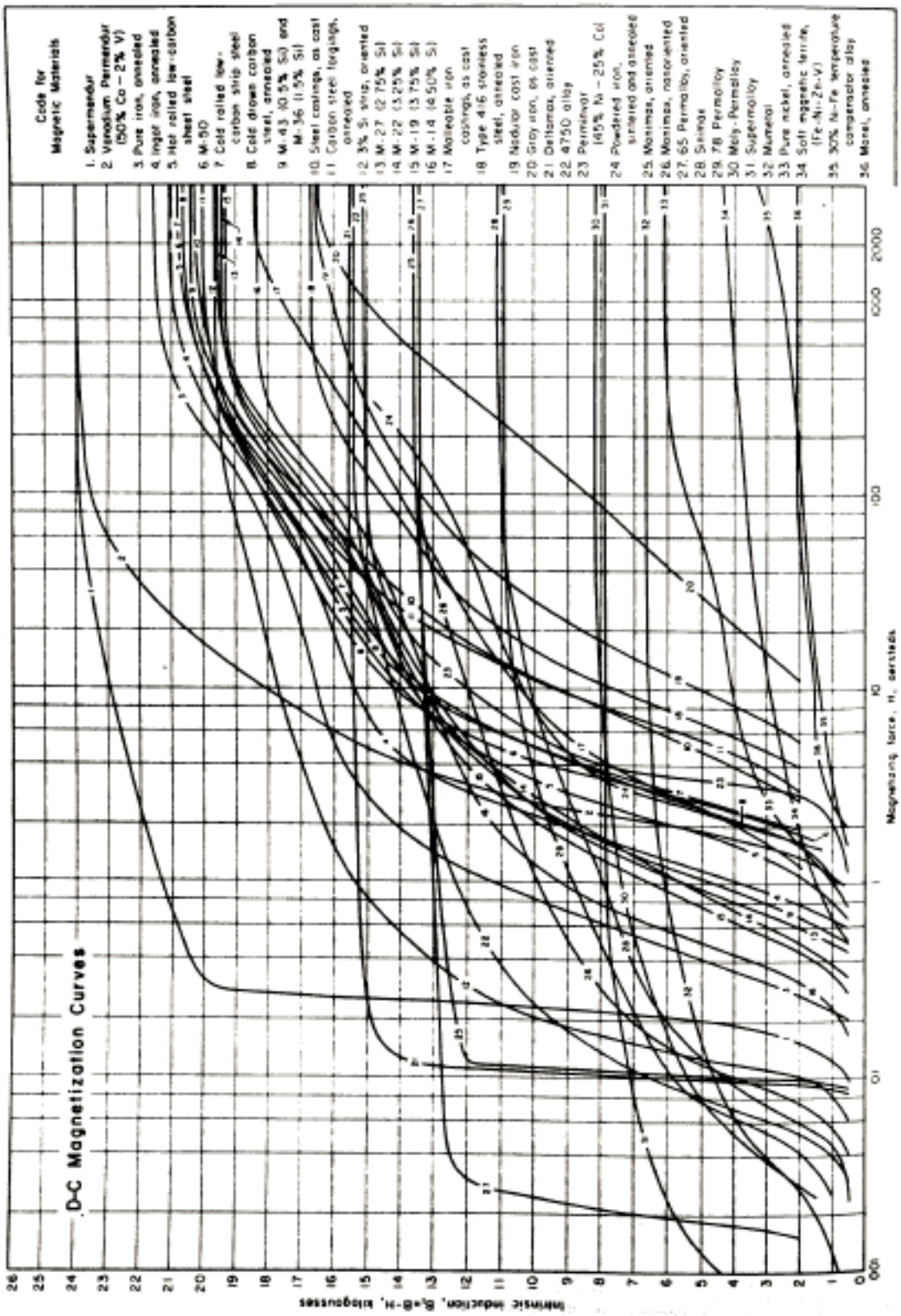

Figure 7-18: B-H Curves of selected magnetic steels [26]

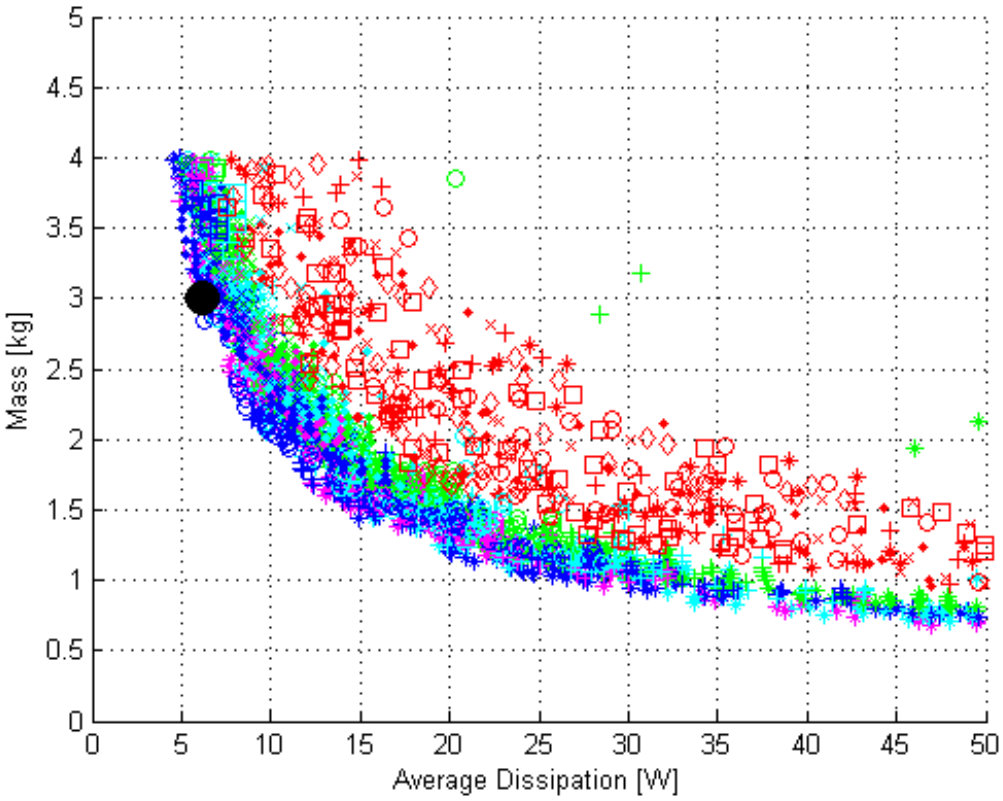

Figure 7-19: M19 and 1T magnets at 1x diameter. The black dot represents the commercial solution. Symbols represent different scalings of axial length.

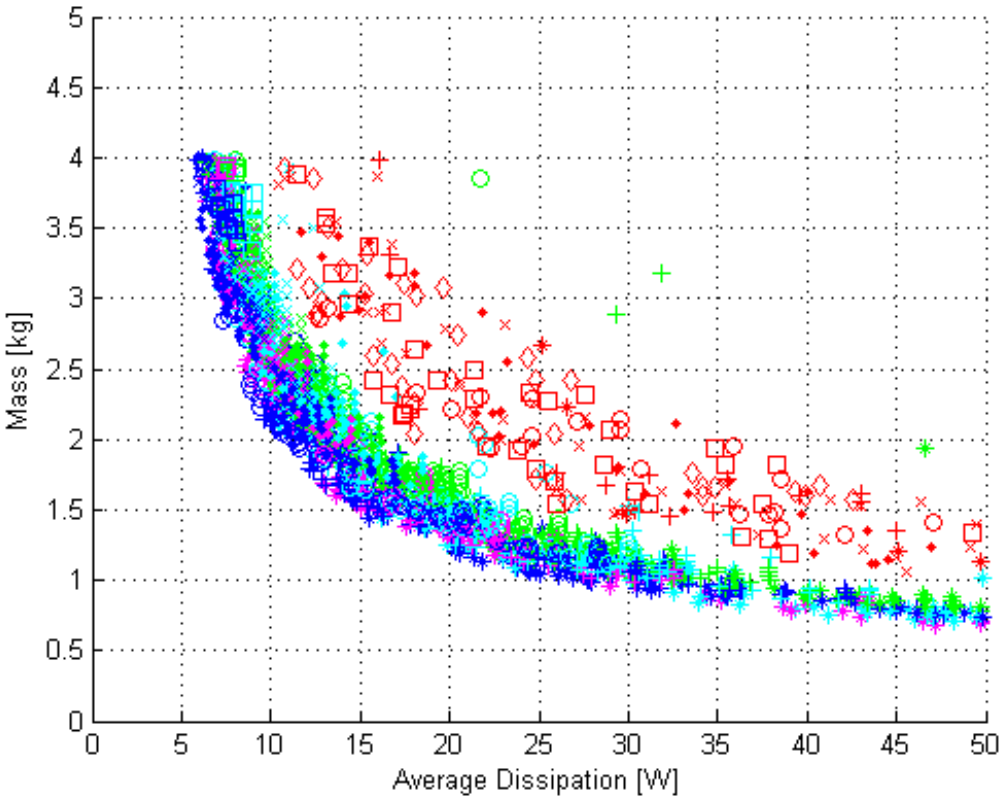

Figure 7-20: M19 and 1T magnets at 1x diameter including core loss. Symbols represent different scalings of axial length.

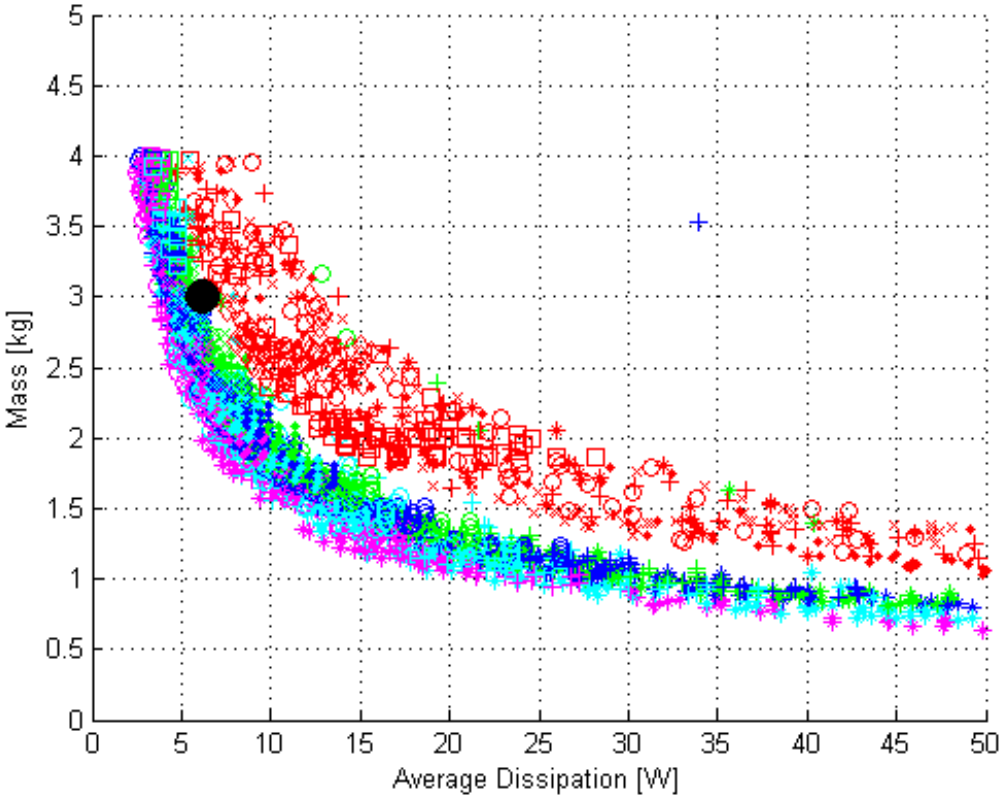

Figure 7-21: M19 and 1T magnets at 1.5x diameter. The black dot represents the commercial solution. Symbols represent different scalings of axial length.

and end turn length.

Figures 7-25 and 7-26 show this analysis performed on machines with an outer radius of half the reference machine. They are also assumed to be geared 5:1, meaning that core loss should be greatly exaggerated. This analysis is performed simply to see the effect of core loss on a geared application, as an machine mounted off-center and driving the wheel through a gearbox is of interest to the design, primarily to allow flexibility with the arrangement of other components.

The figures show that core loss has become approximately 20% of the power dissipated in the machine. This is seen in the increased dissipation numbers between Figures 7-25 and 7-26. In this application, it is especially relevant, as this core loss is present whether or not the machine is being driven. This would require a freewheel built into the application, but it does represent the potential to remove half of the

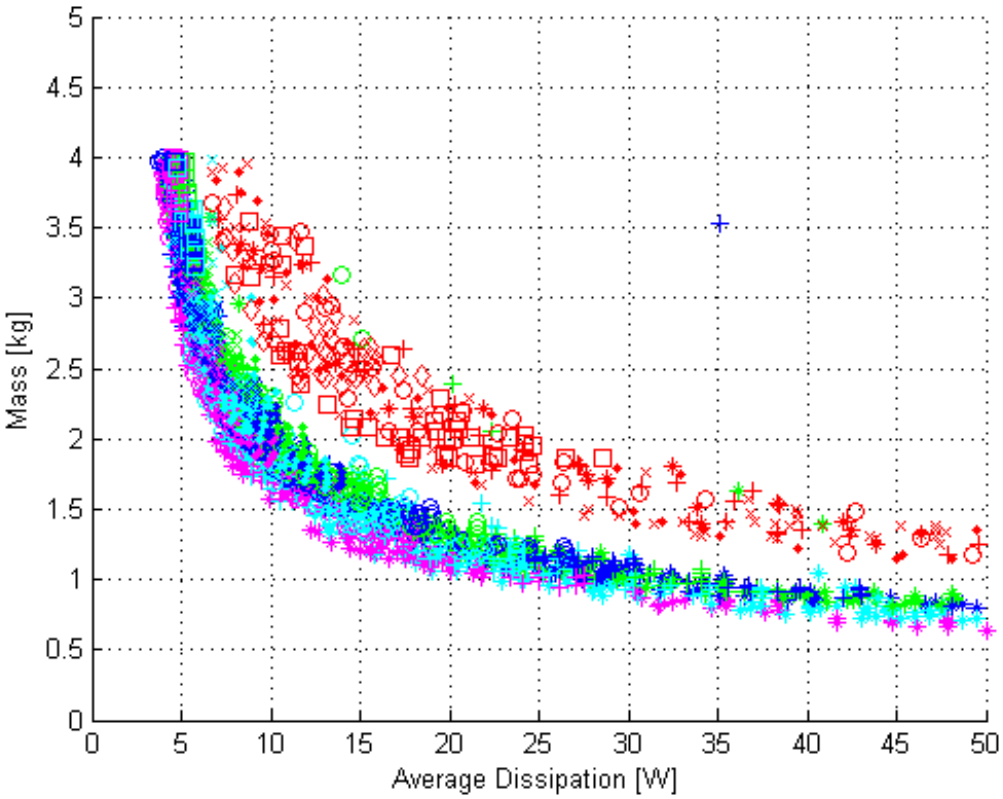

Figure 7-22: M19 and 1T magnets at 1.5x diameter including core loss. Symbols represent different scalings of axial length.

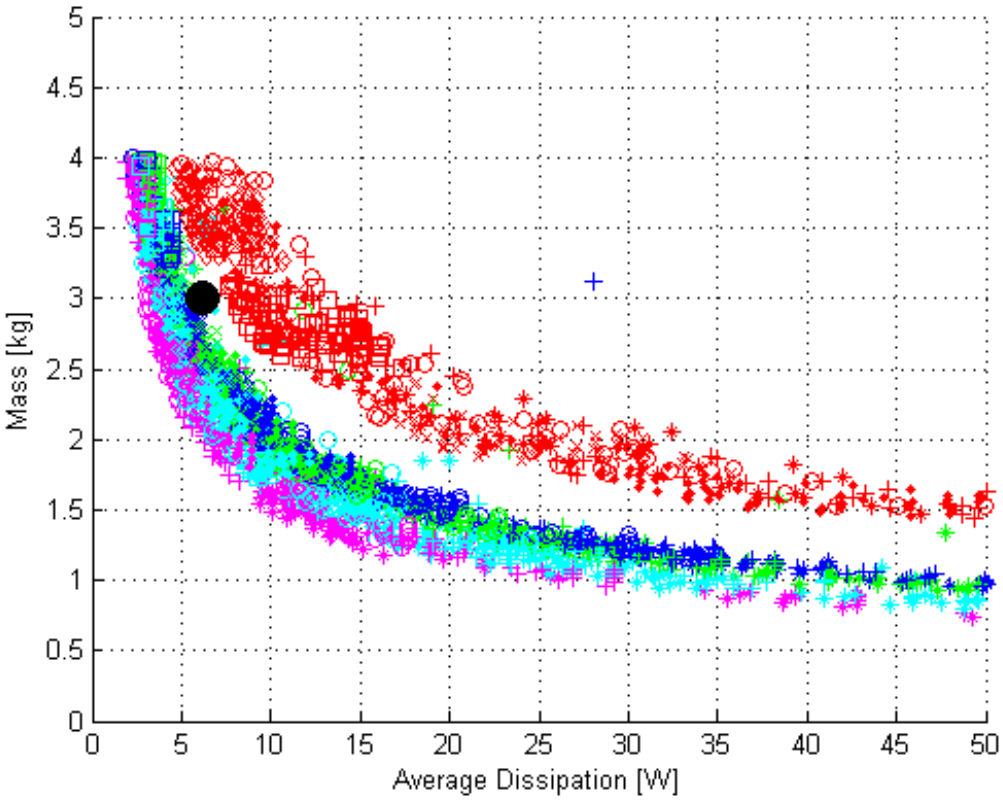

Figure 7-23: M19 and 1T magnets at 2x diameter. The black dot represents the commercial solution. Symbols represent different scalings of axial length.

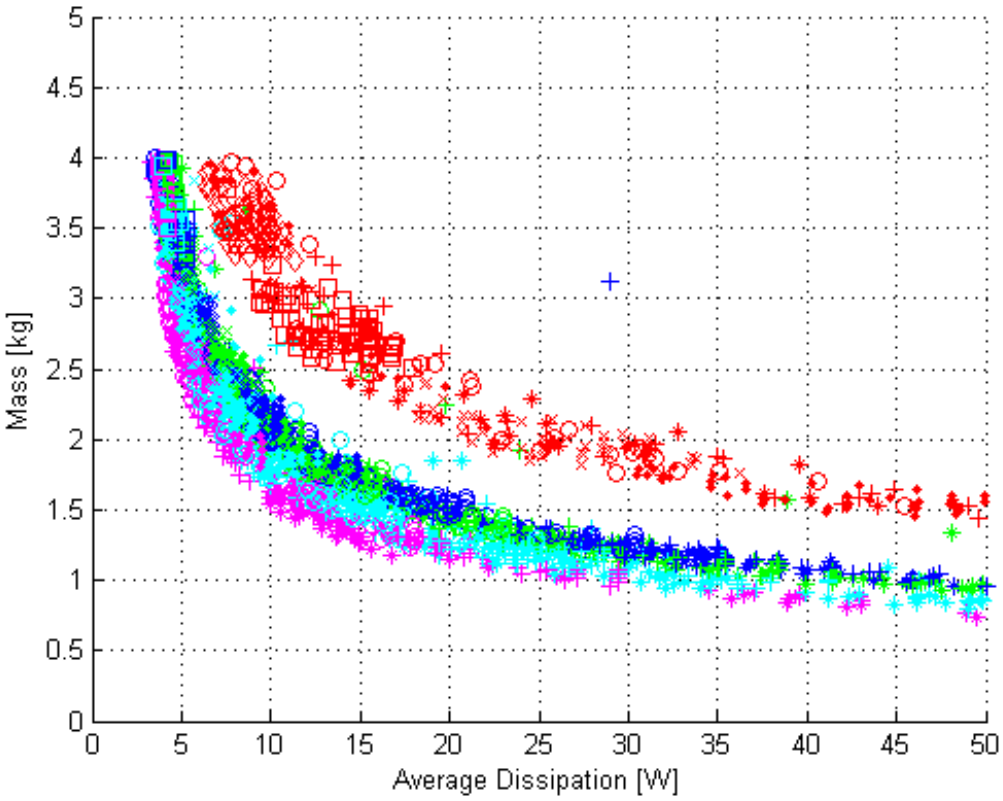

Figure 7-24: M19 and 1T magnets at 2x diameter including core loss. Symbols represent different scalings of axial length.

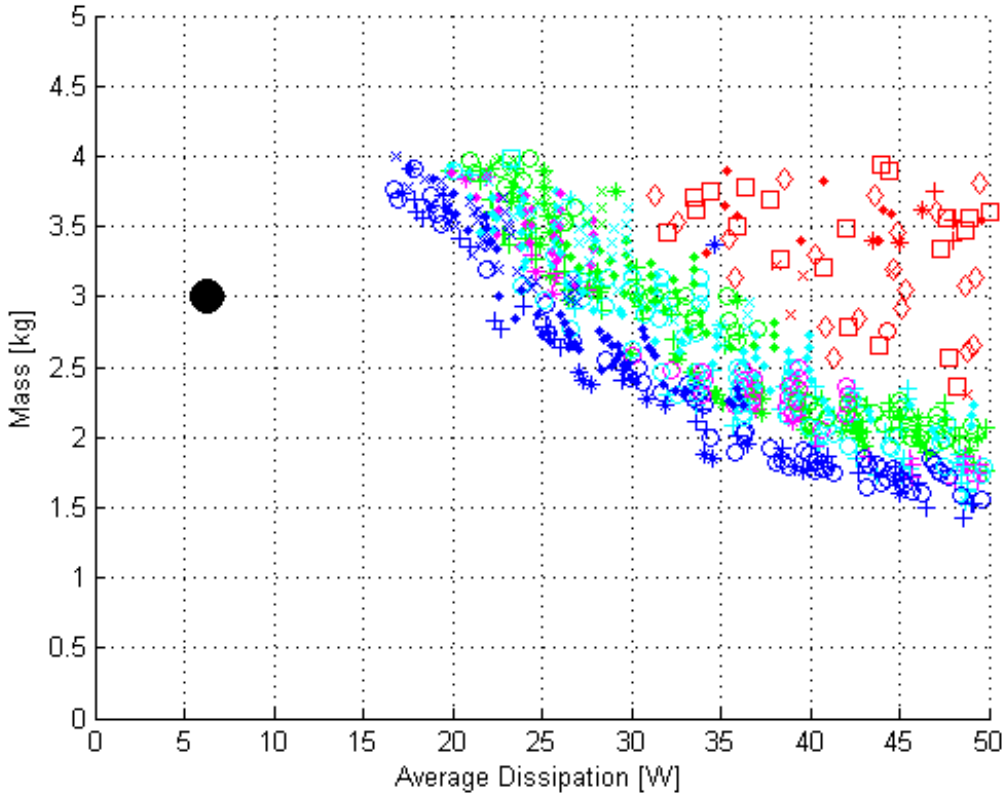

Figure 7-25: M19 and 1T magnets at .5x diameter. The black dot represents the commercial solution. Symbols represent different scalings of axial length.

mass of the machine.

7.2.2 Bicycle Motor Design

The bicycle motors have much different requirements than the cheetah that result in a vastly different motor. This is a traditional application, requiring relatively constant torque for a long period of time, so it is better served by existing machinery. Rotational inertia is less of a concern, as the bicycle does not accelerate quickly (by cheetah standards), allowing for an outrunner configuration where the rotor is on the outside of the motor. This moves the airgap radius further out, increasing torque production with the same shear force on the rotor. By moving to larger numbers of phases, rectangular drive, and larger diameters, performance gains may be realized over commercial solutions even when assuming cheap, lower-performance materials.

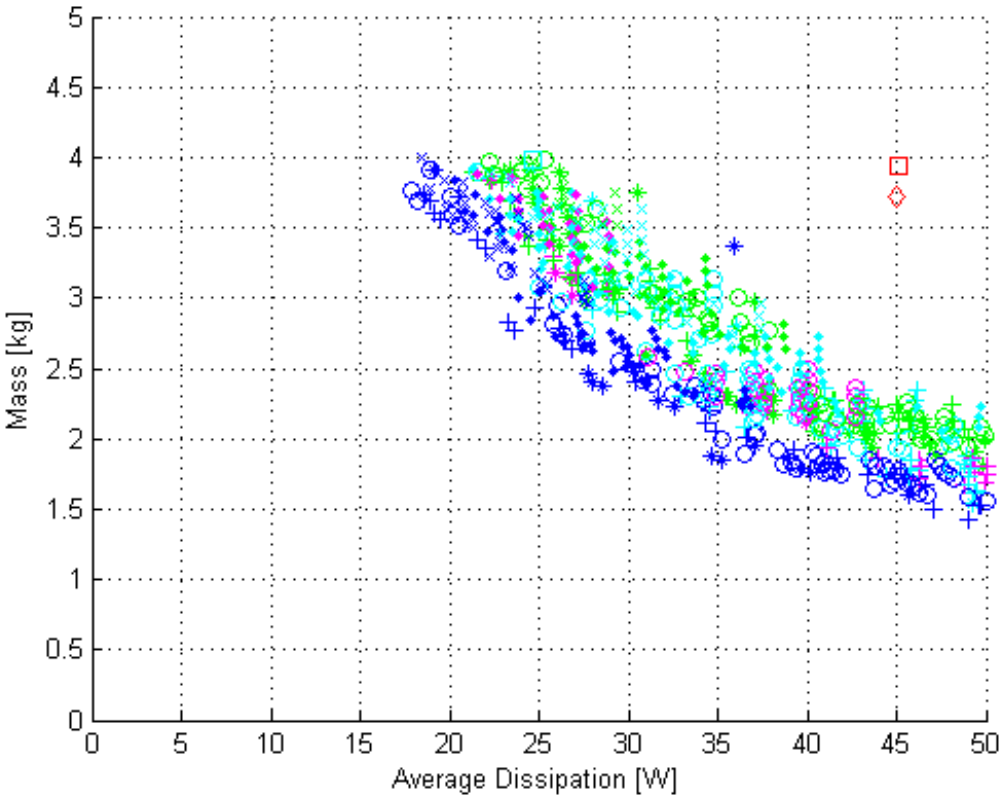

Figure 7-26: M19 and 1T Magnets at .5x diameter including core loss. Symbols represent different scalings of axial length.

In a machine that has twice the diameter, approximately 33% of the mass may be removed. Additionally, this outrunner configuration allows for ease in winding the machine. Windings may be wound on a bobbin and then simply slid over a tooth.

The optimum topologies here have small magnets, meaning that the windings produce a larger portion of the flux in the machine. This has benefits for core loss as well, especially when undriven. In a direct-drive application without a freewheel, a rider must spin the motor while pedaling when the motor is not assisting, meaning that the rider fights core loss in the machine. In the case of a machine that is a smaller diameter which is geared, this loss number may become significant.

7.3 Summary

The modeling/design technique shows significant improvement in both applications at opposite ends of the design spectrum. Good (expensive) steel is a significant fraction of the improvement in the cheetah motor, but the design technique shows improvement over the generation-2 machine [19], which also uses good steel, in the same mechanical envelope. Factors related to the improvement include the use of a square current waveform drive, a high number of phases, and an exhaustive sweep of one region of the design space. A 24% increase in torque density at the same dissipation was predicted for the switch to a square drive [20], and the design study suggests this is about right, to the limit of the difficulty of comparing machines across torque capacity (the machine in [19] is heavily-saturated by the time it reaches design torque).

For the bicycle motor, advantages are less obvious in a machine of equivalent mechanical envelope, but there are several conservative assumptions that could drastically improve these numbers beyond parity. Allowing the selection of larger diameters is shown to dramatically improve performance (again, in the space of mass and efficiency), even with the same conservative assumptions. Geared machines may potentially be used to decrease mass, but require mechanical complexity (a gearbox and a freewheel) to be useful.

Chapter 8

Cheetah Motor

This chapter focuses on the fabrication and experimental performance of the Cheetah motor designed in Chapter 7. The design for the motor was chosen from the locus of points shown in Figure 7-9. The design picked represented the knee in the curve, or the point that lay on the parabola closest to the origin. The design space was restricted to eight phase machines with no more than nine pole pairs. Eight phases or fewer was dictated by the power electronics architecture in the motor drivers, and 9 pole pairs represented a design that was considered buildable. Additionally, 8 phases would allow a close comparison with previous theoretical work [20]. Drawings for the designed machine are contained in Appendix F.

8.1 Construction

The machine was constructed at Walco in Providence, Rhode Island. The steel in the rotor backiron and stator were laser-cut before being annealed and laminated at an unknown third party. Magnets were sourced from a different vendor, and represented the long-lead item in construction. They were epoxied to the rotor core with spacers between each to maintain proper spacing, as they are strongly attracted to both each other and the rotor core. After a mishap in ordering the laminations, the OD of the rotor backiron had to be turned down by approximately 0.5 mm to meet specification. The process may have introduced shorts between laminations, which would increase

core losses. This is less of a concern on the rotor, as it does not see changes in the magnetic flux. The stator was also delivered with a backiron 0.5 mm thinner than specified, resulting in reduced torque predictions, which are included in figures in this chapter. The machine was then wound by hand with six turns of five strands of 27 AWG wire.

After delivery, the machine was first pressed into a spare motor housing for the cheetah, but with the 6:1 planetary gear reduction removed. Figures 8-1 and 8-2 show the machine mounted in the housing. To press the stator into the housing, the rotor was minimally inserted by hand. The assembly was then placed upon a foam pad, and the housing was struck with a mallet, pressing the stator into the housing by taking advantage of the momentum of the relatively heavy stator. The rotor was fitted to a 3-D printed spacer which had keys on both the inner and outer surfaces to constrain slip between the parts. The machine was then assembled by clamping the stator to a bench and inserting a 1/2" rod through the holes in the housing and slowly lowering the stator into place. A magnetic shaft encoder sits in the housing, consisting of an integrated circuit and a magnet on a post. These pieces may be seen in figure 8-1.

8.2 Test

The motor constant of the machine may be determined from the Back Electromotive Force (Back EMF) or by driving current in the windings of the machine and measuring torque. The motor constant is the relationship between the voltage and speed of the machine. It is also the relationship of current to torque if saturation may be ignored. In the case of the cheetah, it may be ignored if the machine is kept within the design specification, as it is roughly linear until saturation, which is predicted to happen around 75 A in this design.

There are many ways to justify the linear relationship between voltage and speed, and current and torque. From first principles, a wire loop rotating through a magnetic field will produce a voltage equal to the change in flux through the loop. Faraday's

Figure 8-1: Stator (left) and permanent-magnet rotor (right). Circuit board is magnetic encoder. Orange cylinder is the 3-D printed spacer with keyways. Shaft encoder is visible in the center of both rotor (magnet on post) and stator (integrated circuit).

Figure 8-2: Assembled machine in cheetah housing

law states that $V = \frac{d\phi}{dt}$, where V is the terminal voltage at, and phi is the flux linked by, the loop. Then $V = \frac{dBA}{dt}$, where A is area of the loop and B is the magnetic flux density in the loop. Removing constant terms, $V = B\frac{dA}{dt}$, $A = l * w$, where A is area of the loop, l is length of the loop, and w is width of the loop. Effective area varies with the cosine of the angle of incidence of the magnetic field. Voltage is then, $V = B * l * w * \sin\theta \frac{d\theta}{dt}$, $\frac{d\theta}{dt} = \omega$. Therefore, $V = B * l * w * \omega * \sin\theta$.

A magnetic field exerts a force on a wire carrying current. The Lorentz force law tells us that $f = I \times B$, where f is force per unit length, I is current, and B is magnetic flux density. Force per unit length may be multiplied by radius to calculate torque per unit length, and then by length Torque = f $*$ l $*$ w = l $*$ w $*$ B $*$ I $*$ $\sin\theta$. Comparing the two equations, $V = B*l*w*\omega*\sin\theta$ and Torque = l$*$w$*$B$*$I$*$$\sin\theta$, the constant $B * A$ (coincidentally flux!) may be removed from both. This results in $V = k * \omega$ and Torque = k $*$ I.

It is important to note that the torque constant derived from the back EMF is not affected by saturation due to current in the windings. The motor constant derived from driving current in the machine and measuring torque measures the *incremental change in flux density by the current in the windings*. Given that the magnets dominate the magnetic field in the machine and that the slope of the BH curve for the material is non-linear, reaching saturation just beyond the operating point, one expects that the motor constant derived from current-torque experiments will necessarily be lower than that from the back EMF measurement (that does not include current).

8.2.1 Back EMF

For the back EMF test, scope leads were attached to each phase of the machine, and the machine was spun by hand. In the test machine, both ends of each winding were available, as the star point was not buried in the windings. The star point was shorted among the 8 phases and grounded. Figure 8-3 shows the resulting waveform of four of the eight phases. Figure 8-4 is a closer view of the waveforms of interest.

The motor constant may be backed out of the zero crossing times for a phase

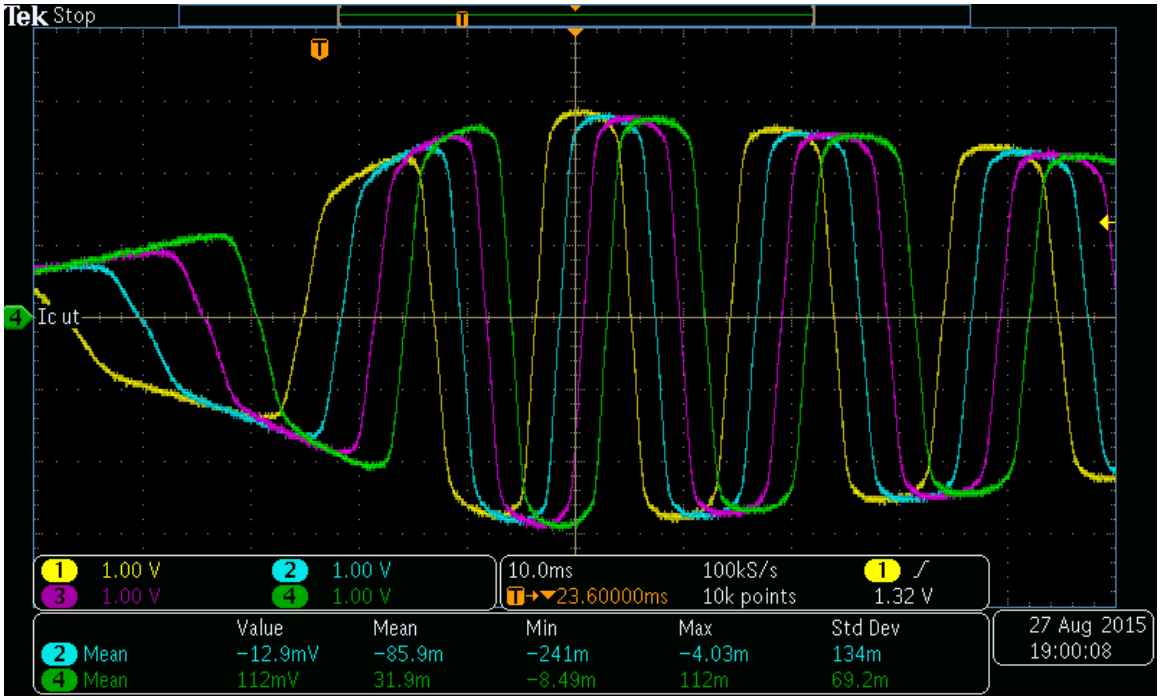

Figure 8-3: Back EMF of phases 1-4 when rotor is spun by hand

Figure 8-4: Back EMF of phases 1-4 when rotor is spun by hand

# magnets	18	-	18	-
# phases	8	-	8	-
half cycle time	9.6E-3	s	8.8E-3	s
Time for revolution	0.1728	s	0.1584	s
speed	36.3610	rad/s	39.666	rad/s
Voltage	2.6	V	2.9	V
k per phase	7.1505E-2	-	7.3109E-2	-
k_e (sum of phases)	0.572	-	0.585	-

Table 8.1: Table showing calculation of motor constant from two instances of back EMF measurement

and the maximum amplitude. The time between zero-crossings corresponds to the amount of time taken for the rotor to rotate one half of a pole pair. Note that this result does not include saturation, nor does it include spatial factors. Table 8.1 shows the results taken from Figure 8-4 as well as a different recorded waveform.

8.2.2 Torque Measurement

To measure torque, the housing was mounted to a milling turntable. A spare cheetah leg section was mounted to the output flange, which was in turn connected to a load cell. The load cell is anchored to a block clamped to the edge of the turntable, which is placed to produce a 90° angle between the output leg and the load cell. Knowledge of the radius of attachment allows calculation of the torque of the machine. The turntable allows rotation of the housing, allowing torque to be measured at different points in the rotation of the machine. This experimental setup is shown in Figure 8-5.

When the machine was constructed, both ends of each coil were brought out of the stator, meaning that the star point was both available and unconnected. This eases measurement of back EMF and torque measurement. To measure torque, since the machine is designed to be driven with a square torque waveform, phases 1-8 are all simply connected in series. Care must be taken to wire the phases in a manner that produces a magnetic field and flux in the direction of constructive interference. The winding diagram is included in Appendix F.

To verify the winding diagram, the machine was spun by hand while watching the

Figure 8-5: Photo of test setup, showing motor mounted in housing. Housing is mounted to milling turntable, and output arm is connected to load cell. The phases are connected together with the terminal block shown at the upper-left of the photo.

Figure 8-6: Scope trace of phases 1,2,5,6

back EMF on phases 1, 2, 5, and 6, as phases 1-4 and phases 5-8 had been separately compared in previous tests. This result is shown in Figure 8-6. This shows the relative phasing of the four phases. The star point was then connected input-1, 1*-2, 2*-3, 3*-4, 4*-8*, 8-7*, 7-6*, 6-5*, 5-output. The resistance of a single phase was calculated to be 0.1667Ω and measured to be 0.1825Ω. This difference may be likely attributed to a difference in end-turn length from that assumed by the model.

To measure torque, a constant current was placed in the windings, all connected in series, and the machine was stepped through positions. The output of the load cell was measured on a multimeter. Figure 8-7 shows close agreement of the measured data to simulated data. This experiment used currents that could be comfortably placed in the windings continuously. They are well short of values where any sort of saturation behavior is expected.

Figure 8-8 shows the performance of the machine at high current. The machine matched well at the two lower currents, but fell 8% short at the maximum design current. The data matches well at 40 A and 50A, which suggests that saturation behavior matches well in this range, but that the machine is more heavily saturating

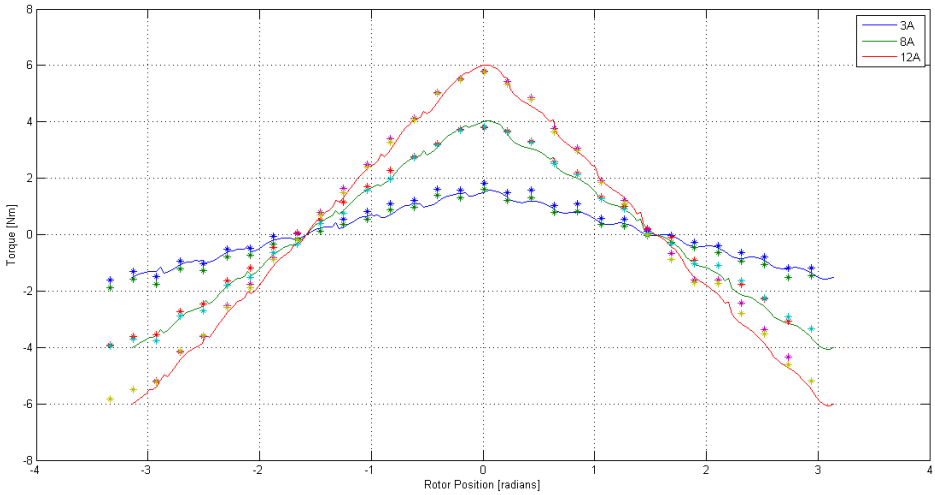

Figure 8-7: Comparison of simulated and measured torque at low current. Asterisks are measurement, lines are simulated data.

than predicted in the 60 A range. The saturation properties of the material in question are sensitive to strain [27], and residual strain from press-fitting of the motor in the housing, or any other assembly or machining process, may have adversely affected the saturation flux density in the stator.

A look at the measured steel data from Chapter 6, shown again in Figure 8-9, provides an alternate explanation. The simulation predicts a maximum flux density of 1.7-2.1 T, depending on rotor position, in the teeth with 60 A in the windings, 1.68-2.1 T at 50 A, and 1.65-1.96 T at 40A. Above 2 T, the difference in field strength (H) required to drive flux in the delivered steel versus the manufacturer data used in the simulation becomes greatly different.

8.2.3 Summary

An 8-phase motor was constructed and its performance measured on the test stand. The machine matched predictions very well at low current and at moderately high current. It performed slightly worse than expected at high currents. This may be explained by manufacturing tolerances or by residual strain in the stator material imparted by pressing it into the housing.

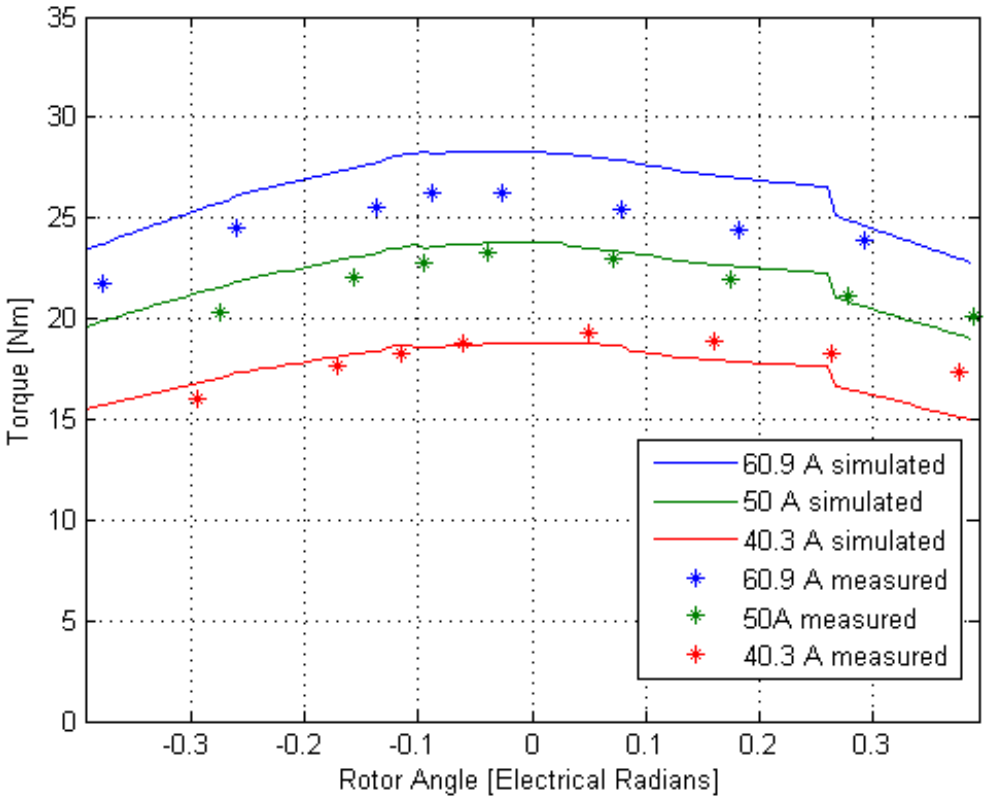

Figure 8-8: Comparison of simulated and measured torque at high current. Asterisks are measurement, lines are simulated data.

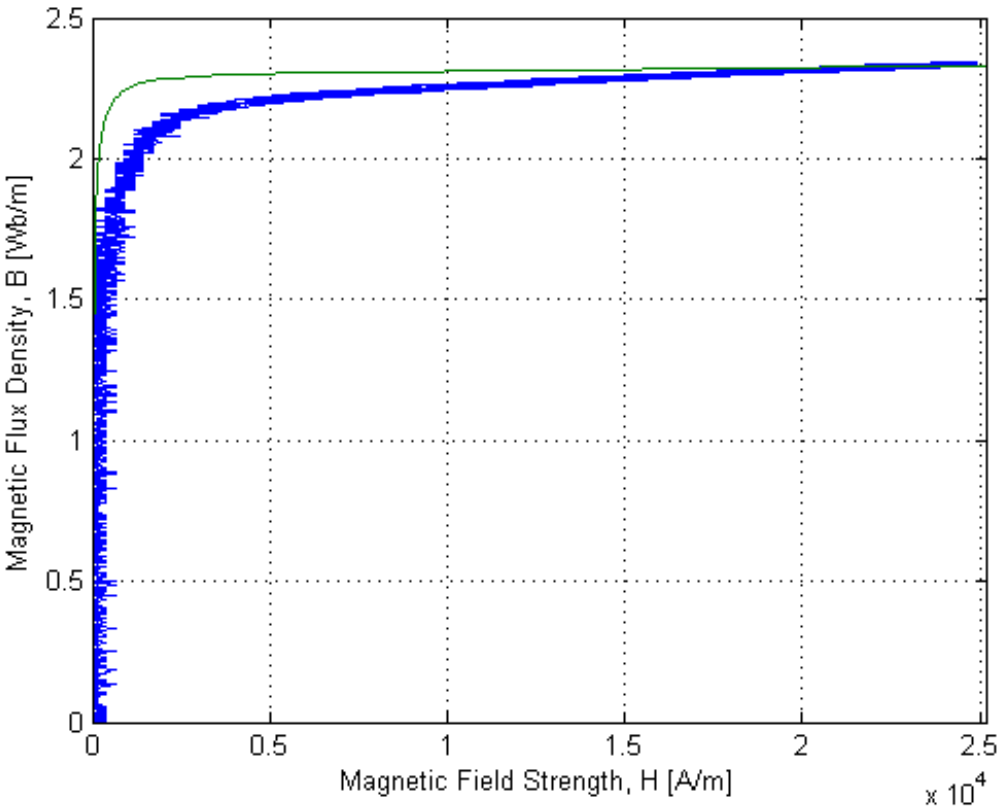

Figure 8-9: BH Curve. Green line shows manufacturer data, Blue line shows measured data.

Chapter 9

Optimal Drive

9.1 Problem Statement

The eight-phase cheetah machine has been designed assuming a square current drive, meaning that all of the phases are driven with the same current, and a phase switches from a positive value of that current to a negative one during a commutation event as the rotor turns. Bannerjee [20] proved that this is the ideal way to drive a machine to maximize torque per mass when saturation in the steel is not considered. Such a pattern most effectively uses steel in the backiron.

To arrive at this conclusion, he considered torque production from each harmonic of the rotor and stator magnetic fields. The rotor field is dominated by the permanent magnets, and their radial field pattern is effectively a square wave in space. Shifting the corresponding harmonic component of the tangential field produced by the stator to produce maximum torque results in a triangle wave pattern. This is illustrated in Figure 9-1.

The tangential field is produced by windings in the stator. The current pattern which produces a triangular field pattern is the spatial derivative of the field pattern, or a square wave. This may be more easily seen with Lorentz's law, $f = q\,(E + v \times B)$, or neglecting electric fields, $f = I \times B$. Anywhere there is a radial magnetic field, there should be an axial current to produce the maximum amount of torque.

Add in saturation, and the problem reasserts itself. The question then becomes

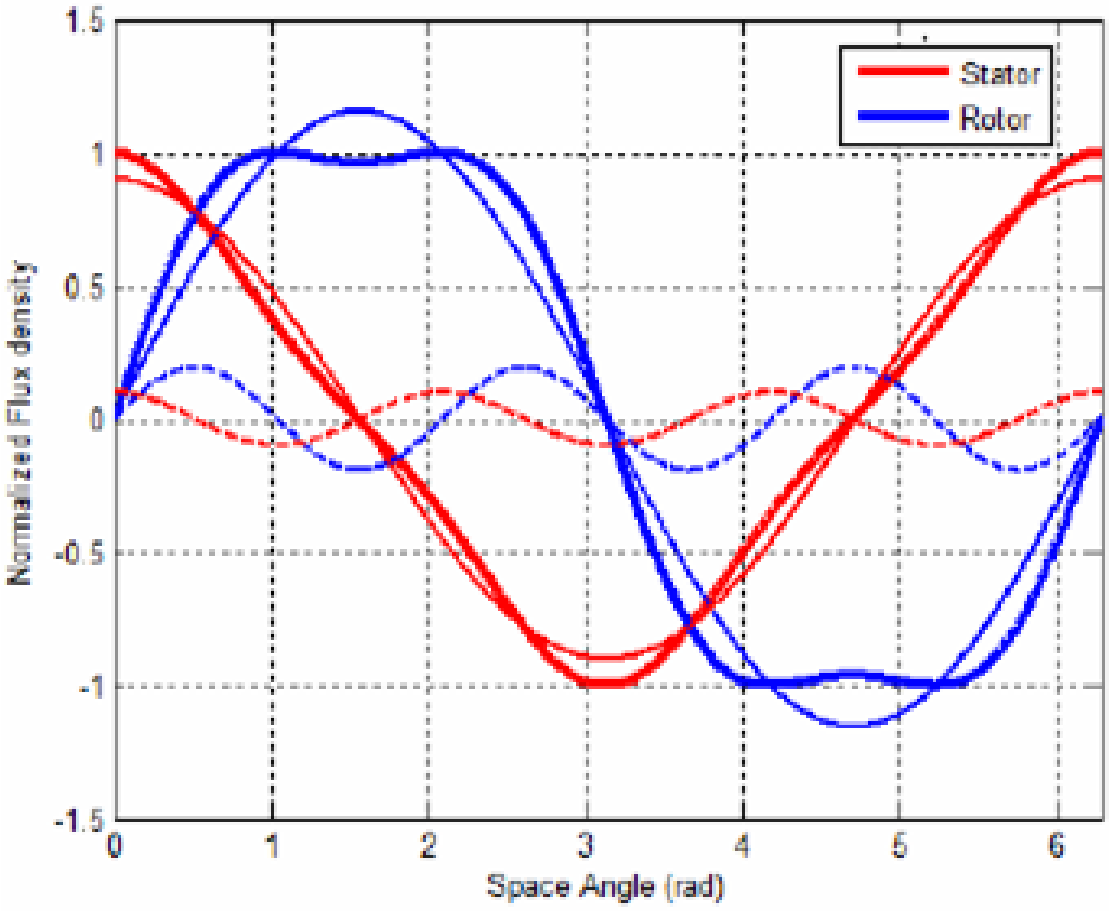

Figure 9-1: Addition of harmonic components of rotor and stator fluxes [20]

how to optimally distribute current in the windings to make the maximum amount of torque with total dissipation held constant.

9.2 Method

The modeling methods developed in the previous chapters enable this solution to be achieved by Monte Carlo methods. The simplest method is to sweep a given number of currents in each phase.

Start by normalizing the design drive current to one. Currents for each phase are then selected in turn from a list of potential scalings. The scalings are squared, summed, and normalized to one. They are then scaled by the original design drive current, thereby holding dissipation in the machine equal to that of the original square-wave design case. The torque produced by the motor is then calculated by the model developed in Chapters 2, 3, and 4. Results from two rotor positions (centered on a pole and at the edge of the commutation window) are shown below.

9.3 Results

In the case where the rotor is centered on a pole, the optimum solution represents only a 0.38% advantage in produced torque. Figure 9-2 shows the torque curves associated with the square drive and optimal drive. Figure 9-3 shows the distribution of current. The waveform has more current concentrated in the slots in the center of the pole and less at the edges. While this is not a large victory for torque production, the shape lends itself to easier commutation, requiring less current swing between phases.

In the case where the rotor is offset but still at the edge of the commutation window, the effects are much more obvious. At the edge of the window, the optimal drive results in a 4.04% increase in torque when dissipation is held constant. Figure 9-4 shows the torque curves associated with the square drive and optimal drive. Figure 9-5 shows the distribution of current. This, too, is a shape that eases commutation, requiring less change in current during the commutation event.

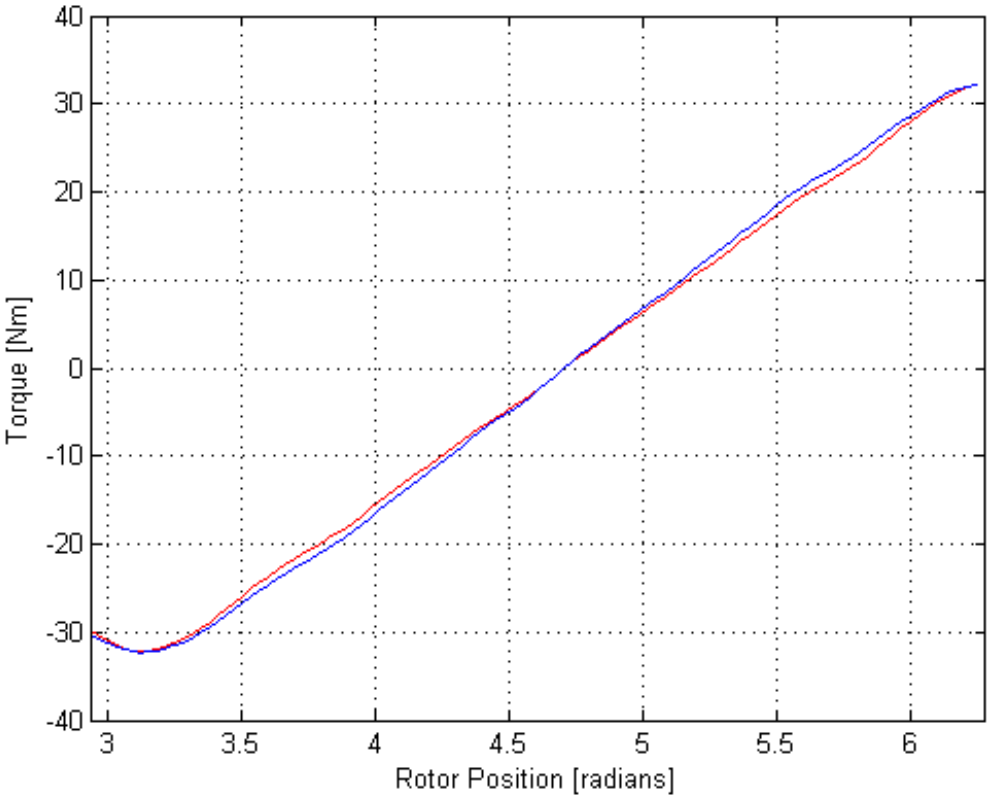

Figure 9-2: Optimal drive (blue) vs. square drive(red) across rotor position

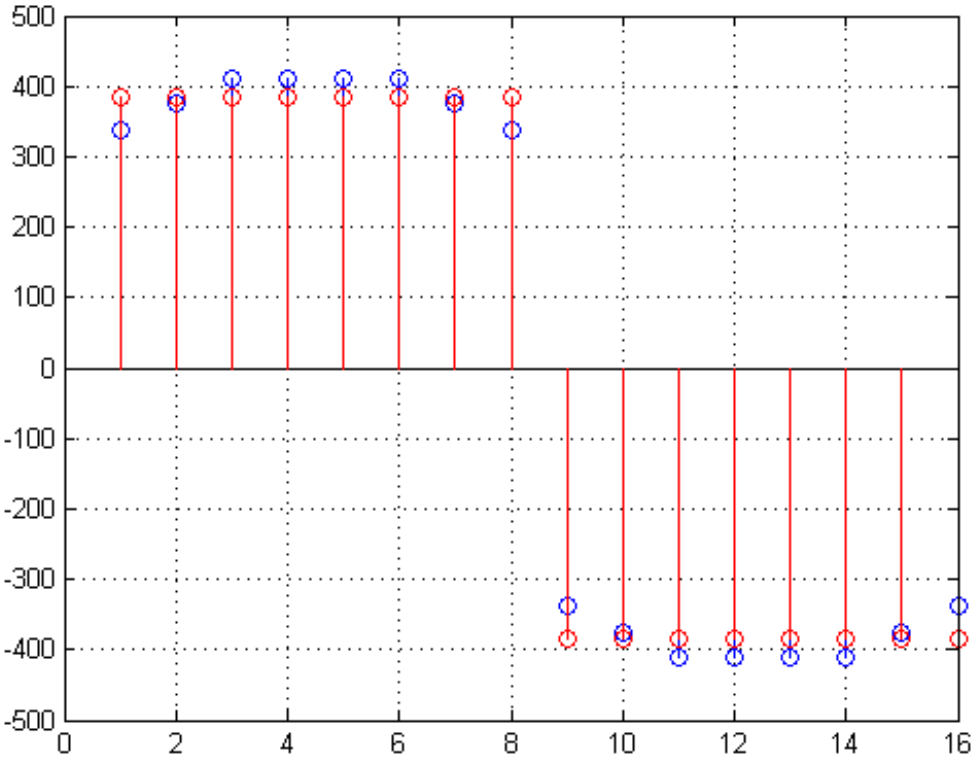

Figure 9-3: Optimal drive currents (blue) vs. square drive currents (red)

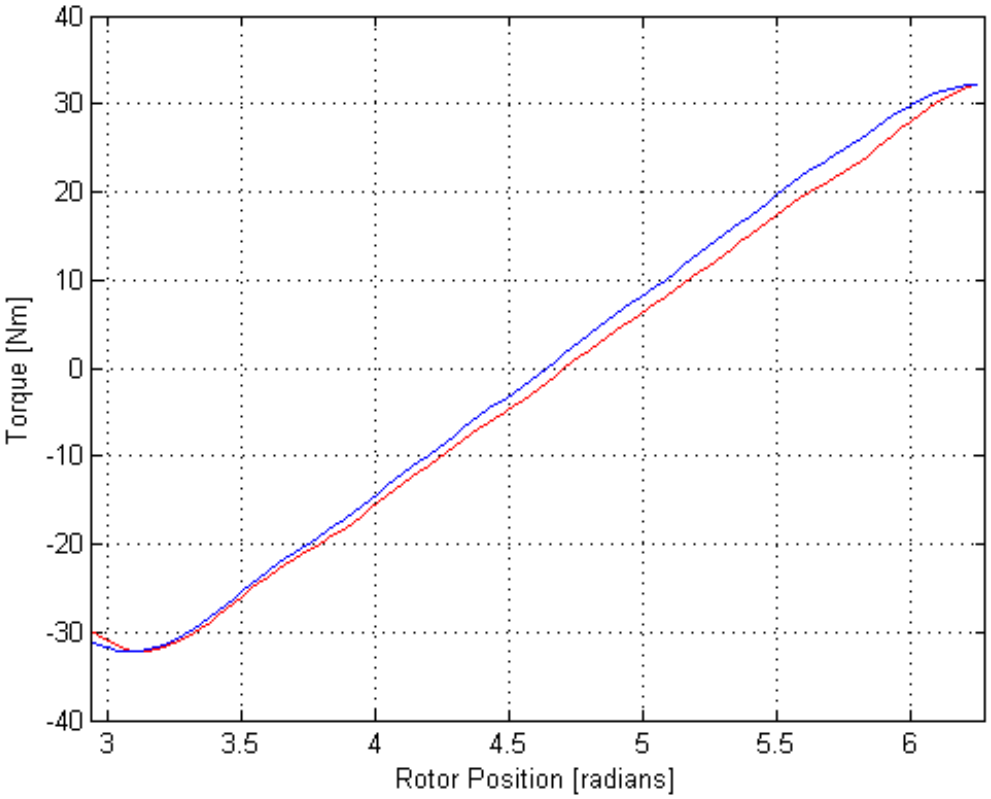

Figure 9-4: Optimal drive (blue) vs. square drive(red) across rotor position

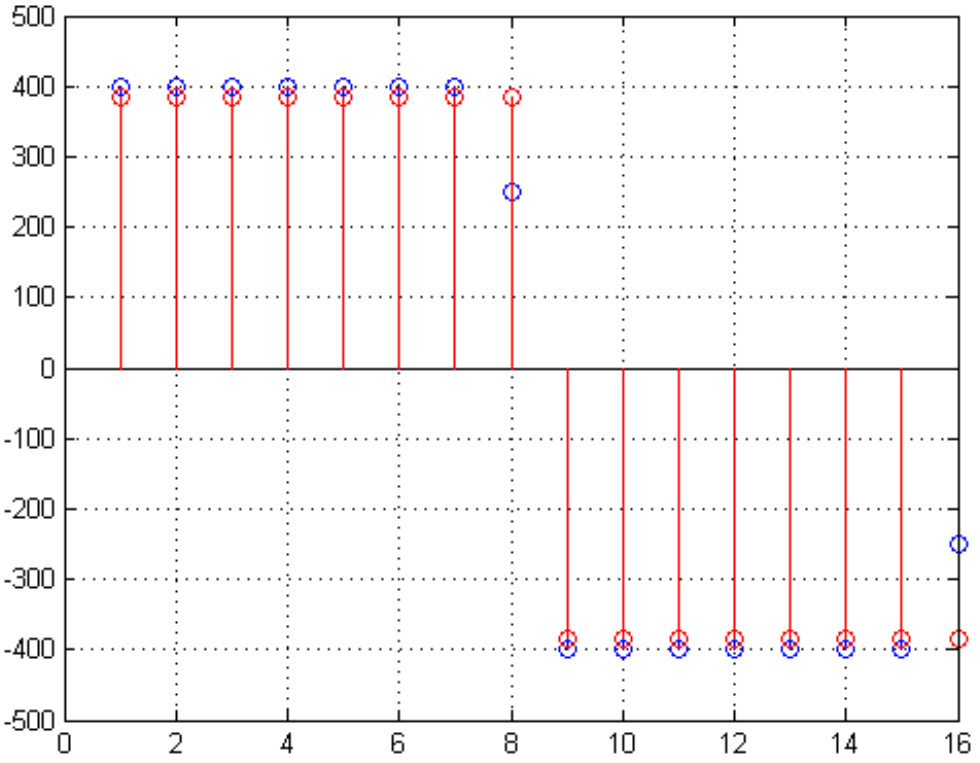

Figure 9-5: Optimal drive currents (blue) vs. square drive currents (red)

9.4 Summary

A fast, accurate modeling method allows sweeping possible winding excitation patterns to find the optimum torque per copper loss. When the rotor is in the center of the commutation window, there is not much torque to gain. When the rotor is at the edge of the window, however, torque production may be increased by more than 4%, helping to smooth torque ripple. Additionally, the current waveform has less current at the edges, making it easier to perform commutation operations.

Chapter 10

Build

The following chapter is based on an interview with Paul Boisse, the head winder at WALCO, a company specializing in motor winding in Providence, Rhode Island, who built the electric machines described in this thesis.

A permanent-magnet synchronous machine has four main parts: the stator, stator windings, magnets, and rotor core. The most expensive and time-consuming step in the process, especially for a machine built in small quantities, is winding the stator. This step dominates nearly all considerations for construction.

There is nearly infinite freedom in cutting the rotor core and stator, as the individual sheets are laser cut or punched before being annealed and laminated. These processes have few if any limitations on geometry on the scales corresponding to a motor for the cheetah. It must be noted that the rotor core does not need to be laminated, as flux does not change significantly during operation. In this case, the material used for the rotor core is a byproduct of cutting the laminations for the stator, so it is used.

Magnets are sintered from powdered material, so they may be made in nearly any shape before being nickel-plated. So long as the magnetization pattern isn't more complicated than magnetizing in a linear or radial direction, a designer is mostly free to specify magnet shapes.

Winding a machine is performed by specialized machines, or in cases of prototype or small production runs, by hand. Issues with winding apply to both situations.

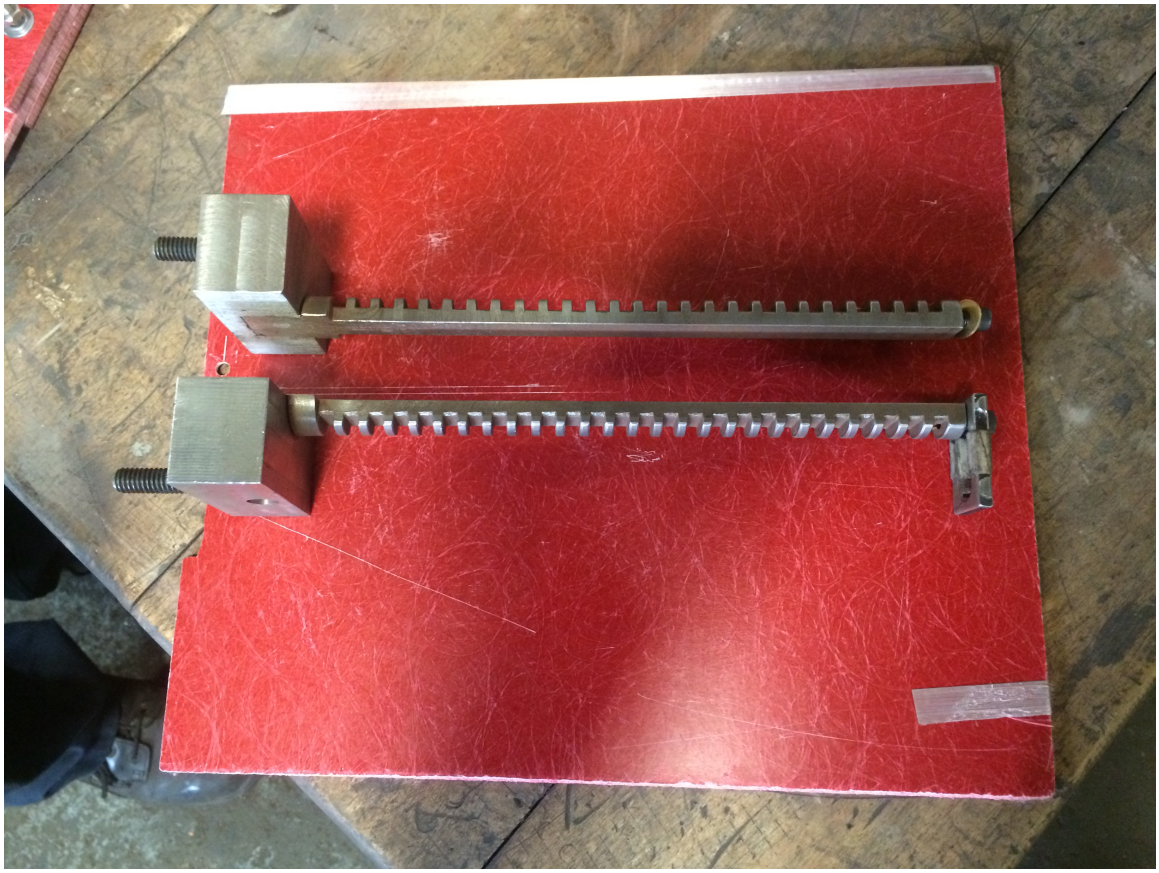

Figure 10-1: Winding form

First, the windings are formed on a machine. Figure 10-1 and Figure 10-2 show the forms upon which the windings are formed from straight wire. The two parts are situated the correct distance apart, and wire is fed on to them as they are spun by the machine, which also properly tensions the wires. This is done for two reasons: first, to eliminate the requirement to form the windings by hand while being threaded into the slots of the machine, and second to prevent the wires from being bent over the edges of the stator core and slot liners, leading to insulation failure. For the motor in question, the appropriate spacing between the forms was too small for the machine, so it was wound by hand outside of the machine. Figure 10-3 shows the installation of the pre-formed coils.

The number of phases represented an organizational problem as well. The winders have specialized racks that are intended to organize three phases of windings. Keeping 8 phases organized and accessible in such a small machine proved to be an issue.

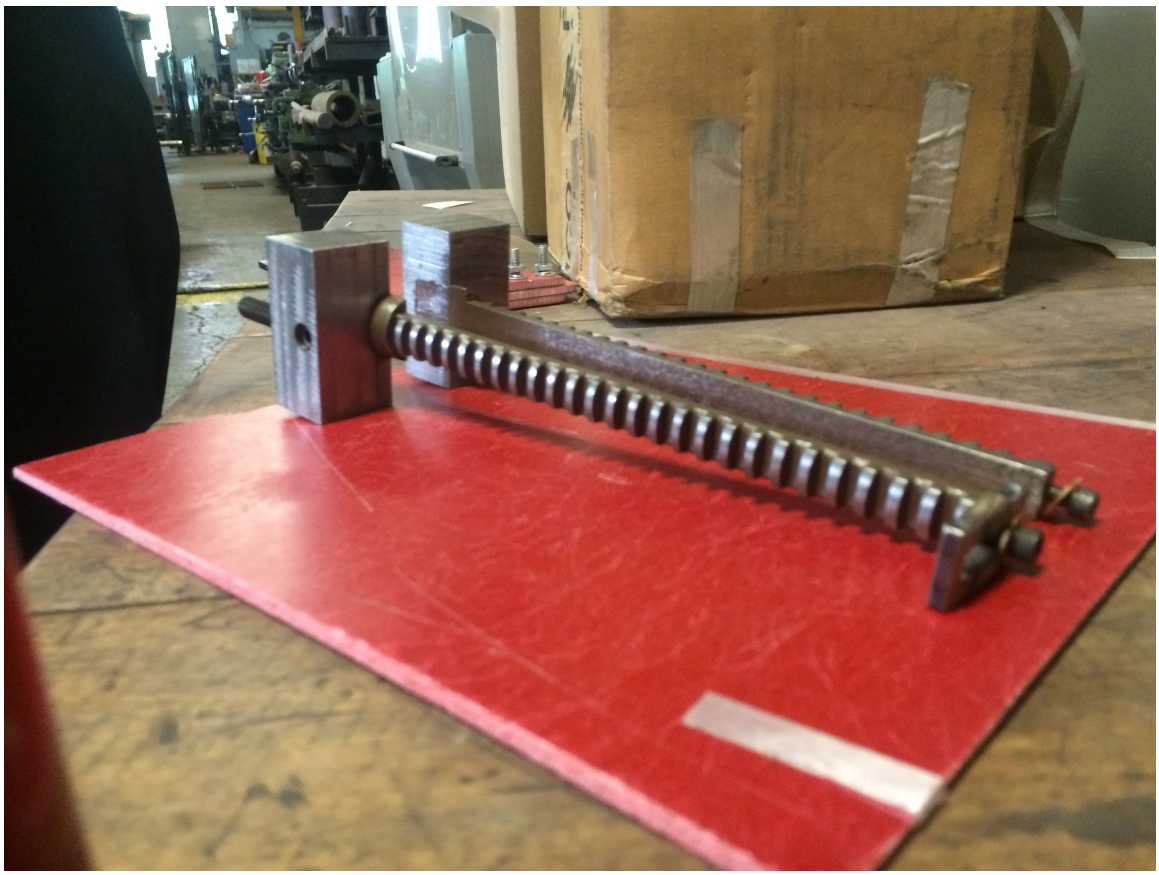

Figure 10-2: Winding form

Figure 10-3: Winding process

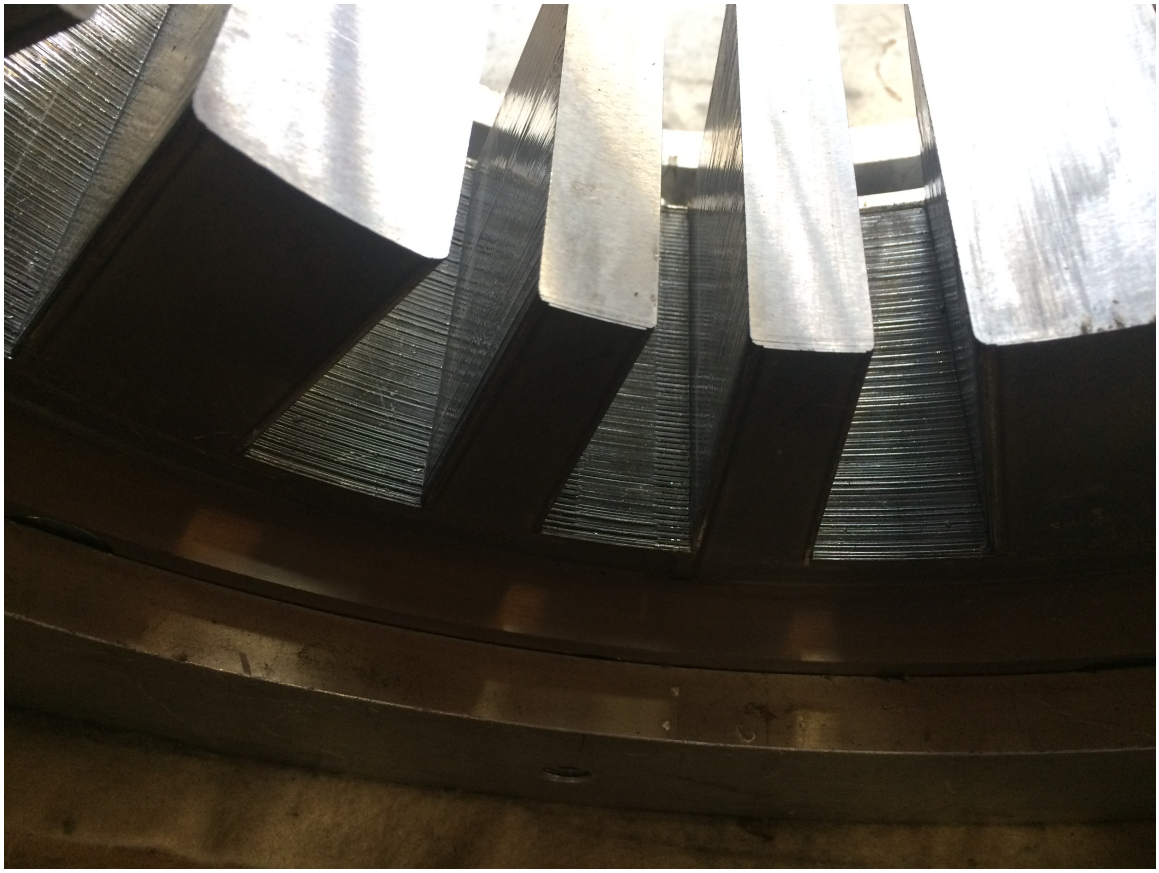

Figure 10-4: Chamfered edges on example electric machine stator

The slots in the machine are then lined with Nomex liners of varying thickness. These are used to protect the insulation on the wire from the sharp edge formed by the edge of the slot. The laminations used to make the rotor core and stator are laser cut or punched from thin sheets of very hard material, resulting in sharp edges that will easily slice both skin and winding insulation. Nomex breaks down when repeatedly stressed, so pre-forming the windings helps to prevent breakdown of the material. To help alleviate some of this concern, edges are often chamfered by opening the slots in the outermost laminations. The angle of the chamfer isn't terribly important. Figure 10-4 shows the edges of teeth in a motor where the slots have been widened in the outer laminations.

Windings themselves are the time-consuming step of the process. The rate-determining step is the number of wires that may be fed through the opening in the slot at one time. In the 8-phase machine built for the cheetah, only one wire

could be pulled through the slot at a time. For this machine, special tools were constructed to enable the installation of windings. Figure 10-5 shows the scale of the slots.

Winding each machine has an associated learning curve when wound by hand. For the 78-tooth Generation-2 Cheetah motors [19], the first ones took one winder more than a week of 8-hour shifts to wind. By the end, some 10 machines later, each machine could be wound in four days. Similarly, the 144-tooth 8-phase machine of Chapter8 took 8 days of 8-hour shifts to wind. They expect a similar learning curve to the 78-tooth machine, as the total number of windings in each is approximately the same (6 turns in the 8-phase machine vs. 12 turns in the gen-2 machine).

Skewed stators present added complexity in the winding process. Geometrically, the skewing process reduces the size of the opening between teeth as well as the area allotted for windings by the cosine of the skew angle. On a machine with a short stack length and small numbers of teeth, this can be severe.

Once the windings have been placed in the machine, wedges are used to capture the windings and slot liners. These, too, are made of Nomex. They come in standard sizes and are commercially available from EIS, Essex, and Brownell. Teeth must be closed to use this method of assembly. The small triangles on the tooth tips that close the slot help eliminate cogging torque, but are also necessary to form a mating surface for the wedge. Wedges are shown in Figure 10-7.

Finally, windings are pressed to make the machine fit in an allowed axial window. For the 8-phase, 144-tooth machine, end turns were made as small as possible on the winding forms and, due to the small axial length of the core, did not need to be pressed. For the 78-tooth machines, the windings had to be pressed after assembly to fit in the same axial envelope. Toothpicks were used as spacers to prevent each turn from cutting through the slot liner on the sharp edge of each slot. Additionally, when pressing the skewed stator machines, further care was required. The windings in the skewed stator were trapezoidal, so they would collapse instead of mushroom when pressed, so they had to be supported.

The windings in these machines are *distributed*, meaning that they span multiple

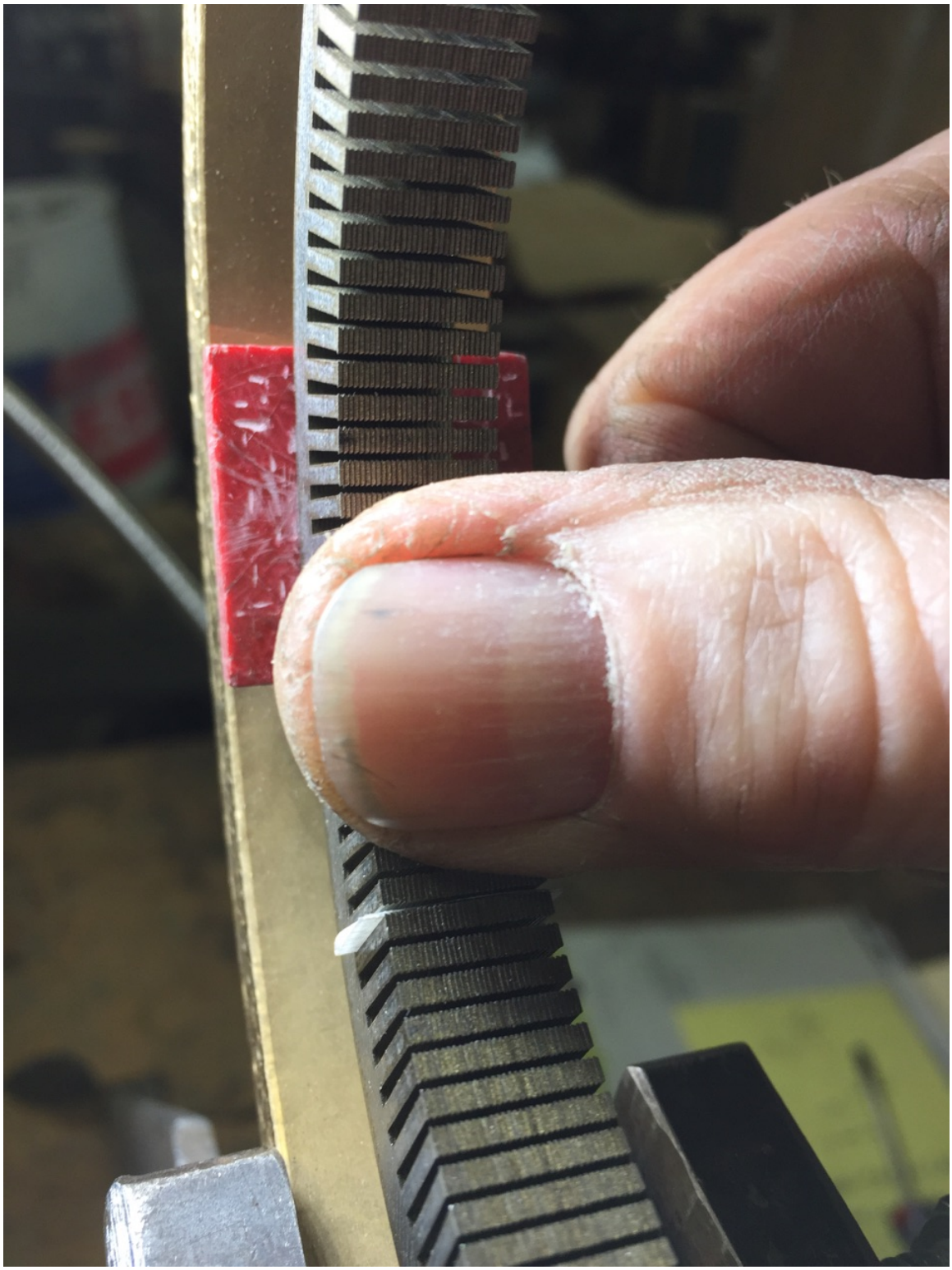

Figure 10-5: Slots next to thumb

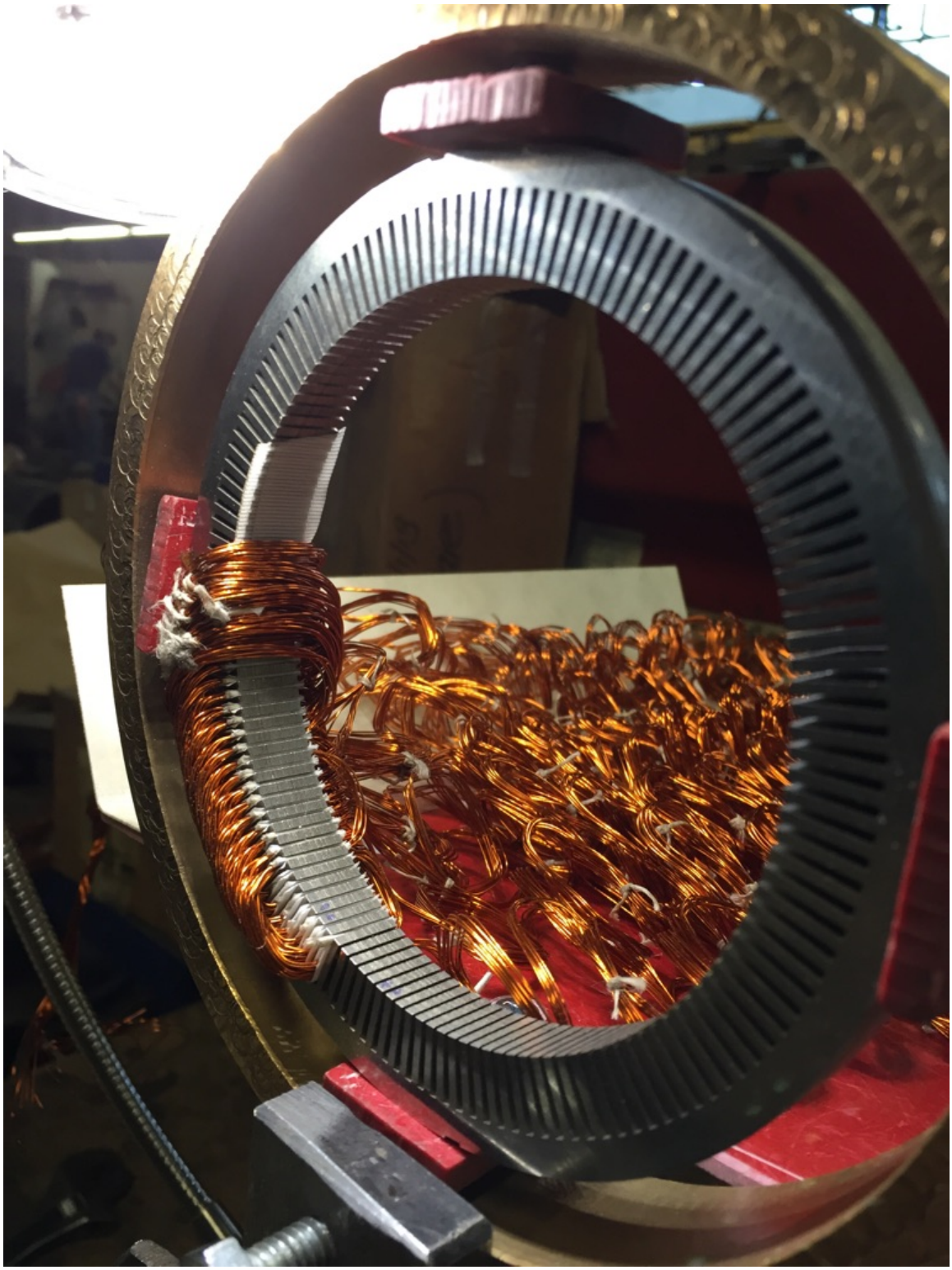

Figure 10-6: Winding process

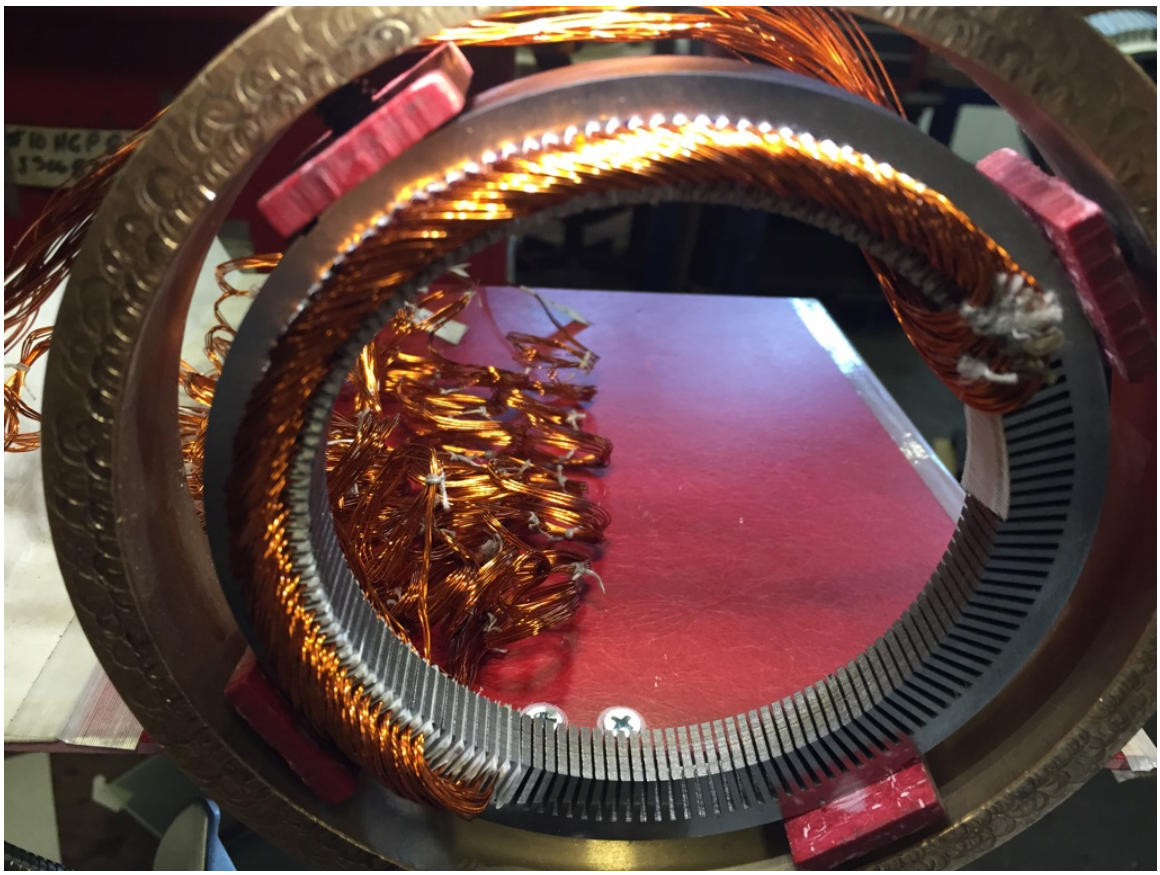

Figure 10-7: Winding process

teeth. Specifically, one side of the winding passes through the stator one direction in a slot in a pole, and the other side passes through the stator in the opposite direction in the corresponding slot in the subsequent pole. In this manner, the winding is continuous around the machine without interruption. Motors may also be wound with a *concentrated* winding, which wraps around each pole in the machine. Such windings present their own challenges, as the end turns must be sufficient to allow the winding into the slot and are then pulled tight. Geometric concerns also present interesting challenges when winding the subsequent tooth.

The method of securing the machine in the housing has little effect on the construction of the machine. Of the machines constructed at Walco, 20% of motors are press fit into aluminum housing and 80% are keyed or use radial pins to secure the motor. Keys may be included in the individual laminations at the laser cutting or stamping phase, or they may be cut into an assembled motor, so long as care is taken to not short the windings.

10.1 Summary

The overall size of the machine makes winding by hand or machine difficult. In a machine the size of the cheetah machines, there simply is not much room to work, for either a robot or a human.

If wire will physically fit in a slot whose area is adjusted to account for slot liners, a machine may be wound. The difficulties in winding come from the width of the opening between teeth. This parameter limits the number of wires that may be inserted in the slot at a time, and is the rate-determining step of the winding process. Unfortunately, this parameter is driven to a minimum value by the desire to minimize cogging torque.

The next most important parameter is the axial envelope in which the machine must fit. In designs where the stack length of the stator laminations takes up the majority of this envelope, the end turns must be wound tight or pressed to the envelope after winding. If there are enough poles such that the length of the end

turns is minimized, this process is made easier.

There is a significant amount of time spent building tools to wind an unusual machine such as the eight-phase machine presented here. The winding bobbins and organization racks for the windings were something completely different than what Walco had used before, and had to be assembled specifically for this machine.

All things being equal, the number of teeth does not factor significantly in the build process. The 78-tooth and 144-tooth machines have approximately the same number of strands of copper (similar bundle, twice as many turns in the 78-tooth machine). Since the slot openings are approximately the same relative to the strands of wire used, build time is very nearly the same.

Chapter 11

Summary, Conclusions & Future Work

11.1 Summary

In Chapters 2 and 3, this thesis covered the development of a novel, fast modeling method for permanent magnet machines consisting of a hybrid model of an explicit maxwell solution and a flux tube solution. It then showed, in Chapter 4, how they could be stitched together and forced to converge. This captured effects such as cogging torque as well as saturation of the core materials. The modeling method was implemented for two topologies of surface-mount permanent-magnet machines. Chapter 6 showed a nearly-exact match with the performance of the Generation-2 Cheetah motor. Chapter 7 details how it was then used to optimize machine design to a given drive cycle, including effects of core loss. In Chapter 8, a machine was built to demonstrate the validity of the model and optimization method and test results matched predictions. Chapter 9 used the modeling method to determine the optimum current pattern for torque per dissipation.

On a parallel track, methods for reducing or eliminating cogging torque were explored in Chapter 5. Two types of machines based on the Generation 2 Cheetah machines were built to demonstrate the virtual elimination of cogging: a skewed rotor machine, and a skewed stator machine. Each demonstrated reduction of a particular

Figure 11-1: Comparison of Stators: 8-phase (front), 3-phase gen-2 (middle), 3-phase commercial solution (back). Each successive stator represents an increase in absolute torque production, a decrease in mass, and an increase in efficiency in the application in question.

cogging harmonic or all of the cogging.

11.2 Conclusions

A fast, accurate modeling technique enables identification of global optima across a design space. In the case of the Cheetah, the mass and dissipation of the machine have been drastically improved. Figure 11-1 shows the evolution of the stators of the machines in the Cheetah. This work has resulted in a substantial reduction in mass of small permanent-magnet synchronous machines, and should enable greater performance capabilities for robots.

Chapter 6 shows that the modeling work of Chapters 2 to 4 results in a model

that captures both motive and cogging torque well. Figure 6-9 shows a near-exact match with measured data on the Generation-2 machine. Chapter 8 shows a good match with torque in a region where the 8-phase machine is saturating in Figure 8-8.

Convergence, detailed in Chapter 4, is tricky. It works only in one direction: flux is used as an input to the flux-tube model, and MMF is used as an input to the continuum model. The solution spirals outward in the other case. This process is illustrated in Figure 4-2.

The code developed to run the model runs fast. Chapter 4 shows an improvement of four orders of magnitude in time over FEA of equal accuracy.

Building a machine of this scale with large numbers of teeth is a challenge. From Chapter 10, it is apparent that a machine of arbitrary feature size may be built, but the 8-phase machine is near a point where the machine gets more difficult to build very quickly. Winding dominates that build process. The primary issue is the size of the opening between teeth, as this determines how quickly the machine may be wound.

Chapter 7 explains the design and optimization process. The cheetah machine is optimized for relatively little steady-state torque with short temporal spikes of high torque. The magnets are comparatively large, making up the majority of the flux in the machine. This results in a machine that is heavily biased towards magnetic structure with small windings. In this way, iron, and flux carrying capacity of the teeth is traded with winding area, or current carrying capability.

Larger numbers of teeth generally improve all aspects of performance until the slot liners become a significant fraction of the slot area. Numbers of poles and phases are traded, with an increasing number of phases allowing greater harmonic content in the flux waveform, while greater numbers of poles make the backiron on both the rotor and stator smaller (the amount of flux contained in a pole, and therefore required to be carried by the backiron, is proportionally reduced). Greater numbers of poles increases the ratio between electrical and mechanical frequency, increasing core losses.

The bicycle motors have much different requirements than the cheetah that result in a vastly different motor. Rotational inertia is less of a concern, as the bicycle does

not accelerate quickly, allowing for an outrunner configuration where the rotor is on the outside of the motor. This moves the airgap radius further out, increasing torque production with the same shear force on the rotor. By moving to larger numbers of phases, rectangular drive, and larger diameters, performance gains may be realized over commercial solutions even when assuming cheap, lower-performance materials. In a machine that has twice the diameter, approximately 33% of the mass may be removed as compared to the commercial solution.

The optimum topologies here have small magnets, meaning that the windings produce a larger portion of the flux in the machine. This has benefits for core loss as well, especially when undriven. In a direct-drive application without a freewheel, a rider must spin the motor while pedaling when the motor is not assisting, meaning that the rider fights core loss in the machine. In the case of a machine that is a smaller diameter which is geared, this loss number may become significant.

The work supports the conclusion that larger numbers of phases are a useful design for different types of permanent magnet machines. Greater control over the flux in a machine allows torque production from higher-order harmonics. It also suggests that a machine that produces most of its flux with permanent magnets is an ideal machine for robotics, where peak torques can be many time the average torque. In a machine optimized for continuous torque, designs favor less flux from the magnets, leading to less steel structure, and more space for windings. Steel and magnets dominate the composition of high-torque, low-duty-cycle machines, and windings are the most important part of constant-torque machines.

A fast, accurate modeling method allows sweeping possible winding excitation patterns to find the optimum torque per copper loss as is demonstrated in Chapter 9. When the rotor is in the center of the commutation window, there is not much torque to gain. When the rotor is at the edge of the window, however, torque production may be increased by more than 4% in the cheetah machine, helping to smooth torque ripple. Additionally, the current waveform has less current at the edges, making it easier to perform commutation operations.

11.3 Future Work

The first area that may be expanded is the operating range of potential machine designs. This work assumed that the greatest efficiency would exist in an operating region short of saturation, where the motor constant doesn't drastically change. For this reason, it assumed a linear current-torque relationship, and calculated dissipation with this assumption. Addition of the saturation region would require interpolating values of current per demanded torque to calculate loss.

This modeling technique is applicable to a wide variety of other machines, the simplest of which is a linear machine. The solutions to Laplace's Equation are known in cartesian, cylindrical, and spherical coordinate systems. Such solutions would all the same technique to be used for linear machines, skewing in cylindrical radial-flux machines, cylindrical axial-flux machines, and spherical machines.

The break from a traditional three-phase machines allows several possibilities related to increased control of flux in the machine. The first possibility is performing flux weakening within a pole. A large phase-count machine will happily run if driven on fewer phases, leaving the other phases to manipulate flux in the machine. One can imagine shorting four of the phases and counteracting flux in the machine. This would effectively lower the motor constant, allowing the machine to be driven beyond the design speed of the machine at the same voltage.

The Flux Tube Model could be expanded in an attempt to capture local saturation effects in the tooth tips. The model presented in this thesis achieved remarkable accuracy with a few simple approximations, but required slight modifications to the motor structure to create accurate results. Adding complexity to the Flux Tube Model may increase accuracy at an acceptable run time increase.

The conformal mapping [16] [17] techniques or the complicated field solutions in slots [13] [15] could be combined with the model presented here to add the ability to encompass motive torque and saturation effects. In particular, the field solutions in slots could be integrated with the flux tube model, as the vector potential is easily calculated on the surface of the inside of the slots from the Flux Tube Model. Run

time would likely be slower than the techniques presented in this thesis, however they could offer more flexibility in dealing with hard saturation.

Appendix A

Motor Simulation Code

```
%% includes Rsupplement to properly calculate cogging
%%

function [Torque,Bmaxst,Bmaxsb,converge] =
motorsim5_sawtooth_vector(k,N,thetaRs,delta,fslot,R5,R4,R3,R2,R1,P,s,gap,Lmotor,M0,mdeg)
num_mainloops = 20;
main_tolerance = .0001;
mu0 = 4*pi*1e-7;

%% Data for Hyperco50 - returns muh50 , Bh50 [Tesla], Hh50 [A/m] into global
 hyperco50data;
 % Hmin = min(Hh50);
 % Hmax = max(Hh50);
 % Bmin = min(Bh50);
 %Bmax = max(Bh50);
 mumin = min(muh50);
 %mumax = max(muh50);

 %% A few physical parameters
 oor = R5;
 sbr = R4;
 sr = R3+gap;
 gr = R3;
 cr = R2;
 br = R1;

 %theta used only for calculating areas
 theta = 2*pi/P/s;

 % Stator Back Iron
 Asb = Lmotor*(oor-sbr);
 lsb = theta*(oor+sbr)/2;

 % Stator Tooth
 Ast = Lmotor*theta*sr*(1-fslot); %tooth area
 Astooth = Lmotor*theta*sr*(1-delta); %closed tooth area
 lst = (oor+sbr)/2-sr;

 Torque = zeros(size(thetaRs));
 Bmaxst = zeros(size(thetaRs));
 Bmaxsb = zeros(size(thetaRs));
 Bmaxrb = zeros(size(thetaRs));
 for AA = 1:size(thetaRs,2)

    thetaR = thetaRs(AA);

    %% Define the teeth...
    tooth = 1:s; %1xN
    middles = (tooth-1).*2*pi/s;
    lowtooth = middles-pi/s+delta*pi/s;
    hightooth = middles+pi/s-delta*pi/s;

    %lowslot = middles-pi/s+fslot*pi/s;
```

```
%highslot = middles+pi/s-fslot*pi/s;

lowtotal = middles-pi/s;
hightotal = middles+pi/s;

lowmod = zeros(size(lowtotal));
highmod = zeros(size(hightotal));
lowtotal(s+1) = lowtotal(1)+2*pi;
lowmod(s+1) = lowmod(1)+2*pi;
for kk = 1:s
   if and(hightotal(kk)<thetaR,thetaR<lowtotal(kk+1)) %if magnet boundary between teeth
      highgap = thetaR-hightotal(kk);
      lowgap = lowtotal(kk+1)-thetaR;
      if highgap<=lowgap
         lowmod(kk+1) = thetaR+highgap;
         highmod(kk) = hightotal(kk);
      else
         lowmod(kk+1) = lowtotal(kk+1);
         highmod(kk) = thetaR-lowgap;
      end
   end
end
lowmod(1) = lowmod(s+1)-2*pi;
lowmod = lowmod(1:s);
lowtotal = lowtotal(1:s);
%toothdiagnostic;


%% Define magnets
lownm = (-pi/2-mdeg*pi/360+thetaR)/P;
highnm = (-pi/2+mdeg*pi/360+thetaR)/P;
lowpm = (pi/2-mdeg*pi/360+thetaR)/P;
highpm = (pi/2+mdeg*pi/360+thetaR)/P;

%% Take fourier coefficients of magnetization
Am = M0./k./pi.*(-sin(k.*P*highnm)+sin(k.*P*lownm)+sin(k.*P*highpm)-sin(k.*P*lowpm));
Bm = M0./k./pi.*(cos(k.*P*highnm)-cos(k.*P*lownm)-cos(k.*P*highpm)+cos(k.*P*lowpm));

%magnetdiagnostic;

%% Compute starting fluxes - assume 1T field phased with magnets in stator teeth to start
Dist = sign(sum(Am*ones(1,s).*cos(k*middles)+Bm*ones(1,s).*sin(k*middles),1));
Dist = Dist + (abs(Dist)<1).*(-sum(Dist));
Phis = Astooth.*Dist;%.*.5;
%grab fluxes at edge of teeth as well
Bhighedge = Dist;
Blowedge = Dist;

 muc = 2000*mumin;

 %          figure()
 %          thetat = linspace(0,2*pi/P,1000);
```

```
105     %
plot(thetat,mu0.*sum(Am*ones(1,size(thetat,2)).*cos(P.*k*thetat)+Bm*ones(1,size(thetat,2)).*sin(P.*k*thetat),1)
)
106     %           title(['Magnet M, Theta = ' num2str(thetaR/pi) 'pi'])
107     %           hold on
108     %           y = zeros(size(tooth));
109     %           plot(middles/P,y,'r.',lows/P,y,'g*',highs/P,y,'b*') %mark boundaries of teeth
110     %           stem(middles/P,Phis./Astooth)
111     %           clear thetat
112
113     dPhis = 1;
114     iter = 1;
115
116
117     %% Calc flux outside core of stator tooth to calc additional reluctance due to fringing
118   %     Rsup = gap*delta/(mu0*Lmotor*theta*sr);
119
120     while and(dPhis>main_tolerance,iter<=num_mainloops)%for nums = 1:num_mainloops %
121       %% Calculate reluctances in stator teeth
122       Btooth = abs(Phis(1:s/2)./Ast);
123       must = (interp1(Bh50,muh50,Btooth,'linear','extrap'))';
124       Rst = lst/Ast./[must;must];
125       %Rst = lst/Ast./[must;must]+Rsup';
126       Rstd = [Rst; Rst];
127
128       %% Calculate Phiprime, fluxes in stator backiron
129       Phiprime = zeros(1,s/2);
130       phisurrogate = [Phis(1:s/2), zeros(1,s/2)];
131       for kk = 1:s/2
132         Phiprime(1,kk) = .5*sum(phisurrogate(1:kk))-.5*sum(phisurrogate(kk+1:end));
133       end
134
135       %% Calculate reluctances in stator backiron
136       Bsb = abs(Phiprime/Asb);
137       musb = (interp1(Bh50,muh50,Bsb,'linear','extrap'))';
138       Rsb = lsb/Asb./[musb;musb];
139       Rsbd = [Rsb; Rsb];
140
141       %% Build flux tube model matrices
142       %initialize matrices.  Make it twice as wide, collapse later to allow
143       %insertion of entries in reference to diagonal
144       Apflux = zeros(s,2*s);
145       Apsource = zeros(s,2*s);
146       Apmmf = zeros(s,2*s);
147
148       %Build matrices corresponding to flux tube model... see handwritten
149       %pages
150       for n = 1:s;
151         Apflux(n,n) = 1+Rstd(n)/Rsbd(n)+Rstd(n)/Rsbd(n+s-1);
152         Apflux(n,n+1) = -Rstd(n+1)/Rsbd(n);
153         Apflux(n,n+s-1) = -Rstd(n+s-1)/Rsbd(n+s-1);
154         Apsource(n,n) = -1/Rsbd(n);
155         Apsource(n,n+s-1) = 1/Rsbd(n+s-1);
```

```
156             Apmmf(n,n) = 1/Rsbd(n)+1/Rsbd(n+s-1);
157             Apmmf(n,n+1) = -1/Rsbd(n);
158             Apmmf(n,n+s-1) = -1/Rsbd(n+s-1);
159         end
160
161         %Now fold matrices back upon themselves to make square matrices
162         Aflux = Apflux(:,1:s)+Apflux(:,s+1:2*s);
163         Asource = Apsource(:,1:s)+Apsource(:,s+1:2*s);
164         Ammf = Apmmf(:,1:s)+Apmmf(:,s+1:2*s);
165
166         Ammf(1,:) = ones(1,size(Ammf,2));
167         Aflux(1,:) = zeros(1,size(Aflux,2));
168         Asource(1,:) = zeros(1,size(Asource,2));
169
170         %phi is input, psi output
171         Psis = (Ammf\(Aflux*Phis'+Asource*N'))';
172
173         psiprime = Psis'-diag(Rst)*Phis';
174         phiprime = (psiprime+N'-[psiprime(2:end);psiprime(1)])./Rsb;
175
176         %% Take fourier components of Hperp
177         deltaPsis = diff([Psis,Psis(1)]); %diff([Psis(end),Psis]);%
178         deltals = sr*theta*delta;    %length between teeth
179         Hperps = deltaPsis./deltals;     %H = dPsi/dl
180
181         Asp = sum(1./k./pi*Hperps.*(sin(k*[lowtooth(2:end),2*pi+lowtooth(1)])-sin(k*hightooth)),2); %calculate
and sum along each tooth, leaving coeffs for each harmonic
182         Bsp = sum(1./k./pi*Hperps.*(cos(k*hightooth)-cos(k*[lowtooth(2:end),2*pi+lowtooth(1)])),2);
183
184         %% Add in sawteeth
185         lowedgeB = [Blowedge(2:end),Blowedge(1)]-Hperps*mu0;
186         highedgeB = Bhighedge-Hperps*mu0;
187         lowtoothend = [lowtooth(2:end),lowtooth(1)+2*pi];
188         hightoothend = hightooth;
189
190         %define slope, height, x1, x2, xz
191         sawnumber = s;
192         slo = zeros(1,sawnumber);
193         x1 = slo;
194         x2 = slo;
195         height = slo;
196         xz = slo;
197 %       x1
198 %       x2
199         for qq = 1:sawnumber;
200 %           thetaR
201 %           lowtoothend(qq)
202 %           hightoothend(qq)
203             if or(and(thetaR<lowtoothend(qq),thetaR>hightoothend(qq)),...
204                 and(mod(thetaR+pi,2*pi)<lowtoothend(qq),mod(thetaR+pi,2*pi)>hightoothend(qq)))
205               %If thetaR or thetaR+pi is inside tooth gap
206 % %             thetaR
207 % %             temp121 = lowtoothend(qq);
```

```
208  % %          hightoothend(qq)
209
210              height(qq) = (abs(highedgeB(qq))+abs(lowedgeB(qq)))/2;
211              height(s+1) = (abs(highedgeB(qq))+abs(lowedgeB(qq)))/2;
212              height(s+2) = (abs(highedgeB(qq))+abs(lowedgeB(qq)))/2;
213
214             slo(qq) = -sign(lowedgeB(qq));
215             x1(qq) = hightoothend(qq);
216             if and(thetaR<lowtoothend(qq),thetaR>hightoothend(qq))
217                x2(qq) = thetaR;%(hightoothend(qq)+lowtoothend(qq))/2;
218             else
219                x2(qq) = mod(thetaR+pi,2*pi);
220             end
221  %             height(qq) = abs(highedgeB(qq));
222             xz(qq) = (x1(qq)+x2(qq))/2;
223             % second half of gap
224             slo(s+1) = -sign(lowedgeB(qq));
225             x1(s+1) = thetaR;%(hightoothend(qq)+lowtoothend(qq))/2;
226             x2(s+1) = lowtoothend(qq)-pi;
227  %             height(s+1) = abs(highedgeB(qq));
228             xz(s+1) = (x1(s+1)+x2(s+1))/2;
229             %overwrite second half of gap+pi
230             slo(s+2) = sign(lowedgeB(qq));
231             x1(s+2) = mod(thetaR+pi,2*pi);%(hightoothend(qq)+lowtoothend(qq))/2+pi;
232             x2(s+2) = mod(lowtoothend(qq),2*pi);
233  %             height(s+2) = abs(highedgeB(qq));
234             xz(s+2) = (x1(s+2)+x2(s+2))/2;
235           else
236              slo(qq) = sign(lowedgeB(qq));
237              x1(qq) = hightoothend(qq);
238              x2(qq) = lowtoothend(qq);
239              height(qq) = (abs(highedgeB(qq))+abs(lowedgeB(qq)))/2;
240              xz(qq) = (hightoothend(qq)+lowtoothend(qq))/2;
241           end
242        end
243  % x1/pi
244  % x2/pi
245  % xz/pi
246
247
248        %calculate fourier harmonics
249        Asaw = 1/mu0*sum(2/pi./k.^2*(sign(slo).*height./(x2-x1)).*(k*(xz-x1).*sin(k*x1)-cos(k*x1)-k*(xz-
x2).*sin(k*x2)+cos(k*x2)),2);
250        Bsaw = 1/mu0*sum(2/pi./k.^2*(sign(slo).*height./(x2-x1)).*(k*(x1-xz).*cos(k*x1)-sin(k*x1)-k*(x2-
xz).*cos(k*x2)+sin(k*x2)),2);
251
252        Asf = Asp+Asaw;
253        Bsf = Bsp+Bsaw;
254  %        hperpdiagnostic;
255
256        %% solve for scalar potential in gap, magnets, and rotor iron
257        WXYZ = zeros(size(k,1),12);
258        for mm = 1:size(k,1)
```

```
259
260         Amaxwell = [-sr^(k(mm)*P-1) sr^(-k(mm)*P-1) 0 0 0 0 0 0 0 0 0 0;
261             0 0 -sr^(k(mm)*P-1) sr^(-k(mm)*P-1) 0 0 0 0 0 0 0 0;
262             -gr^(k(mm)*P-1) -gr^(-k(mm)*P-1) 0 0 gr^(k(mm)*P-1) -gr^(-k(mm)*P-1) 0 0 0 0 0 0;
263             0 0 gr^(k(mm)*P-1) gr^(-k(mm)*P-1) 0 0 -gr^(k(mm)*P-1) -gr^(-k(mm)*P-1) 0 0 0 0;
264             -gr^(k(mm)*P) gr^(-k(mm)*P) 0 0 gr^(k(mm)*P) -gr^(-k(mm)*P) 0 0 0 0 0 0;
265             0 0 -gr^(k(mm)*P) gr^(-k(mm)*P) 0 0 gr^(k(mm)*P) -gr^(-k(mm)*P) 0 0 0 0;
266             0 0 0 0 -mu0*cr^(k(mm)*P-1) mu0*cr^(-k(mm)*P-1) 0 0 muc*cr^(k(mm)*P-1) muc*cr^(-k(mm)*P-1)
0 0;
267             0 0 0 0 0 0 mu0*cr^(k(mm)*P-1) mu0*cr^(-k(mm)*P-1) 0 0 -muc*cr^(k(mm)*P-1) -muc*cr^(-
k(mm)*P-1);
268             0 0 0 0 -cr^(k(mm)*P) cr^(-k(mm)*P) 0 0 cr^(k(mm)*P) -cr^(-k(mm)*P) 0 0;
269             0 0 0 0 0 0 -cr^(k(mm)*P) cr^(-k(mm)*P) 0 0 cr^(k(mm)*P) -cr^(-k(mm)*P);
270             0 0 0 0 0 0 0 0 br^(k(mm)*P-1) br^(-k(mm)*P-1) 0 0;
271             0 0 0 0 0 0 0 0 0 0 br^(k(mm)*P-1) br^(-k(mm)*P-1)];
272
273         Bmaxwell = [Asf(mm);
274             Bsf(mm);
275             cr/gr*Bm(mm);
276             cr/gr*Am(mm);
277             0;
278             0;
279             -mu0*Bm(mm);
280             -mu0*Am(mm);
281             0;
282             0;
283             0;
284             0];
285
286         WXYZ(mm,:) = (Amaxwell\Bmaxwell)';
287     end
288
289     last_Phis = Phis;
290
291     %% Calculate B at stator teeth and integrate to get Phi - Bphi
292     U = mu0.*(-WXYZ(:,1).*sr.^(k.*P-1)-WXYZ(:,2).*sr.^(-k.*P-1));
293     V = mu0.*(WXYZ(:,3).*sr.^(k.*P-1)+WXYZ(:,4).*sr.^(-k.*P-1));
294     Phis = sum(sr*Lmotor.*(V./k/P*ones(size(Phis)).*(sin(k*hightotal)-sin(k*lowtotal))-
U./k/P*ones(size(Phis)).*(cos(k*hightotal)-cos(k*lowtotal))),1);
295
296     Bhighedge =
sum(V*ones(size(hightooth)).*cos(k*hightooth)+U*ones(size(hightooth)).*sin(k*hightooth),1);
297     Blowedge =
sum(V*ones(size(hightooth)).*cos(k*lowtooth)+U*ones(size(hightooth)).*sin(k*lowtooth),1);
298
299     %% Recalculate mu in rotor core - Bphi
300     rad = cr-.5*(cr-br);
301     S = -WXYZ(:,9).*rad.^(k.*P-1)+WXYZ(:,10).*rad.^(-k.*P-1);
302     T = -WXYZ(:,11).*rad.^(k.*P-1)-WXYZ(:,12).*rad.^(-k.*P-1);
303     Hrotormax = sum(S./k/P,1)^2+sum(T./k/P,1)^2;
304     muc = muc-.05*(muc-interp1(Hh50,muh50,Hrotormax,'linear','extrap'));
305
306     %% Check to see if converged
```

```
307         dPhis = sum(abs(Phis-last_Phis)./abs(last_Phis));
308         iter = iter+1;
309     end
310     %Record maximum B
311     Bmaxst(AA) = max(Phis)/Ast;
312     Bmaxsb(AA) = max(phiprime)/Asb;
313     Bmaxrb(AA) = muc*Hrotormax;
314     %disp(['Baxrb = ' num2str(muc*Hrotormax)])
315     %disp(['Mu rotor = ' num2str(muc/(4*pi*1e-7)) '*mu0'])
316
317     %% Now calculate Torque
318     rt = gr+gap/100; %radius at which torque is calculated
319     thetat = linspace(0,2*pi/P,2001);
320     thetat = thetat(1:end-1);
321     U = -WXYZ(:,1).*rt.^(k.*P-1)-WXYZ(:,2).*rt.^(-k.*P-1);
322     V = WXYZ(:,3).*rt.^(k.*P-1)+WXYZ(:,4).*rt.^(-k.*P-1);
323     Hnorm = V*ones(1,size(thetat,2)).*cos(P.*k*thetat)+U*ones(1,size(thetat,2)).*sin(P.*k*thetat);
324     S = 1/rt.*(-WXYZ(:,1).*rt.^(k.*P)+WXYZ(:,2).*rt.^(-k.*P));
325     T = 1/rt.*(-WXYZ(:,3).*rt.^(k.*P)+WXYZ(:,4).*rt.^(-k.*P));
326     Htan = T*ones(1,size(thetat,2)).*sin(P.*k*thetat)+S*ones(1,size(thetat,2)).*cos(P.*k*thetat);
327     shear = mu0.*sum(Hnorm,1).*sum(Htan,1); %combine all harmonics per
328     avgshear = sum(shear)/size(thetat,2);
329     rotorarea = 2*pi*rt*Lmotor;
330     Torque(AA) = rotorarea*rt*avgshear;
331
332     %iter;
333 end
334
335 %iter
336
337 if iter>=num_mainloops
338     converge = 0;
339 elseif iter<num_mainloops
340     converge = 1;
341 end
342
343 %plotvectorpotential;
344 % figure()
345 % plot(thetaRs./pi,Bmaxst,'r*',thetaRs./pi,Bmaxsb,'b*',thetaRs./pi,Bmaxrb,'g*')
346 % legend('Bmax Stator Tooth', 'Bmax Stator Backiron','Bmax Rotor Backiron')
347 % grid on
348
349 % plotfields;
350 % plotscalarpotential;
351 end
```

Appendix B

Motor Optimization Code

The following code sweeps a defined design space and saves torque values corresponding to each design in an output array.

```
clear all
close all
warning('off','all')

% CURRENT BEST DESIGN 2,1,3,5,1,1,3,1

k = ((0:4)*2+1)'; %harmonicsb

% Physical Parameters

 rhohyperco50 = 27679.9047*.293; %[kg/m^3]
 rhomag = 7400;                %[kg/m^3]
 scopper = 5.95e7;             %[siemens]
 rhocopper = 8960;             %[kg/m^3]
 packingfactor = .4711;          % pulled from walco motors with slot liner included

 % Motor Parameters

 max_tq = 30;

 M0= 1.1141e+006;       %magnet strength... corresponds to 1.4T remnant flux density FIXED
 gap = 400e-6;          %motor gap FIXED
 Lmotor = .015;         %axial length FIXED
 R5 = .0635;            %outside FIXED
 delta = .35;          %gap fraction between teeth

 % Variable Parameters
 R1fs = [.55 .57 .59];    %inside of rotor backiron
 R2fs = [.19 .20 .21];   %outisde of rotor backiron
 R3fs = [.35 .40 .45];   %outside surface of magnets
 R4fs = [.75 .77 .79 .80 .82 .84];   %inside of stator backiron

 fslots = [.33 .34 .35 .36];      %slot fraction in stator
 Ps = [7 8 9];%[6 8 13];         %pole pairs
 ss  = [14 16 18];%16;%16;%[6 8 12 16];      %teeth per pole pair (# phases times 2)
 mdegs = 178;%[150 160 170];  %magnet span in degrees... full pitch is 180degrees

 mTorque =
zeros(size(R1fs,2),size(R2fs,2),size(R3fs,2),size(R4fs,2),size(fslots,2),size(Ps,2),size(ss,2),size(mdegs,2));
 Bmaxtooth=
zeros(size(R1fs,2),size(R2fs,2),size(R3fs,2),size(R4fs,2),size(fslots,2),size(Ps,2),size(ss,2),size(mdegs,2));
 Bmaxback= Bmaxtooth;
```

```
maxcurrent = Bmaxtooth;
for aa = 1:size(R1fs,2)
    R1 = R1fs(aa)*R5;
    for bb = 1:size(R2fs,2)
        R2 = R2fs(bb)*(R5-R1)+R1;
        for cc = 1:size(R3fs,2)
            R3 = R3fs(cc)*(R5-R1)+R1;
            for dd = 1:size(R4fs,2)
                R4 = R4fs(dd)*(R5-R1)+R1;
                for ee = 1:size(fslots,2)          %slot fraction
                    fslot = fslots(ee);
                    delta = fslot;
                    for ff = 1:size(Ps,2)          %number of pole pairs
                        P = Ps(ff);
                        for gg = 1:size(ss,2)      %number of phases*2
                            s = ss(gg);
                            for hh = 1:size(mdegs,2)%magnet fraction
                                mdeg = mdegs(hh);

                                adjust = 100;
                                cur = 0;
                                drive = 0;
                                search = 1;
                                Torquetemp = 0;
                                while and(abs(adjust)>5,search<20)
                                    %adjust
                                    cur = cur+adjust;
                                    Current = cur.*ones(1,s/2);
                                    thetaRs = pi/s;
                                    N = [Current, -Current];%zeros(1,6);%
                                    [tq,Bmaxst,Bmaxsb,converge] =
motorsim5(k,N,thetaRs,delta,fslot,R5,R4,R3,R2,R1,P,s,gap,Lmotor,M0,mdeg);
                                    %converge
                                    if cur<0
                                        break
                                    else
                                        if adjust>0
                                            if or(converge == 0,max(Bmaxst,Bmaxsb)>2.4)
                                                adjust = -adjust/2;
                                            end
                                        else
                                            if or(converge == 1,max(Bmaxst,Bmaxsb)<2.4)
```

```
                                adjust = -adjust/2;
                            end
                        end
                        if and(converge == 1,max(Bmaxst,Bmaxsb)<2.4)
%                               Torque(kk) = tq;
%                               drive(kk) = cur;
%                               kk = kk+1;
                            Torquetemp = tq;
                            drive = cur;
                        end
                        search = search+1;
                    end
                end
                if Torquetemp>0
                    Bmaxtooth(aa,bb,cc,dd,ee,ff,gg,hh) = max(Bmaxst);
                    Bmaxback(aa,bb,cc,dd,ee,ff,gg,hh) = max(Bmaxsb);
                    maxcurrent(aa,bb,cc,dd,ee,ff,gg,hh) = drive;
                    mTorque(aa,bb,cc,dd,ee,ff,gg,hh,:) = Torquetemp;
                end
            end
        end
    end
  end
end
```

Appendix C

Optimizer Post-Process Code

The following code is used to post-process the array of motor designs (from the motor optimizer) and display them on a plot depicting power dissipation and mass.

```
%% Post Process parameters... skew and axial length
%% and Score with cheetah data
%% 3-13 added provision to include slot liner

colors = ['r*' 'b*' 'g*' 'c*' 'y*' 'k*'];
sktq = zeros(size(R1fs,2),size(R2fs,2),size(R3fs,2),size(R4fs,2),size(fslots,2),size(Ps,2),size(ss,2),size(mdegs,2));
mtot = sktq;
Rwinding = sktq;
tqconst = sktq;
 L_motor = sktq;
 for aa = 1:size(R1fs,2)
    R1 = R1fs(aa)*R5;
    for bb = 1:size(R2fs,2)
       R2 = R2fs(bb)*(R5-R1)+R1;
       for cc = 1:size(R3fs,2)
          R3 = R3fs(cc)*(R5-R1)+R1;
          for dd = 1:size(R4fs,2)
             R4 = R4fs(dd)*(R5-R1)+R1;
             for ee = 1:size(fslots,2)         %slot fraction
                fslot = fslots(ee);
                for ff = 1:size(Ps,2)         %number of poler pairs
                   P = Ps(ff);
                   for gg = 1:size(ss,2)      %number of phases*2
                      s = ss(gg);
                      for hh = 1:size(mdegs,2)%magnet fraction
                         mdeg = mdegs(hh);


                            tq = mTorque(aa,bb,cc,dd,ee,ff,gg,hh,:);
                            %apply skew
                            sktq(aa,bb,cc,dd,ee,ff,gg,hh) = mean(tq);

                            tqconst(aa,bb,cc,dd,ee,ff,gg,hh) = mean(tq)/maxcurrent(aa,bb,cc,dd,ee,ff,gg,hh);

                            %correct for skew with axial length,
                            %include larger axial lengths
                            L_motor(aa,bb,cc,dd,ee,ff,gg,hh) = (1+(max_tq-mean(tq))/mean(tq))*Lmotor;

                            %% Calculate mass, slot resistance
                            %% A few physical parameters
```

```
41                          oor = R5;
42                          sbr = R4;
43                          sr = R3+gap;
44                          gr = R3;
45                          cr = R2;
46                          br = R1;
47
48                          %theta used only for calculating areas
49                          theta = 2*pi/P/s;
50
51                          % Stator Back Iron
52                          Vsb = pi*(R5^2-R4^2)*L_motor(aa,bb,cc,dd,ee,ff,gg,hh);
53                          msbi = Vsb*rhohyperco50;
54
55                          % Stator Tooth
56                          Ast = L_motor(aa,bb,cc,dd,ee,ff,gg,hh)*theta*sr*(1-fslot); %tooth area
57                          lst = sbr-sr;% CHANGED FROM RELUCTANCE CALCS (oor+sbr)/2-sr;
58                          Vst = Ast*lst*s*P;
59                          mst = Vst*rhohyperco50;
60
61                          % Magnets
62                          lm = R3-R2;
63                          Vmag = pi*(R3^2-R2^2)*L_motor(aa,bb,cc,dd,ee,ff,gg,hh).*mdeg/180;
64                          mmag = Vmag*rhomag;
65
66                          % Rotor
67                          Vrot = pi*(R2^2-R1^2)*L_motor(aa,bb,cc,dd,ee,ff,gg,hh);
68                          mrot = Vrot*rhohyperco50;
69
70                          % Windings
71                          lwinding =  pi^2*(sr+sbr)/P+2*L_motor(aa,bb,cc,dd,ee,ff,gg,hh);
72                          Aliner = .000127*(2*(sbr-sr)+theta*sbr*fslot); %.000127 is liner width
73                          Awinding = ((pi*(sbr^2-sr^2)-P*s*(sbr-sr)*theta*sr*(1-fslot))/P/s-
Aliner)*packingfactor;
74                          mwinding = P*s/2*lwinding*Awinding*rhocopper;
75
76                          mtot(aa,bb,cc,dd,ee,ff,gg,hh) = mrot+mmag+mst+msbi+mwinding;
77                          Rwinding(aa,bb,cc,dd,ee,ff,gg,hh) = lwinding/scopper/Awinding;
78                      end
79                  end
80              end
81          end
```

```
            end
        end
    end
end

%%
load('TenTorqueVelocityPower.mat')
Torque = Power./Jointvelocity;

RLshoulder.speed = Jointvelocity(:,1);
RRshoulder.speed = Jointvelocity(:,3);
FLshoulder.speed = Jointvelocity(:,5);
FRshoulder.speed = Jointvelocity(:,7);

RLshoulder.torque = Torque(:,1);
RRshoulder.torque = Torque(:,3);
FLshoulder.torque = Torque(:,5);
FRshoulder.torque = Torque(:,7);

 RLknee.speed = Jointvelocity(:,2);
 RRknee.speed = Jointvelocity(:,4);
 FLknee.speed = Jointvelocity(:,6);
 FRknee.speed = Jointvelocity(:,8);

 RLknee.torque = Torque(:,2);
 RRknee.torque = Torque(:,4);
 FLknee.torque = Torque(:,6);
 FRknee.torque = Torque(:,8);

 dissipation_scale = diff(time(1:2))/(max(time)-min(time));

 %% Calculate current per torque
 %% Calculate power over cycle
 %% Assume saturated steel for steel loss... only
 % hyperco50data;
 % f = 160/2/pi*P;
 % numwindings = P*s/2;
 % Bmaxst = min(Bmaxst,2);
 % clossst = mst*interp2(Bloss,floss,Loss,Bmaxst,f);
 % Bmaxsb = min(Bmaxsb,2);
 % closssb = msbi*interp2(Bloss,floss,Loss,Bmaxsb,f);
 % losscore = closssb+clossst;
```

```
% losscopper = sum(Current.^2.*Rwinding)*P;
figure()
hold on
ylabel('Mass [kg]')
xlabel('Dissipation [J]')

totalTorque = [RLshoulder.torque; RRshoulder.torque; FLshoulder.torque; FRshoulder.torque; RLknee.torque; RRknee.torque; FLknee.torque; FRknee.torque];

Ptot = zeros(size(R1fs,2),size(R2fs,2),size(R3fs,2),size(R4fs,2),size(fslots,2),size(Ps,2),size(ss,2),size(mdegs,2));
for aa = 1:size(R1fs,2)
    for bb = 1:size(R2fs,2)
        for cc = 1:size(R3fs,2)
            for dd = 1:size(R4fs,2)
                for ee = 1:size(fslots,2)          %slot fraction
                    for ff = 1:size(Ps,2)          %number of pole pairs
                        color = colors(2*ff-1:2*ff);
                        for gg = 1:size(ss,2)      %number of phases*2
                            %color = colors(2*gg-1:2*gg);
                            for hh = 1:size(mdegs,2)%magnet fraction

                                Ireq = abs(totalTorque)./tqconst(aa,bb,cc,dd,ee,ff,gg,hh);
                                Ptot(aa,bb,cc,dd,ee,ff,gg,hh) = dissipation_scale.*sum(Ireq.^2*Rwinding(aa,bb,cc,dd,ee,ff,gg,hh)*Ps(ff)*ss(gg)/2);
                                plot(Ptot(aa,bb,cc,dd,ee,ff,gg,hh),mtot(aa,bb,cc,dd,ee,ff,gg,hh),color)
%                                   if and(and(.658<mtot(aa,bb,cc,dd,ee,ff,gg,hh)<.660,1.58e5<Ptot(aa,bb,cc,dd,ee,ff,gg,hh)<1.6e5),L_motor(aa,bb,cc,dd,ee,ff,gg,hh)<.0025)
%                                       aa
%                                       bb
%                                       cc
%                                       dd
%                                       ee
%                                       ff
%                                       gg
%                                       hh
%                                   end

                            end
                        end
                    end
                end
            end
        end
    end
```

```
161                 end
162               end
163             end
164           end
165         end
166
167         %% Now try a different stack length
168
169         sktq =
zeros(size(R1fs,2),size(R2fs,2),size(R3fs,2),size(R4fs,2),size(fslots,2),size(Ps,2),size(ss,2),size(mdegs,2));
170         mtot = sktq;
171         Rwinding = sktq;
172         tqconst = sktq;
173         L_motor = sktq;
174         for aa = 1:size(R1fs,2)
175           R1 = R1fs(aa)*R5;
176           for bb = 1:size(R2fs,2)
177             R2 = R2fs(bb)*(R5-R1)+R1;
178             for cc = 1:size(R3fs,2)
179               R3 = R3fs(cc)*(R5-R1)+R1;
180               for dd = 1:size(R4fs,2)
181                 R4 = R4fs(dd)*(R5-R1)+R1;
182                 for ee = 1:size(fslots,2)          %slot fraction
183                   fslot = fslots(ee);
184                   for ff = 1:size(Ps,2)          %number of poler pairs
185                     P = Ps(ff);
186                     for gg = 1:size(ss,2)      %number of phases*2
187                       s = ss(gg);
188                       for hh = 1:size(mdegs,2)%magnet fraction
189                         mdeg = mdegs(hh);
190
191
192                           tq = mTorque(aa,bb,cc,dd,ee,ff,gg,hh,:);
193                           %apply skew
194                           sktq(aa,bb,cc,dd,ee,ff,gg,hh) = mean(tq);
195
196                           tqconst(aa,bb,cc,dd,ee,ff,gg,hh) =
mean(tq)/maxcurrent(aa,bb,cc,dd,ee,ff,gg,hh);
197
198                           %correct for skew with axial length,
199                           %include larger axial lengths
```

```
                    L_motor(aa,bb,cc,dd,ee,ff,gg,hh) = 1.25*(1+(max_tq-
mean(tq))/mean(tq))*Lmotor;

                    %% Calculate mass, slot resistance
                    %% A few physical parameters
                    oor = R5;
                    sbr = R4;
                    sr = R3+gap;
                    gr = R3;
                    cr = R2;
                    br = R1;

                    %theta used only for calculating areas
                    theta = 2*pi/P/s;

                    % Stator Back Iron
                    Vsb = pi*(R5^2-R4^2)*L_motor(aa,bb,cc,dd,ee,ff,gg,hh);
                    msbi = Vsb*rhohyperco50;

                    % Stator Tooth
                    Ast = L_motor(aa,bb,cc,dd,ee,ff,gg,hh)*theta*sr*(1-fslot); %tooth area
                    lst = sbr-sr;% CHANGED FROM RELUCTANCE CALCS (oor+sbr)/2-sr;
                    Vst = Ast*lst*s*P;
                    mst = Vst*rhohyperco50;

                    % Magnets
                    lm = R3-R2;
                    Vmag = pi*(R3^2-R2^2)*L_motor(aa,bb,cc,dd,ee,ff,gg,hh).*mdeg/180;
                    mmag = Vmag*rhomag;

                    % Rotor
                    Vrot = pi*(R2^2-R1^2)*L_motor(aa,bb,cc,dd,ee,ff,gg,hh);
                    mrot = Vrot*rhohyperco50;

                    % Windings
                    lwinding =  pi^2*(sr+sbr)/P+2*L_motor(aa,bb,cc,dd,ee,ff,gg,hh);
                    Aliner = .000127*(2*(sbr-sr)+theta*sbr*fslot); %.000127 is liner width
                    Awinding = ((pi*(sbr^2-sr^2)-P*s*(sbr-sr)*theta*sr*(1-fslot))/P/s-
Aliner)*packingfactor;
                    mwinding = P*s/2*lwinding*Awinding*rhocopper;

                    mtot(aa,bb,cc,dd,ee,ff,gg,hh) = mrot+mmag+mst+msbi+mwinding;
```

```
240                         Rwinding(aa,bb,cc,dd,ee,ff,gg,hh) = lwinding/scopper/Awinding;
241                     end
242                   end
243                 end
244               end
245             end
246           end
247     end
248   end
249   Ptot =
zeros(size(R1fs,2),size(R2fs,2),size(R3fs,2),size(R4fs,2),size(fslots,2),size(Ps,2),size(ss,2),size(mdegs,2));
250
251
252   colors = ['r+' 'b+' 'g+' 'c+' 'y+' 'k+'];
253   for aa = 1:size(R1fs,2)
254     for bb = 1:size(R2fs,2)
255       for cc = 1:size(R3fs,2)
256         for dd = 1:size(R4fs,2)
257           for ee = 1:size(fslots,2)          %slot fraction
258             for ff = 1:size(Ps,2)          %number of poler pairs
259               color = colors(2*ff-1:2*ff);
260               for gg = 1:size(ss,2)      %number of phases*2
261                 %color = colors(2*gg-1:2*gg);
262                 for hh = 1:size(mdegs,2)%magnet fraction
263
264                   Ireq = abs(totalTorque)./tqconst(aa,bb,cc,dd,ee,ff,gg,hh)./1.25;
265                   Ptot(aa,bb,cc,dd,ee,ff,gg,hh) =
dissipation_scale.*sum(Ireq.^2*Rwinding(aa,bb,cc,dd,ee,ff,gg,hh)*Ps(ff)*ss(gg)/2);
266                   plot(Ptot(aa,bb,cc,dd,ee,ff,gg,hh),mtot(aa,bb,cc,dd,ee,ff,gg,hh),color)
267                   if and(.84<mtot(aa,bb,cc,dd,ee,ff,gg,hh),mtot(aa,bb,cc,dd,ee,ff,gg,hh)<.87)
268                     if
and(605<Ptot(aa,bb,cc,dd,ee,ff,gg,hh),Ptot(aa,bb,cc,dd,ee,ff,gg,hh)<620)%,L_motor(aa,bb,cc,dd,ee,ff,gg,
hh)<.015)
269                       aa
270                       bb
271                       cc
272                       dd
273                       ee
274                       ff
275                       gg
276                       hh
277                       disp(['mass = ' num2str(mtot(aa,bb,cc,dd,ee,ff,gg,hh))])
```

```
278                         disp(['energy = ' num2str(Ptot(aa,bb,cc,dd,ee,ff,gg,hh))])
279                         L_motor(aa,bb,cc,dd,ee,ff,gg,hh)
280                         end
281                       end
282
283                     end
284                   end
285                 end
286               end
287             end
288           end
289         end
290 end
291
292 %% Now try a different stack length
293
294 sktq =
zeros(size(R1fs,2),size(R2fs,2),size(R3fs,2),size(R4fs,2),size(fslots,2),size(Ps,2),size(ss,2),size(mdegs,2));
295 mtot = sktq;
296 Rwinding = sktq;
297 tqconst = sktq;
298 L_motor = sktq;
299 for aa = 1:size(R1fs,2)
300     R1 = R1fs(aa)*R5;
301     for bb = 1:size(R2fs,2)
302         R2 = R2fs(bb)*(R5-R1)+R1;
303         for cc = 1:size(R3fs,2)
304             R3 = R3fs(cc)*(R5-R1)+R1;
305             for dd = 1:size(R4fs,2)
306                 R4 = R4fs(dd)*(R5-R1)+R1;
307                 for ee = 1:size(fslots,2)          %slot fraction
308                     fslot = fslots(ee);
309                     for ff = 1:size(Ps,2)          %number of poler pairs
310                         P = Ps(ff);
311                         for gg = 1:size(ss,2)      %number of phases*2
312                             s = ss(gg);
313                             for hh = 1:size(mdegs,2)%magnet fraction
314                                 mdeg = mdegs(hh);
315
316
317                                     tq = mTorque(aa,bb,cc,dd,ee,ff,gg,hh,:);
318                                     %apply skew
```

```
319                     sktq(aa,bb,cc,dd,ee,ff,gg,hh) = mean(tq);
320
321                     tqconst(aa,bb,cc,dd,ee,ff,gg,hh) =
mean(tq)/maxcurrent(aa,bb,cc,dd,ee,ff,gg,hh);
322
323                     %correct for skew with axial length,
324                     %include larger axial lengths
325                     L_motor(aa,bb,cc,dd,ee,ff,gg,hh) = 1.125*(1+(max_tq-
mean(tq))/mean(tq))*Lmotor;
326
327                     %% Calculate mass, slot resistance
328                     %% A few physical parameters
329                     oor = R5;
330                     sbr = R4;
331                     sr = R3+gap;
332                     gr = R3;
333                     cr = R2;
334                     br = R1;
335
336                     %theta used only for calculating areas
337                     theta = 2*pi/P/s;
338
339                     % Stator Back Iron
340                     Vsb = pi*(R5^2-R4^2)*L_motor(aa,bb,cc,dd,ee,ff,gg,hh);
341                     msbi = Vsb*rhohyperco50;
342
343                     % Stator Tooth
344                     Ast = L_motor(aa,bb,cc,dd,ee,ff,gg,hh)*theta*sr*(1-fslot); %tooth area
345                     lst = sbr-sr;% CHANGED FROM RELUCTANCE CALCS (oor+sbr)/2-sr;
346                     Vst = Ast*lst*s*P;
347                     mst = Vst*rhohyperco50;
348
349                     % Magnets
350                     lm = R3-R2;
351                     Vmag = pi*(R3^2-R2^2)*L_motor(aa,bb,cc,dd,ee,ff,gg,hh).*mdeg/180;
352                     mmag = Vmag*rhomag;
353
354                     % Rotor
355                     Vrot = pi*(R2^2-R1^2)*L_motor(aa,bb,cc,dd,ee,ff,gg,hh);
356                     mrot = Vrot*rhohyperco50;
357
358                     % Windings
```

```
                        lwinding =  pi^2*(sr+sbr)/P+2*L_motor(aa,bb,cc,dd,ee,ff,gg,hh);
                        Aliner = .000127*(2*(sbr-sr)+theta*sbr*fslot); %.000127 is liner width
                        Awinding = ((pi*(sbr^2-sr^2)-P*s*(sbr-sr)*theta*sr*(1-fslot))/P/s-
Aliner)*packingfactor;
                        mwinding = P*s/2*lwinding*Awinding*rhocopper;

                        mtot(aa,bb,cc,dd,ee,ff,gg,hh) = mrot+mmag+mst+msbi+mwinding;
                        Rwinding(aa,bb,cc,dd,ee,ff,gg,hh) = lwinding/scopper/Awinding;
                    end
                end
            end
        end
    end
  end
  Ptot =
zeros(size(R1fs,2),size(R2fs,2),size(R3fs,2),size(R4fs,2),size(fslots,2),size(Ps,2),size(ss,2),size(mdegs,2));


  colors = ['ro' 'bo' 'go' 'co' 'yo' 'ko'];
  for aa = 1:size(R1fs,2)
    for bb = 1:size(R2fs,2)
      for cc = 1:size(R3fs,2)
        for dd = 1:size(R4fs,2)
          for ee = 1:size(fslots,2)          %slot fraction
            for ff = 1:size(Ps,2)          %number of poler pairs
              color = colors(2*ff-1:2*ff);
              for gg = 1:size(ss,2)      %number of phases*2
                %color = colors(2*gg-1:2*gg);
                for hh = 1:size(mdegs,2)%magnet fraction

                  Ireq = abs(totalTorque)./tqconst(aa,bb,cc,dd,ee,ff,gg,hh)./1.125;
                  Ptot(aa,bb,cc,dd,ee,ff,gg,hh) =
dissipation_scale.*sum(Ireq.^2*Rwinding(aa,bb,cc,dd,ee,ff,gg,hh)*Ps(ff)*ss(gg)/2);
                  plot(Ptot(aa,bb,cc,dd,ee,ff,gg,hh),mtot(aa,bb,cc,dd,ee,ff,gg,hh),color)
                  if and(.84<mtot(aa,bb,cc,dd,ee,ff,gg,hh),mtot(aa,bb,cc,dd,ee,ff,gg,hh)<.87)
                    if
and(605<Ptot(aa,bb,cc,dd,ee,ff,gg,hh),Ptot(aa,bb,cc,dd,ee,ff,gg,hh)<620)%,L_motor(aa,bb,cc,dd,ee,ff,gg,
hh)<.015)
                      aa
                      bb
```

```
396                         cc
397                         dd
398                         ee
399                         ff
400                         gg
401                         hh
402                         disp(['mass = ' num2str(mtot(aa,bb,cc,dd,ee,ff,gg,hh))])
403                         disp(['energy = ' num2str(Ptot(aa,bb,cc,dd,ee,ff,gg,hh))])
404                         end
405                       end
406                     end
407                   end
408                 end
409               end
410             end
411           end
412     end
413 end
414
415 x = 1:1:2000;
416 y = 720./x;
417 plot(x,y)
418 ylim([0 1.5])
419 grid on
```

Appendix D

Hyperco50 Data

Hiperco 50 Strip BH Data

Data obtained from representative ring test specimens from production orders
Tested per ASTM A 773/A 773M and A 596/A 596M

0.15 mm Hiperco 50 865 °C/4hr anneal Yield Strength abt. 210 MPa		0.15 mm Hiperco 50 732 °C/2hr anneal Yield Strength abt. 450 MPa		0.35 mm Hiperco 50 875 °C/4hr anneal Yield Strength abt. 210 MPa		0.35 mm Hiperco 50 766 °C/2hr anneal Yield Strength abt. 345 MPa	
H (Oe)	B (Gauss)	H (Oe)	B (Gauss)	H (Oe)	B (Gauss)	H (Oe)	B (Gauss)
0	0	0	0	0	0	0	0
0.1	200	0.1	150	0.1	425	0.4	110
0.2	706	0.2	309	0.2	631	0.5	341
0.3	1764	0.3	470	0.3	1294	0.6	609
0.4	3728	0.4	630	0.4	3342	0.7	893
0.5	6530	0.5	788	0.5	6896	0.8	1171
0.6	9438	0.6	944	0.6	10687	0.9	1429
0.7	11773	0.7	1103	0.7	13595	1	1654
0.8	13405	0.8	1270	0.8	15497	1.2	2018
0.9	14509	0.9	1457	0.9	16694	1.5	3185
1	15280	1	1678	1	17467	1.6	4388
1.2	16292	1.2	2291	1.2	18378	1.7	6366
1.5	17237	1.5	3908	1.5	19110	1.8	9029
2	18252	1.8	6467	1.8	19575	1.9	11875
3	19454	2	8417	2	19818	2	14311
4	20152	2.2	10264	2.2	20026	2.1	16061
5	20607	2.4	11843	2.4	20210	2.2	17184
6	20925	2.6	13114	2.6	20373	2.4	18268
7	21160	2.8	14108	2.8	20520	2.6	18672
8	21340	3	14884	3	20653	2.8	18869
9	21483	3.2	15496	3.2	20774	3	19013
10	21599	4	17023	4	21165	3.2	19146
15	21955	5	18059	5	21512	4	19683
20	22140	6	18740	6	21762	5	20269
25	22254	7	19243	7	21950	6	20716
30	22333	8	19638	8	22095	7	21049
35	22390	9	19957	9	22211	8	21303
40	22435	10	20220	10	22306	9	21499
45	22471	15	21058	15	22594	10	21655
50	22500	20	21505	20	22737	15	22108
60	22547	25	21783	25	22821	20	22323
70	22584	30	21973	30	22875	25	22447
80	22614	35	22111	35	22913	30	22529
90	22640	40	22217	40	22941	35	22587
100	22662	45	22301	45	22963	40	22631
110	22682	50	22369	50	22980	45	22666
120	22701	60	22474	60	23007	50	22694
130	22718	70	22552	70	23027	60	22739
140	22734	80	22614	80	23044	70	22773
150	22749	90	22664	90	23058	80	22801
160	22764	100	22706	100	23071	90	22825
170	22778	110	22742	110	23083	100	22846
180	22792	120	22774	120	23095	110	22865
190	22805	130	22802	130	23106	120	22883
200	22818	140	22828	140	23117	130	22899
		150	22852	150	23127	140	22914
		160	22874	160	23138	150	22929
		170	22895	170	23148	160	22943
		180	22914	180	23158	170	22956
		190	22933	190	23168	180	22969
		200	22950	200	23178	190	22982
						200	22995

		1350 F for 2 hours				1475 F for 2 hours				1600 F for 2 hours			
Test	Maximum	Core Loss (W/lb)				Core Loss (W/lb)				Core Loss (W/lb)			
Frequency	Flux Density	Thickness (inches)				Thickness (inches)				Thickness (inches)			
(Hz)	(Gauss)	0.006	0.01	1.4E-2	0.02	0.006	0.01	.014	0.02	0.006	0.01	0.014	0.02
60	7500	0.81	0.8	0.8	0.92	0.67	0.76	0.69	0.72	0.33	0.35	0.33	0.39
60	10000	1.26	1.28	1.26	1.41	1	1.15	1.1	1.1	0.52	0.54	0.5	0.61
60	12500	1.73	1.78	1.78	1.96	1.33	1.57	1.51	1.57	0.68	0.72	0.69	0.86
60	15000	2.27	2.33	2.34	2.55	1.73	2.01	1.95	2.06	0.91	0.96	0.89	1.16
60	17500	2.89	2.96	2.95	3.22	2.15	2.51	2.44	2.59	1.16	1.24	1.17	1.53
60	20000	3.61	3.74	3.68	4.03	2.71	3.09	2.98	3.31	1.47	1.59	1.47	1.98
400	7500	5.82	5.74	6.31	8.86	4.58	5.54	5.92	7.66	2.77	3.33	3.54	4.64
400	10000	9.1	9.62	10.8	14.7	7.08	8.68	9.30	12.9	4.26	5.36	5.95	8.57
400	12500	12.8	14.1	16.1	23.6	10.20	12.7	14	20.6	6.2	7.77	9.12	14.28
400	15000	17.1	19.6	22.1	33.9	13.3	17.40	19.40	30.3	8.34	10.73	13.4	22.1
400	17500	21.7	25.5	29.5	47.1	16.90	22.5	26	43.5	11	14.6	19.2	33.6
400	20000	27.2	32.4	38.80	60.3	21.2	28.3	34.20	54.8	13.8	19	25.9	49.1
800	7500	12.4	13.7	15.8	23.2	10	13.3	14.7	20.8	7	8.70	9.9	14.1
800	10000	20	22.9	26.9	41.5	16	21.6	24.2	37.80	10.7	14.6	17.10	27.7
800	12500	28.5	34.1	40.80	67.90	23.1	31.4	36.70	62.4	15.7	21.8	28.1	48.4
800	15000	38.20	47.8	59.6	103.7	30.6	43.8	54	96.4	21.3	31.4	44.1	80.3
800	17500	49.1	64.60	83.5	148.9	39.6	59.1	77	141.8	27.9	44.4	67	124.9
800	20000	60.1	83.3	115.1	201.7	50	77.1	106.6	191	34.9	60.1	89.3	178.5
1600	7500	28.1	32.9	41.1	64.1	23.5	31	38.1	60.5	17.8	24.2	30	46
1600	10000	45.8	57.2	73.3	122.5	38.1	53.2	66.2	119.1	29.3	41.2	56.2	94.6
1600	12500	67.7	87.7	117.9	211.2	56.2	82.6	109.8	206.1	42.3	65.6	96.8	176.7
1600	15000	92	130.1	176.3	331.8	76.8	122.7	171.2	327.1	57.6	101.7	156.3	294.5
1600	17500	120.3	181.4	272.8	490.2	100.2	174.1	258.6	491.6	77.5	150.7	243.7	467.6
1600	20000	149.4	246.2	378.6	697.6	130.8	236.5	370.3	684.5	102.7	207.1	329.3	674.6
2400	7500	46.2	57.6	74.8	130.1	39.6	55.4	70.7	126.7	31.2	44.4	57.7	96.4
2400	10000	76.6	101.4	135.9	248.9	65.8	96.1	130.2	251.5	50.6	79.9	117.2	205.2
2400	12500	113.9	159.5	232	433.6	97.3	153.4	219.6	425.4	75.6	134.8	208.4	374.8
2400	15000	159.1	246.2	371.2	699.5	136	236.5	353.5	669.4	106	209	336.8	633.5
2400	17500	211.5	362.8	568	1067.1	179.3	349.2	535.9	1047.5	151.2	321.8	524.7	994
2400	20000	263.90	499.7	785.1	1515.8	233.2	478.6	762.9	1531.6	192.1	425.3	694	1336.7
3000	7500	69.3	87	106.9	184.8	52.9	73.9	98.6	185.3	44	62.3	85.6	155.3
3000	10000	111.2	144.7	198.6	367.6	87.7	140.4	186.1	370.6	72.1	118	176.8	337.3
3000	12500	156.8	235.1	345.2	635.4	131	225.4	325.6	639.1	106.2	199.7	318.2	596.1
3000	15000	217.3	262.8	540.1	1055.8	183.9	347.4	534	996.5	152.9	321.8	524.7	953
3000	17500	289.1	534.9	848.2	1596.9	254.1	511.8	805.7	1554.3	217.1	488.2	785.2	1499.1
3000	20000	366.7	729.2	1132.2	2262.5	331.1	692.9	1140.6	2193.4	288.8	628.8	1049.4	2088

Table D.1: Core Loss Data for Hyperco50 [31]

Technical Datasheet

CARPENTER

Hiperco® 50 Alloy

Type Analysis

Carbon	0.01 %	**Manganese**	0.05 %
Silicon	0.05 %	**Cobalt**	48.75 %
Columbium/Niobium	0.05 %	**Vanadium**	1.90 %
Iron	49.19 %		

General Information

Description

Hiperco® 50 alloy is an iron-cobalt-vanadium soft magnetic alloy which exhibits high magnetic saturation (24 kilogauss), high D.C. maximum permeability, low D.C. coercive force, and low A.C. core loss.

This alloy is produced in strip form only and contains a small niobium addition for grain refinement during mill processing and final heat treatment of strip.

Applications

Hiperco 50 alloy strip has been used primarily in the manufacture of rotor and stator laminations in motors and generators for aircraft power generation applications.

These laminations are stamped from cold rolled strip and must be final annealed in a protective atmosphere or vacuum environment at a temperature which will provide an optimum combination of mechanical and magnetic properties to withstand the high stresses encountered in service.

Properties

Physical Properties

Specific Gravity	8.12	
Density	0.2930	lb/in³

Mean CTE

77 to 392°F	5.30	x 10⁻⁶ in/in/°F
77 to 752°F	5.60	x 10⁻⁶ in/in/°F
77 to 1112°F	5.80	x 10⁻⁶ in/in/°F
77 to 1472°F	6.30	x 10⁻⁶ in/in/°F

Mean coefficient of thermal expansion

Temperature Range		Coefficient	
77°F to	25°C to	10⁻⁶/°F	10⁻⁶/°C
392	200	5.3	9.5
752	400	5.6	10.1
1112	600	5.8	10.5
1472	800	6.3	11.3

Thermal Conductivity	206.8	BTU-in/hr/ft²/°F
Modulus of Elasticity (E)	30.0	x 10³ ksi
Electrical Resistivity (70°F)	241.0	ohm-cir-mil/ft
Curie Temperature	1720	°F

Magnetic Properties

Typical A.C. core loss values at frequencies of 60, 400, 800 and 1600 Hz are shown for common lamination strip thicknesses of 0.006” (0.15 mm), 0.010” (0.25 mm) and 0.014” (0.35 mm), heat treated at two final heat treating temperatures (1600°F [871°C] and 1400°F [760°]) for 2 hours, cooled at 180°F (100°C)/hr. Typical core loss values cover the induction range of 10 kilogauss (1T) to 20 kilogauss (2T).

Hiperco® 50 Alloy

The magnetic data were determined on ring laminations 1.50” O.D. x 1.25” I.D. x thickness per ASTM A-697 taking special precautions to assure the retention of a sinusoidal flux wave form.

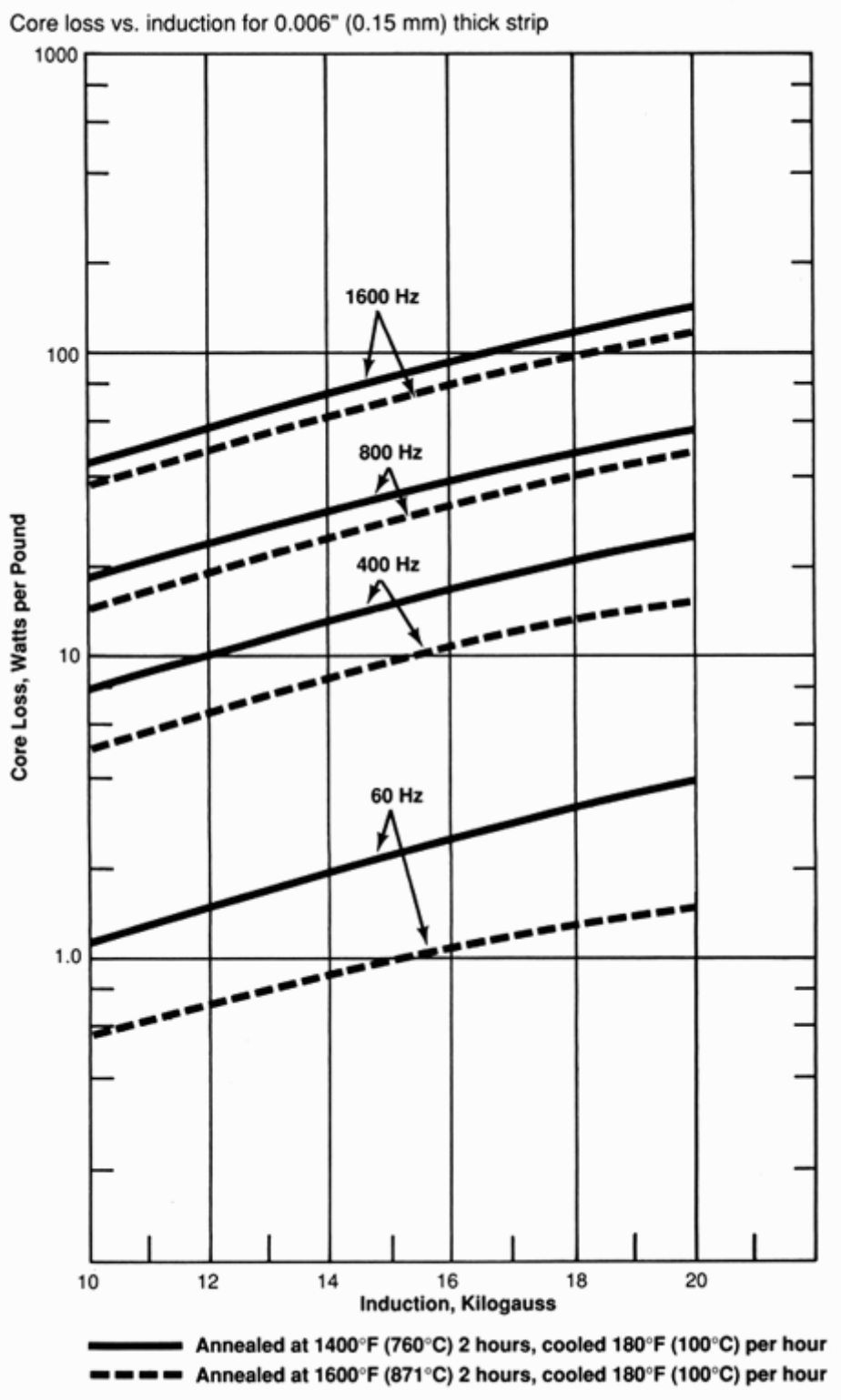

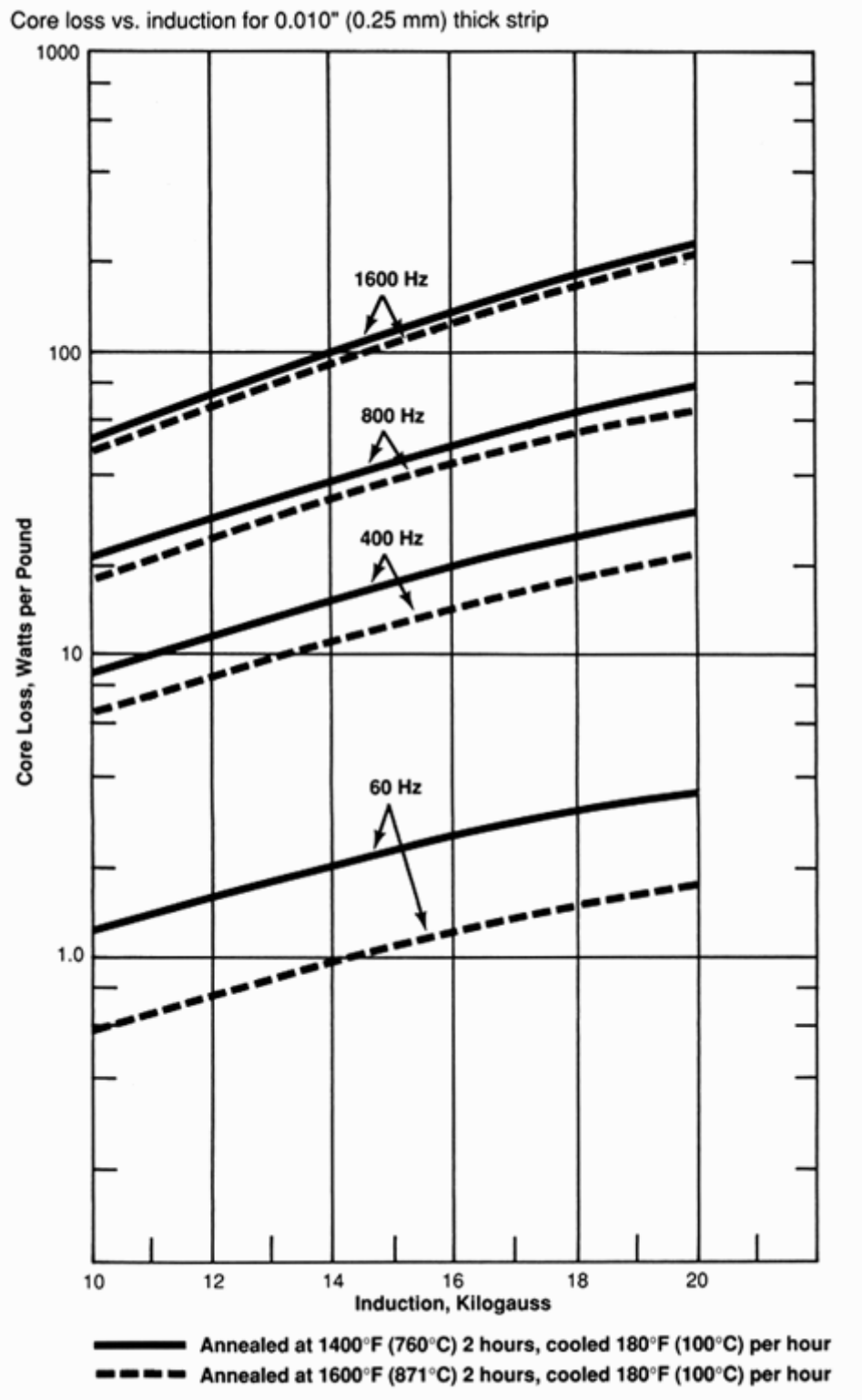
Core loss vs. induction for 0.010" (0.25 mm) thick strip
1000
100
10
1.0
Core Loss, Watts per Pound
1600 Hz
800 Hz
400 Hz
60 Hz
10
12
14
16
18
20
Induction, Kilogauss
Annealed at 1400°F (760°C) 2 hours, cooled 180°F (100°C) per hour
Annealed at 1600°F (871°C) 2 hours, cooled 180°F (100°C) per hour

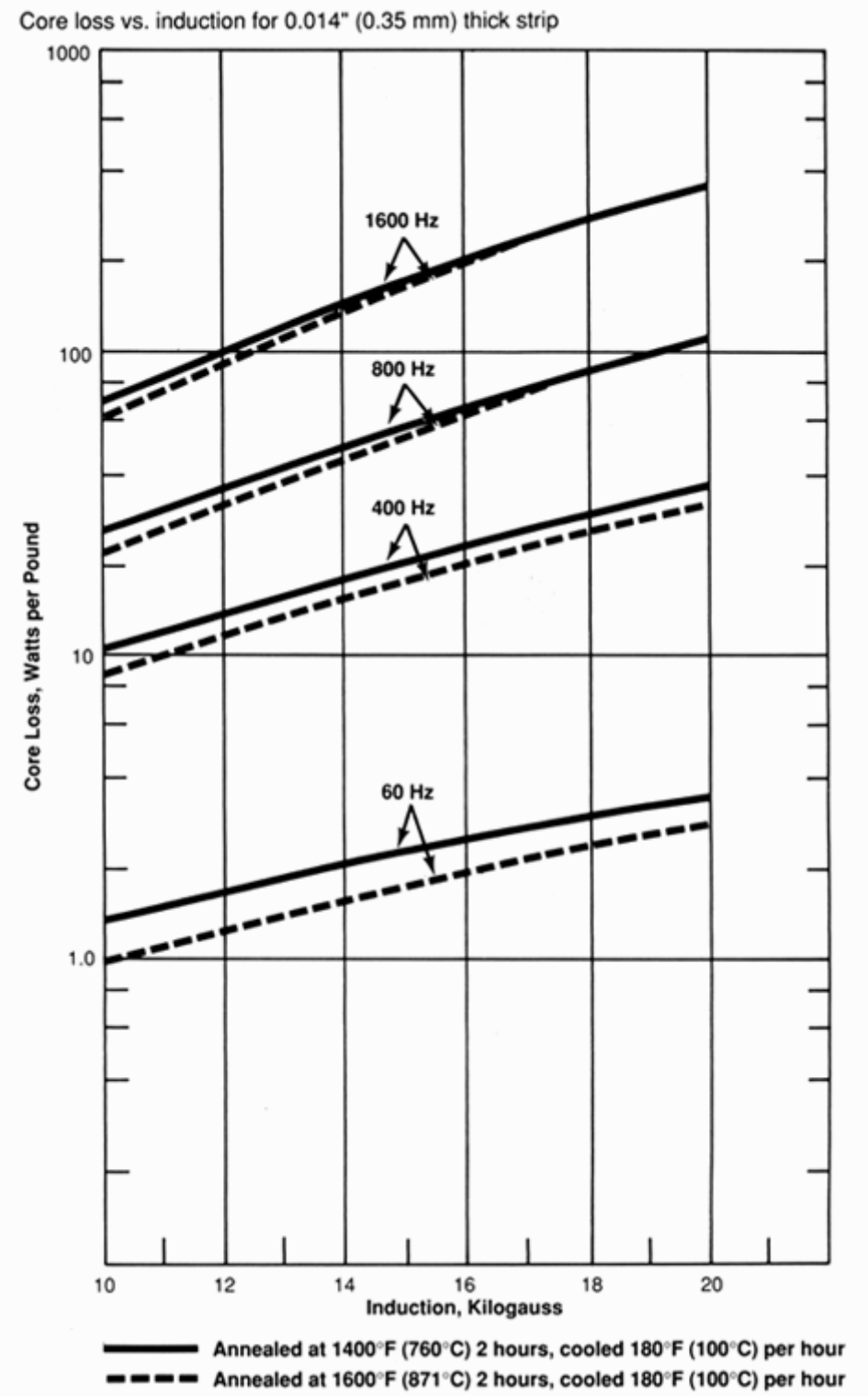
Core loss vs. induction for 0.014" (0.35 mm) thick strip
1000
100
10
1.0
Core Loss, Watts per Pound
1600 Hz
800 Hz
400 Hz
60 Hz
10
12
14
16
18
20
Induction, Kilogauss
Annealed at 1400°F (760°C) 2 hours, cooled 180°F (100°C) per hour
Annealed at 1600°F (871°C) 2 hours, cooled 180°F (100°C) per hour

Hiperco® 50 Alloy

Typical D.C. Magnetic Properties - Hiperco Alloy 50

Typical D.C. induction values in kilogauss from different magnetizing forces in oersteds are shown below for different strip thicknesses after a 1600°F (871°C) anneal for 2 hours, cooled at 180°F (100°C)/hour heat treatment. The magnetic data was determined on ring laminations 1.50" O.D. x 1.25" I.D. per ASTM A596.

Strip Thickness	@ 10 Oe	@ 50 Oe	@ 100 Oe	@ 200 Oe
.006"	21.2 Kg	23.0 Kg	23.6 Kg	24.4 Kg
.010"	21.6 Kg	22.9 Kg	23.5 Kg	24.2 Kg
.014"	21.7 Kg	23.0 Kg	23.6 Kg	24.3 Kg

Induction		
10 Oe, 0.00600 in	21200	G
10 Oe, 0.0100 in	21600	G
10 Oe, 0.0140 in	21700	G
50 Oe, 0.0100 in	22900	G
50 Oe, 0.0140 in	23000	G
50 Oe, 0.00600 in	23000	G
100 Oe, 0.0100 in	23500	G
100 Oe, 0.0140 in	23600	G
100 Oe, 0.00600 in	23600	G
200 Oe, 0.0100 in	24200	G
200 Oe, 0.0140 in	24300	G
200 Oe, 0.00600 in	24400	G

Typical Mechanical Properties

Typical Mechanical Properties - Hiperco Alloy 50

Tensile Strength		0.2%Yield Strength		% Elongation in 2" (50.8 mm)	Hardness Rockwell C
ksi	MPa	ksi	MPa		
As Cold Rolled					
195	1345	185	1275	1	36
After Heat Treatment - 1400°F (760°C) for 2 hrs. and cooled at 180°F (100°C)/hr.					
0.006" (0.15 mm) Thick Strip					
120	827	65	448	8	—
0.014" (0.35 mm) Thick Strip					
125	861	70	483	9	—
After Heat Treatment - 1550°F (843°C) for 2 hrs. and cooled at 180°F (100°C)/hr.					
0.006" (0.15 mm) Thick Strip					
115	792	57	393	8	—
0.014" (0.35 mm) Thick Strip					
118	813	63	434	9	—

Heat Treatment

It is important to avoid any contamination of the finished parts during the heat treatment. All parts must be cleaned thoroughly to remove any surface contaminants prior to annealing.

Batch heat treating in a sealed retort or welded box-type furnace is recommended. Thoroughly degreased and cleaned laminations can usually be stacked without an insulating media separation. To obtain the best degree of lamination flatness, a light weight can be placed on top of the stack It may be necessary to determine the correct amount of weight to assure that there is no sticking of the laminations within the stack height employed.

A dry hydrogen atmosphere or a high vacuum is recommended to minimize oxide contamination of the parts during annealing. When hydrogen is employed, the entry dew point should be dryer than -60°F (-51°C) and the exit dew point dryer than about -40°F (-40°C) when the inside retort temperature is above 900°F (482°C).

Anneal parts at 1300/1600°F (704/871°C) for 2 to 4 hours in dry hydrogen or vacuum and cool at 150/350°F (83/194°C) per hour until 600°F (316°C) is reached, after which any cooling rate can be employed. The exact heat treat temperature to be employed will depend upon the particular application and the desired compromise between magnetic and mechanical properties. With increasing temperature from 1300 to 1600°F (704 to 871°C), the magnetic properties improve while the yield and tensile strengths decrease. The temperature at no time should exceed 1600°F (871°C) as an upper limit, as the soft magnetic characteristics start to decline due to formation of an austenitic phase.

For certain A.C. applications, improved magnetic characteristics and/or lower core loss are realized by creating a thin oxide layer on the surface of the annealed laminations. The surface oxide layer can be achieved by heating in an oxygen bearing atmosphere in the range of 600 to 900°F (316 to 480°C) for about 30 to 60 minutes. The exact baking parameters must be determined for the annealing facility employed and the thickness of oxide layer desired.

Other Information

Applicable Specifications

- ASTM A801 Alloy Type 1
- MIL A 47182

Forms Manufactured

Strip - Up to approximately 9" wide and thicknesses from 0.004" to 0.050" (0.102 to 1.3 mm) in the cold rolled unannealed condition only.

- Strip

Technical Articles

- A Guide to Etching Specialty Alloys for Microstructural Evaluation
- A Simplified Method of Selecting Soft Magnetic Alloys
- High Strength and High Induction Co27-Fe-C0.23 Soft Magnetic Alloy for Forge Application
- Soft Magnetic Alloys with Improved Corrosion Resistance

Edition Date: 12/01/1990

DC Normal Induction - Special Soft Magnetic Alloys

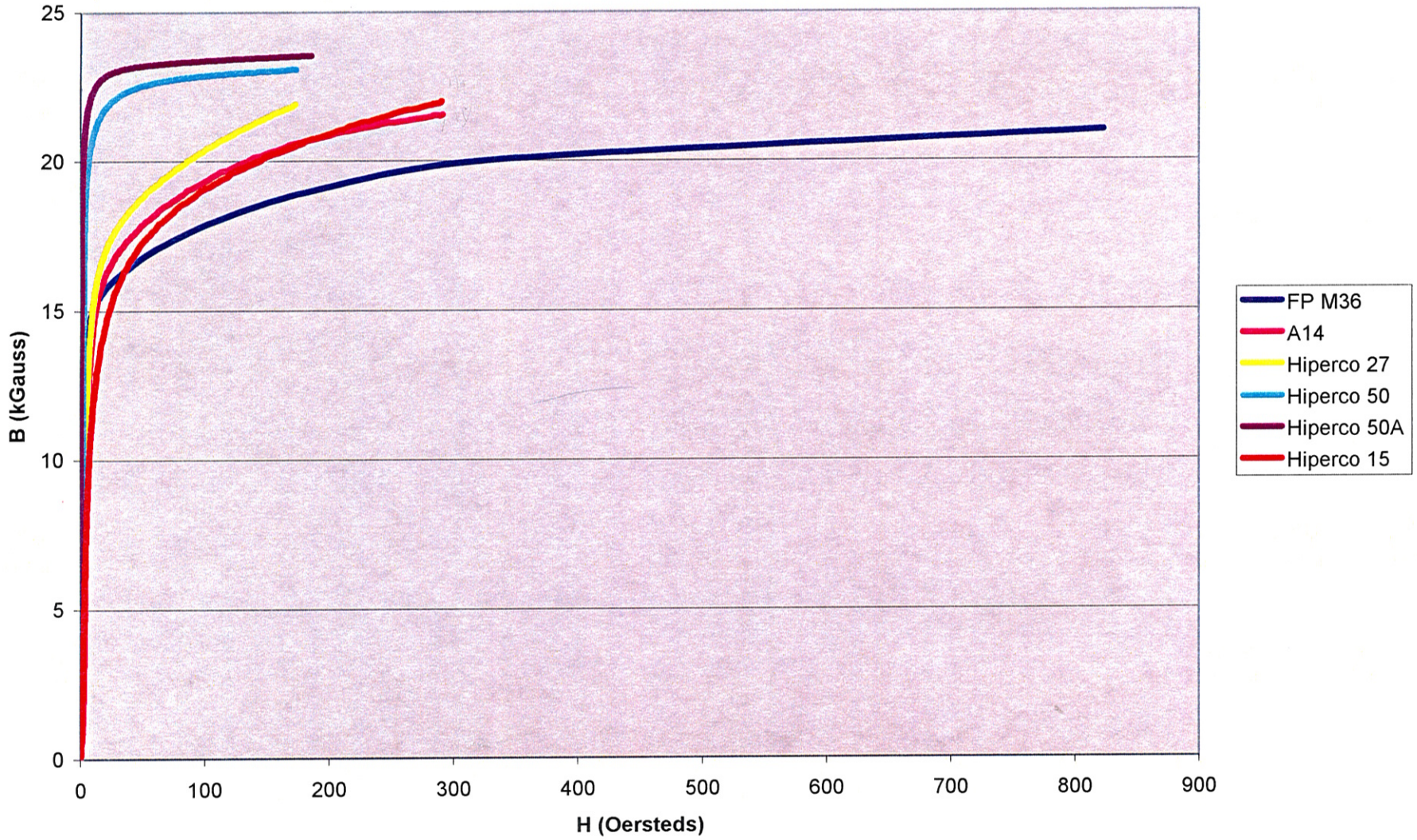

Appendix E

Speed Comparison with Comsol

This appendix shows results of allowing Comsol to run to a certain number of iterations to allow a speed comparison with the method presented in Chapters 2, 3, and 4. It supports conclusions reached in Chapter 4.

E.1 One Iteration

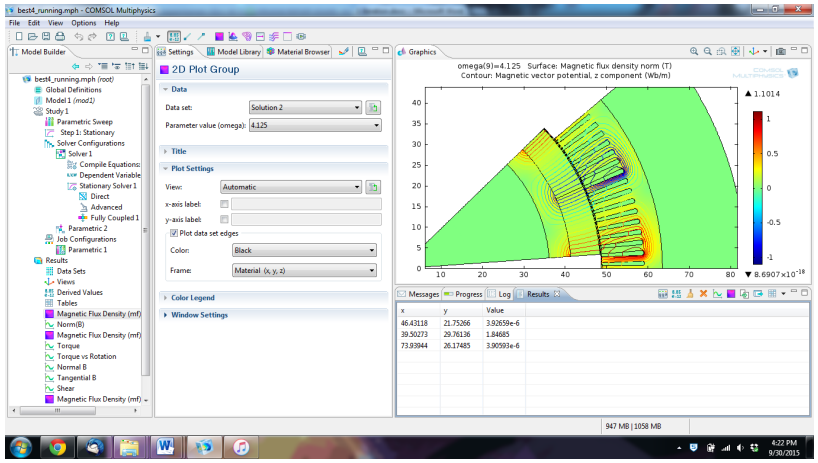

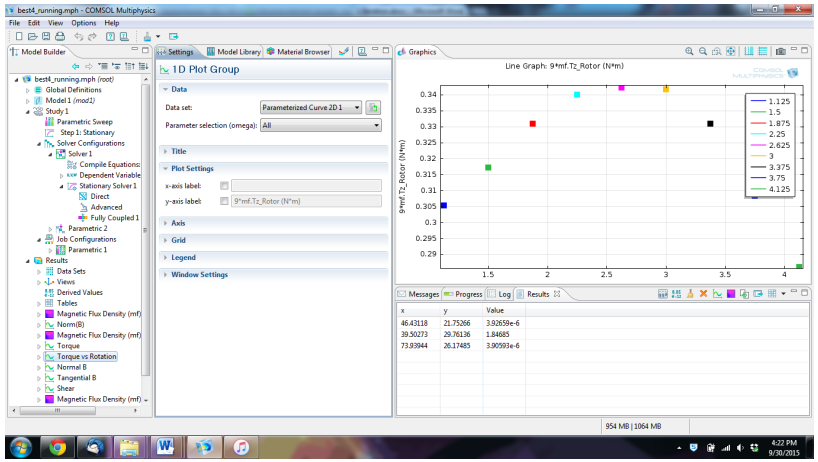


```
============================================================
Parameter omega = 1.125.
Number of vertex elements: 10
Number of boundary elements: 121
Stationary Solver 1 in Solver 1 started at 30-Sep-2015 16:17:59.
Nonlinear solver
Number of degrees of freedom solved for: 37017.
Nonsymmetric matrix found.
Scales for dependent variables:
mod1.A: 1
mod1.root.mod1.mf.VCoil_1_ode: 0.19
mod1.root.mod1.mf.VCoil_2_ode: 0.19
mod1.root.mod1.mf.VCoil_3_ode: 0.19
mod1.root.mod1.mf.VCoil_4_ode: 0.19
mod1.root.mod1.mf.VCoil_5_ode: 0.19
mod1.root.mod1.mf.VCoil_6_ode: 0.19
mod1.root.mod1.mf.VCoil_7_ode: 0.19
mod1.root.mod1.mf.VCoil_8_ode: 0.19
mod1.root.mod1.mf.VCoil_9_ode: 0.19
mod1.root.mod1.mf.VCoil_10_ode: 0.19
mod1.root.mod1.mf.VCoil_11_ode: 0.19
mod1.root.mod1.mf.VCoil_12_ode: 0.19
mod1.root.mod1.mf.VCoil_13_ode: 0.19
mod1.root.mod1.mf.VCoil_14_ode: 0.19
mod1.root.mod1.mf.VCoil_15_ode: 0.19
mod1.root.mod1.mf.VCoil_16_ode: 0.19
Iter      ErrEst     Damping    Stepsize #Res #Jac #Sol
   1       0.044   0.1000000       0.049    3    1    3
Stationary Solver 1 in Solver 1: Solution time: 1 s.
Parameter omega = 1.5.
Number of vertex elements: 10
Number of boundary elements: 122
Stationary Solver 1 in Solver 1 started at 30-Sep-2015 16:18:08.
Nonlinear solver
Number of degrees of freedom solved for: 36911.
Nonsymmetric matrix found.
Scales for dependent variables:
mod1.A: 1
mod1.root.mod1.mf.VCoil_1_ode: 0.19
mod1.root.mod1.mf.VCoil_2_ode: 0.19
mod1.root.mod1.mf.VCoil_3_ode: 0.19
mod1.root.mod1.mf.VCoil_4_ode: 0.19
mod1.root.mod1.mf.VCoil_5_ode: 0.19
mod1.root.mod1.mf.VCoil_6_ode: 0.19
mod1.root.mod1.mf.VCoil_7_ode: 0.19
mod1.root.mod1.mf.VCoil_8_ode: 0.19
mod1.root.mod1.mf.VCoil_9_ode: 0.19
mod1.root.mod1.mf.VCoil_10_ode: 0.19
mod1.root.mod1.mf.VCoil_11_ode: 0.19
mod1.root.mod1.mf.VCoil_12_ode: 0.19
mod1.root.mod1.mf.VCoil_13_ode: 0.19
mod1.root.mod1.mf.VCoil_14_ode: 0.19
mod1.root.mod1.mf.VCoil_15_ode: 0.19
mod1.root.mod1.mf.VCoil_16_ode: 0.19
Iter      ErrEst     Damping    Stepsize #Res #Jac #Sol
   1       0.045   0.1000000        0.05    3    1    3
Stationary Solver 1 in Solver 1: Solution time: 1 s.
Parameter omega = 1.875.
Number of vertex elements: 10
Number of boundary elements: 123
Stationary Solver 1 in Solver 1 started at 30-Sep-2015 16:18:17.
Nonlinear solver
Number of degrees of freedom solved for: 36825.
Nonsymmetric matrix found.
Scales for dependent variables:
```

```
mod1.A: 1
mod1.root.mod1.mf.VCoil_1_ode: 0.19
mod1.root.mod1.mf.VCoil_2_ode: 0.19
mod1.root.mod1.mf.VCoil_3_ode: 0.19
mod1.root.mod1.mf.VCoil_4_ode: 0.19
mod1.root.mod1.mf.VCoil_5_ode: 0.19
mod1.root.mod1.mf.VCoil_6_ode: 0.19
mod1.root.mod1.mf.VCoil_7_ode: 0.19
mod1.root.mod1.mf.VCoil_8_ode: 0.19
mod1.root.mod1.mf.VCoil_9_ode: 0.19
mod1.root.mod1.mf.VCoil_10_ode: 0.19
mod1.root.mod1.mf.VCoil_11_ode: 0.19
mod1.root.mod1.mf.VCoil_12_ode: 0.19
mod1.root.mod1.mf.VCoil_13_ode: 0.19
mod1.root.mod1.mf.VCoil_14_ode: 0.19
mod1.root.mod1.mf.VCoil_15_ode: 0.19
mod1.root.mod1.mf.VCoil_16_ode: 0.19
Iter      ErrEst     Damping    Stepsize #Res #Jac #Sol
   1       0.046   0.1000000       0.051    3    1    3
Stationary Solver 1 in Solver 1: Solution time: 1 s.
Parameter omega = 2.25.
Number of vertex elements: 10
Number of boundary elements: 124
Stationary Solver 1 in Solver 1 started at 30-Sep-2015 16:18:25.
Nonlinear solver
Number of degrees of freedom solved for: 36647.
Nonsymmetric matrix found.
Scales for dependent variables:
mod1.A: 1
mod1.root.mod1.mf.VCoil_1_ode: 0.19
mod1.root.mod1.mf.VCoil_2_ode: 0.19
mod1.root.mod1.mf.VCoil_3_ode: 0.19
mod1.root.mod1.mf.VCoil_4_ode: 0.19
mod1.root.mod1.mf.VCoil_5_ode: 0.19
mod1.root.mod1.mf.VCoil_6_ode: 0.19
mod1.root.mod1.mf.VCoil_7_ode: 0.19
mod1.root.mod1.mf.VCoil_8_ode: 0.19
mod1.root.mod1.mf.VCoil_9_ode: 0.19
mod1.root.mod1.mf.VCoil_10_ode: 0.19
mod1.root.mod1.mf.VCoil_11_ode: 0.19
mod1.root.mod1.mf.VCoil_12_ode: 0.19
mod1.root.mod1.mf.VCoil_13_ode: 0.19
mod1.root.mod1.mf.VCoil_14_ode: 0.19
mod1.root.mod1.mf.VCoil_15_ode: 0.19
mod1.root.mod1.mf.VCoil_16_ode: 0.19
Iter      ErrEst     Damping    Stepsize #Res #Jac #Sol
   1       0.047   0.1000000       0.052    3    1    3
Stationary Solver 1 in Solver 1: Solution time: 1 s.
Parameter omega = 2.625.
Number of vertex elements: 10
Number of boundary elements: 125
Stationary Solver 1 in Solver 1 started at 30-Sep-2015 16:18:34.
Nonlinear solver
Number of degrees of freedom solved for: 36885.
Nonsymmetric matrix found.
Scales for dependent variables:
mod1.A: 1
mod1.root.mod1.mf.VCoil_1_ode: 0.19
mod1.root.mod1.mf.VCoil_2_ode: 0.19
mod1.root.mod1.mf.VCoil_3_ode: 0.19
mod1.root.mod1.mf.VCoil_4_ode: 0.19
mod1.root.mod1.mf.VCoil_5_ode: 0.19
mod1.root.mod1.mf.VCoil_6_ode: 0.19
mod1.root.mod1.mf.VCoil_7_ode: 0.19
mod1.root.mod1.mf.VCoil_8_ode: 0.19
mod1.root.mod1.mf.VCoil_9_ode: 0.19
mod1.root.mod1.mf.VCoil_10_ode: 0.19
mod1.root.mod1.mf.VCoil_11_ode: 0.19
mod1.root.mod1.mf.VCoil_12_ode: 0.19
mod1.root.mod1.mf.VCoil_13_ode: 0.19
mod1.root.mod1.mf.VCoil_14_ode: 0.19
mod1.root.mod1.mf.VCoil_15_ode: 0.19
mod1.root.mod1.mf.VCoil_16_ode: 0.19
Iter      ErrEst     Damping    Stepsize #Res #Jac #Sol
   1       0.048   0.1000000       0.053    3    1    3
Stationary Solver 1 in Solver 1: Solution time: 1 s.
Parameter omega = 3.0.
Number of vertex elements: 10
Number of boundary elements: 126
Stationary Solver 1 in Solver 1 started at 30-Sep-2015 16:18:43.
Nonlinear solver
Number of degrees of freedom solved for: 36759.
Nonsymmetric matrix found.
Scales for dependent variables:
mod1.A: 1
mod1.root.mod1.mf.VCoil_1_ode: 0.19
mod1.root.mod1.mf.VCoil_2_ode: 0.19
mod1.root.mod1.mf.VCoil_3_ode: 0.19
mod1.root.mod1.mf.VCoil_4_ode: 0.19
mod1.root.mod1.mf.VCoil_5_ode: 0.19
mod1.root.mod1.mf.VCoil_6_ode: 0.19
mod1.root.mod1.mf.VCoil_7_ode: 0.19
mod1.root.mod1.mf.VCoil_8_ode: 0.19
mod1.root.mod1.mf.VCoil_9_ode: 0.19
mod1.root.mod1.mf.VCoil_10_ode: 0.19
mod1.root.mod1.mf.VCoil_11_ode: 0.19
mod1.root.mod1.mf.VCoil_12_ode: 0.19
mod1.root.mod1.mf.VCoil_13_ode: 0.19
mod1.root.mod1.mf.VCoil_14_ode: 0.19
mod1.root.mod1.mf.VCoil_15_ode: 0.19
mod1.root.mod1.mf.VCoil_16_ode: 0.19
Iter      ErrEst     Damping    Stepsize #Res #Jac #Sol
   1       0.049   0.1000000       0.054    3    1    3
Stationary Solver 1 in Solver 1: Solution time: 1 s.
Parameter omega = 3.375.
Number of vertex elements: 10
Number of boundary elements: 127
Stationary Solver 1 in Solver 1 started at 30-Sep-2015 16:18:52.
Nonlinear solver
Number of degrees of freedom solved for: 36841.
Nonsymmetric matrix found.
Scales for dependent variables:
mod1.A: 1
mod1.root.mod1.mf.VCoil_1_ode: 0.19
```

```
mod1.root.mod1.mf.VCoil_2_ode: 0.19
mod1.root.mod1.mf.VCoil_3_ode: 0.19
mod1.root.mod1.mf.VCoil_4_ode: 0.19
mod1.root.mod1.mf.VCoil_5_ode: 0.19
mod1.root.mod1.mf.VCoil_6_ode: 0.19
mod1.root.mod1.mf.VCoil_7_ode: 0.19
mod1.root.mod1.mf.VCoil_8_ode: 0.19
mod1.root.mod1.mf.VCoil_9_ode: 0.19
mod1.root.mod1.mf.VCoil_10_ode: 0.19
mod1.root.mod1.mf.VCoil_11_ode: 0.19
mod1.root.mod1.mf.VCoil_12_ode: 0.19
mod1.root.mod1.mf.VCoil_13_ode: 0.19
mod1.root.mod1.mf.VCoil_14_ode: 0.19
mod1.root.mod1.mf.VCoil_15_ode: 0.19
mod1.root.mod1.mf.VCoil_16_ode: 0.19
Iter      ErrEst     Damping    Stepsize #Res #Jac #Sol
   1        0.05   0.1000000       0.055    3    1    3
Stationary Solver 1 in Solver 1: Solution time: 2 s.
Parameter omega = 3.75.
Number of vertex elements: 10
Number of boundary elements: 128
Stationary Solver 1 in Solver 1 started at 30-Sep-2015 16:19:01.
Nonlinear solver
Number of degrees of freedom solved for: 36827.
Nonsymmetric matrix found.
Scales for dependent variables:
mod1.A: 1
mod1.root.mod1.mf.VCoil_1_ode: 0.19
mod1.root.mod1.mf.VCoil_2_ode: 0.19
mod1.root.mod1.mf.VCoil_3_ode: 0.19
mod1.root.mod1.mf.VCoil_4_ode: 0.19
mod1.root.mod1.mf.VCoil_5_ode: 0.19
mod1.root.mod1.mf.VCoil_6_ode: 0.19
mod1.root.mod1.mf.VCoil_7_ode: 0.19
mod1.root.mod1.mf.VCoil_8_ode: 0.19
mod1.root.mod1.mf.VCoil_9_ode: 0.19
mod1.root.mod1.mf.VCoil_10_ode: 0.19
mod1.root.mod1.mf.VCoil_11_ode: 0.19
mod1.root.mod1.mf.VCoil_12_ode: 0.19
mod1.root.mod1.mf.VCoil_13_ode: 0.19
mod1.root.mod1.mf.VCoil_14_ode: 0.19
mod1.root.mod1.mf.VCoil_15_ode: 0.19
mod1.root.mod1.mf.VCoil_16_ode: 0.19
Iter      ErrEst     Damping    Stepsize #Res #Jac #Sol
   1       0.051   0.1000000       0.056    3    1    3
Stationary Solver 1 in Solver 1: Solution time: 2 s.
Parameter omega = 4.125.
Number of vertex elements: 10
Number of boundary elements: 129
Stationary Solver 1 in Solver 1 started at 30-Sep-2015 16:19:10.
Nonlinear solver
Number of degrees of freedom solved for: 36869.
Nonsymmetric matrix found.
Scales for dependent variables:
mod1.A: 1
mod1.root.mod1.mf.VCoil_1_ode: 0.19
mod1.root.mod1.mf.VCoil_2_ode: 0.19
mod1.root.mod1.mf.VCoil_3_ode: 0.19
mod1.root.mod1.mf.VCoil_4_ode: 0.19
mod1.root.mod1.mf.VCoil_5_ode: 0.19
mod1.root.mod1.mf.VCoil_6_ode: 0.19
mod1.root.mod1.mf.VCoil_7_ode: 0.19
mod1.root.mod1.mf.VCoil_8_ode: 0.19
mod1.root.mod1.mf.VCoil_9_ode: 0.19
mod1.root.mod1.mf.VCoil_10_ode: 0.19
mod1.root.mod1.mf.VCoil_11_ode: 0.19
mod1.root.mod1.mf.VCoil_12_ode: 0.19
mod1.root.mod1.mf.VCoil_13_ode: 0.19
mod1.root.mod1.mf.VCoil_14_ode: 0.19
mod1.root.mod1.mf.VCoil_15_ode: 0.19
mod1.root.mod1.mf.VCoil_16_ode: 0.19
Iter      ErrEst     Damping    Stepsize #Res #Jac #Sol
   1       0.051   0.1000000       0.057    3    1    3
Stationary Solver 1 in Solver 1: Solution time: 2 s.
```

E.2 Ten Iterations

10 iterations

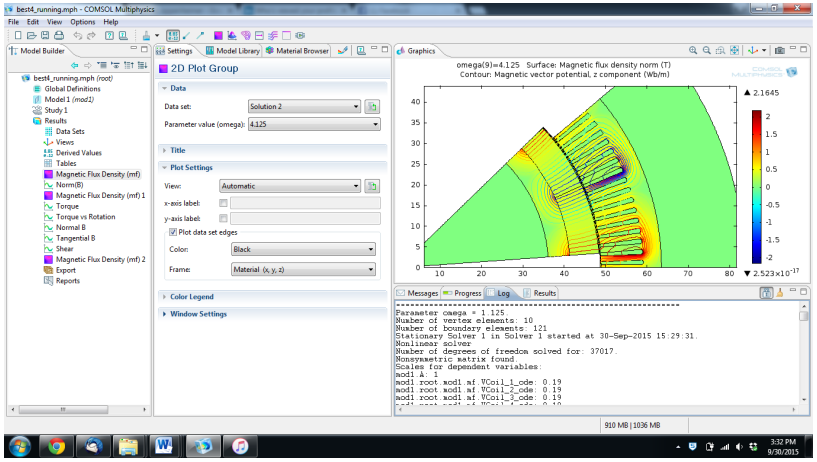

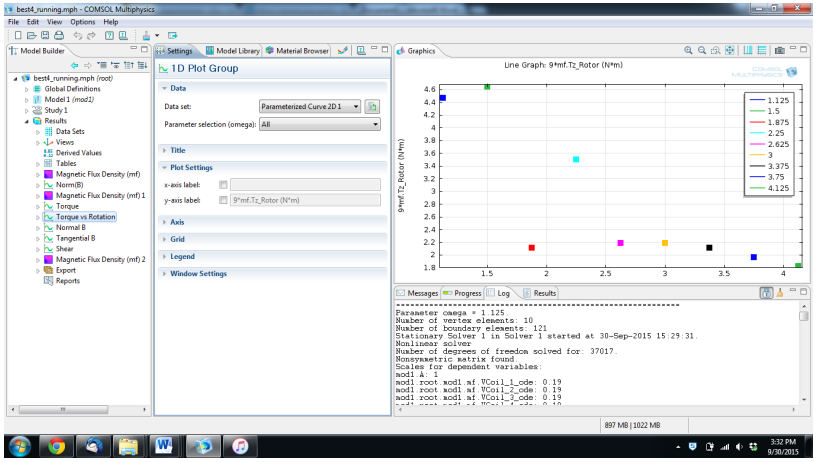

==========

```
Parameter omega = 1.125.
Number of vertex elements: 10
Number of boundary elements: 121
Stationary Solver 1 in Solver 1 started at 30-Sep-2015 15:29:31.
Nonlinear solver
Number of degrees of freedom solved for: 37017.
Nonsymmetric matrix found.
Scales for dependent variables:
mod1.A: 1
mod1.root.mod1.mf.VCoil_1_ode: 0.19
mod1.root.mod1.mf.VCoil_2_ode: 0.19
mod1.root.mod1.mf.VCoil_3_ode: 0.19
mod1.root.mod1.mf.VCoil_4_ode: 0.19
mod1.root.mod1.mf.VCoil_5_ode: 0.19
mod1.root.mod1.mf.VCoil_6_ode: 0.19
mod1.root.mod1.mf.VCoil_7_ode: 0.19
mod1.root.mod1.mf.VCoil_8_ode: 0.19
mod1.root.mod1.mf.VCoil_9_ode: 0.19
mod1.root.mod1.mf.VCoil_10_ode: 0.19
mod1.root.mod1.mf.VCoil_11_ode: 0.19
mod1.root.mod1.mf.VCoil_12_ode: 0.19
mod1.root.mod1.mf.VCoil_13_ode: 0.19
mod1.root.mod1.mf.VCoil_14_ode: 0.19
mod1.root.mod1.mf.VCoil_15_ode: 0.19
mod1.root.mod1.mf.VCoil_16_ode: 0.19
Iter      ErrEst     Damping    Stepsize #Res #Jac #Sol
   1       0.044   0.1000000       0.049     3     1     3
   2       0.041   0.1000000       0.046     5     2     6
   3       0.039   0.1000000       0.044     7     3     9
   4       0.041   0.0100000       0.041    10     4    13
   5       0.039   0.1000000       0.043    11     5    15
   6        0.04   0.0100000       0.041    14     6    19
   7       0.042   0.0100000       0.043    16     7    22
   8       0.044   0.0100000       0.044    18     8    25
   9       0.046   0.0100000       0.046    20     9    28
  10       0.048   0.0100000       0.048    22    10    31
Stationary Solver 1 in Solver 1: Solution time: 9 s.
Parameter omega = 1.5.
Number of vertex elements: 10
Number of boundary elements: 122
Stationary Solver 1 in Solver 1 started at 30-Sep-2015 15:29:47.
Nonlinear solver
Number of degrees of freedom solved for: 36911.
Nonsymmetric matrix found.
Scales for dependent variables:
mod1.A: 1
mod1.root.mod1.mf.VCoil_1_ode: 0.19
mod1.root.mod1.mf.VCoil_2_ode: 0.19
mod1.root.mod1.mf.VCoil_3_ode: 0.19
mod1.root.mod1.mf.VCoil_4_ode: 0.19
mod1.root.mod1.mf.VCoil_5_ode: 0.19
mod1.root.mod1.mf.VCoil_6_ode: 0.19
mod1.root.mod1.mf.VCoil_7_ode: 0.19
mod1.root.mod1.mf.VCoil_8_ode: 0.19
mod1.root.mod1.mf.VCoil_9_ode: 0.19
mod1.root.mod1.mf.VCoil_10_ode: 0.19
mod1.root.mod1.mf.VCoil_11_ode: 0.19
```

```
mod1.root.mod1.mf.VCoil_12_ode: 0.19
mod1.root.mod1.mf.VCoil_13_ode: 0.19
mod1.root.mod1.mf.VCoil_14_ode: 0.19
mod1.root.mod1.mf.VCoil_15_ode: 0.19
mod1.root.mod1.mf.VCoil_16_ode: 0.19
```

Iter	ErrEst	Damping	Stepsize	#Res	#Jac	#Sol
1	0.045	0.1000000	0.05	3	1	3
2	0.042	0.1000000	0.047	5	2	6
3	0.041	0.1000000	0.044	7	3	9
4	0.039	0.1000000	0.042	9	4	12
5	0.04	0.0100000	0.04	12	5	16
6	0.041	0.0100000	0.042	14	6	19
7	0.043	0.0100000	0.044	16	7	22
8	0.045	0.0100000	0.046	18	8	25
9	0.047	0.0100000	0.047	20	9	28
10	0.049	0.0100000	0.049	22	10	31

```
Stationary Solver 1 in Solver 1: Solution time: 9 s.
Parameter omega = 1.875.
Number of vertex elements: 10
Number of boundary elements: 123
Stationary Solver 1 in Solver 1 started at 30-Sep-2015 15:30:04.
Nonlinear solver
Number of degrees of freedom solved for: 36825.
Nonsymmetric matrix found.
Scales for dependent variables:
mod1.A: 1
mod1.root.mod1.mf.VCoil_1_ode: 0.19
mod1.root.mod1.mf.VCoil_2_ode: 0.19
mod1.root.mod1.mf.VCoil_3_ode: 0.19
mod1.root.mod1.mf.VCoil_4_ode: 0.19
mod1.root.mod1.mf.VCoil_5_ode: 0.19
mod1.root.mod1.mf.VCoil_6_ode: 0.19
mod1.root.mod1.mf.VCoil_7_ode: 0.19
mod1.root.mod1.mf.VCoil_8_ode: 0.19
mod1.root.mod1.mf.VCoil_9_ode: 0.19
mod1.root.mod1.mf.VCoil_10_ode: 0.19
mod1.root.mod1.mf.VCoil_11_ode: 0.19
mod1.root.mod1.mf.VCoil_12_ode: 0.19
mod1.root.mod1.mf.VCoil_13_ode: 0.19
mod1.root.mod1.mf.VCoil_14_ode: 0.19
mod1.root.mod1.mf.VCoil_15_ode: 0.19
mod1.root.mod1.mf.VCoil_16_ode: 0.19
```

Iter	ErrEst	Damping	Stepsize	#Res	#Jac	#Sol
1	0.046	0.1000000	0.051	3	1	3
2	0.043	0.1000000	0.048	5	2	6
3	0.045	0.0100000	0.045	8	3	10
4	0.047	0.0100000	0.047	10	4	13
5	0.049	0.0100000	0.049	12	5	16
6	0.051	0.0100000	0.051	14	6	19
7	0.053	0.0100000	0.054	16	7	22
8	0.055	0.0100000	0.056	18	8	25
9	0.058	0.0100000	0.058	20	9	28
10	0.06	0.0100000	0.061	22	10	31

```
Stationary Solver 1 in Solver 1: Solution time: 11 s.
Parameter omega = 2.25.
Number of vertex elements: 10
Number of boundary elements: 124
Stationary Solver 1 in Solver 1 started at 30-Sep-2015 15:30:22.
Nonlinear solver
Number of degrees of freedom solved for: 36647.
Nonsymmetric matrix found.
Scales for dependent variables:
mod1.A: 1
mod1.root.mod1.mf.VCoil_1_ode: 0.19
mod1.root.mod1.mf.VCoil_2_ode: 0.19
mod1.root.mod1.mf.VCoil_3_ode: 0.19
mod1.root.mod1.mf.VCoil_4_ode: 0.19
mod1.root.mod1.mf.VCoil_5_ode: 0.19
mod1.root.mod1.mf.VCoil_6_ode: 0.19
mod1.root.mod1.mf.VCoil_7_ode: 0.19
mod1.root.mod1.mf.VCoil_8_ode: 0.19
mod1.root.mod1.mf.VCoil_9_ode: 0.19
mod1.root.mod1.mf.VCoil_10_ode: 0.19
mod1.root.mod1.mf.VCoil_11_ode: 0.19
mod1.root.mod1.mf.VCoil_12_ode: 0.19
mod1.root.mod1.mf.VCoil_13_ode: 0.19
mod1.root.mod1.mf.VCoil_14_ode: 0.19
mod1.root.mod1.mf.VCoil_15_ode: 0.19
mod1.root.mod1.mf.VCoil_16_ode: 0.19
```

Iter	ErrEst	Damping	Stepsize	#Res	#Jac	#Sol
1	0.047	0.1000000	0.052	3	1	3
2	0.044	0.1000000	0.049	5	2	6
3	0.046	0.0100000	0.046	8	3	10
4	0.048	0.0100000	0.048	10	4	13
5	0.05	0.0100000	0.05	12	5	16
6	0.048	0.1000000	0.052	13	6	18
7	0.049	0.0100000	0.05	16	7	22
8	0.051	0.0100000	0.052	18	8	25
9	0.054	0.0100000	0.054	20	9	28
10	0.056	0.0100000	0.056	22	10	31

```
Stationary Solver 1 in Solver 1: Solution time: 11 s.
Parameter omega = 2.625.
Number of vertex elements: 10
Number of boundary elements: 125
Stationary Solver 1 in Solver 1 started at 30-Sep-2015 15:30:42.
Nonlinear solver
Number of degrees of freedom solved for: 36885.
Nonsymmetric matrix found.
Scales for dependent variables:
mod1.A: 1
mod1.root.mod1.mf.VCoil_1_ode: 0.19
mod1.root.mod1.mf.VCoil_2_ode: 0.19
mod1.root.mod1.mf.VCoil_3_ode: 0.19
mod1.root.mod1.mf.VCoil_4_ode: 0.19
mod1.root.mod1.mf.VCoil_5_ode: 0.19
mod1.root.mod1.mf.VCoil_6_ode: 0.19
mod1.root.mod1.mf.VCoil_7_ode: 0.19
mod1.root.mod1.mf.VCoil_8_ode: 0.19
mod1.root.mod1.mf.VCoil_9_ode: 0.19
mod1.root.mod1.mf.VCoil_10_ode: 0.19
mod1.root.mod1.mf.VCoil_11_ode: 0.19
mod1.root.mod1.mf.VCoil_12_ode: 0.19
mod1.root.mod1.mf.VCoil_13_ode: 0.19
mod1.root.mod1.mf.VCoil_14_ode: 0.19
```

```
mod1.root.mod1.mf.VCoil_15_ode: 0.19
mod1.root.mod1.mf.VCoil_16_ode: 0.19
Iter      ErrEst     Damping    Stepsize #Res #Jac #Sol
   1       0.048   0.1000000       0.053    3    1    3
   2       0.045   0.1000000        0.05    5    2    6
   3       0.047   0.0100000       0.047    8    3   10
   4       0.049   0.0100000       0.049   10    4   13
   5       0.051   0.0100000       0.051   12    5   16
   6       0.053   0.0100000       0.054   14    6   19
   7       0.055   0.0100000       0.056   16    7   22
   8       0.058   0.0100000       0.058   18    8   25
   9        0.06   0.0100000       0.061   20    9   28
  10       0.063   0.0100000       0.063   22   10   31
Stationary Solver 1 in Solver 1: Solution time: 10 s.
Parameter omega = 3.0.
Number of vertex elements: 10
Number of boundary elements: 126
Stationary Solver 1 in Solver 1 started at 30-Sep-2015 15:31:00.
Nonlinear solver
Number of degrees of freedom solved for: 36759.
Nonsymmetric matrix found.
Scales for dependent variables:
mod1.A: 1
mod1.root.mod1.mf.VCoil_1_ode: 0.19
mod1.root.mod1.mf.VCoil_2_ode: 0.19
mod1.root.mod1.mf.VCoil_3_ode: 0.19
mod1.root.mod1.mf.VCoil_4_ode: 0.19
mod1.root.mod1.mf.VCoil_5_ode: 0.19
mod1.root.mod1.mf.VCoil_6_ode: 0.19
mod1.root.mod1.mf.VCoil_7_ode: 0.19
mod1.root.mod1.mf.VCoil_8_ode: 0.19
mod1.root.mod1.mf.VCoil_9_ode: 0.19
mod1.root.mod1.mf.VCoil_10_ode: 0.19
mod1.root.mod1.mf.VCoil_11_ode: 0.19
mod1.root.mod1.mf.VCoil_12_ode: 0.19
mod1.root.mod1.mf.VCoil_13_ode: 0.19
mod1.root.mod1.mf.VCoil_14_ode: 0.19
mod1.root.mod1.mf.VCoil_15_ode: 0.19
mod1.root.mod1.mf.VCoil_16_ode: 0.19
Iter      ErrEst     Damping    Stepsize #Res #Jac #Sol
   1       0.049   0.1000000       0.054    3    1    3
   2       0.046   0.1000000       0.051    5    2    6
   3       0.048   0.0100000       0.048    8    3   10
   4        0.05   0.0100000        0.05   10    4   13
   5       0.052   0.0100000       0.052   12    5   16
   6       0.054   0.0100000       0.055   14    6   19
   7       0.056   0.0100000       0.057   16    7   22
   8       0.059   0.0100000       0.059   18    8   25
   9       0.061   0.0100000       0.062   20    9   28
  10       0.064   0.0100000       0.065   22   10   31
Stationary Solver 1 in Solver 1: Solution time: 10 s.
Parameter omega = 3.375.
Number of vertex elements: 10
Number of boundary elements: 127
Stationary Solver 1 in Solver 1 started at 30-Sep-2015 15:31:18.
Nonlinear solver
Number of degrees of freedom solved for: 36841.
Nonsymmetric matrix found.
Scales for dependent variables:
mod1.A: 1
mod1.root.mod1.mf.VCoil_1_ode: 0.19
mod1.root.mod1.mf.VCoil_2_ode: 0.19
mod1.root.mod1.mf.VCoil_3_ode: 0.19
mod1.root.mod1.mf.VCoil_4_ode: 0.19
mod1.root.mod1.mf.VCoil_5_ode: 0.19
mod1.root.mod1.mf.VCoil_6_ode: 0.19
mod1.root.mod1.mf.VCoil_7_ode: 0.19
mod1.root.mod1.mf.VCoil_8_ode: 0.19
mod1.root.mod1.mf.VCoil_9_ode: 0.19
mod1.root.mod1.mf.VCoil_10_ode: 0.19
mod1.root.mod1.mf.VCoil_11_ode: 0.19
mod1.root.mod1.mf.VCoil_12_ode: 0.19
mod1.root.mod1.mf.VCoil_13_ode: 0.19
mod1.root.mod1.mf.VCoil_14_ode: 0.19
mod1.root.mod1.mf.VCoil_15_ode: 0.19
mod1.root.mod1.mf.VCoil_16_ode: 0.19
Iter      ErrEst     Damping    Stepsize #Res #Jac #Sol
   1        0.05   0.1000000       0.055    3    1    3
   2       0.047   0.1000000       0.052    5    2    6
   3       0.049   0.0100000       0.049    8    3   10
   4       0.051   0.0100000       0.051   10    4   13
   5       0.053   0.0100000       0.054   12    5   16
   6       0.055   0.0100000       0.056   14    6   19
   7       0.058   0.0100000       0.058   16    7   22
   8        0.06   0.0100000       0.061   18    8   25
   9       0.063   0.0100000       0.063   20    9   28
  10       0.065   0.0100000       0.066   22   10   31
Stationary Solver 1 in Solver 1: Solution time: 10 s.
Parameter omega = 3.75.
Number of vertex elements: 10
Number of boundary elements: 128
Stationary Solver 1 in Solver 1 started at 30-Sep-2015 15:31:35.
Nonlinear solver
Number of degrees of freedom solved for: 36827.
Nonsymmetric matrix found.
Scales for dependent variables:
mod1.A: 1
mod1.root.mod1.mf.VCoil_1_ode: 0.19
mod1.root.mod1.mf.VCoil_2_ode: 0.19
mod1.root.mod1.mf.VCoil_3_ode: 0.19
mod1.root.mod1.mf.VCoil_4_ode: 0.19
mod1.root.mod1.mf.VCoil_5_ode: 0.19
mod1.root.mod1.mf.VCoil_6_ode: 0.19
mod1.root.mod1.mf.VCoil_7_ode: 0.19
mod1.root.mod1.mf.VCoil_8_ode: 0.19
mod1.root.mod1.mf.VCoil_9_ode: 0.19
mod1.root.mod1.mf.VCoil_10_ode: 0.19
mod1.root.mod1.mf.VCoil_11_ode: 0.19
mod1.root.mod1.mf.VCoil_12_ode: 0.19
mod1.root.mod1.mf.VCoil_13_ode: 0.19
mod1.root.mod1.mf.VCoil_14_ode: 0.19
mod1.root.mod1.mf.VCoil_15_ode: 0.19
mod1.root.mod1.mf.VCoil_16_ode: 0.19
Iter      ErrEst     Damping    Stepsize #Res #Jac #Sol
```

```
   1       0.051   0.1000000       0.056    3    1    3
   2       0.048   0.1000000       0.053    5    2    6
   3        0.05   0.0100000        0.05    8    3   10
   4       0.052   0.0100000       0.052   10    4   13
   5       0.054   0.0100000       0.055   12    5   16
   6       0.056   0.0100000       0.057   14    6   19
   7       0.059   0.0100000       0.059   16    7   22
   8       0.061   0.0100000       0.062   18    8   25
   9       0.064   0.0100000       0.065   20    9   28
  10       0.067   0.0100000       0.067   22   10   31
Stationary Solver 1 in Solver 1: Solution time: 10 s.
Parameter omega = 4.125.
Number of vertex elements: 10
Number of boundary elements: 129
Stationary Solver 1 in Solver 1 started at 30-Sep-2015 15:31:53.
Nonlinear solver
Number of degrees of freedom solved for: 36869.
Nonsymmetric matrix found.
Scales for dependent variables:
mod1.A: 1
mod1.root.mod1.mf.VCoil_1_ode: 0.19
mod1.root.mod1.mf.VCoil_2_ode: 0.19
mod1.root.mod1.mf.VCoil_3_ode: 0.19
mod1.root.mod1.mf.VCoil_4_ode: 0.19
mod1.root.mod1.mf.VCoil_5_ode: 0.19
mod1.root.mod1.mf.VCoil_6_ode: 0.19
mod1.root.mod1.mf.VCoil_7_ode: 0.19
mod1.root.mod1.mf.VCoil_8_ode: 0.19
mod1.root.mod1.mf.VCoil_9_ode: 0.19
mod1.root.mod1.mf.VCoil_10_ode: 0.19
mod1.root.mod1.mf.VCoil_11_ode: 0.19
mod1.root.mod1.mf.VCoil_12_ode: 0.19
mod1.root.mod1.mf.VCoil_13_ode: 0.19
mod1.root.mod1.mf.VCoil_14_ode: 0.19
mod1.root.mod1.mf.VCoil_15_ode: 0.19
mod1.root.mod1.mf.VCoil_16_ode: 0.19
Iter      ErrEst     Damping    Stepsize #Res #Jac #Sol
   1       0.051   0.1000000       0.057    3    1    3
   2       0.048   0.1000000       0.054    5    2    6
   3        0.05   0.0100000       0.051    8    3   10
   4       0.053   0.0100000       0.053   10    4   13
   5       0.055   0.0100000       0.055   12    5   16
   6       0.057   0.0100000       0.058   14    6   19
   7        0.06   0.0100000        0.06   16    7   22
   8       0.062   0.0100000       0.063   18    8   25
   9       0.065   0.0100000       0.065   20    9   28
  10       0.067   0.0100000       0.068   22   10   31
Stationary Solver 1 in Solver 1: Solution time: 10 s.
```

E.3 Fifty Iterations

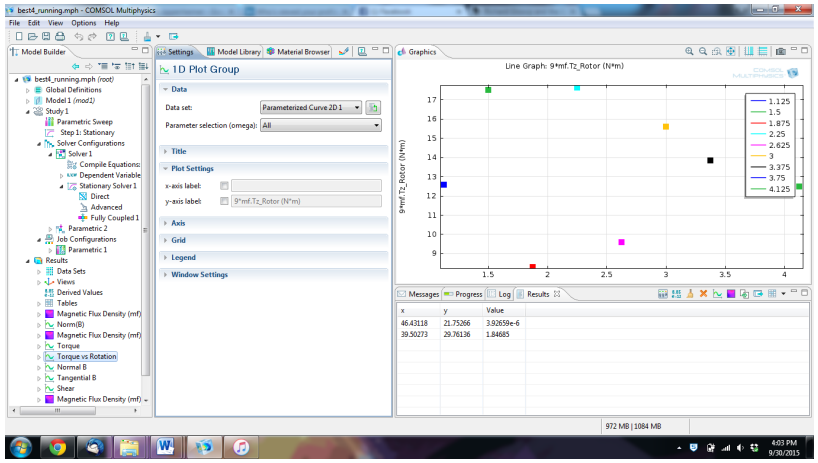

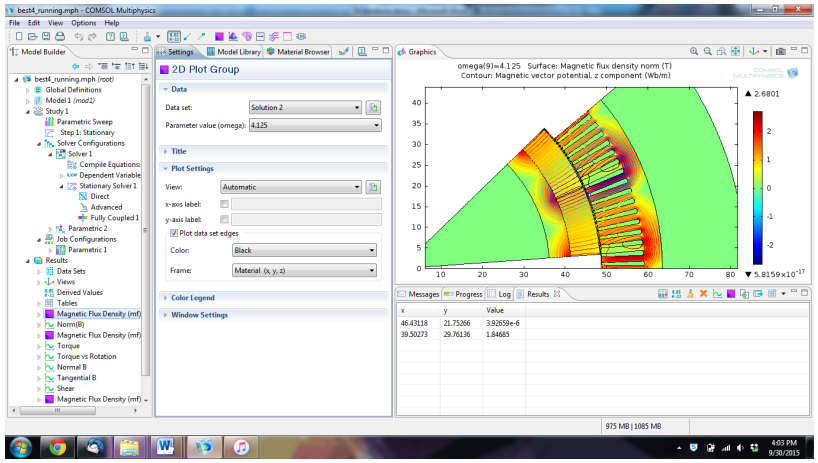


```
================================================================
Parameter omega = 1.125.
Number of vertex elements: 10
Number of boundary elements: 121
Stationary Solver 1 in Solver 1 started at 30-Sep-2015 15:55:06.
Nonlinear solver
Number of degrees of freedom solved for: 37017.
Nonsymmetric matrix found.
```

```
Scales for dependent variables:
mod1.A: 1
mod1.root.mod1.mf.VCoil_1_ode: 0.19
mod1.root.mod1.mf.VCoil_2_ode: 0.19
mod1.root.mod1.mf.VCoil_3_ode: 0.19
mod1.root.mod1.mf.VCoil_4_ode: 0.19
mod1.root.mod1.mf.VCoil_5_ode: 0.19
mod1.root.mod1.mf.VCoil_6_ode: 0.19
mod1.root.mod1.mf.VCoil_7_ode: 0.19
mod1.root.mod1.mf.VCoil_8_ode: 0.19
mod1.root.mod1.mf.VCoil_9_ode: 0.19
mod1.root.mod1.mf.VCoil_10_ode: 0.19
mod1.root.mod1.mf.VCoil_11_ode: 0.19
mod1.root.mod1.mf.VCoil_12_ode: 0.19
mod1.root.mod1.mf.VCoil_13_ode: 0.19
mod1.root.mod1.mf.VCoil_14_ode: 0.19
mod1.root.mod1.mf.VCoil_15_ode: 0.19
mod1.root.mod1.mf.VCoil_16_ode: 0.19
```

Iter	ErrEst	Damping	Stepsize	#Res	#Jac	#Sol
1	0.044	0.1000000	0.049	3	1	3
2	0.041	0.1000000	0.046	5	2	6
3	0.039	0.1000000	0.044	7	3	9
4	0.041	0.0100000	0.041	10	4	13
5	0.039	0.1000000	0.043	11	5	15
6	0.04	0.0100000	0.041	14	6	19
7	0.042	0.0100000	0.043	16	7	22
8	0.044	0.0100000	0.044	18	8	25
9	0.046	0.0100000	0.046	20	9	28
10	0.048	0.0100000	0.048	22	10	31
11	0.05	0.0100000	0.05	24	11	34
12	0.052	0.0100000	0.052	26	12	37
13	0.054	0.0100000	0.055	28	13	40
14	0.057	0.0100000	0.057	30	14	43
15	0.059	0.0100000	0.059	32	15	46
16	0.061	0.0100000	0.062	34	16	49
17	0.064	0.0100000	0.065	36	17	52
18	0.067	0.0100000	0.067	38	18	55
19	0.07	0.0100000	0.07	40	19	58
20	0.073	0.0100000	0.073	42	20	61
21	0.076	0.0100000	0.076	44	21	64
22	0.079	0.0100000	0.08	46	22	67
23	0.082	0.0100000	0.083	48	23	70
24	0.086	0.0100000	0.087	50	24	73
25	0.089	0.0100000	0.09	52	25	76
26	0.093	0.0100000	0.094	54	26	79
27	0.097	0.0100000	0.098	56	27	82
28	0.1	0.0100000	0.1	58	28	85
29	0.11	0.0100000	0.11	60	29	88
30	0.11	0.0165913	0.11	62	30	91
31	0.11	0.0165913	0.12	64	31	94
32	0.12	0.0165913	0.12	66	32	97
33	0.12	0.0165913	0.12	68	33	100
34	0.13	0.0165913	0.13	70	34	103
35	0.13	0.0165913	0.13	72	35	106
36	0.14	0.0165913	0.14	74	36	109
37	0.14	0.0165913	0.14	76	37	112
38	0.14	0.0165913	0.15	78	38	115

```
  39        0.15   0.0165913        0.15   80   39  118
  40        0.15   0.0165913        0.16   82   40  121
  41        0.16   0.0165913        0.16   84   41  124
  42        0.17   0.0165913        0.17   86   42  127
  43        0.17   0.0165913        0.17   88   43  130
  44        0.18   0.0165913        0.18   90   44  133
  45        0.18   0.0165913        0.19   92   45  136
  46        0.19   0.0165913        0.19   94   46  139
  47         0.2   0.0165913         0.2   96   47  142
  48         0.2   0.0165913        0.21   98   48  145
  49        0.21   0.0165913        0.21  100   49  148
  50        0.22   0.0165913        0.22  102   50  151
Stationary Solver 1 in Solver 1: Solution time: 45 s.
Parameter omega = 1.5.
Number of vertex elements: 10
Number of boundary elements: 122
Stationary Solver 1 in Solver 1 started at 30-Sep-2015 15:55:57.
Nonlinear solver
Number of degrees of freedom solved for: 36911.
Nonsymmetric matrix found.
Scales for dependent variables:
mod1.A: 1
mod1.root.mod1.mf.VCoil_1_ode: 0.19
mod1.root.mod1.mf.VCoil_2_ode: 0.19
mod1.root.mod1.mf.VCoil_3_ode: 0.19
mod1.root.mod1.mf.VCoil_4_ode: 0.19
mod1.root.mod1.mf.VCoil_5_ode: 0.19
mod1.root.mod1.mf.VCoil_6_ode: 0.19
mod1.root.mod1.mf.VCoil_7_ode: 0.19
mod1.root.mod1.mf.VCoil_8_ode: 0.19
mod1.root.mod1.mf.VCoil_9_ode: 0.19
mod1.root.mod1.mf.VCoil_10_ode: 0.19
mod1.root.mod1.mf.VCoil_11_ode: 0.19
mod1.root.mod1.mf.VCoil_12_ode: 0.19
mod1.root.mod1.mf.VCoil_13_ode: 0.19
mod1.root.mod1.mf.VCoil_14_ode: 0.19
mod1.root.mod1.mf.VCoil_15_ode: 0.19
mod1.root.mod1.mf.VCoil_16_ode: 0.19
Iter      ErrEst     Damping    Stepsize #Res #Jac #Sol
   1       0.045   0.1000000        0.05    3    1    3
   2       0.042   0.1000000       0.047    5    2    6
   3       0.041   0.1000000       0.044    7    3    9
   4       0.039   0.1000000       0.042    9    4   12
   5        0.04   0.0100000        0.04   12    5   16
   6       0.041   0.0100000       0.042   14    6   19
   7       0.043   0.0100000       0.044   16    7   22
   8       0.045   0.0100000       0.046   18    8   25
   9       0.047   0.0100000       0.047   20    9   28
  10       0.049   0.0100000       0.049   22   10   31
  11       0.051   0.0100000       0.052   24   11   34
  12       0.053   0.0100000       0.054   26   12   37
  13       0.056   0.0100000       0.056   28   13   40
  14       0.058   0.0100000       0.058   30   14   43
  15        0.06   0.0100000       0.061   32   15   46
  16       0.063   0.0100000       0.064   34   16   49
  17       0.066   0.0100000       0.066   36   17   52
  18       0.068   0.0100000       0.069   38   18   55
  19       0.071   0.0100000       0.072   40   19   58
  20       0.074   0.0100000       0.075   42   20   61
  21       0.078   0.0100000       0.078   44   21   64
  22       0.081   0.0100000       0.082   46   22   67
  23       0.084   0.0100000       0.085   48   23   70
  24       0.088   0.0100000       0.089   50   24   73
  25       0.092   0.0100000       0.093   52   25   76
  26       0.096   0.0100000       0.097   54   26   79
  27         0.1   0.0100000         0.1   56   27   82
  28         0.1   0.0100000        0.11   58   28   85
  29        0.11   0.0100000        0.11   60   29   88
  30        0.11   0.0100000        0.11   62   30   91
  31        0.12   0.0100000        0.12   64   31   94
  32        0.12   0.0100000        0.12   66   32   97
  33        0.13   0.0100000        0.13   68   33  100
  34        0.13   0.0100000        0.13   70   34  103
  35        0.14   0.0100000        0.14   72   35  106
  36        0.14   0.0100000        0.15   74   36  109
  37        0.15   0.0100000        0.15   76   37  112
  38        0.16   0.0100000        0.16   78   38  115
  39        0.16   0.0100000        0.16   80   39  118
  40        0.17   0.0100000        0.17   82   40  121
  41        0.18   0.0100000        0.18   84   41  124
  42        0.18   0.0100000        0.19   86   42  127
  43        0.19   0.1000000        0.19   87   43  129
  44        0.17   0.0645361        0.18   89   44  132
  45        0.17   0.0645361        0.18   91   45  135
  46        0.16   0.0645361        0.18   93   46  138
  47        0.16   0.0645361        0.17   95   47  141
  48        0.16   0.0645361        0.17   97   48  144
  49        0.16   0.0645361        0.17   99   49  147
  50        0.15   0.0645361        0.17  101   50  150
Stationary Solver 1 in Solver 1: Solution time: 48 s.
Parameter omega = 1.875.
Number of vertex elements: 10
Number of boundary elements: 123
Stationary Solver 1 in Solver 1 started at 30-Sep-2015 15:56:53.
Nonlinear solver
Number of degrees of freedom solved for: 36825.
Nonsymmetric matrix found.
Scales for dependent variables:
mod1.A: 1
mod1.root.mod1.mf.VCoil_1_ode: 0.19
mod1.root.mod1.mf.VCoil_2_ode: 0.19
mod1.root.mod1.mf.VCoil_3_ode: 0.19
mod1.root.mod1.mf.VCoil_4_ode: 0.19
mod1.root.mod1.mf.VCoil_5_ode: 0.19
mod1.root.mod1.mf.VCoil_6_ode: 0.19
mod1.root.mod1.mf.VCoil_7_ode: 0.19
mod1.root.mod1.mf.VCoil_8_ode: 0.19
mod1.root.mod1.mf.VCoil_9_ode: 0.19
mod1.root.mod1.mf.VCoil_10_ode: 0.19
mod1.root.mod1.mf.VCoil_11_ode: 0.19
mod1.root.mod1.mf.VCoil_12_ode: 0.19
mod1.root.mod1.mf.VCoil_13_ode: 0.19
mod1.root.mod1.mf.VCoil_14_ode: 0.19
mod1.root.mod1.mf.VCoil_15_ode: 0.19
```

```
mod1.root.mod1.mf.VCoil_16_ode: 0.19
Iter      ErrEst     Damping    Stepsize #Res #Jac #Sol
   1       0.046   0.1000000       0.051    3    1    3
   2       0.043   0.1000000       0.048    5    2    6
   3       0.045   0.0100000       0.045    8    3   10
   4       0.047   0.0100000       0.047   10    4   13
   5       0.049   0.0100000       0.049   12    5   16
   6       0.051   0.0100000       0.051   14    6   19
   7       0.053   0.0100000       0.054   16    7   22
   8       0.055   0.0100000       0.056   18    8   25
   9       0.058   0.0100000       0.058   20    9   28
  10        0.06   0.0100000       0.061   22   10   31
  11       0.063   0.0100000       0.063   24   11   34
  12       0.065   0.0100000       0.066   26   12   37
  13       0.068   0.0100000       0.069   28   13   40
  14       0.071   0.0100000       0.071   30   14   43
  15       0.074   0.0100000       0.074   32   15   46
  16       0.077   0.0100000       0.078   34   16   49
  17        0.08   0.0100000       0.081   36   17   52
  18       0.084   0.0100000       0.084   38   18   55
  19       0.087   0.0100000       0.088   40   19   58
  20       0.091   0.0100000       0.092   42   20   61
  21       0.094   0.0100000       0.095   44   21   64
  22       0.099   0.0100000         0.1   46   22   67
  23         0.1   0.0100000         0.1   48   23   70
  24        0.11   0.0100000        0.11   50   24   73
  25        0.11   0.0100000        0.11   52   25   76
  26        0.12   0.0100000        0.12   54   26   79
  27        0.12   0.0100000        0.12   56   27   82
  28        0.13   0.0100000        0.13   58   28   85
  29        0.13   0.0100000        0.13   60   29   88
  30        0.14   0.0100000        0.14   62   30   91
  31        0.14   0.0100000        0.14   64   31   94
  32        0.15   0.0100000        0.15   66   32   97
  33        0.16   0.0100000        0.16   68   33  100
  34        0.16   0.0100000        0.16   70   34  103
  35        0.17   0.0100000        0.17   72   35  106
  36        0.18   0.0100000        0.18   74   36  109
  37        0.18   0.0100000        0.19   76   37  112
  38        0.19   0.0100000        0.19   78   38  115
  39         0.2   0.0100000         0.2   80   39  118
  40        0.21   0.0100000        0.21   82   40  121
  41        0.22   0.0100000        0.22   84   41  124
  42        0.23   0.0100000        0.23   86   42  127
  43        0.23   0.0100000        0.24   88   43  130
  44        0.24   0.0100000        0.25   90   44  133
  45        0.25   0.0100000        0.26   92   45  136
  46        0.26   0.0100000        0.27   94   46  139
  47        0.28   0.0100000        0.28   96   47  142
  48        0.29   0.0100000        0.29   98   48  145
  49         0.3   0.0100000         0.3  100   49  148
  50        0.31   0.0100000        0.31  102   50  151
Stationary Solver 1 in Solver 1: Solution time: 45 s.
Parameter omega = 2.25.
Number of vertex elements: 10
Number of boundary elements: 124
Stationary Solver 1 in Solver 1 started at 30-Sep-2015 15:57:45.
Nonlinear solver
Number of degrees of freedom solved for: 36647.
Nonsymmetric matrix found.
Scales for dependent variables:
mod1.A: 1
mod1.root.mod1.mf.VCoil_1_ode: 0.19
mod1.root.mod1.mf.VCoil_2_ode: 0.19
mod1.root.mod1.mf.VCoil_3_ode: 0.19
mod1.root.mod1.mf.VCoil_4_ode: 0.19
mod1.root.mod1.mf.VCoil_5_ode: 0.19
mod1.root.mod1.mf.VCoil_6_ode: 0.19
mod1.root.mod1.mf.VCoil_7_ode: 0.19
mod1.root.mod1.mf.VCoil_8_ode: 0.19
mod1.root.mod1.mf.VCoil_9_ode: 0.19
mod1.root.mod1.mf.VCoil_10_ode: 0.19
mod1.root.mod1.mf.VCoil_11_ode: 0.19
mod1.root.mod1.mf.VCoil_12_ode: 0.19
mod1.root.mod1.mf.VCoil_13_ode: 0.19
mod1.root.mod1.mf.VCoil_14_ode: 0.19
mod1.root.mod1.mf.VCoil_15_ode: 0.19
mod1.root.mod1.mf.VCoil_16_ode: 0.19
Iter      ErrEst     Damping    Stepsize #Res #Jac #Sol
   1       0.047   0.1000000       0.052    3    1    3
   2       0.044   0.1000000       0.049    5    2    6
   3       0.046   0.0100000       0.046    8    3   10
   4       0.048   0.0100000       0.048   10    4   13
   5        0.05   0.0100000        0.05   12    5   16
   6       0.048   0.1000000       0.052   13    6   18
   7       0.049   0.0100000        0.05   16    7   22
   8       0.051   0.0100000       0.052   18    8   25
   9       0.054   0.0100000       0.054   20    9   28
  10       0.056   0.0100000       0.056   22   10   31
  11       0.058   0.0100000       0.059   24   11   34
  12       0.061   0.0100000       0.061   26   12   37
  13       0.063   0.0100000       0.064   28   13   40
  14       0.066   0.0100000       0.067   30   14   43
  15       0.069   0.0100000        0.07   32   15   46
  16       0.072   0.0100000       0.073   34   16   49
  17       0.075   0.0100000       0.076   36   17   52
  18       0.078   0.0100000       0.079   38   18   55
  19       0.082   0.0100000       0.082   40   19   58
  20       0.085   0.0100000       0.086   42   20   61
  21       0.089   0.0100000        0.09   44   21   64
  22       0.093   0.0100000       0.093   46   22   67
  23       0.097   0.0100000       0.097   48   23   70
  24         0.1   0.0100000         0.1   50   24   73
  25         0.1   0.0100000        0.11   52   25   76
  26        0.11   0.0100000        0.11   54   26   79
  27        0.11   0.0100000        0.12   56   27   82
  28        0.12   0.0100000        0.12   58   28   85
  29        0.12   0.0100000        0.13   60   29   88
  30        0.13   0.0100000        0.13   62   30   91
  31        0.13   0.0100000        0.14   64   31   94
  32        0.14   0.0100000        0.14   66   32   97
  33        0.15   0.0100000        0.15   68   33  100
  34        0.15   0.0100000        0.15   70   34  103
  35        0.16   0.0100000        0.16   72   35  106
```

```
  36        0.16   0.0100000        0.17   74   36  109
  37        0.17   0.0100000        0.17   76   37  112
  38        0.18   0.0100000        0.18   78   38  115
  39        0.19   0.0100000        0.19   80   39  118
  40        0.18   0.1000000        0.19   81   40  120
  41        0.17   0.0625646        0.18   83   41  123
  42        0.17   0.0625646        0.18   85   42  126
  43        0.17   0.0625646        0.18   87   43  129
  44        0.16   0.0625646        0.18   89   44  132
  45        0.16   0.0625646        0.17   91   45  135
  46        0.16   0.0625646        0.17   93   46  138
  47        0.16   0.0625646        0.17   95   47  141
  48        0.17   0.0062565        0.17   98   48  145
  49        0.17   0.0625646        0.17   99   49  147
  50        0.17   0.0192446        0.17  101   50  150
Stationary Solver 1 in Solver 1: Solution time: 44 s.
Parameter omega = 2.625.
Number of vertex elements: 10
Number of boundary elements: 125
Stationary Solver 1 in Solver 1 started at 30-Sep-2015 15:58:36.
Nonlinear solver
Number of degrees of freedom solved for: 36885.
Nonsymmetric matrix found.
Scales for dependent variables:
mod1.A: 1
mod1.root.mod1.mf.VCoil_1_ode: 0.19
mod1.root.mod1.mf.VCoil_2_ode: 0.19
mod1.root.mod1.mf.VCoil_3_ode: 0.19
mod1.root.mod1.mf.VCoil_4_ode: 0.19
mod1.root.mod1.mf.VCoil_5_ode: 0.19
mod1.root.mod1.mf.VCoil_6_ode: 0.19
mod1.root.mod1.mf.VCoil_7_ode: 0.19
mod1.root.mod1.mf.VCoil_8_ode: 0.19
mod1.root.mod1.mf.VCoil_9_ode: 0.19
mod1.root.mod1.mf.VCoil_10_ode: 0.19
mod1.root.mod1.mf.VCoil_11_ode: 0.19
mod1.root.mod1.mf.VCoil_12_ode: 0.19
mod1.root.mod1.mf.VCoil_13_ode: 0.19
mod1.root.mod1.mf.VCoil_14_ode: 0.19
mod1.root.mod1.mf.VCoil_15_ode: 0.19
mod1.root.mod1.mf.VCoil_16_ode: 0.19
Iter      ErrEst     Damping    Stepsize #Res #Jac #Sol
   1       0.048   0.1000000       0.053    3    1    3
   2       0.045   0.1000000        0.05    5    2    6
   3       0.047   0.0100000       0.047    8    3   10
   4       0.049   0.0100000       0.049   10    4   13
   5       0.051   0.0100000       0.051   12    5   16
   6       0.053   0.0100000       0.054   14    6   19
   7       0.055   0.0100000       0.056   16    7   22
   8       0.058   0.0100000       0.058   18    8   25
   9        0.06   0.0100000       0.061   20    9   28
  10       0.063   0.0100000       0.063   22   10   31
  11       0.065   0.0100000       0.066   24   11   34
  12       0.068   0.0100000       0.069   26   12   37
  13       0.071   0.0100000       0.072   28   13   40
  14       0.074   0.0100000       0.075   30   14   43
  15       0.077   0.0100000       0.078   32   15   46
  16        0.08   0.0100000       0.081   34   16   49
  17       0.084   0.0100000       0.085   36   17   52
  18       0.087   0.0100000       0.088   38   18   55
  19       0.091   0.0100000       0.092   40   19   58
  20       0.095   0.0100000       0.096   42   20   61
  21       0.099   0.0100000         0.1   44   21   64
  22         0.1   0.0100000         0.1   46   22   67
  23        0.11   0.0100000        0.11   48   23   70
  24        0.11   0.0100000        0.11   50   24   73
  25        0.12   0.0100000        0.12   52   25   76
  26        0.12   0.0100000        0.12   54   26   79
  27        0.13   0.0100000        0.13   56   27   82
  28        0.13   0.0100000        0.13   58   28   85
  29        0.14   0.0100000        0.14   60   29   88
  30        0.14   0.0100000        0.15   62   30   91
  31        0.15   0.0100000        0.15   64   31   94
  32        0.16   0.0100000        0.16   66   32   97
  33        0.16   0.0100000        0.16   68   33  100
  34        0.17   0.0100000        0.17   70   34  103
  35        0.18   0.0100000        0.18   72   35  106
  36        0.18   0.0100000        0.19   74   36  109
  37        0.19   0.0100000        0.19   76   37  112
  38         0.2   0.0100000         0.2   78   38  115
  39        0.21   0.0100000        0.21   80   39  118
  40        0.22   0.0100000        0.22   82   40  121
  41        0.22   0.0100000        0.23   84   41  124
  42        0.23   0.0114514        0.23   86   42  127
  43        0.24   0.0130367        0.24   88   43  130
  44        0.25   0.0130367        0.25   90   44  133
  45        0.26   0.0130367        0.26   92   45  136
  46        0.26   0.0213471        0.27   94   46  139
  47        0.27   0.0213471        0.28   96   47  142
  48        0.28   0.0213471        0.28   98   48  145
  49        0.29   0.0213471        0.29  100   49  148
  50        0.29   0.0213471         0.3  102   50  151
Stationary Solver 1 in Solver 1: Solution time: 44 s.
Parameter omega = 3.0.
Number of vertex elements: 10
Number of boundary elements: 126
Stationary Solver 1 in Solver 1 started at 30-Sep-2015 15:59:27.
Nonlinear solver
Number of degrees of freedom solved for: 36759.
Nonsymmetric matrix found.
Scales for dependent variables:
mod1.A: 1
mod1.root.mod1.mf.VCoil_1_ode: 0.19
mod1.root.mod1.mf.VCoil_2_ode: 0.19
mod1.root.mod1.mf.VCoil_3_ode: 0.19
mod1.root.mod1.mf.VCoil_4_ode: 0.19
mod1.root.mod1.mf.VCoil_5_ode: 0.19
mod1.root.mod1.mf.VCoil_6_ode: 0.19
mod1.root.mod1.mf.VCoil_7_ode: 0.19
mod1.root.mod1.mf.VCoil_8_ode: 0.19
mod1.root.mod1.mf.VCoil_9_ode: 0.19
mod1.root.mod1.mf.VCoil_10_ode: 0.19
mod1.root.mod1.mf.VCoil_11_ode: 0.19
mod1.root.mod1.mf.VCoil_12_ode: 0.19
```

```
mod1.root.mod1.mf.VCoil_13_ode: 0.19
mod1.root.mod1.mf.VCoil_14_ode: 0.19
mod1.root.mod1.mf.VCoil_15_ode: 0.19
mod1.root.mod1.mf.VCoil_16_ode: 0.19
```

Iter	ErrEst	Damping	Stepsize	#Res	#Jac	#Sol
1	0.049	0.1000000	0.054	3	1	3
2	0.046	0.1000000	0.051	5	2	6
3	0.048	0.0100000	0.048	8	3	10
4	0.05	0.0100000	0.05	10	4	13
5	0.052	0.0100000	0.052	12	5	16
6	0.054	0.0100000	0.055	14	6	19
7	0.056	0.0100000	0.057	16	7	22
8	0.059	0.0100000	0.059	18	8	25
9	0.061	0.0100000	0.062	20	9	28
10	0.064	0.0100000	0.065	22	10	31
11	0.067	0.0100000	0.067	24	11	34
12	0.069	0.0100000	0.07	26	12	37
13	0.072	0.0100000	0.073	28	13	40
14	0.075	0.0100000	0.076	30	14	43
15	0.079	0.0100000	0.079	32	15	46
16	0.082	0.0100000	0.083	34	16	49
17	0.086	0.0100000	0.086	36	17	52
18	0.089	0.0100000	0.09	38	18	55
19	0.093	0.0100000	0.094	40	19	58
20	0.097	0.0100000	0.098	42	20	61
21	0.1	0.0100000	0.1	44	21	64
22	0.11	0.0100000	0.11	46	22	67
23	0.11	0.0100000	0.11	48	23	70
24	0.11	0.0100000	0.12	50	24	73
25	0.12	0.0100000	0.12	52	25	76
26	0.12	0.0100000	0.13	54	26	79
27	0.13	0.0100000	0.13	56	27	82
28	0.14	0.0100000	0.14	58	28	85
29	0.14	0.0100000	0.14	60	29	88
30	0.15	0.0100000	0.15	62	30	91
31	0.15	0.0100000	0.15	64	31	94
32	0.16	0.0100000	0.16	66	32	97
33	0.17	0.0100000	0.17	68	33	100
34	0.17	0.0100000	0.17	70	34	103
35	0.18	0.0100000	0.18	72	35	106
36	0.19	0.0100000	0.19	74	36	109
37	0.18	0.1000000	0.19	75	37	111
38	0.17	0.0403578	0.18	77	38	114
39	0.18	0.0403578	0.18	79	39	117
40	0.18	0.0403578	0.19	81	40	120
41	0.18	0.0403578	0.19	83	41	123
42	0.18	0.0403578	0.19	85	42	126
43	0.18	0.0403578	0.19	87	43	129
44	0.19	0.0403578	0.19	89	44	132
45	0.19	0.0403578	0.2	91	45	135
46	0.19	0.0403578	0.2	93	46	138
47	0.19	0.0403578	0.2	95	47	141
48	0.2	0.0403578	0.2	97	48	144
49	0.2	0.0403578	0.21	99	49	147
50	0.2	0.0403578	0.21	101	50	150

```
Stationary Solver 1 in Solver 1: Solution time: 47 s.
Parameter omega = 3.375.
Number of vertex elements: 10
Number of boundary elements: 127
Stationary Solver 1 in Solver 1 started at 30-Sep-2015 16:00:22.
Nonlinear solver
Number of degrees of freedom solved for: 36841.
Nonsymmetric matrix found.
Scales for dependent variables:
mod1.A: 1
mod1.root.mod1.mf.VCoil_1_ode: 0.19
mod1.root.mod1.mf.VCoil_2_ode: 0.19
mod1.root.mod1.mf.VCoil_3_ode: 0.19
mod1.root.mod1.mf.VCoil_4_ode: 0.19
mod1.root.mod1.mf.VCoil_5_ode: 0.19
mod1.root.mod1.mf.VCoil_6_ode: 0.19
mod1.root.mod1.mf.VCoil_7_ode: 0.19
mod1.root.mod1.mf.VCoil_8_ode: 0.19
mod1.root.mod1.mf.VCoil_9_ode: 0.19
mod1.root.mod1.mf.VCoil_10_ode: 0.19
mod1.root.mod1.mf.VCoil_11_ode: 0.19
mod1.root.mod1.mf.VCoil_12_ode: 0.19
mod1.root.mod1.mf.VCoil_13_ode: 0.19
mod1.root.mod1.mf.VCoil_14_ode: 0.19
mod1.root.mod1.mf.VCoil_15_ode: 0.19
mod1.root.mod1.mf.VCoil_16_ode: 0.19
```

Iter	ErrEst	Damping	Stepsize	#Res	#Jac	#Sol
1	0.05	0.1000000	0.055	3	1	3
2	0.047	0.1000000	0.052	5	2	6
3	0.049	0.0100000	0.049	8	3	10
4	0.051	0.0100000	0.051	10	4	13
5	0.053	0.0100000	0.054	12	5	16
6	0.055	0.0100000	0.056	14	6	19
7	0.058	0.0100000	0.058	16	7	22
8	0.06	0.0100000	0.061	18	8	25
9	0.063	0.0100000	0.063	20	9	28
10	0.065	0.0100000	0.066	22	10	31
11	0.068	0.0100000	0.069	24	11	34
12	0.071	0.0100000	0.072	26	12	37
13	0.074	0.0100000	0.075	28	13	40
14	0.077	0.0100000	0.078	30	14	43
15	0.081	0.0100000	0.081	32	15	46
16	0.084	0.0100000	0.085	34	16	49
17	0.088	0.0100000	0.089	36	17	52
18	0.091	0.0100000	0.092	38	18	55
19	0.095	0.0100000	0.096	40	19	58
20	0.099	0.0100000	0.1	42	20	61
21	0.1	0.0100000	0.1	44	21	64
22	0.11	0.0100000	0.11	46	22	67
23	0.11	0.0100000	0.11	48	23	70
24	0.12	0.0100000	0.12	50	24	73
25	0.12	0.0100000	0.12	52	25	76
26	0.13	0.0100000	0.13	54	26	79
27	0.13	0.0100000	0.13	56	27	82
28	0.14	0.0100000	0.14	58	28	85
29	0.14	0.0100000	0.14	60	29	88
30	0.15	0.0100000	0.15	62	30	91
31	0.15	0.0100000	0.16	64	31	94
32	0.16	0.0100000	0.16	66	32	97

```
  33        0.17   0.0100000        0.17   68   33  100
  34        0.17   0.1000000        0.17   69   34  102
  35        0.16   0.0290886        0.16   71   35  105
  36        0.16   0.0290886        0.17   73   36  108
  37        0.17   0.0290886        0.17   75   37  111
  38        0.17   0.0290886        0.18   77   38  114
  39        0.17   0.0290886        0.18   79   39  117
  40        0.18   0.0290886        0.18   81   40  120
  41        0.18   0.0290886        0.19   83   41  123
  42        0.19   0.0290886        0.19   85   42  126
  43        0.19   0.0290886         0.2   87   43  129
  44        0.19   0.0290886         0.2   89   44  132
  45         0.2   0.0290886         0.2   91   45  135
  46         0.2   0.0290886        0.21   93   46  138
  47        0.21   0.0290886        0.21   95   47  141
  48        0.21   0.0290886        0.22   97   48  144
  49        0.22   0.0290886        0.22   99   49  147
  50        0.22   0.0290886        0.23  101   50  150
Stationary Solver 1 in Solver 1: Solution time: 46 s.
Parameter omega = 3.75.
Number of vertex elements: 10
Number of boundary elements: 128
Stationary Solver 1 in Solver 1 started at 30-Sep-2015 16:01:16.
Nonlinear solver
Number of degrees of freedom solved for: 36827.
Nonsymmetric matrix found.
Scales for dependent variables:
mod1.A: 1
mod1.root.mod1.mf.VCoil_1_ode: 0.19
mod1.root.mod1.mf.VCoil_2_ode: 0.19
mod1.root.mod1.mf.VCoil_3_ode: 0.19
mod1.root.mod1.mf.VCoil_4_ode: 0.19
mod1.root.mod1.mf.VCoil_5_ode: 0.19
mod1.root.mod1.mf.VCoil_6_ode: 0.19
mod1.root.mod1.mf.VCoil_7_ode: 0.19
mod1.root.mod1.mf.VCoil_8_ode: 0.19
mod1.root.mod1.mf.VCoil_9_ode: 0.19
mod1.root.mod1.mf.VCoil_10_ode: 0.19
mod1.root.mod1.mf.VCoil_11_ode: 0.19
mod1.root.mod1.mf.VCoil_12_ode: 0.19
mod1.root.mod1.mf.VCoil_13_ode: 0.19
mod1.root.mod1.mf.VCoil_14_ode: 0.19
mod1.root.mod1.mf.VCoil_15_ode: 0.19
mod1.root.mod1.mf.VCoil_16_ode: 0.19
Iter      ErrEst     Damping    Stepsize #Res #Jac #Sol
   1       0.051   0.1000000       0.056    3    1    3
   2       0.048   0.1000000       0.053    5    2    6
   3        0.05   0.0100000        0.05    8    3   10
   4       0.052   0.0100000       0.052   10    4   13
   5       0.054   0.0100000       0.055   12    5   16
   6       0.056   0.0100000       0.057   14    6   19
   7       0.059   0.0100000       0.059   16    7   22
   8       0.061   0.0100000       0.062   18    8   25
   9       0.064   0.0100000       0.065   20    9   28
  10       0.067   0.0100000       0.067   22   10   31
  11       0.069   0.0100000        0.07   24   11   34
  12       0.072   0.0100000       0.073   26   12   37
  13       0.076   0.0100000       0.076   28   13   40
  14       0.079   0.0100000        0.08   30   14   43
  15       0.082   0.0100000       0.083   32   15   46
  16       0.086   0.0100000       0.087   34   16   49
  17       0.089   0.0100000        0.09   36   17   52
  18       0.093   0.0100000       0.094   38   18   55
  19       0.097   0.0100000       0.098   40   19   58
  20         0.1   0.0100000         0.1   42   20   61
  21        0.11   0.0100000        0.11   44   21   64
  22        0.11   0.0100000        0.11   46   22   67
  23        0.11   0.0100000        0.12   48   23   70
  24        0.12   0.0100000        0.12   50   24   73
  25        0.12   0.0100000        0.13   52   25   76
  26        0.13   0.0100000        0.13   54   26   79
  27        0.13   0.0100000        0.14   56   27   82
  28        0.14   0.0100000        0.14   58   28   85
  29        0.14   0.0100000        0.15   60   29   88
  30        0.15   0.0100000        0.15   62   30   91
  31        0.14   0.1000000        0.16   63   31   93
  32        0.15   0.0100000        0.15   66   32   97
  33        0.14   0.1000000        0.15   67   33   99
  34        0.15   0.1000000        0.15   69   34  102
  35        0.14   0.0328079        0.14   71   35  105
  36        0.14   0.0328079        0.14   73   36  108
  37        0.14   0.0328079        0.14   75   37  111
  38        0.14   0.0328079        0.15   77   38  114
  39        0.15   0.0328079        0.15   79   39  117
  40        0.15   0.0328079        0.15   81   40  120
  41        0.15   0.0328079        0.16   83   41  123
  42        0.15   0.0328079        0.16   85   42  126
  43        0.16   0.0328079        0.16   87   43  129
  44        0.16   0.0328079        0.16   89   44  132
  45        0.16   0.0328079        0.16   91   45  135
  46        0.16   0.0328079        0.17   93   46  138
  47        0.16   0.0328079        0.17   95   47  141
  48        0.16   0.0328079        0.17   97   48  144
  49        0.17   0.0328079        0.17   99   49  147
  50        0.17   0.0328079        0.17  101   50  150
Stationary Solver 1 in Solver 1: Solution time: 43 s.
Parameter omega = 4.125.
Number of vertex elements: 10
Number of boundary elements: 129
Stationary Solver 1 in Solver 1 started at 30-Sep-2015 16:02:06.
Nonlinear solver
Number of degrees of freedom solved for: 36869.
Nonsymmetric matrix found.
Scales for dependent variables:
mod1.A: 1
mod1.root.mod1.mf.VCoil_1_ode: 0.19
mod1.root.mod1.mf.VCoil_2_ode: 0.19
mod1.root.mod1.mf.VCoil_3_ode: 0.19
mod1.root.mod1.mf.VCoil_4_ode: 0.19
mod1.root.mod1.mf.VCoil_5_ode: 0.19
mod1.root.mod1.mf.VCoil_6_ode: 0.19
mod1.root.mod1.mf.VCoil_7_ode: 0.19
mod1.root.mod1.mf.VCoil_8_ode: 0.19
mod1.root.mod1.mf.VCoil_9_ode: 0.19
```

```
mod1.root.mod1.mf.VCoil_10_ode: 0.19
mod1.root.mod1.mf.VCoil_11_ode: 0.19
mod1.root.mod1.mf.VCoil_12_ode: 0.19
mod1.root.mod1.mf.VCoil_13_ode: 0.19
mod1.root.mod1.mf.VCoil_14_ode: 0.19
mod1.root.mod1.mf.VCoil_15_ode: 0.19
mod1.root.mod1.mf.VCoil_16_ode: 0.19
```

Iter	ErrEst	Damping	Stepsize	#Res	#Jac	#Sol
1	0.051	0.1000000	0.057	3	1	3
2	0.048	0.1000000	0.054	5	2	6
3	0.05	0.0100000	0.051	8	3	10
4	0.053	0.0100000	0.053	10	4	13
5	0.055	0.0100000	0.055	12	5	16
6	0.057	0.0100000	0.058	14	6	19
7	0.06	0.0100000	0.06	16	7	22
8	0.062	0.0100000	0.063	18	8	25
9	0.065	0.0100000	0.065	20	9	28
10	0.067	0.0100000	0.068	22	10	31
11	0.07	0.0100000	0.071	24	11	34
12	0.073	0.0100000	0.074	26	12	37
13	0.077	0.0100000	0.077	28	13	40
14	0.08	0.0100000	0.081	30	14	43
15	0.083	0.0100000	0.084	32	15	46
16	0.087	0.0100000	0.088	34	16	49
17	0.091	0.0100000	0.092	36	17	52
18	0.095	0.0100000	0.096	38	18	55
19	0.098	0.0100000	0.099	40	19	58
20	0.1	0.0100000	0.1	42	20	61
21	0.11	0.0100000	0.11	44	21	64
22	0.11	0.0100000	0.11	46	22	67
23	0.12	0.0100000	0.12	48	23	70
24	0.12	0.0100000	0.12	50	24	73
25	0.12	0.0100000	0.13	52	25	76
26	0.13	0.0100000	0.13	54	26	79
27	0.13	0.0100000	0.14	56	27	82
28	0.14	0.0100000	0.14	58	28	85
29	0.13	0.1000000	0.15	59	29	87
30	0.14	0.0087288	0.14	62	30	91
31	0.13	0.0872879	0.14	63	31	93
32	0.14	0.0087288	0.14	66	32	97
33	0.13	0.0872879	0.14	67	33	99
34	0.13	0.0872879	0.14	69	34	102
35	0.13	0.0087288	0.13	72	35	106
36	0.14	0.0087288	0.14	74	36	109
37	0.14	0.0087288	0.15	76	37	112
38	0.15	0.0087288	0.15	78	38	115
39	0.16	0.0087288	0.16	80	39	118
40	0.16	0.0087288	0.17	82	40	121
41	0.17	0.0087288	0.17	84	41	124
42	0.18	0.0087288	0.18	86	42	127
43	0.19	0.0087288	0.19	88	43	130
44	0.19	0.0087288	0.2	90	44	133
45	0.2	0.0087288	0.2	92	45	136
46	0.21	0.0087288	0.21	94	46	139
47	0.22	0.0087288	0.22	96	47	142
48	0.23	0.0087288	0.23	98	48	145
49	0.23	0.0872879	0.24	99	49	147
50	0.22	0.0355868	0.23	101	50	150

```
Stationary Solver 1 in Solver 1: Solution time: 42 s.
```

E.4 Seventy-five Iterations

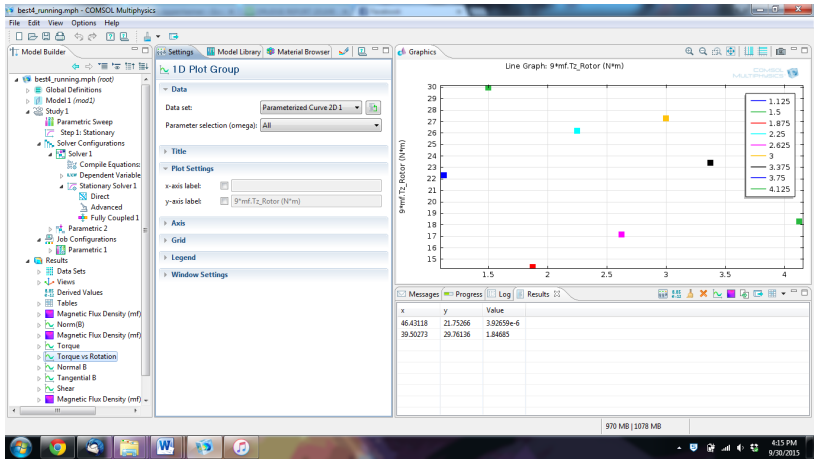

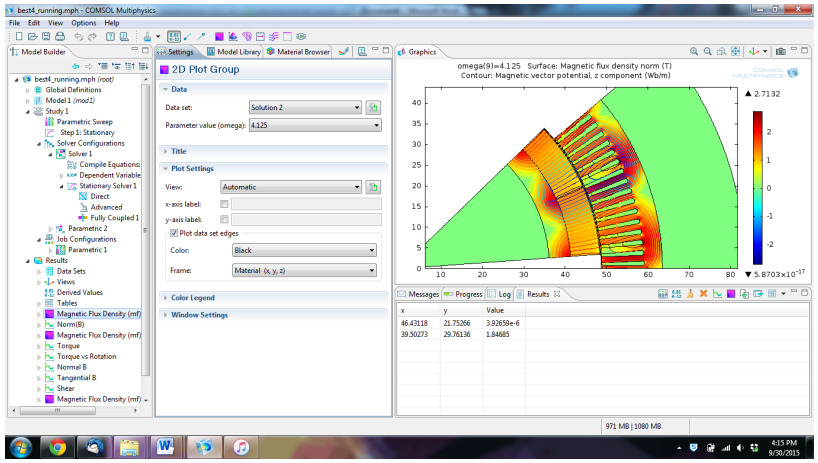


```
================================================================
Parameter omega = 1.125.
Number of vertex elements: 10
Number of boundary elements: 121
Stationary Solver 1 in Solver 1 started at 30-Sep-2015 16:04:11.
Nonlinear solver
Number of degrees of freedom solved for: 37017.
Nonsymmetric matrix found.
```

```
Scales for dependent variables:
mod1.A: 1
mod1.root.mod1.mf.VCoil_1_ode: 0.19
mod1.root.mod1.mf.VCoil_2_ode: 0.19
mod1.root.mod1.mf.VCoil_3_ode: 0.19
mod1.root.mod1.mf.VCoil_4_ode: 0.19
mod1.root.mod1.mf.VCoil_5_ode: 0.19
mod1.root.mod1.mf.VCoil_6_ode: 0.19
mod1.root.mod1.mf.VCoil_7_ode: 0.19
mod1.root.mod1.mf.VCoil_8_ode: 0.19
mod1.root.mod1.mf.VCoil_9_ode: 0.19
mod1.root.mod1.mf.VCoil_10_ode: 0.19
mod1.root.mod1.mf.VCoil_11_ode: 0.19
mod1.root.mod1.mf.VCoil_12_ode: 0.19
mod1.root.mod1.mf.VCoil_13_ode: 0.19
mod1.root.mod1.mf.VCoil_14_ode: 0.19
mod1.root.mod1.mf.VCoil_15_ode: 0.19
mod1.root.mod1.mf.VCoil_16_ode: 0.19
```

Iter	ErrEst	Damping	Stepsize	#Res	#Jac	#Sol
1	0.044	0.1000000	0.049	3	1	3
2	0.041	0.1000000	0.046	5	2	6
3	0.039	0.1000000	0.044	7	3	9
4	0.041	0.0100000	0.041	10	4	13
5	0.039	0.1000000	0.043	11	5	15
6	0.04	0.0100000	0.041	14	6	19
7	0.042	0.0100000	0.043	16	7	22
8	0.044	0.0100000	0.044	18	8	25
9	0.046	0.0100000	0.046	20	9	28
10	0.048	0.0100000	0.048	22	10	31
11	0.05	0.0100000	0.05	24	11	34
12	0.052	0.0100000	0.052	26	12	37
13	0.054	0.0100000	0.055	28	13	40
14	0.057	0.0100000	0.057	30	14	43
15	0.059	0.0100000	0.059	32	15	46
16	0.061	0.0100000	0.062	34	16	49
17	0.064	0.0100000	0.065	36	17	52
18	0.067	0.0100000	0.067	38	18	55
19	0.07	0.0100000	0.07	40	19	58
20	0.073	0.0100000	0.073	42	20	61
21	0.076	0.0100000	0.076	44	21	64
22	0.079	0.0100000	0.08	46	22	67
23	0.082	0.0100000	0.083	48	23	70
24	0.086	0.0100000	0.087	50	24	73
25	0.089	0.0100000	0.09	52	25	76
26	0.093	0.0100000	0.094	54	26	79
27	0.097	0.0100000	0.098	56	27	82
28	0.1	0.0100000	0.1	58	28	85
29	0.11	0.0100000	0.11	60	29	88
30	0.11	0.0165913	0.11	62	30	91
31	0.11	0.0165913	0.12	64	31	94
32	0.12	0.0165913	0.12	66	32	97
33	0.12	0.0165913	0.12	68	33	100
34	0.13	0.0165913	0.13	70	34	103
35	0.13	0.0165913	0.13	72	35	106
36	0.14	0.0165913	0.14	74	36	109
37	0.14	0.0165913	0.14	76	37	112
38	0.14	0.0165913	0.15	78	38	115

39	0.15	0.0165913	0.15	80	39	118
40	0.15	0.0165913	0.16	82	40	121
41	0.16	0.0165913	0.16	84	41	124
42	0.17	0.0165913	0.17	86	42	127
43	0.17	0.0165913	0.17	88	43	130
44	0.18	0.0165913	0.18	90	44	133
45	0.18	0.0165913	0.19	92	45	136
46	0.19	0.0165913	0.19	94	46	139
47	0.2	0.0165913	0.2	96	47	142
48	0.2	0.0165913	0.21	98	48	145
49	0.21	0.0165913	0.21	100	49	148
50	0.22	0.0165913	0.22	102	50	151
51	0.22	0.0165913	0.23	104	51	154
52	0.23	0.0165913	0.23	106	52	157
53	0.24	0.0165913	0.24	108	53	160
54	0.24	0.0165913	0.25	110	54	163
55	0.25	0.0165913	0.25	112	55	166
56	0.26	0.0165913	0.26	114	56	169
57	0.26	0.0165913	0.26	116	57	172
58	0.26	0.0165913	0.27	118	58	175
59	0.26	0.0165913	0.27	120	59	178
60	0.27	0.0165913	0.27	122	60	181
61	0.27	0.0165913	0.27	124	61	184
62	0.27	0.0165913	0.27	126	62	187
63	0.27	0.0165913	0.27	128	63	190
64	0.26	0.0165913	0.27	130	64	193
65	0.26	0.0165913	0.27	132	65	196
66	0.26	0.0165913	0.26	134	66	199
67	0.26	0.0165913	0.26	136	67	202
68	0.26	0.0165913	0.26	138	68	205
69	0.25	0.0165913	0.26	140	69	208
70	0.25	0.0165913	0.25	142	70	211
71	0.21	0.1659130	0.24	143	71	213
72	0.18	0.1000000	0.2	145	72	216
73	0.16	0.1000000	0.18	147	73	219
74	0.15	0.1000000	0.16	149	74	222
75	0.13	0.1000000	0.14	151	75	225

Stationary Solver 1 in Solver 1: Solution time: 69 s. (1 minute, 9 seconds)
Parameter omega = 1.5.
Number of vertex elements: 10
Number of boundary elements: 122
Stationary Solver 1 in Solver 1 started at 30-Sep-2015 16:05:27.
Nonlinear solver
Number of degrees of freedom solved for: 36911.
Nonsymmetric matrix found.
Scales for dependent variables:
mod1.A: 1
mod1.root.mod1.mf.VCoil_1_ode: 0.19
mod1.root.mod1.mf.VCoil_2_ode: 0.19
mod1.root.mod1.mf.VCoil_3_ode: 0.19
mod1.root.mod1.mf.VCoil_4_ode: 0.19
mod1.root.mod1.mf.VCoil_5_ode: 0.19
mod1.root.mod1.mf.VCoil_6_ode: 0.19
mod1.root.mod1.mf.VCoil_7_ode: 0.19
mod1.root.mod1.mf.VCoil_8_ode: 0.19
mod1.root.mod1.mf.VCoil_9_ode: 0.19
mod1.root.mod1.mf.VCoil_10_ode: 0.19
mod1.root.mod1.mf.VCoil_11_ode: 0.19
mod1.root.mod1.mf.VCoil_12_ode: 0.19
mod1.root.mod1.mf.VCoil_13_ode: 0.19
mod1.root.mod1.mf.VCoil_14_ode: 0.19
mod1.root.mod1.mf.VCoil_15_ode: 0.19
mod1.root.mod1.mf.VCoil_16_ode: 0.19

Iter	ErrEst	Damping	Stepsize	#Res	#Jac	#Sol
1	0.045	0.1000000	0.05	3	1	3
2	0.042	0.1000000	0.047	5	2	6
3	0.041	0.1000000	0.044	7	3	9
4	0.039	0.1000000	0.042	9	4	12
5	0.04	0.0100000	0.04	12	5	16
6	0.041	0.0100000	0.042	14	6	19
7	0.043	0.0100000	0.044	16	7	22
8	0.045	0.0100000	0.046	18	8	25
9	0.047	0.0100000	0.047	20	9	28
10	0.049	0.0100000	0.049	22	10	31
11	0.051	0.0100000	0.052	24	11	34
12	0.053	0.0100000	0.054	26	12	37
13	0.056	0.0100000	0.056	28	13	40
14	0.058	0.0100000	0.058	30	14	43
15	0.06	0.0100000	0.061	32	15	46
16	0.063	0.0100000	0.064	34	16	49
17	0.066	0.0100000	0.066	36	17	52
18	0.068	0.0100000	0.069	38	18	55
19	0.071	0.0100000	0.072	40	19	58
20	0.074	0.0100000	0.075	42	20	61
21	0.078	0.0100000	0.078	44	21	64
22	0.081	0.0100000	0.082	46	22	67
23	0.084	0.0100000	0.085	48	23	70
24	0.088	0.0100000	0.089	50	24	73
25	0.092	0.0100000	0.093	52	25	76
26	0.096	0.0100000	0.097	54	26	79
27	0.1	0.0100000	0.1	56	27	82
28	0.1	0.0100000	0.11	58	28	85
29	0.11	0.0100000	0.11	60	29	88
30	0.11	0.0100000	0.11	62	30	91
31	0.12	0.0100000	0.12	64	31	94
32	0.12	0.0100000	0.12	66	32	97
33	0.13	0.0100000	0.13	68	33	100
34	0.13	0.0100000	0.13	70	34	103
35	0.14	0.0100000	0.14	72	35	106
36	0.14	0.0100000	0.15	74	36	109
37	0.15	0.0100000	0.15	76	37	112
38	0.16	0.0100000	0.16	78	38	115
39	0.16	0.0100000	0.16	80	39	118
40	0.17	0.0100000	0.17	82	40	121
41	0.18	0.0100000	0.18	84	41	124
42	0.18	0.0100000	0.19	86	42	127
43	0.19	0.1000000	0.19	87	43	129
44	0.17	0.0645361	0.18	89	44	132
45	0.17	0.0645361	0.18	91	45	135
46	0.16	0.0645361	0.18	93	46	138
47	0.16	0.0645361	0.17	95	47	141
48	0.16	0.0645361	0.17	97	48	144
49	0.16	0.0645361	0.17	99	49	147
50	0.15	0.0645361	0.17	101	50	150

51	0.15	0.0645361	0.16	103	51	153
52	0.15	0.0645361	0.16	105	52	156
53	0.14	0.0645361	0.15	107	53	159
54	0.14	0.0645361	0.15	109	54	162
55	0.13	0.0645361	0.14	111	55	165
56	0.13	0.0645361	0.14	113	56	168
57	0.12	0.0523015	0.13	115	57	171
58	0.12	0.0523015	0.12	117	58	174
59	0.11	0.0523015	0.12	119	59	177
60	0.11	0.0523015	0.11	121	60	180
61	0.1	0.0523015	0.11	123	61	183
62	0.098	0.0523015	0.1	125	62	186
63	0.093	0.0523015	0.099	127	63	189
64	0.089	0.0523015	0.094	129	64	192
65	0.085	0.0523015	0.09	131	65	195
66	0.081	0.0523015	0.085	133	66	198
67	0.077	0.0523015	0.081	135	67	201
68	0.074	0.0523015	0.078	137	68	204
69	0.07	0.0523015	0.074	139	69	207
70	0.067	0.0523015	0.07	141	70	210
71	0.063	0.0523015	0.067	143	71	213
72	0.064	0.5230153	0.061	144	72	215
73	0.026	0.1153894	0.029	146	73	218
74	0.015	0.4111196	0.026	148	74	221
75	0.0088	0.4439298	0.015	150	75	224

Stationary Solver 1 in Solver 1: Solution time: 66 s. (1 minute, 6 seconds)
Parameter omega = 1.875.
Number of vertex elements: 10
Number of boundary elements: 123
Stationary Solver 1 in Solver 1 started at 30-Sep-2015 16:06:40.
Nonlinear solver
Number of degrees of freedom solved for: 36825.
Nonsymmetric matrix found.
Scales for dependent variables:
mod1.A: 1
mod1.root.mod1.mf.VCoil_1_ode: 0.19
mod1.root.mod1.mf.VCoil_2_ode: 0.19
mod1.root.mod1.mf.VCoil_3_ode: 0.19
mod1.root.mod1.mf.VCoil_4_ode: 0.19
mod1.root.mod1.mf.VCoil_5_ode: 0.19
mod1.root.mod1.mf.VCoil_6_ode: 0.19
mod1.root.mod1.mf.VCoil_7_ode: 0.19
mod1.root.mod1.mf.VCoil_8_ode: 0.19
mod1.root.mod1.mf.VCoil_9_ode: 0.19
mod1.root.mod1.mf.VCoil_10_ode: 0.19
mod1.root.mod1.mf.VCoil_11_ode: 0.19
mod1.root.mod1.mf.VCoil_12_ode: 0.19
mod1.root.mod1.mf.VCoil_13_ode: 0.19
mod1.root.mod1.mf.VCoil_14_ode: 0.19
mod1.root.mod1.mf.VCoil_15_ode: 0.19
mod1.root.mod1.mf.VCoil_16_ode: 0.19

Iter	ErrEst	Damping	Stepsize	#Res	#Jac	#Sol
1	0.046	0.1000000	0.051	3	1	3
2	0.043	0.1000000	0.048	5	2	6
3	0.045	0.0100000	0.045	8	3	10
4	0.047	0.0100000	0.047	10	4	13
5	0.049	0.0100000	0.049	12	5	16
6	0.051	0.0100000	0.051	14	6	19
7	0.053	0.0100000	0.054	16	7	22
8	0.055	0.0100000	0.056	18	8	25
9	0.058	0.0100000	0.058	20	9	28
10	0.06	0.0100000	0.061	22	10	31
11	0.063	0.0100000	0.063	24	11	34
12	0.065	0.0100000	0.066	26	12	37
13	0.068	0.0100000	0.069	28	13	40
14	0.071	0.0100000	0.071	30	14	43
15	0.074	0.0100000	0.074	32	15	46
16	0.077	0.0100000	0.078	34	16	49
17	0.08	0.0100000	0.081	36	17	52
18	0.084	0.0100000	0.084	38	18	55
19	0.087	0.0100000	0.088	40	19	58
20	0.091	0.0100000	0.092	42	20	61
21	0.094	0.0100000	0.095	44	21	64
22	0.099	0.0100000	0.1	46	22	67
23	0.1	0.0100000	0.1	48	23	70
24	0.11	0.0100000	0.11	50	24	73
25	0.11	0.0100000	0.11	52	25	76
26	0.12	0.0100000	0.12	54	26	79
27	0.12	0.0100000	0.12	56	27	82
28	0.13	0.0100000	0.13	58	28	85
29	0.13	0.0100000	0.13	60	29	88
30	0.14	0.0100000	0.14	62	30	91
31	0.14	0.0100000	0.14	64	31	94
32	0.15	0.0100000	0.15	66	32	97
33	0.16	0.0100000	0.16	68	33	100
34	0.16	0.0100000	0.16	70	34	103
35	0.17	0.0100000	0.17	72	35	106
36	0.18	0.0100000	0.18	74	36	109
37	0.18	0.0100000	0.19	76	37	112
38	0.19	0.0100000	0.19	78	38	115
39	0.2	0.0100000	0.2	80	39	118
40	0.21	0.0100000	0.21	82	40	121
41	0.22	0.0100000	0.22	84	41	124
42	0.23	0.0100000	0.23	86	42	127
43	0.23	0.0100000	0.24	88	43	130
44	0.24	0.0100000	0.25	90	44	133
45	0.25	0.0100000	0.26	92	45	136
46	0.26	0.0100000	0.27	94	46	139
47	0.28	0.0100000	0.28	96	47	142
48	0.29	0.0100000	0.29	98	48	145
49	0.3	0.0100000	0.3	100	49	148
50	0.31	0.0100000	0.31	102	50	151
51	0.32	0.0100000	0.33	104	51	154
52	0.34	0.0100000	0.34	106	52	157
53	0.35	0.0100000	0.35	108	53	160
54	0.36	0.0100000	0.37	110	54	163
55	0.38	0.0118020	0.38	112	55	166
56	0.39	0.0118020	0.4	114	56	169
57	0.4	0.0118020	0.41	116	57	172
58	0.42	0.0118020	0.42	118	58	175
59	0.42	0.0173061	0.43	120	59	178
60	0.43	0.0173061	0.43	122	60	181
61	0.43	0.0173061	0.44	124	61	184
62	0.43	0.0173061	0.44	126	62	187

63	0.43	0.0173061	0.44	128	63	190
64	0.43	0.0173061	0.44	130	64	193
65	0.43	0.0180233	0.44	132	65	196
66	0.43	0.0180233	0.43	134	66	199
67	0.42	0.0180233	0.43	136	67	202
68	0.42	0.0180233	0.43	138	68	205
69	0.41	0.0180233	0.42	140	69	208
70	0.41	0.0180233	0.41	142	70	211
71	0.4	0.0180233	0.41	144	71	214
72	0.39	0.0180233	0.4	146	72	217
73	0.39	0.0180233	0.39	148	73	220
74	0.38	0.0180233	0.39	150	74	223
75	0.38	0.0180233	0.38	152	75	226

Stationary Solver 1 in Solver 1: Solution time: 72 s. (1 minute, 12 seconds)
Parameter omega = 2.25.
Number of vertex elements: 10
Number of boundary elements: 124
Stationary Solver 1 in Solver 1 started at 30-Sep-2015 16:07:59.
Nonlinear solver
Number of degrees of freedom solved for: 36647.
Nonsymmetric matrix found.
Scales for dependent variables:
mod1.A: 1
mod1.root.mod1.mf.VCoil_1_ode: 0.19
mod1.root.mod1.mf.VCoil_2_ode: 0.19
mod1.root.mod1.mf.VCoil_3_ode: 0.19
mod1.root.mod1.mf.VCoil_4_ode: 0.19
mod1.root.mod1.mf.VCoil_5_ode: 0.19
mod1.root.mod1.mf.VCoil_6_ode: 0.19
mod1.root.mod1.mf.VCoil_7_ode: 0.19
mod1.root.mod1.mf.VCoil_8_ode: 0.19
mod1.root.mod1.mf.VCoil_9_ode: 0.19
mod1.root.mod1.mf.VCoil_10_ode: 0.19
mod1.root.mod1.mf.VCoil_11_ode: 0.19
mod1.root.mod1.mf.VCoil_12_ode: 0.19
mod1.root.mod1.mf.VCoil_13_ode: 0.19
mod1.root.mod1.mf.VCoil_14_ode: 0.19
mod1.root.mod1.mf.VCoil_15_ode: 0.19
mod1.root.mod1.mf.VCoil_16_ode: 0.19

Iter	ErrEst	Damping	Stepsize	#Res	#Jac	#Sol
1	0.047	0.1000000	0.052	3	1	3
2	0.044	0.1000000	0.049	5	2	6
3	0.046	0.0100000	0.046	8	3	10
4	0.048	0.0100000	0.048	10	4	13
5	0.05	0.0100000	0.05	12	5	16
6	0.048	0.1000000	0.052	13	6	18
7	0.049	0.0100000	0.05	16	7	22
8	0.051	0.0100000	0.052	18	8	25
9	0.054	0.0100000	0.054	20	9	28
10	0.056	0.0100000	0.056	22	10	31
11	0.058	0.0100000	0.059	24	11	34
12	0.061	0.0100000	0.061	26	12	37
13	0.063	0.0100000	0.064	28	13	40
14	0.066	0.0100000	0.067	30	14	43
15	0.069	0.0100000	0.07	32	15	46
16	0.072	0.0100000	0.073	34	16	49
17	0.075	0.0100000	0.076	36	17	52
18	0.078	0.0100000	0.079	38	18	55
19	0.082	0.0100000	0.082	40	19	58
20	0.085	0.0100000	0.086	42	20	61
21	0.089	0.0100000	0.09	44	21	64
22	0.093	0.0100000	0.093	46	22	67
23	0.097	0.0100000	0.097	48	23	70
24	0.1	0.0100000	0.1	50	24	73
25	0.1	0.0100000	0.11	52	25	76
26	0.11	0.0100000	0.11	54	26	79
27	0.11	0.0100000	0.12	56	27	82
28	0.12	0.0100000	0.12	58	28	85
29	0.12	0.0100000	0.13	60	29	88
30	0.13	0.0100000	0.13	62	30	91
31	0.13	0.0100000	0.14	64	31	94
32	0.14	0.0100000	0.14	66	32	97
33	0.15	0.0100000	0.15	68	33	100
34	0.15	0.0100000	0.15	70	34	103
35	0.16	0.0100000	0.16	72	35	106
36	0.16	0.0100000	0.17	74	36	109
37	0.17	0.0100000	0.17	76	37	112
38	0.18	0.0100000	0.18	78	38	115
39	0.19	0.0100000	0.19	80	39	118
40	0.18	0.1000000	0.19	81	40	120
41	0.17	0.0625646	0.18	83	41	123
42	0.17	0.0625646	0.18	85	42	126
43	0.17	0.0625646	0.18	87	43	129
44	0.16	0.0625646	0.18	89	44	132
45	0.16	0.0625646	0.17	91	45	135
46	0.16	0.0625646	0.17	93	46	138
47	0.16	0.0625646	0.17	95	47	141
48	0.17	0.0062565	0.17	98	48	145
49	0.17	0.0625646	0.17	99	49	147
50	0.17	0.0192446	0.17	101	50	150
51	0.17	0.0192446	0.18	103	51	153
52	0.18	0.0192446	0.18	105	52	156
53	0.18	0.0192446	0.18	107	53	159
54	0.18	0.0192446	0.19	109	54	162
55	0.19	0.0192446	0.19	111	55	165
56	0.19	0.0192446	0.19	113	56	168
57	0.19	0.0192446	0.19	115	57	171
58	0.19	0.0192446	0.19	117	58	174
59	0.19	0.0192446	0.19	119	59	177
60	0.19	0.0192446	0.19	121	60	180
61	0.18	0.1924456	0.18	122	61	182
62	0.14	0.0540705	0.15	124	62	185
63	0.13	0.0461513	0.14	126	63	188
64	0.13	0.0461513	0.13	128	64	191
65	0.12	0.0461513	0.13	130	65	194
66	0.12	0.0461513	0.12	132	66	197
67	0.11	0.0461513	0.12	134	67	200
68	0.11	0.0461513	0.11	136	68	203
69	0.1	0.0461513	0.11	138	69	206
70	0.099	0.0461513	0.1	140	70	209
71	0.095	0.0461513	0.1	142	71	212
72	0.091	0.0461513	0.096	144	72	215
73	0.088	0.0461513	0.092	146	73	218
74	0.084	0.0461513	0.088	148	74	221

```
  75        0.08   0.0461513       0.084  150   75  224
Stationary Solver 1 in Solver 1: Solution time: 81 s. (1 minute, 21 seconds)
Parameter omega = 2.625.
Number of vertex elements: 10
Number of boundary elements: 125
Stationary Solver 1 in Solver 1 started at 30-Sep-2015 16:09:27.
Nonlinear solver
Number of degrees of freedom solved for: 36885.
Nonsymmetric matrix found.
Scales for dependent variables:
mod1.A: 1
mod1.root.mod1.mf.VCoil_1_ode: 0.19
mod1.root.mod1.mf.VCoil_2_ode: 0.19
mod1.root.mod1.mf.VCoil_3_ode: 0.19
mod1.root.mod1.mf.VCoil_4_ode: 0.19
mod1.root.mod1.mf.VCoil_5_ode: 0.19
mod1.root.mod1.mf.VCoil_6_ode: 0.19
mod1.root.mod1.mf.VCoil_7_ode: 0.19
mod1.root.mod1.mf.VCoil_8_ode: 0.19
mod1.root.mod1.mf.VCoil_9_ode: 0.19
mod1.root.mod1.mf.VCoil_10_ode: 0.19
mod1.root.mod1.mf.VCoil_11_ode: 0.19
mod1.root.mod1.mf.VCoil_12_ode: 0.19
mod1.root.mod1.mf.VCoil_13_ode: 0.19
mod1.root.mod1.mf.VCoil_14_ode: 0.19
mod1.root.mod1.mf.VCoil_15_ode: 0.19
mod1.root.mod1.mf.VCoil_16_ode: 0.19
```

Iter	ErrEst	Damping	Stepsize	#Res	#Jac	#Sol
1	0.048	0.1000000	0.053	3	1	3
2	0.045	0.1000000	0.05	5	2	6
3	0.047	0.0100000	0.047	8	3	10
4	0.049	0.0100000	0.049	10	4	13
5	0.051	0.0100000	0.051	12	5	16
6	0.053	0.0100000	0.054	14	6	19
7	0.055	0.0100000	0.056	16	7	22
8	0.058	0.0100000	0.058	18	8	25
9	0.06	0.0100000	0.061	20	9	28
10	0.063	0.0100000	0.063	22	10	31
11	0.065	0.0100000	0.066	24	11	34
12	0.068	0.0100000	0.069	26	12	37
13	0.071	0.0100000	0.072	28	13	40
14	0.074	0.0100000	0.075	30	14	43
15	0.077	0.0100000	0.078	32	15	46
16	0.08	0.0100000	0.081	34	16	49
17	0.084	0.0100000	0.085	36	17	52
18	0.087	0.0100000	0.088	38	18	55
19	0.091	0.0100000	0.092	40	19	58
20	0.095	0.0100000	0.096	42	20	61
21	0.099	0.0100000	0.1	44	21	64
22	0.1	0.0100000	0.1	46	22	67
23	0.11	0.0100000	0.11	48	23	70
24	0.11	0.0100000	0.11	50	24	73
25	0.12	0.0100000	0.12	52	25	76
26	0.12	0.0100000	0.12	54	26	79
27	0.13	0.0100000	0.13	56	27	82
28	0.13	0.0100000	0.13	58	28	85
29	0.14	0.0100000	0.14	60	29	88
30	0.14	0.0100000	0.15	62	30	91
31	0.15	0.0100000	0.15	64	31	94
32	0.16	0.0100000	0.16	66	32	97
33	0.16	0.0100000	0.16	68	33	100
34	0.17	0.0100000	0.17	70	34	103
35	0.18	0.0100000	0.18	72	35	106
36	0.18	0.0100000	0.19	74	36	109
37	0.19	0.0100000	0.19	76	37	112
38	0.2	0.0100000	0.2	78	38	115
39	0.21	0.0100000	0.21	80	39	118
40	0.22	0.0100000	0.22	82	40	121
41	0.22	0.0100000	0.23	84	41	124
42	0.23	0.0114514	0.23	86	42	127
43	0.24	0.0130367	0.24	88	43	130
44	0.25	0.0130367	0.25	90	44	133
45	0.26	0.0130367	0.26	92	45	136
46	0.26	0.0213471	0.27	94	46	139
47	0.27	0.0213471	0.28	96	47	142
48	0.28	0.0213471	0.28	98	48	145
49	0.29	0.0213471	0.29	100	49	148
50	0.29	0.0213471	0.3	102	50	151
51	0.3	0.0213471	0.31	104	51	154
52	0.31	0.0213471	0.32	106	52	157
53	0.32	0.0213471	0.33	108	53	160
54	0.33	0.0213471	0.34	110	54	163
55	0.34	0.0213471	0.34	112	55	166
56	0.34	0.0213471	0.35	114	56	169
57	0.35	0.0213471	0.36	116	57	172
58	0.35	0.0213471	0.36	118	58	175
59	0.35	0.0213471	0.36	120	59	178
60	0.36	0.0213471	0.36	122	60	181
61	0.35	0.0213471	0.36	124	61	184
62	0.35	0.0213471	0.36	126	62	187
63	0.35	0.0213471	0.36	128	63	190
64	0.35	0.0213471	0.36	130	64	193
65	0.34	0.0213471	0.35	132	65	196
66	0.34	0.0213471	0.35	134	66	199
67	0.33	0.0213471	0.34	136	67	202
68	0.33	0.0213471	0.34	138	68	205
69	0.32	0.0213471	0.33	140	69	208
70	0.32	0.0213471	0.32	142	70	211
71	0.31	0.0213471	0.32	144	71	214
72	0.3	0.0213471	0.31	146	72	217
73	0.3	0.0213471	0.31	148	73	220
74	0.29	0.0213471	0.3	150	74	223
75	0.29	0.0213471	0.29	152	75	226

```
Stationary Solver 1 in Solver 1: Solution time: 70 s. (1 minute, 10 seconds)
Parameter omega = 3.0.
Number of vertex elements: 10
Number of boundary elements: 126
Stationary Solver 1 in Solver 1 started at 30-Sep-2015 16:10:45.
Nonlinear solver
Number of degrees of freedom solved for: 36759.
Nonsymmetric matrix found.
Scales for dependent variables:
mod1.A: 1
mod1.root.mod1.mf.VCoil_1_ode: 0.19
```

```
mod1.root.mod1.mf.VCoil_2_ode: 0.19
mod1.root.mod1.mf.VCoil_3_ode: 0.19
mod1.root.mod1.mf.VCoil_4_ode: 0.19
mod1.root.mod1.mf.VCoil_5_ode: 0.19
mod1.root.mod1.mf.VCoil_6_ode: 0.19
mod1.root.mod1.mf.VCoil_7_ode: 0.19
mod1.root.mod1.mf.VCoil_8_ode: 0.19
mod1.root.mod1.mf.VCoil_9_ode: 0.19
mod1.root.mod1.mf.VCoil_10_ode: 0.19
mod1.root.mod1.mf.VCoil_11_ode: 0.19
mod1.root.mod1.mf.VCoil_12_ode: 0.19
mod1.root.mod1.mf.VCoil_13_ode: 0.19
mod1.root.mod1.mf.VCoil_14_ode: 0.19
mod1.root.mod1.mf.VCoil_15_ode: 0.19
mod1.root.mod1.mf.VCoil_16_ode: 0.19
```

Iter	ErrEst	Damping	Stepsize	#Res	#Jac	#Sol
1	0.049	0.1000000	0.054	3	1	3
2	0.046	0.1000000	0.051	5	2	6
3	0.048	0.0100000	0.048	8	3	10
4	0.05	0.0100000	0.05	10	4	13
5	0.052	0.0100000	0.052	12	5	16
6	0.054	0.0100000	0.055	14	6	19
7	0.056	0.0100000	0.057	16	7	22
8	0.059	0.0100000	0.059	18	8	25
9	0.061	0.0100000	0.062	20	9	28
10	0.064	0.0100000	0.065	22	10	31
11	0.067	0.0100000	0.067	24	11	34
12	0.069	0.0100000	0.07	26	12	37
13	0.072	0.0100000	0.073	28	13	40
14	0.075	0.0100000	0.076	30	14	43
15	0.079	0.0100000	0.079	32	15	46
16	0.082	0.0100000	0.083	34	16	49
17	0.086	0.0100000	0.086	36	17	52
18	0.089	0.0100000	0.09	38	18	55
19	0.093	0.0100000	0.094	40	19	58
20	0.097	0.0100000	0.098	42	20	61
21	0.1	0.0100000	0.1	44	21	64
22	0.11	0.0100000	0.11	46	22	67
23	0.11	0.0100000	0.11	48	23	70
24	0.11	0.0100000	0.12	50	24	73
25	0.12	0.0100000	0.12	52	25	76
26	0.12	0.0100000	0.13	54	26	79
27	0.13	0.0100000	0.13	56	27	82
28	0.14	0.0100000	0.14	58	28	85
29	0.14	0.0100000	0.14	60	29	88
30	0.15	0.0100000	0.15	62	30	91
31	0.15	0.0100000	0.15	64	31	94
32	0.16	0.0100000	0.16	66	32	97
33	0.17	0.0100000	0.17	68	33	100
34	0.17	0.0100000	0.17	70	34	103
35	0.18	0.0100000	0.18	72	35	106
36	0.19	0.0100000	0.19	74	36	109
37	0.18	0.1000000	0.19	75	37	111
38	0.17	0.0403578	0.18	77	38	114
39	0.18	0.0403578	0.18	79	39	117
40	0.18	0.0403578	0.19	81	40	120
41	0.18	0.0403578	0.19	83	41	123
42	0.18	0.0403578	0.19	85	42	126
43	0.18	0.0403578	0.19	87	43	129
44	0.19	0.0403578	0.19	89	44	132
45	0.19	0.0403578	0.2	91	45	135
46	0.19	0.0403578	0.2	93	46	138
47	0.19	0.0403578	0.2	95	47	141
48	0.2	0.0403578	0.2	97	48	144
49	0.2	0.0403578	0.21	99	49	147
50	0.2	0.0403578	0.21	101	50	150
51	0.2	0.0403578	0.21	103	51	153
52	0.2	0.0403578	0.21	105	52	156
53	0.2	0.0403578	0.21	107	53	159
54	0.19	0.0403578	0.2	109	54	162
55	0.19	0.0403578	0.2	111	55	165
56	0.19	0.0403578	0.19	113	56	168
57	0.18	0.0403578	0.19	115	57	171
58	0.18	0.0403578	0.18	117	58	174
59	0.17	0.0403578	0.18	119	59	177
60	0.17	0.0403578	0.17	121	60	180
61	0.16	0.0403578	0.17	123	61	183
62	0.16	0.0403578	0.16	125	62	186
63	0.16	0.0256437	0.16	127	63	189
64	0.13	0.1430420	0.15	128	64	191
65	0.12	0.1000000	0.13	130	65	194
66	0.1	0.1000000	0.12	132	66	197
67	0.093	0.1000000	0.1	134	67	200
68	0.084	0.1000000	0.093	136	68	203
69	0.075	0.1000000	0.084	138	69	206
70	0.067	0.1000000	0.075	140	70	209
71	0.06	0.1000000	0.067	142	71	212
72	0.054	0.1000000	0.06	144	72	215
73	0.049	0.1000000	0.054	146	73	218
74	0.044	0.1000000	0.049	148	74	221
75	0.04	0.1000000	0.044	150	75	224

```
Stationary Solver 1 in Solver 1: Solution time: 63 s. (1 minute, 3 seconds)
Parameter omega = 3.375.
Number of vertex elements: 10
Number of boundary elements: 127
Stationary Solver 1 in Solver 1 started at 30-Sep-2015 16:11:55.
Nonlinear solver
Number of degrees of freedom solved for: 36841.
Nonsymmetric matrix found.
Scales for dependent variables:
mod1.A: 1
mod1.root.mod1.mf.VCoil_1_ode: 0.19
mod1.root.mod1.mf.VCoil_2_ode: 0.19
mod1.root.mod1.mf.VCoil_3_ode: 0.19
mod1.root.mod1.mf.VCoil_4_ode: 0.19
mod1.root.mod1.mf.VCoil_5_ode: 0.19
mod1.root.mod1.mf.VCoil_6_ode: 0.19
mod1.root.mod1.mf.VCoil_7_ode: 0.19
mod1.root.mod1.mf.VCoil_8_ode: 0.19
mod1.root.mod1.mf.VCoil_9_ode: 0.19
mod1.root.mod1.mf.VCoil_10_ode: 0.19
mod1.root.mod1.mf.VCoil_11_ode: 0.19
mod1.root.mod1.mf.VCoil_12_ode: 0.19
mod1.root.mod1.mf.VCoil_13_ode: 0.19
```

```
mod1.root.mod1.mf.VCoil_14_ode: 0.19
mod1.root.mod1.mf.VCoil_15_ode: 0.19
mod1.root.mod1.mf.VCoil_16_ode: 0.19
```

Iter	ErrEst	Damping	Stepsize	#Res	#Jac	#Sol
1	0.05	0.1000000	0.055	3	1	3
2	0.047	0.1000000	0.052	5	2	6
3	0.049	0.0100000	0.049	8	3	10
4	0.051	0.0100000	0.051	10	4	13
5	0.053	0.0100000	0.054	12	5	16
6	0.055	0.0100000	0.056	14	6	19
7	0.058	0.0100000	0.058	16	7	22
8	0.06	0.0100000	0.061	18	8	25
9	0.063	0.0100000	0.063	20	9	28
10	0.065	0.0100000	0.066	22	10	31
11	0.068	0.0100000	0.069	24	11	34
12	0.071	0.0100000	0.072	26	12	37
13	0.074	0.0100000	0.075	28	13	40
14	0.077	0.0100000	0.078	30	14	43
15	0.081	0.0100000	0.081	32	15	46
16	0.084	0.0100000	0.085	34	16	49
17	0.088	0.0100000	0.089	36	17	52
18	0.091	0.0100000	0.092	38	18	55
19	0.095	0.0100000	0.096	40	19	58
20	0.099	0.0100000	0.1	42	20	61
21	0.1	0.0100000	0.1	44	21	64
22	0.11	0.0100000	0.11	46	22	67
23	0.11	0.0100000	0.11	48	23	70
24	0.12	0.0100000	0.12	50	24	73
25	0.12	0.0100000	0.12	52	25	76
26	0.13	0.0100000	0.13	54	26	79
27	0.13	0.0100000	0.13	56	27	82
28	0.14	0.0100000	0.14	58	28	85
29	0.14	0.0100000	0.14	60	29	88
30	0.15	0.0100000	0.15	62	30	91
31	0.15	0.0100000	0.16	64	31	94
32	0.16	0.0100000	0.16	66	32	97
33	0.17	0.0100000	0.17	68	33	100
34	0.17	0.1000000	0.17	69	34	102
35	0.16	0.0290886	0.16	71	35	105
36	0.16	0.0290886	0.17	73	36	108
37	0.17	0.0290886	0.17	75	37	111
38	0.17	0.0290886	0.18	77	38	114
39	0.17	0.0290886	0.18	79	39	117
40	0.18	0.0290886	0.18	81	40	120
41	0.18	0.0290886	0.19	83	41	123
42	0.19	0.0290886	0.19	85	42	126
43	0.19	0.0290886	0.2	87	43	129
44	0.19	0.0290886	0.2	89	44	132
45	0.2	0.0290886	0.2	91	45	135
46	0.2	0.0290886	0.21	93	46	138
47	0.21	0.0290886	0.21	95	47	141
48	0.21	0.0290886	0.22	97	48	144
49	0.22	0.0290886	0.22	99	49	147
50	0.22	0.0290886	0.23	101	50	150
51	0.23	0.0290886	0.23	103	51	153
52	0.23	0.0290886	0.24	105	52	156
53	0.23	0.0290886	0.24	107	53	159
54	0.23	0.0290886	0.24	109	54	162
55	0.23	0.0290886	0.23	111	55	165
56	0.23	0.0290886	0.23	113	56	168
57	0.22	0.0290886	0.23	115	57	171
58	0.22	0.0290886	0.23	117	58	174
59	0.22	0.0290886	0.22	119	59	177
60	0.21	0.0290886	0.22	121	60	180
61	0.21	0.0290886	0.22	123	61	183
62	0.21	0.0290886	0.21	125	62	186
63	0.2	0.0290886	0.21	127	63	189
64	0.2	0.0290886	0.2	129	64	192
65	0.19	0.0290886	0.2	131	65	195
66	0.19	0.0290886	0.2	133	66	198
67	0.19	0.0290886	0.19	135	67	201
68	0.18	0.0172647	0.18	137	68	204
69	0.16	0.1726466	0.18	138	69	206
70	0.14	0.0661292	0.15	140	70	209
71	0.13	0.0661292	0.14	142	71	212
72	0.12	0.0661292	0.13	144	72	215
73	0.11	0.0661292	0.12	146	73	218
74	0.1	0.0661292	0.11	148	74	221
75	0.096	0.0661292	0.1	150	75	224

```
Stationary Solver 1 in Solver 1: Solution time: 66 s. (1 minute, 6 seconds)
Parameter omega = 3.75.
Number of vertex elements: 10
Number of boundary elements: 128
Stationary Solver 1 in Solver 1 started at 30-Sep-2015 16:13:10.
Nonlinear solver
Number of degrees of freedom solved for: 36827.
Nonsymmetric matrix found.
Scales for dependent variables:
mod1.A: 1
mod1.root.mod1.mf.VCoil_1_ode: 0.19
mod1.root.mod1.mf.VCoil_2_ode: 0.19
mod1.root.mod1.mf.VCoil_3_ode: 0.19
mod1.root.mod1.mf.VCoil_4_ode: 0.19
mod1.root.mod1.mf.VCoil_5_ode: 0.19
mod1.root.mod1.mf.VCoil_6_ode: 0.19
mod1.root.mod1.mf.VCoil_7_ode: 0.19
mod1.root.mod1.mf.VCoil_8_ode: 0.19
mod1.root.mod1.mf.VCoil_9_ode: 0.19
mod1.root.mod1.mf.VCoil_10_ode: 0.19
mod1.root.mod1.mf.VCoil_11_ode: 0.19
mod1.root.mod1.mf.VCoil_12_ode: 0.19
mod1.root.mod1.mf.VCoil_13_ode: 0.19
mod1.root.mod1.mf.VCoil_14_ode: 0.19
mod1.root.mod1.mf.VCoil_15_ode: 0.19
mod1.root.mod1.mf.VCoil_16_ode: 0.19
```

Iter	ErrEst	Damping	Stepsize	#Res	#Jac	#Sol
1	0.051	0.1000000	0.056	3	1	3
2	0.048	0.1000000	0.053	5	2	6
3	0.05	0.0100000	0.05	8	3	10
4	0.052	0.0100000	0.052	10	4	13
5	0.054	0.0100000	0.055	12	5	16
6	0.056	0.0100000	0.057	14	6	19
7	0.059	0.0100000	0.059	16	7	22
8	0.061	0.0100000	0.062	18	8	25

```
 9       0.064   0.0100000       0.065   20    9   28
10       0.067   0.0100000       0.067   22   10   31
11       0.069   0.0100000        0.07   24   11   34
12       0.072   0.0100000       0.073   26   12   37
13       0.076   0.0100000       0.076   28   13   40
14       0.079   0.0100000        0.08   30   14   43
15       0.082   0.0100000       0.083   32   15   46
16       0.086   0.0100000       0.087   34   16   49
17       0.089   0.0100000        0.09   36   17   52
18       0.093   0.0100000       0.094   38   18   55
19       0.097   0.0100000       0.098   40   19   58
20         0.1   0.0100000         0.1   42   20   61
21        0.11   0.0100000        0.11   44   21   64
22        0.11   0.0100000        0.11   46   22   67
23        0.11   0.0100000        0.12   48   23   70
24        0.12   0.0100000        0.12   50   24   73
25        0.12   0.0100000        0.13   52   25   76
26        0.13   0.0100000        0.13   54   26   79
27        0.13   0.0100000        0.14   56   27   82
28        0.14   0.0100000        0.14   58   28   85
29        0.14   0.0100000        0.15   60   29   88
30        0.15   0.0100000        0.15   62   30   91
31        0.14   0.1000000        0.16   63   31   93
32        0.15   0.0100000        0.15   66   32   97
33        0.14   0.1000000        0.15   67   33   99
34        0.15   0.1000000        0.15   69   34  102
35        0.14   0.0328079        0.14   71   35  105
36        0.14   0.0328079        0.14   73   36  108
37        0.14   0.0328079        0.14   75   37  111
38        0.14   0.0328079        0.15   77   38  114
39        0.15   0.0328079        0.15   79   39  117
40        0.15   0.0328079        0.15   81   40  120
41        0.15   0.0328079        0.16   83   41  123
42        0.15   0.0328079        0.16   85   42  126
43        0.16   0.0328079        0.16   87   43  129
44        0.16   0.0328079        0.16   89   44  132
45        0.16   0.0328079        0.16   91   45  135
46        0.16   0.0328079        0.17   93   46  138
47        0.16   0.0328079        0.17   95   47  141
48        0.16   0.0328079        0.17   97   48  144
49        0.17   0.0328079        0.17   99   49  147
50        0.17   0.0328079        0.17  101   50  150
51        0.17   0.0328079        0.18  103   51  153
52        0.17   0.0328079        0.18  105   52  156
53        0.17   0.0328079        0.18  107   53  159
54        0.17   0.0328079        0.17  109   54  162
55        0.16   0.0284580        0.17  111   55  165
56        0.16   0.0284580        0.17  113   56  168
57        0.16   0.0284580        0.17  115   57  171
58        0.16   0.0284580        0.16  117   58  174
59        0.16   0.0284580        0.16  119   59  177
60        0.15   0.0284580        0.16  121   60  180
61        0.15   0.0284580        0.16  123   61  183
62        0.15   0.0284580        0.15  125   62  186
63        0.15   0.0284580        0.15  127   63  189
64        0.14   0.0284580        0.15  129   64  192
65        0.14   0.0284580        0.14  131   65  195
66        0.14   0.0284580        0.14  133   66  198
67        0.13   0.0284580        0.14  135   67  201
68        0.13   0.0284580        0.13  137   68  204
69        0.13   0.0284580        0.13  139   69  207
70        0.12   0.0284580        0.13  141   70  210
71        0.12   0.0284580        0.13  143   71  213
72        0.12   0.0284580        0.12  145   72  216
73        0.11   0.2845801        0.11  146   73  218
74       0.072   0.0697177       0.078  148   74  221
75       0.067   0.0697177       0.072  150   75  224
Stationary Solver 1 in Solver 1: Solution time: 66 s. (1 minute, 6 seconds)
Parameter omega = 4.125.
Number of vertex elements: 10
Number of boundary elements: 129
Stationary Solver 1 in Solver 1 started at 30-Sep-2015 16:14:23.
Nonlinear solver
Number of degrees of freedom solved for: 36869.
Nonsymmetric matrix found.
Scales for dependent variables:
mod1.A: 1
mod1.root.mod1.mf.VCoil_1_ode: 0.19
mod1.root.mod1.mf.VCoil_2_ode: 0.19
mod1.root.mod1.mf.VCoil_3_ode: 0.19
mod1.root.mod1.mf.VCoil_4_ode: 0.19
mod1.root.mod1.mf.VCoil_5_ode: 0.19
mod1.root.mod1.mf.VCoil_6_ode: 0.19
mod1.root.mod1.mf.VCoil_7_ode: 0.19
mod1.root.mod1.mf.VCoil_8_ode: 0.19
mod1.root.mod1.mf.VCoil_9_ode: 0.19
mod1.root.mod1.mf.VCoil_10_ode: 0.19
mod1.root.mod1.mf.VCoil_11_ode: 0.19
mod1.root.mod1.mf.VCoil_12_ode: 0.19
mod1.root.mod1.mf.VCoil_13_ode: 0.19
mod1.root.mod1.mf.VCoil_14_ode: 0.19
mod1.root.mod1.mf.VCoil_15_ode: 0.19
mod1.root.mod1.mf.VCoil_16_ode: 0.19
Iter      ErrEst     Damping    Stepsize #Res #Jac #Sol
   1       0.051   0.1000000       0.057    3    1    3
   2       0.048   0.1000000       0.054    5    2    6
   3        0.05   0.0100000       0.051    8    3   10
   4       0.053   0.0100000       0.053   10    4   13
   5       0.055   0.0100000       0.055   12    5   16
   6       0.057   0.0100000       0.058   14    6   19
   7        0.06   0.0100000        0.06   16    7   22
   8       0.062   0.0100000       0.063   18    8   25
   9       0.065   0.0100000       0.065   20    9   28
  10       0.067   0.0100000       0.068   22   10   31
  11        0.07   0.0100000       0.071   24   11   34
  12       0.073   0.0100000       0.074   26   12   37
  13       0.077   0.0100000       0.077   28   13   40
  14        0.08   0.0100000       0.081   30   14   43
  15       0.083   0.0100000       0.084   32   15   46
  16       0.087   0.0100000       0.088   34   16   49
  17       0.091   0.0100000       0.092   36   17   52
  18       0.095   0.0100000       0.096   38   18   55
  19       0.098   0.0100000       0.099   40   19   58
  20         0.1   0.0100000         0.1   42   20   61
```

21	0.11	0.0100000	0.11	44	21	64
22	0.11	0.0100000	0.11	46	22	67
23	0.12	0.0100000	0.12	48	23	70
24	0.12	0.0100000	0.12	50	24	73
25	0.12	0.0100000	0.13	52	25	76
26	0.13	0.0100000	0.13	54	26	79
27	0.13	0.0100000	0.14	56	27	82
28	0.14	0.0100000	0.14	58	28	85
29	0.13	0.1000000	0.15	59	29	87
30	0.14	0.0087288	0.14	62	30	91
31	0.13	0.0872879	0.14	63	31	93
32	0.14	0.0087288	0.14	66	32	97
33	0.13	0.0872879	0.14	67	33	99
34	0.13	0.0872879	0.14	69	34	102
35	0.13	0.0087288	0.13	72	35	106
36	0.14	0.0087288	0.14	74	36	109
37	0.14	0.0087288	0.15	76	37	112
38	0.15	0.0087288	0.15	78	38	115
39	0.16	0.0087288	0.16	80	39	118
40	0.16	0.0087288	0.17	82	40	121
41	0.17	0.0087288	0.17	84	41	124
42	0.18	0.0087288	0.18	86	42	127
43	0.19	0.0087288	0.19	88	43	130
44	0.19	0.0087288	0.2	90	44	133
45	0.2	0.0087288	0.2	92	45	136
46	0.21	0.0087288	0.21	94	46	139
47	0.22	0.0087288	0.22	96	47	142
48	0.23	0.0087288	0.23	98	48	145
49	0.23	0.0872879	0.24	99	49	147
50	0.22	0.0355868	0.23	101	50	150
51	0.22	0.0355868	0.23	103	51	153
52	0.22	0.0355868	0.23	105	52	156
53	0.22	0.0355868	0.23	107	53	159
54	0.22	0.0355868	0.22	109	54	162
55	0.21	0.0355868	0.22	111	55	165
56	0.21	0.0355868	0.22	113	56	168
57	0.21	0.0355868	0.22	115	57	171
58	0.23	0.0081895	0.23	117	58	174
59	0.23	0.0081895	0.23	119	59	177
60	0.21	0.0213455	0.21	120	60	179
61	0.21	0.0213455	0.21	122	61	182
62	0.2	0.0213455	0.21	124	62	185
63	0.2	0.0213455	0.21	126	63	188
64	0.2	0.0213455	0.2	128	64	191
65	0.2	0.0213455	0.2	130	65	194
66	0.19	0.0213455	0.2	132	66	197
67	0.19	0.0213455	0.19	134	67	200
68	0.19	0.0213455	0.19	136	68	203
69	0.18	0.0213455	0.19	138	69	206
70	0.18	0.0213455	0.19	140	70	209
71	0.18	0.0213455	0.18	142	71	212
72	0.18	0.0213455	0.18	144	72	215
73	0.17	0.0213455	0.18	146	73	218
74	0.17	0.0213455	0.17	148	74	221
75	0.17	0.0213455	0.17	150	75	224

Stationary Solver 1 in Solver 1: Solution time: 62 s. (1 minute, 2 seconds)

E.5 Eighty-five Iterations

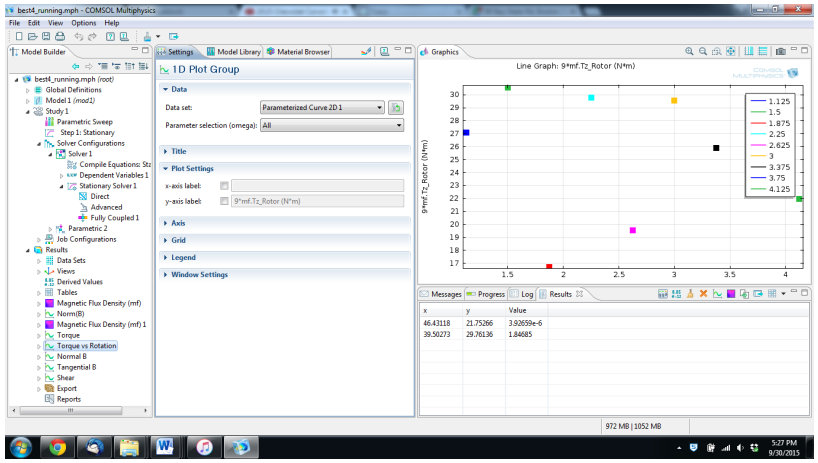

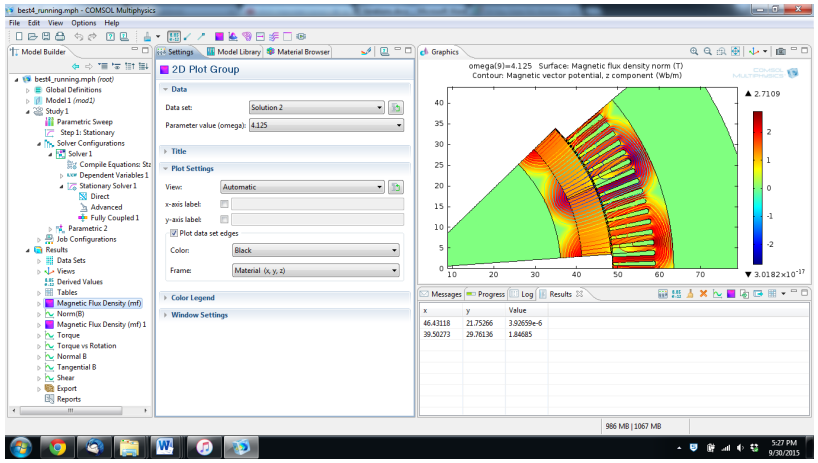


```
============================================================
Parameter omega = 1.125.
Number of vertex elements: 10
Number of boundary elements: 121
Number of vertex elements: 109
Number of boundary elements: 1534
Number of elements: 18344
Minimum element quality: 0.2929
Stationary Solver 1 in Solver 1 started at 30-Sep-2015 17:14:23.
Nonlinear solver
Number of degrees of freedom solved for: 37017.
Nonsymmetric matrix found.
Scales for dependent variables:
mod1.A: 1
mod1.root.mod1.mf.VCoil_1_ode: 0.19
mod1.root.mod1.mf.VCoil_2_ode: 0.19
mod1.root.mod1.mf.VCoil_3_ode: 0.19
mod1.root.mod1.mf.VCoil_4_ode: 0.19
mod1.root.mod1.mf.VCoil_5_ode: 0.19
mod1.root.mod1.mf.VCoil_6_ode: 0.19
mod1.root.mod1.mf.VCoil_7_ode: 0.19
mod1.root.mod1.mf.VCoil_8_ode: 0.19
mod1.root.mod1.mf.VCoil_9_ode: 0.19
mod1.root.mod1.mf.VCoil_10_ode: 0.19
mod1.root.mod1.mf.VCoil_11_ode: 0.19
mod1.root.mod1.mf.VCoil_12_ode: 0.19
mod1.root.mod1.mf.VCoil_13_ode: 0.19
mod1.root.mod1.mf.VCoil_14_ode: 0.19
mod1.root.mod1.mf.VCoil_15_ode: 0.19
mod1.root.mod1.mf.VCoil_16_ode: 0.19
```

Iter	ErrEst	Damping	Stepsize	#Res	#Jac	#Sol
1	0.044	0.1000000	0.049	3	1	3
2	0.041	0.1000000	0.046	5	2	6
3	0.039	0.1000000	0.044	7	3	9
4	0.041	0.0100000	0.041	10	4	13
5	0.039	0.1000000	0.043	11	5	15
6	0.04	0.0100000	0.041	14	6	19
7	0.042	0.0100000	0.043	16	7	22
8	0.044	0.0100000	0.044	18	8	25
9	0.046	0.0100000	0.046	20	9	28
10	0.048	0.0100000	0.048	22	10	31
11	0.05	0.0100000	0.05	24	11	34
12	0.052	0.0100000	0.052	26	12	37
13	0.054	0.0100000	0.055	28	13	40
14	0.057	0.0100000	0.057	30	14	43
15	0.059	0.0100000	0.059	32	15	46
16	0.061	0.0100000	0.062	34	16	49
17	0.064	0.0100000	0.065	36	17	52
18	0.067	0.0100000	0.067	38	18	55
19	0.07	0.0100000	0.07	40	19	58
20	0.073	0.0100000	0.073	42	20	61
21	0.076	0.0100000	0.076	44	21	64
22	0.079	0.0100000	0.08	46	22	67
23	0.082	0.0100000	0.083	48	23	70
24	0.086	0.0100000	0.087	50	24	73
25	0.089	0.0100000	0.09	52	25	76
26	0.093	0.0100000	0.094	54	26	79
27	0.097	0.0100000	0.098	56	27	82
28	0.1	0.0100000	0.1	58	28	85
29	0.11	0.0100000	0.11	60	29	88
30	0.11	0.0165913	0.11	62	30	91
31	0.11	0.0165913	0.12	64	31	94
32	0.12	0.0165913	0.12	66	32	97

33	0.12	0.0165913	0.12	68	33	100
34	0.13	0.0165913	0.13	70	34	103
35	0.13	0.0165913	0.13	72	35	106
36	0.14	0.0165913	0.14	74	36	109
37	0.14	0.0165913	0.14	76	37	112
38	0.14	0.0165913	0.15	78	38	115
39	0.15	0.0165913	0.15	80	39	118
40	0.15	0.0165913	0.16	82	40	121
41	0.16	0.0165913	0.16	84	41	124
42	0.17	0.0165913	0.17	86	42	127
43	0.17	0.0165913	0.17	88	43	130
44	0.18	0.0165913	0.18	90	44	133
45	0.18	0.0165913	0.19	92	45	136
46	0.19	0.0165913	0.19	94	46	139
47	0.2	0.0165913	0.2	96	47	142
48	0.2	0.0165913	0.21	98	48	145
49	0.21	0.0165913	0.21	100	49	148
50	0.22	0.0165913	0.22	102	50	151
51	0.22	0.0165913	0.23	104	51	154
52	0.23	0.0165913	0.23	106	52	157
53	0.24	0.0165913	0.24	108	53	160
54	0.24	0.0165913	0.25	110	54	163
55	0.25	0.0165913	0.25	112	55	166
56	0.26	0.0165913	0.26	114	56	169
57	0.26	0.0165913	0.26	116	57	172
58	0.26	0.0165913	0.27	118	58	175
59	0.26	0.0165913	0.27	120	59	178
60	0.27	0.0165913	0.27	122	60	181
61	0.27	0.0165913	0.27	124	61	184
62	0.27	0.0165913	0.27	126	62	187
63	0.27	0.0165913	0.27	128	63	190
64	0.26	0.0165913	0.27	130	64	193
65	0.26	0.0165913	0.27	132	65	196
66	0.26	0.0165913	0.26	134	66	199
67	0.26	0.0165913	0.26	136	67	202
68	0.26	0.0165913	0.26	138	68	205
69	0.25	0.0165913	0.26	140	69	208
70	0.25	0.0165913	0.25	142	70	211
71	0.21	0.1659130	0.24	143	71	213
72	0.18	0.1000000	0.2	145	72	216
73	0.16	0.1000000	0.18	147	73	219
74	0.15	0.1000000	0.16	149	74	222
75	0.13	0.1000000	0.14	151	75	225
76	0.11	0.0966479	0.13	153	76	228
77	0.1	0.0966479	0.11	155	77	231
78	0.092	0.0966479	0.1	157	78	234
79	0.083	0.0966479	0.092	159	79	237
80	0.075	0.0966479	0.083	161	80	240
81	0.067	0.0966479	0.074	163	81	243
82	0.061	0.0966479	0.067	165	82	246
83	0.055	0.0966479	0.061	167	83	249
84	0.049	0.0966479	0.055	169	84	252
85	0.045	0.0966479	0.049	171	85	255

Stationary Solver 1 in Solver 1: Solution time: 73 s. (1 minute, 13 seconds)
Parameter omega = 1.5.
Number of vertex elements: 10
Number of boundary elements: 122

Number of vertex elements: 109
Number of boundary elements: 1533
Number of elements: 18290
Minimum element quality: 0.5991
Stationary Solver 1 in Solver 1 started at 30-Sep-2015 17:15:44.
Nonlinear solver
Number of degrees of freedom solved for: 36911.
Nonsymmetric matrix found.
Scales for dependent variables:
mod1.A: 1
mod1.root.mod1.mf.VCoil_1_ode: 0.19
mod1.root.mod1.mf.VCoil_2_ode: 0.19
mod1.root.mod1.mf.VCoil_3_ode: 0.19
mod1.root.mod1.mf.VCoil_4_ode: 0.19
mod1.root.mod1.mf.VCoil_5_ode: 0.19
mod1.root.mod1.mf.VCoil_6_ode: 0.19
mod1.root.mod1.mf.VCoil_7_ode: 0.19
mod1.root.mod1.mf.VCoil_8_ode: 0.19
mod1.root.mod1.mf.VCoil_9_ode: 0.19
mod1.root.mod1.mf.VCoil_10_ode: 0.19
mod1.root.mod1.mf.VCoil_11_ode: 0.19
mod1.root.mod1.mf.VCoil_12_ode: 0.19
mod1.root.mod1.mf.VCoil_13_ode: 0.19
mod1.root.mod1.mf.VCoil_14_ode: 0.19
mod1.root.mod1.mf.VCoil_15_ode: 0.19
mod1.root.mod1.mf.VCoil_16_ode: 0.19

Iter	ErrEst	Damping	Stepsize	#Res	#Jac	#Sol
1	0.045	0.1000000	0.05	3	1	3
2	0.042	0.1000000	0.047	5	2	6
3	0.041	0.1000000	0.044	7	3	9
4	0.039	0.1000000	0.042	9	4	12
5	0.04	0.0100000	0.04	12	5	16
6	0.041	0.0100000	0.042	14	6	19
7	0.043	0.0100000	0.044	16	7	22
8	0.045	0.0100000	0.046	18	8	25
9	0.047	0.0100000	0.047	20	9	28
10	0.049	0.0100000	0.049	22	10	31
11	0.051	0.0100000	0.052	24	11	34
12	0.053	0.0100000	0.054	26	12	37
13	0.056	0.0100000	0.056	28	13	40
14	0.058	0.0100000	0.058	30	14	43
15	0.06	0.0100000	0.061	32	15	46
16	0.063	0.0100000	0.064	34	16	49
17	0.066	0.0100000	0.066	36	17	52
18	0.068	0.0100000	0.069	38	18	55
19	0.071	0.0100000	0.072	40	19	58
20	0.074	0.0100000	0.075	42	20	61
21	0.078	0.0100000	0.078	44	21	64
22	0.081	0.0100000	0.082	46	22	67
23	0.084	0.0100000	0.085	48	23	70
24	0.088	0.0100000	0.089	50	24	73
25	0.092	0.0100000	0.093	52	25	76
26	0.096	0.0100000	0.097	54	26	79
27	0.1	0.0100000	0.1	56	27	82
28	0.1	0.0100000	0.11	58	28	85
29	0.11	0.0100000	0.11	60	29	88
30	0.11	0.0100000	0.11	62	30	91

31	0.12	0.0100000	0.12	64	31	94
32	0.12	0.0100000	0.12	66	32	97
33	0.13	0.0100000	0.13	68	33	100
34	0.13	0.0100000	0.13	70	34	103
35	0.14	0.0100000	0.14	72	35	106
36	0.14	0.0100000	0.15	74	36	109
37	0.15	0.0100000	0.15	76	37	112
38	0.16	0.0100000	0.16	78	38	115
39	0.16	0.0100000	0.16	80	39	118
40	0.17	0.0100000	0.17	82	40	121
41	0.18	0.0100000	0.18	84	41	124
42	0.18	0.0100000	0.19	86	42	127
43	0.19	0.1000000	0.19	87	43	129
44	0.17	0.0645361	0.18	89	44	132
45	0.17	0.0645361	0.18	91	45	135
46	0.16	0.0645361	0.18	93	46	138
47	0.16	0.0645361	0.17	95	47	141
48	0.16	0.0645361	0.17	97	48	144
49	0.16	0.0645361	0.17	99	49	147
50	0.15	0.0645361	0.17	101	50	150
51	0.15	0.0645361	0.16	103	51	153
52	0.15	0.0645361	0.16	105	52	156
53	0.14	0.0645361	0.15	107	53	159
54	0.14	0.0645361	0.15	109	54	162
55	0.13	0.0645361	0.14	111	55	165
56	0.13	0.0645361	0.14	113	56	168
57	0.12	0.0523015	0.13	115	57	171
58	0.12	0.0523015	0.12	117	58	174
59	0.11	0.0523015	0.12	119	59	177
60	0.11	0.0523015	0.11	121	60	180
61	0.1	0.0523015	0.11	123	61	183
62	0.098	0.0523015	0.1	125	62	186
63	0.093	0.0523015	0.099	127	63	189
64	0.089	0.0523015	0.094	129	64	192
65	0.085	0.0523015	0.09	131	65	195
66	0.081	0.0523015	0.085	133	66	198
67	0.077	0.0523015	0.081	135	67	201
68	0.074	0.0523015	0.078	137	68	204
69	0.07	0.0523015	0.074	139	69	207
70	0.067	0.0523015	0.07	141	70	210
71	0.063	0.0523015	0.067	143	71	213
72	0.064	0.5230153	0.061	144	72	215
73	0.026	0.1153894	0.029	146	73	218
74	0.015	0.4111196	0.026	148	74	221
75	0.0088	0.4439298	0.015	150	75	224
76	0.0072	0.1556226	0.0085	152	76	227
77	0.0044	1.0000000	0.0083	153	77	229
78	8.3e-005	1.0000000	0.00049	154	78	231

Stationary Solver 1 in Solver 1: Solution time: 68 s. (1 minute, 8 seconds)
Parameter omega = 1.875.
Number of vertex elements: 10
Number of boundary elements: 123
Number of vertex elements: 109
Number of boundary elements: 1533
Number of elements: 18246
Minimum element quality: 0.5685
Stationary Solver 1 in Solver 1 started at 30-Sep-2015 17:17:00.

Nonlinear solver
Number of degrees of freedom solved for: 36825.
Nonsymmetric matrix found.
Scales for dependent variables:
mod1.A: 1
mod1.root.mod1.mf.VCoil_1_ode: 0.19
mod1.root.mod1.mf.VCoil_2_ode: 0.19
mod1.root.mod1.mf.VCoil_3_ode: 0.19
mod1.root.mod1.mf.VCoil_4_ode: 0.19
mod1.root.mod1.mf.VCoil_5_ode: 0.19
mod1.root.mod1.mf.VCoil_6_ode: 0.19
mod1.root.mod1.mf.VCoil_7_ode: 0.19
mod1.root.mod1.mf.VCoil_8_ode: 0.19
mod1.root.mod1.mf.VCoil_9_ode: 0.19
mod1.root.mod1.mf.VCoil_10_ode: 0.19
mod1.root.mod1.mf.VCoil_11_ode: 0.19
mod1.root.mod1.mf.VCoil_12_ode: 0.19
mod1.root.mod1.mf.VCoil_13_ode: 0.19
mod1.root.mod1.mf.VCoil_14_ode: 0.19
mod1.root.mod1.mf.VCoil_15_ode: 0.19
mod1.root.mod1.mf.VCoil_16_ode: 0.19

Iter	ErrEst	Damping	Stepsize	#Res	#Jac	#Sol
1	0.046	0.1000000	0.051	3	1	3
2	0.043	0.1000000	0.048	5	2	6
3	0.045	0.0100000	0.045	8	3	10
4	0.047	0.0100000	0.047	10	4	13
5	0.049	0.0100000	0.049	12	5	16
6	0.051	0.0100000	0.051	14	6	19
7	0.053	0.0100000	0.054	16	7	22
8	0.055	0.0100000	0.056	18	8	25
9	0.058	0.0100000	0.058	20	9	28
10	0.06	0.0100000	0.061	22	10	31
11	0.063	0.0100000	0.063	24	11	34
12	0.065	0.0100000	0.066	26	12	37
13	0.068	0.0100000	0.069	28	13	40
14	0.071	0.0100000	0.071	30	14	43
15	0.074	0.0100000	0.074	32	15	46
16	0.077	0.0100000	0.078	34	16	49
17	0.08	0.0100000	0.081	36	17	52
18	0.084	0.0100000	0.084	38	18	55
19	0.087	0.0100000	0.088	40	19	58
20	0.091	0.0100000	0.092	42	20	61
21	0.094	0.0100000	0.095	44	21	64
22	0.099	0.0100000	0.1	46	22	67
23	0.1	0.0100000	0.1	48	23	70
24	0.11	0.0100000	0.11	50	24	73
25	0.11	0.0100000	0.11	52	25	76
26	0.12	0.0100000	0.12	54	26	79
27	0.12	0.0100000	0.12	56	27	82
28	0.13	0.0100000	0.13	58	28	85
29	0.13	0.0100000	0.13	60	29	88
30	0.14	0.0100000	0.14	62	30	91
31	0.14	0.0100000	0.14	64	31	94
32	0.15	0.0100000	0.15	66	32	97
33	0.16	0.0100000	0.16	68	33	100
34	0.16	0.0100000	0.16	70	34	103
35	0.17	0.0100000	0.17	72	35	106

36	0.18	0.0100000	0.18	74	36	109
37	0.18	0.0100000	0.19	76	37	112
38	0.19	0.0100000	0.19	78	38	115
39	0.2	0.0100000	0.2	80	39	118
40	0.21	0.0100000	0.21	82	40	121
41	0.22	0.0100000	0.22	84	41	124
42	0.23	0.0100000	0.23	86	42	127
43	0.23	0.0100000	0.24	88	43	130
44	0.24	0.0100000	0.25	90	44	133
45	0.25	0.0100000	0.26	92	45	136
46	0.26	0.0100000	0.27	94	46	139
47	0.28	0.0100000	0.28	96	47	142
48	0.29	0.0100000	0.29	98	48	145
49	0.3	0.0100000	0.3	100	49	148
50	0.31	0.0100000	0.31	102	50	151
51	0.32	0.0100000	0.33	104	51	154
52	0.34	0.0100000	0.34	106	52	157
53	0.35	0.0100000	0.35	108	53	160
54	0.36	0.0100000	0.37	110	54	163
55	0.38	0.0118020	0.38	112	55	166
56	0.39	0.0118020	0.4	114	56	169
57	0.4	0.0118020	0.41	116	57	172
58	0.42	0.0118020	0.42	118	58	175
59	0.42	0.0173061	0.43	120	59	178
60	0.43	0.0173061	0.43	122	60	181
61	0.43	0.0173061	0.44	124	61	184
62	0.43	0.0173061	0.44	126	62	187
63	0.43	0.0173061	0.44	128	63	190
64	0.43	0.0173061	0.44	130	64	193
65	0.43	0.0180233	0.44	132	65	196
66	0.43	0.0180233	0.43	134	66	199
67	0.42	0.0180233	0.43	136	67	202
68	0.42	0.0180233	0.43	138	68	205
69	0.41	0.0180233	0.42	140	69	208
70	0.41	0.0180233	0.41	142	70	211
71	0.4	0.0180233	0.41	144	71	214
72	0.39	0.0180233	0.4	146	72	217
73	0.39	0.0180233	0.39	148	73	220
74	0.38	0.0180233	0.39	150	74	223
75	0.38	0.0180233	0.38	152	75	226
76	0.37	0.0180233	0.38	154	76	229
77	0.36	0.0180233	0.37	156	77	232
78	0.36	0.0180233	0.36	158	78	235
79	0.35	0.0180233	0.36	160	79	238
80	0.34	0.0180233	0.35	162	80	241
81	0.34	0.0180233	0.34	164	81	244
82	0.33	0.0180233	0.34	166	82	247
83	0.32	0.0180233	0.33	168	83	250
84	0.32	0.0180233	0.32	170	84	253
85	0.31	0.0180233	0.32	172	85	256

Stationary Solver 1 in Solver 1: Solution time: 76 s. (1 minute, 16 seconds)
Parameter omega = 2.25.
Number of vertex elements: 10
Number of boundary elements: 124
Number of vertex elements: 109
Number of boundary elements: 1531
Number of elements: 18156

Minimum element quality: 0.5803
Stationary Solver 1 in Solver 1 started at 30-Sep-2015 17:18:25.
Nonlinear solver
Number of degrees of freedom solved for: 36647.
Nonsymmetric matrix found.
Scales for dependent variables:
mod1.A: 1
mod1.root.mod1.mf.VCoil_1_ode: 0.19
mod1.root.mod1.mf.VCoil_2_ode: 0.19
mod1.root.mod1.mf.VCoil_3_ode: 0.19
mod1.root.mod1.mf.VCoil_4_ode: 0.19
mod1.root.mod1.mf.VCoil_5_ode: 0.19
mod1.root.mod1.mf.VCoil_6_ode: 0.19
mod1.root.mod1.mf.VCoil_7_ode: 0.19
mod1.root.mod1.mf.VCoil_8_ode: 0.19
mod1.root.mod1.mf.VCoil_9_ode: 0.19
mod1.root.mod1.mf.VCoil_10_ode: 0.19
mod1.root.mod1.mf.VCoil_11_ode: 0.19
mod1.root.mod1.mf.VCoil_12_ode: 0.19
mod1.root.mod1.mf.VCoil_13_ode: 0.19
mod1.root.mod1.mf.VCoil_14_ode: 0.19
mod1.root.mod1.mf.VCoil_15_ode: 0.19
mod1.root.mod1.mf.VCoil_16_ode: 0.19

Iter	ErrEst	Damping	Stepsize	#Res	#Jac	#Sol
1	0.047	0.1000000	0.052	3	1	3
2	0.044	0.1000000	0.049	5	2	6
3	0.046	0.0100000	0.046	8	3	10
4	0.048	0.0100000	0.048	10	4	13
5	0.05	0.0100000	0.05	12	5	16
6	0.048	0.1000000	0.052	13	6	18
7	0.049	0.0100000	0.05	16	7	22
8	0.051	0.0100000	0.052	18	8	25
9	0.054	0.0100000	0.054	20	9	28
10	0.056	0.0100000	0.056	22	10	31
11	0.058	0.0100000	0.059	24	11	34
12	0.061	0.0100000	0.061	26	12	37
13	0.063	0.0100000	0.064	28	13	40
14	0.066	0.0100000	0.067	30	14	43
15	0.069	0.0100000	0.07	32	15	46
16	0.072	0.0100000	0.073	34	16	49
17	0.075	0.0100000	0.076	36	17	52
18	0.078	0.0100000	0.079	38	18	55
19	0.082	0.0100000	0.082	40	19	58
20	0.085	0.0100000	0.086	42	20	61
21	0.089	0.0100000	0.09	44	21	64
22	0.093	0.0100000	0.093	46	22	67
23	0.097	0.0100000	0.097	48	23	70
24	0.1	0.0100000	0.1	50	24	73
25	0.1	0.0100000	0.11	52	25	76
26	0.11	0.0100000	0.11	54	26	79
27	0.11	0.0100000	0.12	56	27	82
28	0.12	0.0100000	0.12	58	28	85
29	0.12	0.0100000	0.13	60	29	88
30	0.13	0.0100000	0.13	62	30	91
31	0.13	0.0100000	0.14	64	31	94
32	0.14	0.0100000	0.14	66	32	97
33	0.15	0.0100000	0.15	68	33	100

34	0.15	0.0100000	0.15	70	34	103
35	0.16	0.0100000	0.16	72	35	106
36	0.16	0.0100000	0.17	74	36	109
37	0.17	0.0100000	0.17	76	37	112
38	0.18	0.0100000	0.18	78	38	115
39	0.19	0.0100000	0.19	80	39	118
40	0.18	0.1000000	0.19	81	40	120
41	0.17	0.0625646	0.18	83	41	123
42	0.17	0.0625646	0.18	85	42	126
43	0.17	0.0625646	0.18	87	43	129
44	0.16	0.0625646	0.18	89	44	132
45	0.16	0.0625646	0.17	91	45	135
46	0.16	0.0625646	0.17	93	46	138
47	0.16	0.0625646	0.17	95	47	141
48	0.17	0.0062565	0.17	98	48	145
49	0.17	0.0625646	0.17	99	49	147
50	0.17	0.0192446	0.17	101	50	150
51	0.17	0.0192446	0.18	103	51	153
52	0.18	0.0192446	0.18	105	52	156
53	0.18	0.0192446	0.18	107	53	159
54	0.18	0.0192446	0.19	109	54	162
55	0.19	0.0192446	0.19	111	55	165
56	0.19	0.0192446	0.19	113	56	168
57	0.19	0.0192446	0.19	115	57	171
58	0.19	0.0192446	0.19	117	58	174
59	0.19	0.0192446	0.19	119	59	177
60	0.19	0.0192446	0.19	121	60	180
61	0.18	0.1924456	0.18	122	61	182
62	0.14	0.0540705	0.15	124	62	185
63	0.13	0.0461513	0.14	126	63	188
64	0.13	0.0461513	0.13	128	64	191
65	0.12	0.0461513	0.13	130	65	194
66	0.12	0.0461513	0.12	132	66	197
67	0.11	0.0461513	0.12	134	67	200
68	0.11	0.0461513	0.11	136	68	203
69	0.1	0.0461513	0.11	138	69	206
70	0.099	0.0461513	0.1	140	70	209
71	0.095	0.0461513	0.1	142	71	212
72	0.091	0.0461513	0.096	144	72	215
73	0.088	0.0461513	0.092	146	73	218
74	0.084	0.0461513	0.088	148	74	221
75	0.08	0.0461513	0.084	150	75	224
76	0.076	0.0461513	0.08	152	76	227
77	0.073	0.0461513	0.077	154	77	230
78	0.07	0.0461513	0.073	156	78	233
79	0.067	0.0461513	0.07	158	79	236
80	0.064	0.0461513	0.067	160	80	239
81	0.061	0.0461513	0.064	162	81	242
82	0.058	0.0461513	0.061	164	82	245
83	0.055	0.0461513	0.058	166	83	248
84	0.04	0.4615128	0.054	167	84	250
85	0.02	0.3214642	0.029	169	85	253

Stationary Solver 1 in Solver 1: Solution time: 72 s. (1 minute, 12 seconds)
Parameter omega = 2.625.
Number of vertex elements: 10
Number of boundary elements: 125
Number of vertex elements: 109
Number of boundary elements: 1535
Number of elements: 18274
Minimum element quality: 0.5875
Stationary Solver 1 in Solver 1 started at 30-Sep-2015 17:19:45.
Nonlinear solver
Number of degrees of freedom solved for: 36885.
Nonsymmetric matrix found.
Scales for dependent variables:
mod1.A: 1
mod1.root.mod1.mf.VCoil_1_ode: 0.19
mod1.root.mod1.mf.VCoil_2_ode: 0.19
mod1.root.mod1.mf.VCoil_3_ode: 0.19
mod1.root.mod1.mf.VCoil_4_ode: 0.19
mod1.root.mod1.mf.VCoil_5_ode: 0.19
mod1.root.mod1.mf.VCoil_6_ode: 0.19
mod1.root.mod1.mf.VCoil_7_ode: 0.19
mod1.root.mod1.mf.VCoil_8_ode: 0.19
mod1.root.mod1.mf.VCoil_9_ode: 0.19
mod1.root.mod1.mf.VCoil_10_ode: 0.19
mod1.root.mod1.mf.VCoil_11_ode: 0.19
mod1.root.mod1.mf.VCoil_12_ode: 0.19
mod1.root.mod1.mf.VCoil_13_ode: 0.19
mod1.root.mod1.mf.VCoil_14_ode: 0.19
mod1.root.mod1.mf.VCoil_15_ode: 0.19
mod1.root.mod1.mf.VCoil_16_ode: 0.19

Iter	ErrEst	Damping	Stepsize	#Res	#Jac	#Sol
1	0.048	0.1000000	0.053	3	1	3
2	0.045	0.1000000	0.05	5	2	6
3	0.047	0.0100000	0.047	8	3	10
4	0.049	0.0100000	0.049	10	4	13
5	0.051	0.0100000	0.051	12	5	16
6	0.053	0.0100000	0.054	14	6	19
7	0.055	0.0100000	0.056	16	7	22
8	0.058	0.0100000	0.058	18	8	25
9	0.06	0.0100000	0.061	20	9	28
10	0.063	0.0100000	0.063	22	10	31
11	0.065	0.0100000	0.066	24	11	34
12	0.068	0.0100000	0.069	26	12	37
13	0.071	0.0100000	0.072	28	13	40
14	0.074	0.0100000	0.075	30	14	43
15	0.077	0.0100000	0.078	32	15	46
16	0.08	0.0100000	0.081	34	16	49
17	0.084	0.0100000	0.085	36	17	52
18	0.087	0.0100000	0.088	38	18	55
19	0.091	0.0100000	0.092	40	19	58
20	0.095	0.0100000	0.096	42	20	61
21	0.099	0.0100000	0.1	44	21	64
22	0.1	0.0100000	0.1	46	22	67
23	0.11	0.0100000	0.11	48	23	70
24	0.11	0.0100000	0.11	50	24	73
25	0.12	0.0100000	0.12	52	25	76
26	0.12	0.0100000	0.12	54	26	79
27	0.13	0.0100000	0.13	56	27	82
28	0.13	0.0100000	0.13	58	28	85
29	0.14	0.0100000	0.14	60	29	88
30	0.14	0.0100000	0.15	62	30	91
31	0.15	0.0100000	0.15	64	31	94

32	0.16	0.0100000	0.16	66	32	97
33	0.16	0.0100000	0.16	68	33	100
34	0.17	0.0100000	0.17	70	34	103
35	0.18	0.0100000	0.18	72	35	106
36	0.18	0.0100000	0.19	74	36	109
37	0.19	0.0100000	0.19	76	37	112
38	0.2	0.0100000	0.2	78	38	115
39	0.21	0.0100000	0.21	80	39	118
40	0.22	0.0100000	0.22	82	40	121
41	0.22	0.0100000	0.23	84	41	124
42	0.23	0.0114514	0.23	86	42	127
43	0.24	0.0130367	0.24	88	43	130
44	0.25	0.0130367	0.25	90	44	133
45	0.26	0.0130367	0.26	92	45	136
46	0.26	0.0213471	0.27	94	46	139
47	0.27	0.0213471	0.28	96	47	142
48	0.28	0.0213471	0.28	98	48	145
49	0.29	0.0213471	0.29	100	49	148
50	0.29	0.0213471	0.3	102	50	151
51	0.3	0.0213471	0.31	104	51	154
52	0.31	0.0213471	0.32	106	52	157
53	0.32	0.0213471	0.33	108	53	160
54	0.33	0.0213471	0.34	110	54	163
55	0.34	0.0213471	0.34	112	55	166
56	0.34	0.0213471	0.35	114	56	169
57	0.35	0.0213471	0.36	116	57	172
58	0.35	0.0213471	0.36	118	58	175
59	0.35	0.0213471	0.36	120	59	178
60	0.36	0.0213471	0.36	122	60	181
61	0.35	0.0213471	0.36	124	61	184
62	0.35	0.0213471	0.36	126	62	187
63	0.35	0.0213471	0.36	128	63	190
64	0.35	0.0213471	0.36	130	64	193
65	0.34	0.0213471	0.35	132	65	196
66	0.34	0.0213471	0.35	134	66	199
67	0.33	0.0213471	0.34	136	67	202
68	0.33	0.0213471	0.34	138	68	205
69	0.32	0.0213471	0.33	140	69	208
70	0.32	0.0213471	0.32	142	70	211
71	0.31	0.0213471	0.32	144	71	214
72	0.3	0.0213471	0.31	146	72	217
73	0.3	0.0213471	0.31	148	73	220
74	0.29	0.0213471	0.3	150	74	223
75	0.29	0.0213471	0.29	152	75	226
76	0.28	0.0213471	0.29	154	76	229
77	0.27	0.0213471	0.28	156	77	232
78	0.27	0.0213471	0.28	158	78	235
79	0.26	0.0213471	0.27	160	79	238
80	0.26	0.0213471	0.26	162	80	241
81	0.25	0.0213471	0.26	164	81	244
82	0.25	0.0213471	0.25	166	82	247
83	0.24	0.0213471	0.25	168	83	250
84	0.24	0.0213471	0.24	170	84	253
85	0.23	0.0213471	0.24	172	85	256

Stationary Solver 1 in Solver 1: Solution time: 72 s. (1 minute, 12 seconds)
Parameter omega = 3.0.
Number of vertex elements: 10
Number of boundary elements: 126
Number of vertex elements: 109
Number of boundary elements: 1533
Number of elements: 18210
Minimum element quality: 0.3629
Stationary Solver 1 in Solver 1 started at 30-Sep-2015 17:21:06.
Nonlinear solver
Number of degrees of freedom solved for: 36759.
Nonsymmetric matrix found.
Scales for dependent variables:
mod1.A: 1
mod1.root.mod1.mf.VCoil_1_ode: 0.19
mod1.root.mod1.mf.VCoil_2_ode: 0.19
mod1.root.mod1.mf.VCoil_3_ode: 0.19
mod1.root.mod1.mf.VCoil_4_ode: 0.19
mod1.root.mod1.mf.VCoil_5_ode: 0.19
mod1.root.mod1.mf.VCoil_6_ode: 0.19
mod1.root.mod1.mf.VCoil_7_ode: 0.19
mod1.root.mod1.mf.VCoil_8_ode: 0.19
mod1.root.mod1.mf.VCoil_9_ode: 0.19
mod1.root.mod1.mf.VCoil_10_ode: 0.19
mod1.root.mod1.mf.VCoil_11_ode: 0.19
mod1.root.mod1.mf.VCoil_12_ode: 0.19
mod1.root.mod1.mf.VCoil_13_ode: 0.19
mod1.root.mod1.mf.VCoil_14_ode: 0.19
mod1.root.mod1.mf.VCoil_15_ode: 0.19
mod1.root.mod1.mf.VCoil_16_ode: 0.19

Iter	ErrEst	Damping	Stepsize	#Res	#Jac	#Sol
1	0.049	0.1000000	0.054	3	1	3
2	0.046	0.1000000	0.051	5	2	6
3	0.048	0.0100000	0.048	8	3	10
4	0.05	0.0100000	0.05	10	4	13
5	0.052	0.0100000	0.052	12	5	16
6	0.054	0.0100000	0.055	14	6	19
7	0.056	0.0100000	0.057	16	7	22
8	0.059	0.0100000	0.059	18	8	25
9	0.061	0.0100000	0.062	20	9	28
10	0.064	0.0100000	0.065	22	10	31
11	0.067	0.0100000	0.067	24	11	34
12	0.069	0.0100000	0.07	26	12	37
13	0.072	0.0100000	0.073	28	13	40
14	0.075	0.0100000	0.076	30	14	43
15	0.079	0.0100000	0.079	32	15	46
16	0.082	0.0100000	0.083	34	16	49
17	0.086	0.0100000	0.086	36	17	52
18	0.089	0.0100000	0.09	38	18	55
19	0.093	0.0100000	0.094	40	19	58
20	0.097	0.0100000	0.098	42	20	61
21	0.1	0.0100000	0.1	44	21	64
22	0.11	0.0100000	0.11	46	22	67
23	0.11	0.0100000	0.11	48	23	70
24	0.11	0.0100000	0.12	50	24	73
25	0.12	0.0100000	0.12	52	25	76
26	0.12	0.0100000	0.13	54	26	79
27	0.13	0.0100000	0.13	56	27	82
28	0.14	0.0100000	0.14	58	28	85
29	0.14	0.0100000	0.14	60	29	88

30	0.15	0.0100000	0.15	62	30	91
31	0.15	0.0100000	0.15	64	31	94
32	0.16	0.0100000	0.16	66	32	97
33	0.17	0.0100000	0.17	68	33	100
34	0.17	0.0100000	0.17	70	34	103
35	0.18	0.0100000	0.18	72	35	106
36	0.19	0.0100000	0.19	74	36	109
37	0.18	0.1000000	0.19	75	37	111
38	0.17	0.0403578	0.18	77	38	114
39	0.18	0.0403578	0.18	79	39	117
40	0.18	0.0403578	0.19	81	40	120
41	0.18	0.0403578	0.19	83	41	123
42	0.18	0.0403578	0.19	85	42	126
43	0.18	0.0403578	0.19	87	43	129
44	0.19	0.0403578	0.19	89	44	132
45	0.19	0.0403578	0.2	91	45	135
46	0.19	0.0403578	0.2	93	46	138
47	0.19	0.0403578	0.2	95	47	141
48	0.2	0.0403578	0.2	97	48	144
49	0.2	0.0403578	0.21	99	49	147
50	0.2	0.0403578	0.21	101	50	150
51	0.2	0.0403578	0.21	103	51	153
52	0.2	0.0403578	0.21	105	52	156
53	0.2	0.0403578	0.21	107	53	159
54	0.19	0.0403578	0.2	109	54	162
55	0.19	0.0403578	0.2	111	55	165
56	0.19	0.0403578	0.19	113	56	168
57	0.18	0.0403578	0.19	115	57	171
58	0.18	0.0403578	0.18	117	58	174
59	0.17	0.0403578	0.18	119	59	177
60	0.17	0.0403578	0.17	121	60	180
61	0.16	0.0403578	0.17	123	61	183
62	0.16	0.0403578	0.16	125	62	186
63	0.16	0.0256437	0.16	127	63	189
64	0.13	0.1430420	0.15	128	64	191
65	0.12	0.1000000	0.13	130	65	194
66	0.1	0.1000000	0.12	132	66	197
67	0.093	0.1000000	0.1	134	67	200
68	0.084	0.1000000	0.093	136	68	203
69	0.075	0.1000000	0.084	138	69	206
70	0.067	0.1000000	0.075	140	70	209
71	0.06	0.1000000	0.067	142	71	212
72	0.054	0.1000000	0.06	144	72	215
73	0.049	0.1000000	0.054	146	73	218
74	0.044	0.1000000	0.049	148	74	221
75	0.04	0.1000000	0.044	150	75	224
76	0.036	0.1000000	0.04	152	76	227
77	0.032	0.1000000	0.036	154	77	230
78	0.029	0.1000000	0.032	156	78	233
79	0.026	0.1000000	0.029	158	79	236
80	0.024	0.1000000	0.026	160	80	239
81	0.021	0.1000000	0.024	162	81	242
82	0.019	0.1000000	0.022	164	82	245
83	0.018	0.1000000	0.02	166	83	248
84	0.014	0.2185642	0.018	168	84	251
85	0.013	1.0000000	0.014	169	85	253

Stationary Solver 1 in Solver 1: Solution time: 78 s. (1 minute, 18 seconds)

Parameter omega = 3.375.
Number of vertex elements: 10
Number of boundary elements: 127
Number of vertex elements: 109
Number of boundary elements: 1536
Number of elements: 18250
Minimum element quality: 0.5665
Stationary Solver 1 in Solver 1 started at 30-Sep-2015 17:22:32.
Nonlinear solver
Number of degrees of freedom solved for: 36841.
Nonsymmetric matrix found.
Scales for dependent variables:
mod1.A: 1
mod1.root.mod1.mf.VCoil_1_ode: 0.19
mod1.root.mod1.mf.VCoil_2_ode: 0.19
mod1.root.mod1.mf.VCoil_3_ode: 0.19
mod1.root.mod1.mf.VCoil_4_ode: 0.19
mod1.root.mod1.mf.VCoil_5_ode: 0.19
mod1.root.mod1.mf.VCoil_6_ode: 0.19
mod1.root.mod1.mf.VCoil_7_ode: 0.19
mod1.root.mod1.mf.VCoil_8_ode: 0.19
mod1.root.mod1.mf.VCoil_9_ode: 0.19
mod1.root.mod1.mf.VCoil_10_ode: 0.19
mod1.root.mod1.mf.VCoil_11_ode: 0.19
mod1.root.mod1.mf.VCoil_12_ode: 0.19
mod1.root.mod1.mf.VCoil_13_ode: 0.19
mod1.root.mod1.mf.VCoil_14_ode: 0.19
mod1.root.mod1.mf.VCoil_15_ode: 0.19
mod1.root.mod1.mf.VCoil_16_ode: 0.19

Iter	ErrEst	Damping	Stepsize	#Res	#Jac	#Sol
1	0.05	0.1000000	0.055	3	1	3
2	0.047	0.1000000	0.052	5	2	6
3	0.049	0.0100000	0.049	8	3	10
4	0.051	0.0100000	0.051	10	4	13
5	0.053	0.0100000	0.054	12	5	16
6	0.055	0.0100000	0.056	14	6	19
7	0.058	0.0100000	0.058	16	7	22
8	0.06	0.0100000	0.061	18	8	25
9	0.063	0.0100000	0.063	20	9	28
10	0.065	0.0100000	0.066	22	10	31
11	0.068	0.0100000	0.069	24	11	34
12	0.071	0.0100000	0.072	26	12	37
13	0.074	0.0100000	0.075	28	13	40
14	0.077	0.0100000	0.078	30	14	43
15	0.081	0.0100000	0.081	32	15	46
16	0.084	0.0100000	0.085	34	16	49
17	0.088	0.0100000	0.089	36	17	52
18	0.091	0.0100000	0.092	38	18	55
19	0.095	0.0100000	0.096	40	19	58
20	0.099	0.0100000	0.1	42	20	61
21	0.1	0.0100000	0.1	44	21	64
22	0.11	0.0100000	0.11	46	22	67
23	0.11	0.0100000	0.11	48	23	70
24	0.12	0.0100000	0.12	50	24	73
25	0.12	0.0100000	0.12	52	25	76
26	0.13	0.0100000	0.13	54	26	79
27	0.13	0.0100000	0.13	56	27	82

28	0.14	0.0100000	0.14	58	28	85
29	0.14	0.0100000	0.14	60	29	88
30	0.15	0.0100000	0.15	62	30	91
31	0.15	0.0100000	0.16	64	31	94
32	0.16	0.0100000	0.16	66	32	97
33	0.17	0.0100000	0.17	68	33	100
34	0.17	0.1000000	0.17	69	34	102
35	0.16	0.0290886	0.16	71	35	105
36	0.16	0.0290886	0.17	73	36	108
37	0.17	0.0290886	0.17	75	37	111
38	0.17	0.0290886	0.18	77	38	114
39	0.17	0.0290886	0.18	79	39	117
40	0.18	0.0290886	0.18	81	40	120
41	0.18	0.0290886	0.19	83	41	123
42	0.19	0.0290886	0.19	85	42	126
43	0.19	0.0290886	0.2	87	43	129
44	0.19	0.0290886	0.2	89	44	132
45	0.2	0.0290886	0.2	91	45	135
46	0.2	0.0290886	0.21	93	46	138
47	0.21	0.0290886	0.21	95	47	141
48	0.21	0.0290886	0.22	97	48	144
49	0.22	0.0290886	0.22	99	49	147
50	0.22	0.0290886	0.23	101	50	150
51	0.23	0.0290886	0.23	103	51	153
52	0.23	0.0290886	0.24	105	52	156
53	0.23	0.0290886	0.24	107	53	159
54	0.23	0.0290886	0.24	109	54	162
55	0.23	0.0290886	0.23	111	55	165
56	0.23	0.0290886	0.23	113	56	168
57	0.22	0.0290886	0.23	115	57	171
58	0.22	0.0290886	0.23	117	58	174
59	0.22	0.0290886	0.22	119	59	177
60	0.21	0.0290886	0.22	121	60	180
61	0.21	0.0290886	0.22	123	61	183
62	0.21	0.0290886	0.21	125	62	186
63	0.2	0.0290886	0.21	127	63	189
64	0.2	0.0290886	0.2	129	64	192
65	0.19	0.0290886	0.2	131	65	195
66	0.19	0.0290886	0.2	133	66	198
67	0.19	0.0290886	0.19	135	67	201
68	0.18	0.0172647	0.18	137	68	204
69	0.16	0.1726466	0.18	138	69	206
70	0.14	0.0661292	0.15	140	70	209
71	0.13	0.0661292	0.14	142	71	212
72	0.12	0.0661292	0.13	144	72	215
73	0.11	0.0661292	0.12	146	73	218
74	0.1	0.0661292	0.11	148	74	221
75	0.096	0.0661292	0.1	150	75	224
76	0.089	0.0661292	0.095	152	76	227
77	0.082	0.0661292	0.088	154	77	230
78	0.077	0.0661292	0.082	156	78	233
79	0.071	0.0661292	0.076	158	79	236
80	0.067	0.0661292	0.071	160	80	239
81	0.062	0.0661292	0.066	162	81	242
82	0.058	0.0661292	0.062	164	82	245
83	0.055	0.0661292	0.058	166	83	248
84	0.051	0.0661292	0.055	168	84	251
85	0.048	0.0661292	0.051	170	85	254

Stationary Solver 1 in Solver 1: Solution time: 84 s. (1 minute, 24 seconds)
Parameter omega = 3.75.
Number of vertex elements: 10
Number of boundary elements: 128
Number of vertex elements: 109
Number of boundary elements: 1538
Number of elements: 18242
Minimum element quality: 0.5374
Stationary Solver 1 in Solver 1 started at 30-Sep-2015 17:24:07.
Nonlinear solver
Number of degrees of freedom solved for: 36827.
Nonsymmetric matrix found.
Scales for dependent variables:
mod1.A: 1
mod1.root.mod1.mf.VCoil_1_ode: 0.19
mod1.root.mod1.mf.VCoil_2_ode: 0.19
mod1.root.mod1.mf.VCoil_3_ode: 0.19
mod1.root.mod1.mf.VCoil_4_ode: 0.19
mod1.root.mod1.mf.VCoil_5_ode: 0.19
mod1.root.mod1.mf.VCoil_6_ode: 0.19
mod1.root.mod1.mf.VCoil_7_ode: 0.19
mod1.root.mod1.mf.VCoil_8_ode: 0.19
mod1.root.mod1.mf.VCoil_9_ode: 0.19
mod1.root.mod1.mf.VCoil_10_ode: 0.19
mod1.root.mod1.mf.VCoil_11_ode: 0.19
mod1.root.mod1.mf.VCoil_12_ode: 0.19
mod1.root.mod1.mf.VCoil_13_ode: 0.19
mod1.root.mod1.mf.VCoil_14_ode: 0.19
mod1.root.mod1.mf.VCoil_15_ode: 0.19
mod1.root.mod1.mf.VCoil_16_ode: 0.19

Iter	ErrEst	Damping	Stepsize	#Res	#Jac	#Sol
1	0.051	0.1000000	0.056	3	1	3
2	0.048	0.1000000	0.053	5	2	6
3	0.05	0.0100000	0.05	8	3	10
4	0.052	0.0100000	0.052	10	4	13
5	0.054	0.0100000	0.055	12	5	16
6	0.056	0.0100000	0.057	14	6	19
7	0.059	0.0100000	0.059	16	7	22
8	0.061	0.0100000	0.062	18	8	25
9	0.064	0.0100000	0.065	20	9	28
10	0.067	0.0100000	0.067	22	10	31
11	0.069	0.0100000	0.07	24	11	34
12	0.072	0.0100000	0.073	26	12	37
13	0.076	0.0100000	0.076	28	13	40
14	0.079	0.0100000	0.08	30	14	43
15	0.082	0.0100000	0.083	32	15	46
16	0.086	0.0100000	0.087	34	16	49
17	0.089	0.0100000	0.09	36	17	52
18	0.093	0.0100000	0.094	38	18	55
19	0.097	0.0100000	0.098	40	19	58
20	0.1	0.0100000	0.1	42	20	61
21	0.11	0.0100000	0.11	44	21	64
22	0.11	0.0100000	0.11	46	22	67
23	0.11	0.0100000	0.12	48	23	70
24	0.12	0.0100000	0.12	50	24	73
25	0.12	0.0100000	0.13	52	25	76

26	0.13	0.0100000	0.13	54	26	79
27	0.13	0.0100000	0.14	56	27	82
28	0.14	0.0100000	0.14	58	28	85
29	0.14	0.0100000	0.15	60	29	88
30	0.15	0.0100000	0.15	62	30	91
31	0.14	0.1000000	0.16	63	31	93
32	0.15	0.0100000	0.15	66	32	97
33	0.14	0.1000000	0.15	67	33	99
34	0.15	0.1000000	0.15	69	34	102
35	0.14	0.0328079	0.14	71	35	105
36	0.14	0.0328079	0.14	73	36	108
37	0.14	0.0328079	0.14	75	37	111
38	0.14	0.0328079	0.15	77	38	114
39	0.15	0.0328079	0.15	79	39	117
40	0.15	0.0328079	0.15	81	40	120
41	0.15	0.0328079	0.16	83	41	123
42	0.15	0.0328079	0.16	85	42	126
43	0.16	0.0328079	0.16	87	43	129
44	0.16	0.0328079	0.16	89	44	132
45	0.16	0.0328079	0.16	91	45	135
46	0.16	0.0328079	0.17	93	46	138
47	0.16	0.0328079	0.17	95	47	141
48	0.16	0.0328079	0.17	97	48	144
49	0.17	0.0328079	0.17	99	49	147
50	0.17	0.0328079	0.17	101	50	150
51	0.17	0.0328079	0.18	103	51	153
52	0.17	0.0328079	0.18	105	52	156
53	0.17	0.0328079	0.18	107	53	159
54	0.17	0.0328079	0.17	109	54	162
55	0.16	0.0284580	0.17	111	55	165
56	0.16	0.0284580	0.17	113	56	168
57	0.16	0.0284580	0.17	115	57	171
58	0.16	0.0284580	0.16	117	58	174
59	0.16	0.0284580	0.16	119	59	177
60	0.15	0.0284580	0.16	121	60	180
61	0.15	0.0284580	0.16	123	61	183
62	0.15	0.0284580	0.15	125	62	186
63	0.15	0.0284580	0.15	127	63	189
64	0.14	0.0284580	0.15	129	64	192
65	0.14	0.0284580	0.14	131	65	195
66	0.14	0.0284580	0.14	133	66	198
67	0.13	0.0284580	0.14	135	67	201
68	0.13	0.0284580	0.13	137	68	204
69	0.13	0.0284580	0.13	139	69	207
70	0.12	0.0284580	0.13	141	70	210
71	0.12	0.0284580	0.13	143	71	213
72	0.12	0.0284580	0.12	145	72	216
73	0.11	0.2845801	0.11	146	73	218
74	0.072	0.0697177	0.078	148	74	221
75	0.067	0.0697177	0.072	150	75	224
76	0.062	0.0697177	0.067	152	76	227
77	0.058	0.0697177	0.062	154	77	230
78	0.054	0.0697177	0.058	156	78	233
79	0.051	0.0697177	0.054	158	79	236
80	0.047	0.0697177	0.051	160	80	239
81	0.044	0.0697177	0.048	162	81	242
82	0.041	0.0697177	0.045	164	82	245
83	0.039	0.0697177	0.042	166	83	248
84	0.036	0.0697177	0.039	168	84	251
85	0.034	0.0697177	0.036	170	85	254

Stationary Solver 1 in Solver 1: Solution time: 81 s. (1 minute, 21 seconds)
Parameter omega = 4.125.
Number of vertex elements: 10
Number of boundary elements: 129
Number of vertex elements: 109
Number of boundary elements: 1539
Number of elements: 18262
Minimum element quality: 0.5176
Stationary Solver 1 in Solver 1 started at 30-Sep-2015 17:25:36.
Nonlinear solver
Number of degrees of freedom solved for: 36869.
Nonsymmetric matrix found.
Scales for dependent variables:
mod1.A: 1
mod1.root.mod1.mf.VCoil_1_ode: 0.19
mod1.root.mod1.mf.VCoil_2_ode: 0.19
mod1.root.mod1.mf.VCoil_3_ode: 0.19
mod1.root.mod1.mf.VCoil_4_ode: 0.19
mod1.root.mod1.mf.VCoil_5_ode: 0.19
mod1.root.mod1.mf.VCoil_6_ode: 0.19
mod1.root.mod1.mf.VCoil_7_ode: 0.19
mod1.root.mod1.mf.VCoil_8_ode: 0.19
mod1.root.mod1.mf.VCoil_9_ode: 0.19
mod1.root.mod1.mf.VCoil_10_ode: 0.19
mod1.root.mod1.mf.VCoil_11_ode: 0.19
mod1.root.mod1.mf.VCoil_12_ode: 0.19
mod1.root.mod1.mf.VCoil_13_ode: 0.19
mod1.root.mod1.mf.VCoil_14_ode: 0.19
mod1.root.mod1.mf.VCoil_15_ode: 0.19
mod1.root.mod1.mf.VCoil_16_ode: 0.19

Iter	ErrEst	Damping	Stepsize	#Res	#Jac	#Sol
1	0.051	0.1000000	0.057	3	1	3
2	0.048	0.1000000	0.054	5	2	6
3	0.05	0.0100000	0.051	8	3	10
4	0.053	0.0100000	0.053	10	4	13
5	0.055	0.0100000	0.055	12	5	16
6	0.057	0.0100000	0.058	14	6	19
7	0.06	0.0100000	0.06	16	7	22
8	0.062	0.0100000	0.063	18	8	25
9	0.065	0.0100000	0.065	20	9	28
10	0.067	0.0100000	0.068	22	10	31
11	0.07	0.0100000	0.071	24	11	34
12	0.073	0.0100000	0.074	26	12	37
13	0.077	0.0100000	0.077	28	13	40
14	0.08	0.0100000	0.081	30	14	43
15	0.083	0.0100000	0.084	32	15	46
16	0.087	0.0100000	0.088	34	16	49
17	0.091	0.0100000	0.092	36	17	52
18	0.095	0.0100000	0.096	38	18	55
19	0.098	0.0100000	0.099	40	19	58
20	0.1	0.0100000	0.1	42	20	61
21	0.11	0.0100000	0.11	44	21	64
22	0.11	0.0100000	0.11	46	22	67
23	0.12	0.0100000	0.12	48	23	70

24	0.12	0.0100000	0.12	50	24	73
25	0.12	0.0100000	0.13	52	25	76
26	0.13	0.0100000	0.13	54	26	79
27	0.13	0.0100000	0.14	56	27	82
28	0.14	0.0100000	0.14	58	28	85
29	0.13	0.1000000	0.15	59	29	87
30	0.14	0.0087288	0.14	62	30	91
31	0.13	0.0872879	0.14	63	31	93
32	0.14	0.0087288	0.14	66	32	97
33	0.13	0.0872879	0.14	67	33	99
34	0.13	0.0872879	0.14	69	34	102
35	0.13	0.0087288	0.13	72	35	106
36	0.14	0.0087288	0.14	74	36	109
37	0.14	0.0087288	0.15	76	37	112
38	0.15	0.0087288	0.15	78	38	115
39	0.16	0.0087288	0.16	80	39	118
40	0.16	0.0087288	0.17	82	40	121
41	0.17	0.0087288	0.17	84	41	124
42	0.18	0.0087288	0.18	86	42	127
43	0.19	0.0087288	0.19	88	43	130
44	0.19	0.0087288	0.2	90	44	133
45	0.2	0.0087288	0.2	92	45	136
46	0.21	0.0087288	0.21	94	46	139
47	0.22	0.0087288	0.22	96	47	142
48	0.23	0.0087288	0.23	98	48	145
49	0.23	0.0872879	0.24	99	49	147
50	0.22	0.0355868	0.23	101	50	150
51	0.22	0.0355868	0.23	103	51	153
52	0.22	0.0355868	0.23	105	52	156
53	0.22	0.0355868	0.23	107	53	159
54	0.22	0.0355868	0.22	109	54	162
55	0.21	0.0355868	0.22	111	55	165
56	0.21	0.0355868	0.22	113	56	168
57	0.21	0.0355868	0.22	115	57	171
58	0.23	0.0081895	0.23	117	58	174
59	0.23	0.0081895	0.23	119	59	177
60	0.21	0.0213455	0.21	120	60	179
61	0.21	0.0213455	0.21	122	61	182
62	0.2	0.0213455	0.21	124	62	185
63	0.2	0.0213455	0.21	126	63	188
64	0.2	0.0213455	0.2	128	64	191
65	0.2	0.0213455	0.2	130	65	194
66	0.19	0.0213455	0.2	132	66	197
67	0.19	0.0213455	0.19	134	67	200
68	0.19	0.0213455	0.19	136	68	203
69	0.18	0.0213455	0.19	138	69	206
70	0.18	0.0213455	0.19	140	70	209
71	0.18	0.0213455	0.18	142	71	212
72	0.18	0.0213455	0.18	144	72	215
73	0.17	0.0213455	0.18	146	73	218
74	0.17	0.0213455	0.17	148	74	221
75	0.17	0.0213455	0.17	150	75	224
76	0.16	0.0213455	0.17	152	76	227
77	0.16	0.0213455	0.17	154	77	230
78	0.16	0.0213455	0.16	156	78	233
79	0.16	0.0213455	0.16	158	79	236
80	0.14	0.2134550	0.15	159	80	238
81	0.1	0.0685852	0.11	161	81	241
82	0.096	0.0685852	0.1	163	82	244
83	0.088	0.0685852	0.095	165	83	247
84	0.082	0.0685852	0.088	167	84	250
85	0.076	0.0685852	0.082	169	85	253

Stationary Solver 1 in Solver 1: Solution time: 81 s. (1 minute, 21 seconds)

E.6 Ninety Iterations

90 iterations

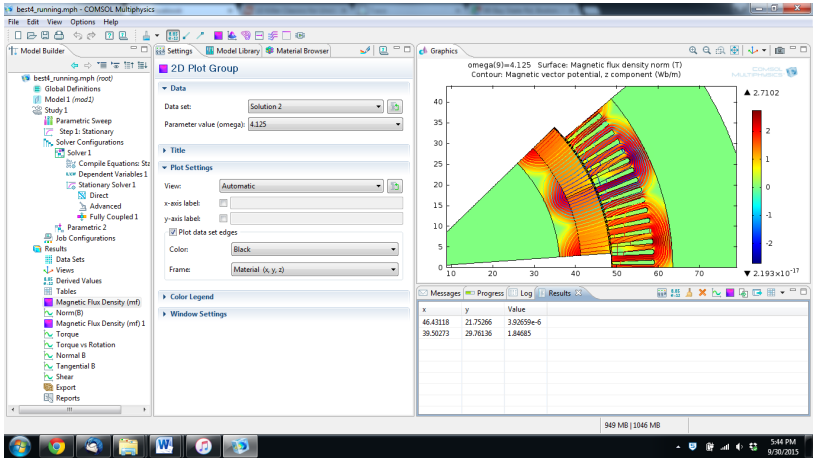

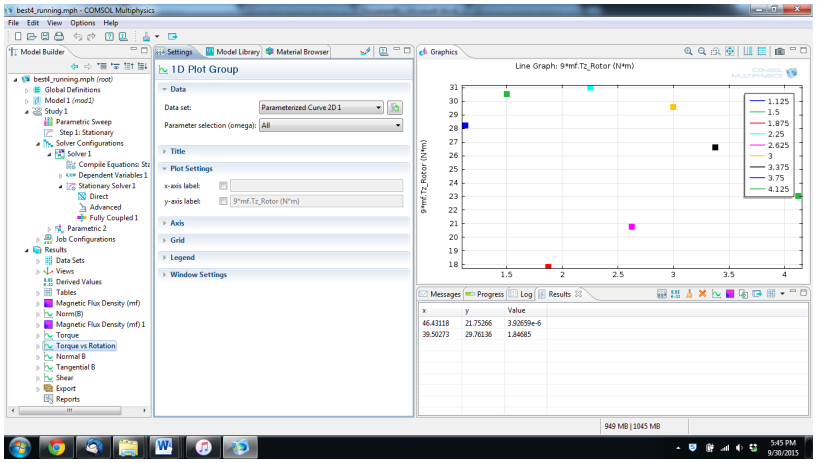


```
================================================================
Parameter omega = 1.125.
Number of vertex elements: 10
Number of boundary elements: 121
Stationary Solver 1 in Solver 1 started at 30-Sep-2015 17:31:45.
Nonlinear solver
Number of degrees of freedom solved for: 37017.
Nonsymmetric matrix found.
Scales for dependent variables:
mod1.A: 1
mod1.root.mod1.mf.VCoil_1_ode: 0.19
mod1.root.mod1.mf.VCoil_2_ode: 0.19
mod1.root.mod1.mf.VCoil_3_ode: 0.19
mod1.root.mod1.mf.VCoil_4_ode: 0.19
mod1.root.mod1.mf.VCoil_5_ode: 0.19
mod1.root.mod1.mf.VCoil_6_ode: 0.19
mod1.root.mod1.mf.VCoil_7_ode: 0.19
mod1.root.mod1.mf.VCoil_8_ode: 0.19
mod1.root.mod1.mf.VCoil_9_ode: 0.19
mod1.root.mod1.mf.VCoil_10_ode: 0.19
mod1.root.mod1.mf.VCoil_11_ode: 0.19
mod1.root.mod1.mf.VCoil_12_ode: 0.19
mod1.root.mod1.mf.VCoil_13_ode: 0.19
mod1.root.mod1.mf.VCoil_14_ode: 0.19
mod1.root.mod1.mf.VCoil_15_ode: 0.19
mod1.root.mod1.mf.VCoil_16_ode: 0.19
```

Iter	ErrEst	Damping	Stepsize	#Res	#Jac	#Sol
1	0.044	0.1000000	0.049	3	1	3
2	0.041	0.1000000	0.046	5	2	6
3	0.039	0.1000000	0.044	7	3	9
4	0.041	0.0100000	0.041	10	4	13
5	0.039	0.1000000	0.043	11	5	15
6	0.04	0.0100000	0.041	14	6	19
7	0.042	0.0100000	0.043	16	7	22
8	0.044	0.0100000	0.044	18	8	25
9	0.046	0.0100000	0.046	20	9	28
10	0.048	0.0100000	0.048	22	10	31
11	0.05	0.0100000	0.05	24	11	34
12	0.052	0.0100000	0.052	26	12	37
13	0.054	0.0100000	0.055	28	13	40
14	0.057	0.0100000	0.057	30	14	43
15	0.059	0.0100000	0.059	32	15	46
16	0.061	0.0100000	0.062	34	16	49
17	0.064	0.0100000	0.065	36	17	52
18	0.067	0.0100000	0.067	38	18	55
19	0.07	0.0100000	0.07	40	19	58
20	0.073	0.0100000	0.073	42	20	61
21	0.076	0.0100000	0.076	44	21	64
22	0.079	0.0100000	0.08	46	22	67
23	0.082	0.0100000	0.083	48	23	70
24	0.086	0.0100000	0.087	50	24	73
25	0.089	0.0100000	0.09	52	25	76
26	0.093	0.0100000	0.094	54	26	79
27	0.097	0.0100000	0.098	56	27	82
28	0.1	0.0100000	0.1	58	28	85
29	0.11	0.0100000	0.11	60	29	88
30	0.11	0.0165913	0.11	62	30	91
31	0.11	0.0165913	0.12	64	31	94
32	0.12	0.0165913	0.12	66	32	97
33	0.12	0.0165913	0.12	68	33	100
34	0.13	0.0165913	0.13	70	34	103
35	0.13	0.0165913	0.13	72	35	106
36	0.14	0.0165913	0.14	74	36	109

37	0.14	0.0165913	0.14	76	37	112
38	0.14	0.0165913	0.15	78	38	115
39	0.15	0.0165913	0.15	80	39	118
40	0.15	0.0165913	0.16	82	40	121
41	0.16	0.0165913	0.16	84	41	124
42	0.17	0.0165913	0.17	86	42	127
43	0.17	0.0165913	0.17	88	43	130
44	0.18	0.0165913	0.18	90	44	133
45	0.18	0.0165913	0.19	92	45	136
46	0.19	0.0165913	0.19	94	46	139
47	0.2	0.0165913	0.2	96	47	142
48	0.2	0.0165913	0.21	98	48	145
49	0.21	0.0165913	0.21	100	49	148
50	0.22	0.0165913	0.22	102	50	151
51	0.22	0.0165913	0.23	104	51	154
52	0.23	0.0165913	0.23	106	52	157
53	0.24	0.0165913	0.24	108	53	160
54	0.24	0.0165913	0.25	110	54	163
55	0.25	0.0165913	0.25	112	55	166
56	0.26	0.0165913	0.26	114	56	169
57	0.26	0.0165913	0.26	116	57	172
58	0.26	0.0165913	0.27	118	58	175
59	0.26	0.0165913	0.27	120	59	178
60	0.27	0.0165913	0.27	122	60	181
61	0.27	0.0165913	0.27	124	61	184
62	0.27	0.0165913	0.27	126	62	187
63	0.27	0.0165913	0.27	128	63	190
64	0.26	0.0165913	0.27	130	64	193
65	0.26	0.0165913	0.27	132	65	196
66	0.26	0.0165913	0.26	134	66	199
67	0.26	0.0165913	0.26	136	67	202
68	0.26	0.0165913	0.26	138	68	205
69	0.25	0.0165913	0.26	140	69	208
70	0.25	0.0165913	0.25	142	70	211
71	0.21	0.1659130	0.24	143	71	213
72	0.18	0.1000000	0.2	145	72	216
73	0.16	0.1000000	0.18	147	73	219
74	0.15	0.1000000	0.16	149	74	222
75	0.13	0.1000000	0.14	151	75	225
76	0.11	0.0966479	0.13	153	76	228
77	0.1	0.0966479	0.11	155	77	231
78	0.092	0.0966479	0.1	157	78	234
79	0.083	0.0966479	0.092	159	79	237
80	0.075	0.0966479	0.083	161	80	240
81	0.067	0.0966479	0.074	163	81	243
82	0.061	0.0966479	0.067	165	82	246
83	0.055	0.0966479	0.061	167	83	249
84	0.049	0.0966479	0.055	169	84	252
85	0.045	0.0966479	0.049	171	85	255
86	0.04	0.0966479	0.045	173	86	258
87	0.037	0.0966479	0.04	175	87	261
88	0.033	0.0966479	0.036	177	88	264
89	0.03	0.0966479	0.033	179	89	267
90	0.027	0.0966479	0.03	181	90	270

Stationary Solver 1 in Solver 1: Solution time: 99 s. (1 minute, 39 seconds)
Parameter omega = 1.5.
Number of vertex elements: 10

Number of boundary elements: 122
Stationary Solver 1 in Solver 1 started at 30-Sep-2015 17:33:33.
Nonlinear solver
Number of degrees of freedom solved for: 36911.
Nonsymmetric matrix found.
Scales for dependent variables:
mod1.A: 1
mod1.root.mod1.mf.VCoil_1_ode: 0.19
mod1.root.mod1.mf.VCoil_2_ode: 0.19
mod1.root.mod1.mf.VCoil_3_ode: 0.19
mod1.root.mod1.mf.VCoil_4_ode: 0.19
mod1.root.mod1.mf.VCoil_5_ode: 0.19
mod1.root.mod1.mf.VCoil_6_ode: 0.19
mod1.root.mod1.mf.VCoil_7_ode: 0.19
mod1.root.mod1.mf.VCoil_8_ode: 0.19
mod1.root.mod1.mf.VCoil_9_ode: 0.19
mod1.root.mod1.mf.VCoil_10_ode: 0.19
mod1.root.mod1.mf.VCoil_11_ode: 0.19
mod1.root.mod1.mf.VCoil_12_ode: 0.19
mod1.root.mod1.mf.VCoil_13_ode: 0.19
mod1.root.mod1.mf.VCoil_14_ode: 0.19
mod1.root.mod1.mf.VCoil_15_ode: 0.19
mod1.root.mod1.mf.VCoil_16_ode: 0.19

Iter	ErrEst	Damping	Stepsize	#Res	#Jac	#Sol
1	0.045	0.1000000	0.05	3	1	3
2	0.042	0.1000000	0.047	5	2	6
3	0.041	0.1000000	0.044	7	3	9
4	0.039	0.1000000	0.042	9	4	12
5	0.04	0.0100000	0.04	12	5	16
6	0.041	0.0100000	0.042	14	6	19
7	0.043	0.0100000	0.044	16	7	22
8	0.045	0.0100000	0.046	18	8	25
9	0.047	0.0100000	0.047	20	9	28
10	0.049	0.0100000	0.049	22	10	31
11	0.051	0.0100000	0.052	24	11	34
12	0.053	0.0100000	0.054	26	12	37
13	0.056	0.0100000	0.056	28	13	40
14	0.058	0.0100000	0.058	30	14	43
15	0.06	0.0100000	0.061	32	15	46
16	0.063	0.0100000	0.064	34	16	49
17	0.066	0.0100000	0.066	36	17	52
18	0.068	0.0100000	0.069	38	18	55
19	0.071	0.0100000	0.072	40	19	58
20	0.074	0.0100000	0.075	42	20	61
21	0.078	0.0100000	0.078	44	21	64
22	0.081	0.0100000	0.082	46	22	67
23	0.084	0.0100000	0.085	48	23	70
24	0.088	0.0100000	0.089	50	24	73
25	0.092	0.0100000	0.093	52	25	76
26	0.096	0.0100000	0.097	54	26	79
27	0.1	0.0100000	0.1	56	27	82
28	0.1	0.0100000	0.11	58	28	85
29	0.11	0.0100000	0.11	60	29	88
30	0.11	0.0100000	0.11	62	30	91
31	0.12	0.0100000	0.12	64	31	94
32	0.12	0.0100000	0.12	66	32	97
33	0.13	0.0100000	0.13	68	33	100

```
  34        0.13   0.0100000        0.13   70   34  103
  35        0.14   0.0100000        0.14   72   35  106
  36        0.14   0.0100000        0.15   74   36  109
  37        0.15   0.0100000        0.15   76   37  112
  38        0.16   0.0100000        0.16   78   38  115
  39        0.16   0.0100000        0.16   80   39  118
  40        0.17   0.0100000        0.17   82   40  121
  41        0.18   0.0100000        0.18   84   41  124
  42        0.18   0.0100000        0.19   86   42  127
  43        0.19   0.1000000        0.19   87   43  129
  44        0.17   0.0645361        0.18   89   44  132
  45        0.17   0.0645361        0.18   91   45  135
  46        0.16   0.0645361        0.18   93   46  138
  47        0.16   0.0645361        0.17   95   47  141
  48        0.16   0.0645361        0.17   97   48  144
  49        0.16   0.0645361        0.17   99   49  147
  50        0.15   0.0645361        0.17  101   50  150
  51        0.15   0.0645361        0.16  103   51  153
  52        0.15   0.0645361        0.16  105   52  156
  53        0.14   0.0645361        0.15  107   53  159
  54        0.14   0.0645361        0.15  109   54  162
  55        0.13   0.0645361        0.14  111   55  165
  56        0.13   0.0645361        0.14  113   56  168
  57        0.12   0.0523015        0.13  115   57  171
  58        0.12   0.0523015        0.12  117   58  174
  59        0.11   0.0523015        0.12  119   59  177
  60        0.11   0.0523015        0.11  121   60  180
  61         0.1   0.0523015        0.11  123   61  183
  62       0.098   0.0523015         0.1  125   62  186
  63       0.093   0.0523015       0.099  127   63  189
  64       0.089   0.0523015       0.094  129   64  192
  65       0.085   0.0523015        0.09  131   65  195
  66       0.081   0.0523015       0.085  133   66  198
  67       0.077   0.0523015       0.081  135   67  201
  68       0.074   0.0523015       0.078  137   68  204
  69        0.07   0.0523015       0.074  139   69  207
  70       0.067   0.0523015        0.07  141   70  210
  71       0.063   0.0523015       0.067  143   71  213
  72       0.064   0.5230153       0.061  144   72  215
  73       0.026   0.1153894       0.029  146   73  218
  74       0.015   0.4111196       0.026  148   74  221
  75      0.0088   0.4439298       0.015  150   75  224
  76      0.0072   0.1556226      0.0085  152   76  227
  77      0.0044   1.0000000      0.0083  153   77  229
  78   8.3e-005   1.0000000     0.00049  154   78  231
Stationary Solver 1 in Solver 1: Solution time: 76 s. (1 minute, 16 seconds)
Parameter omega = 1.875.
Number of vertex elements: 10
Number of boundary elements: 123
Stationary Solver 1 in Solver 1 started at 30-Sep-2015 17:34:57.
Nonlinear solver
Number of degrees of freedom solved for: 36825.
Nonsymmetric matrix found.
Scales for dependent variables:
mod1.A: 1
mod1.root.mod1.mf.VCoil_1_ode: 0.19
mod1.root.mod1.mf.VCoil_2_ode: 0.19
mod1.root.mod1.mf.VCoil_3_ode: 0.19
mod1.root.mod1.mf.VCoil_4_ode: 0.19
mod1.root.mod1.mf.VCoil_5_ode: 0.19
mod1.root.mod1.mf.VCoil_6_ode: 0.19
mod1.root.mod1.mf.VCoil_7_ode: 0.19
mod1.root.mod1.mf.VCoil_8_ode: 0.19
mod1.root.mod1.mf.VCoil_9_ode: 0.19
mod1.root.mod1.mf.VCoil_10_ode: 0.19
mod1.root.mod1.mf.VCoil_11_ode: 0.19
mod1.root.mod1.mf.VCoil_12_ode: 0.19
mod1.root.mod1.mf.VCoil_13_ode: 0.19
mod1.root.mod1.mf.VCoil_14_ode: 0.19
mod1.root.mod1.mf.VCoil_15_ode: 0.19
mod1.root.mod1.mf.VCoil_16_ode: 0.19
Iter      ErrEst     Damping    Stepsize #Res #Jac #Sol
   1       0.046   0.1000000       0.051    3    1    3
   2       0.043   0.1000000       0.048    5    2    6
   3       0.045   0.0100000       0.045    8    3   10
   4       0.047   0.0100000       0.047   10    4   13
   5       0.049   0.0100000       0.049   12    5   16
   6       0.051   0.0100000       0.051   14    6   19
   7       0.053   0.0100000       0.054   16    7   22
   8       0.055   0.0100000       0.056   18    8   25
   9       0.058   0.0100000       0.058   20    9   28
  10        0.06   0.0100000       0.061   22   10   31
  11       0.063   0.0100000       0.063   24   11   34
  12       0.065   0.0100000       0.066   26   12   37
  13       0.068   0.0100000       0.069   28   13   40
  14       0.071   0.0100000       0.071   30   14   43
  15       0.074   0.0100000       0.074   32   15   46
  16       0.077   0.0100000       0.078   34   16   49
  17        0.08   0.0100000       0.081   36   17   52
  18       0.084   0.0100000       0.084   38   18   55
  19       0.087   0.0100000       0.088   40   19   58
  20       0.091   0.0100000       0.092   42   20   61
  21       0.094   0.0100000       0.095   44   21   64
  22       0.099   0.0100000         0.1   46   22   67
  23         0.1   0.0100000         0.1   48   23   70
  24        0.11   0.0100000        0.11   50   24   73
  25        0.11   0.0100000        0.11   52   25   76
  26        0.12   0.0100000        0.12   54   26   79
  27        0.12   0.0100000        0.12   56   27   82
  28        0.13   0.0100000        0.13   58   28   85
  29        0.13   0.0100000        0.13   60   29   88
  30        0.14   0.0100000        0.14   62   30   91
  31        0.14   0.0100000        0.14   64   31   94
  32        0.15   0.0100000        0.15   66   32   97
  33        0.16   0.0100000        0.16   68   33  100
  34        0.16   0.0100000        0.16   70   34  103
  35        0.17   0.0100000        0.17   72   35  106
  36        0.18   0.0100000        0.18   74   36  109
  37        0.18   0.0100000        0.19   76   37  112
  38        0.19   0.0100000        0.19   78   38  115
  39         0.2   0.0100000         0.2   80   39  118
  40        0.21   0.0100000        0.21   82   40  121
  41        0.22   0.0100000        0.22   84   41  124
  42        0.23   0.0100000        0.23   86   42  127
```

43	0.23	0.0100000	0.24	88	43	130
44	0.24	0.0100000	0.25	90	44	133
45	0.25	0.0100000	0.26	92	45	136
46	0.26	0.0100000	0.27	94	46	139
47	0.28	0.0100000	0.28	96	47	142
48	0.29	0.0100000	0.29	98	48	145
49	0.3	0.0100000	0.3	100	49	148
50	0.31	0.0100000	0.31	102	50	151
51	0.32	0.0100000	0.33	104	51	154
52	0.34	0.0100000	0.34	106	52	157
53	0.35	0.0100000	0.35	108	53	160
54	0.36	0.0100000	0.37	110	54	163
55	0.38	0.0118020	0.38	112	55	166
56	0.39	0.0118020	0.4	114	56	169
57	0.4	0.0118020	0.41	116	57	172
58	0.42	0.0118020	0.42	118	58	175
59	0.42	0.0173061	0.43	120	59	178
60	0.43	0.0173061	0.43	122	60	181
61	0.43	0.0173061	0.44	124	61	184
62	0.43	0.0173061	0.44	126	62	187
63	0.43	0.0173061	0.44	128	63	190
64	0.43	0.0173061	0.44	130	64	193
65	0.43	0.0180233	0.44	132	65	196
66	0.43	0.0180233	0.43	134	66	199
67	0.42	0.0180233	0.43	136	67	202
68	0.42	0.0180233	0.43	138	68	205
69	0.41	0.0180233	0.42	140	69	208
70	0.41	0.0180233	0.41	142	70	211
71	0.4	0.0180233	0.41	144	71	214
72	0.39	0.0180233	0.4	146	72	217
73	0.39	0.0180233	0.39	148	73	220
74	0.38	0.0180233	0.39	150	74	223
75	0.38	0.0180233	0.38	152	75	226
76	0.37	0.0180233	0.38	154	76	229
77	0.36	0.0180233	0.37	156	77	232
78	0.36	0.0180233	0.36	158	78	235
79	0.35	0.0180233	0.36	160	79	238
80	0.34	0.0180233	0.35	162	80	241
81	0.34	0.0180233	0.34	164	81	244
82	0.33	0.0180233	0.34	166	82	247
83	0.32	0.0180233	0.33	168	83	250
84	0.32	0.0180233	0.32	170	84	253
85	0.31	0.0180233	0.32	172	85	256
86	0.31	0.0180233	0.31	174	86	259
87	0.3	0.0180233	0.3	176	87	262
88	0.29	0.0180233	0.3	178	88	265
89	0.29	0.0180233	0.29	180	89	268
90	0.28	0.0180233	0.29	182	90	271

Stationary Solver 1 in Solver 1: Solution time: 86 s. (1 minute, 26 seconds)
Parameter omega = 2.25.
Number of vertex elements: 10
Number of boundary elements: 124
Stationary Solver 1 in Solver 1 started at 30-Sep-2015 17:36:30.
Nonlinear solver
Number of degrees of freedom solved for: 36647.
Nonsymmetric matrix found.
Scales for dependent variables:

mod1.A: 1
mod1.root.mod1.mf.VCoil_1_ode: 0.19
mod1.root.mod1.mf.VCoil_2_ode: 0.19
mod1.root.mod1.mf.VCoil_3_ode: 0.19
mod1.root.mod1.mf.VCoil_4_ode: 0.19
mod1.root.mod1.mf.VCoil_5_ode: 0.19
mod1.root.mod1.mf.VCoil_6_ode: 0.19
mod1.root.mod1.mf.VCoil_7_ode: 0.19
mod1.root.mod1.mf.VCoil_8_ode: 0.19
mod1.root.mod1.mf.VCoil_9_ode: 0.19
mod1.root.mod1.mf.VCoil_10_ode: 0.19
mod1.root.mod1.mf.VCoil_11_ode: 0.19
mod1.root.mod1.mf.VCoil_12_ode: 0.19
mod1.root.mod1.mf.VCoil_13_ode: 0.19
mod1.root.mod1.mf.VCoil_14_ode: 0.19
mod1.root.mod1.mf.VCoil_15_ode: 0.19
mod1.root.mod1.mf.VCoil_16_ode: 0.19

Iter	ErrEst	Damping	Stepsize	#Res	#Jac	#Sol
1	0.047	0.1000000	0.052	3	1	3
2	0.044	0.1000000	0.049	5	2	6
3	0.046	0.0100000	0.046	8	3	10
4	0.048	0.0100000	0.048	10	4	13
5	0.05	0.0100000	0.05	12	5	16
6	0.048	0.1000000	0.052	13	6	18
7	0.049	0.0100000	0.05	16	7	22
8	0.051	0.0100000	0.052	18	8	25
9	0.054	0.0100000	0.054	20	9	28
10	0.056	0.0100000	0.056	22	10	31
11	0.058	0.0100000	0.059	24	11	34
12	0.061	0.0100000	0.061	26	12	37
13	0.063	0.0100000	0.064	28	13	40
14	0.066	0.0100000	0.067	30	14	43
15	0.069	0.0100000	0.07	32	15	46
16	0.072	0.0100000	0.073	34	16	49
17	0.075	0.0100000	0.076	36	17	52
18	0.078	0.0100000	0.079	38	18	55
19	0.082	0.0100000	0.082	40	19	58
20	0.085	0.0100000	0.086	42	20	61
21	0.089	0.0100000	0.09	44	21	64
22	0.093	0.0100000	0.093	46	22	67
23	0.097	0.0100000	0.097	48	23	70
24	0.1	0.0100000	0.1	50	24	73
25	0.1	0.0100000	0.11	52	25	76
26	0.11	0.0100000	0.11	54	26	79
27	0.11	0.0100000	0.12	56	27	82
28	0.12	0.0100000	0.12	58	28	85
29	0.12	0.0100000	0.13	60	29	88
30	0.13	0.0100000	0.13	62	30	91
31	0.13	0.0100000	0.14	64	31	94
32	0.14	0.0100000	0.14	66	32	97
33	0.15	0.0100000	0.15	68	33	100
34	0.15	0.0100000	0.15	70	34	103
35	0.16	0.0100000	0.16	72	35	106
36	0.16	0.0100000	0.17	74	36	109
37	0.17	0.0100000	0.17	76	37	112
38	0.18	0.0100000	0.18	78	38	115
39	0.19	0.0100000	0.19	80	39	118

40	0.18	0.1000000	0.19	81	40	120
41	0.17	0.0625646	0.18	83	41	123
42	0.17	0.0625646	0.18	85	42	126
43	0.17	0.0625646	0.18	87	43	129
44	0.16	0.0625646	0.18	89	44	132
45	0.16	0.0625646	0.17	91	45	135
46	0.16	0.0625646	0.17	93	46	138
47	0.16	0.0625646	0.17	95	47	141
48	0.17	0.0062565	0.17	98	48	145
49	0.17	0.0625646	0.17	99	49	147
50	0.17	0.0192446	0.17	101	50	150
51	0.17	0.0192446	0.18	103	51	153
52	0.18	0.0192446	0.18	105	52	156
53	0.18	0.0192446	0.18	107	53	159
54	0.18	0.0192446	0.19	109	54	162
55	0.19	0.0192446	0.19	111	55	165
56	0.19	0.0192446	0.19	113	56	168
57	0.19	0.0192446	0.19	115	57	171
58	0.19	0.0192446	0.19	117	58	174
59	0.19	0.0192446	0.19	119	59	177
60	0.19	0.0192446	0.19	121	60	180
61	0.18	0.1924456	0.18	122	61	182
62	0.14	0.0540705	0.15	124	62	185
63	0.13	0.0461513	0.14	126	63	188
64	0.13	0.0461513	0.13	128	64	191
65	0.12	0.0461513	0.13	130	65	194
66	0.12	0.0461513	0.12	132	66	197
67	0.11	0.0461513	0.12	134	67	200
68	0.11	0.0461513	0.11	136	68	203
69	0.1	0.0461513	0.11	138	69	206
70	0.099	0.0461513	0.1	140	70	209
71	0.095	0.0461513	0.1	142	71	212
72	0.091	0.0461513	0.096	144	72	215
73	0.088	0.0461513	0.092	146	73	218
74	0.084	0.0461513	0.088	148	74	221
75	0.08	0.0461513	0.084	150	75	224
76	0.076	0.0461513	0.08	152	76	227
77	0.073	0.0461513	0.077	154	77	230
78	0.07	0.0461513	0.073	156	78	233
79	0.067	0.0461513	0.07	158	79	236
80	0.064	0.0461513	0.067	160	80	239
81	0.061	0.0461513	0.064	162	81	242
82	0.058	0.0461513	0.061	164	82	245
83	0.055	0.0461513	0.058	166	83	248
84	0.04	0.4615128	0.054	167	84	250
85	0.02	0.3214642	0.029	169	85	253
86	0.014	0.2734717	0.02	171	86	256
87	0.0081	1.0000000	0.014	172	87	258
88	0.00039	1.0000000	0.0017	173	88	260

Stationary Solver 1 in Solver 1: Solution time: 73 s. (1 minute, 13 seconds)
Parameter omega = 2.625.
Number of vertex elements: 10
Number of boundary elements: 125
Stationary Solver 1 in Solver 1 started at 30-Sep-2015 17:37:50.
Nonlinear solver
Number of degrees of freedom solved for: 36885.
Nonsymmetric matrix found.

Scales for dependent variables:
mod1.A: 1
mod1.root.mod1.mf.VCoil_1_ode: 0.19
mod1.root.mod1.mf.VCoil_2_ode: 0.19
mod1.root.mod1.mf.VCoil_3_ode: 0.19
mod1.root.mod1.mf.VCoil_4_ode: 0.19
mod1.root.mod1.mf.VCoil_5_ode: 0.19
mod1.root.mod1.mf.VCoil_6_ode: 0.19
mod1.root.mod1.mf.VCoil_7_ode: 0.19
mod1.root.mod1.mf.VCoil_8_ode: 0.19
mod1.root.mod1.mf.VCoil_9_ode: 0.19
mod1.root.mod1.mf.VCoil_10_ode: 0.19
mod1.root.mod1.mf.VCoil_11_ode: 0.19
mod1.root.mod1.mf.VCoil_12_ode: 0.19
mod1.root.mod1.mf.VCoil_13_ode: 0.19
mod1.root.mod1.mf.VCoil_14_ode: 0.19
mod1.root.mod1.mf.VCoil_15_ode: 0.19
mod1.root.mod1.mf.VCoil_16_ode: 0.19

Iter	ErrEst	Damping	Stepsize	#Res	#Jac	#Sol
1	0.048	0.1000000	0.053	3	1	3
2	0.045	0.1000000	0.05	5	2	6
3	0.047	0.0100000	0.047	8	3	10
4	0.049	0.0100000	0.049	10	4	13
5	0.051	0.0100000	0.051	12	5	16
6	0.053	0.0100000	0.054	14	6	19
7	0.055	0.0100000	0.056	16	7	22
8	0.058	0.0100000	0.058	18	8	25
9	0.06	0.0100000	0.061	20	9	28
10	0.063	0.0100000	0.063	22	10	31
11	0.065	0.0100000	0.066	24	11	34
12	0.068	0.0100000	0.069	26	12	37
13	0.071	0.0100000	0.072	28	13	40
14	0.074	0.0100000	0.075	30	14	43
15	0.077	0.0100000	0.078	32	15	46
16	0.08	0.0100000	0.081	34	16	49
17	0.084	0.0100000	0.085	36	17	52
18	0.087	0.0100000	0.088	38	18	55
19	0.091	0.0100000	0.092	40	19	58
20	0.095	0.0100000	0.096	42	20	61
21	0.099	0.0100000	0.1	44	21	64
22	0.1	0.0100000	0.1	46	22	67
23	0.11	0.0100000	0.11	48	23	70
24	0.11	0.0100000	0.11	50	24	73
25	0.12	0.0100000	0.12	52	25	76
26	0.12	0.0100000	0.12	54	26	79
27	0.13	0.0100000	0.13	56	27	82
28	0.13	0.0100000	0.13	58	28	85
29	0.14	0.0100000	0.14	60	29	88
30	0.14	0.0100000	0.15	62	30	91
31	0.15	0.0100000	0.15	64	31	94
32	0.16	0.0100000	0.16	66	32	97
33	0.16	0.0100000	0.16	68	33	100
34	0.17	0.0100000	0.17	70	34	103
35	0.18	0.0100000	0.18	72	35	106
36	0.18	0.0100000	0.19	74	36	109
37	0.19	0.0100000	0.19	76	37	112
38	0.2	0.0100000	0.2	78	38	115

39	0.21	0.0100000	0.21	80	39	118
40	0.22	0.0100000	0.22	82	40	121
41	0.22	0.0100000	0.23	84	41	124
42	0.23	0.0114514	0.23	86	42	127
43	0.24	0.0130367	0.24	88	43	130
44	0.25	0.0130367	0.25	90	44	133
45	0.26	0.0130367	0.26	92	45	136
46	0.26	0.0213471	0.27	94	46	139
47	0.27	0.0213471	0.28	96	47	142
48	0.28	0.0213471	0.28	98	48	145
49	0.29	0.0213471	0.29	100	49	148
50	0.29	0.0213471	0.3	102	50	151
51	0.3	0.0213471	0.31	104	51	154
52	0.31	0.0213471	0.32	106	52	157
53	0.32	0.0213471	0.33	108	53	160
54	0.33	0.0213471	0.34	110	54	163
55	0.34	0.0213471	0.34	112	55	166
56	0.34	0.0213471	0.35	114	56	169
57	0.35	0.0213471	0.36	116	57	172
58	0.35	0.0213471	0.36	118	58	175
59	0.35	0.0213471	0.36	120	59	178
60	0.36	0.0213471	0.36	122	60	181
61	0.35	0.0213471	0.36	124	61	184
62	0.35	0.0213471	0.36	126	62	187
63	0.35	0.0213471	0.36	128	63	190
64	0.35	0.0213471	0.36	130	64	193
65	0.34	0.0213471	0.35	132	65	196
66	0.34	0.0213471	0.35	134	66	199
67	0.33	0.0213471	0.34	136	67	202
68	0.33	0.0213471	0.34	138	68	205
69	0.32	0.0213471	0.33	140	69	208
70	0.32	0.0213471	0.32	142	70	211
71	0.31	0.0213471	0.32	144	71	214
72	0.3	0.0213471	0.31	146	72	217
73	0.3	0.0213471	0.31	148	73	220
74	0.29	0.0213471	0.3	150	74	223
75	0.29	0.0213471	0.29	152	75	226
76	0.28	0.0213471	0.29	154	76	229
77	0.27	0.0213471	0.28	156	77	232
78	0.27	0.0213471	0.28	158	78	235
79	0.26	0.0213471	0.27	160	79	238
80	0.26	0.0213471	0.26	162	80	241
81	0.25	0.0213471	0.26	164	81	244
82	0.25	0.0213471	0.25	166	82	247
83	0.24	0.0213471	0.25	168	83	250
84	0.24	0.0213471	0.24	170	84	253
85	0.23	0.0213471	0.24	172	85	256
86	0.23	0.0213471	0.23	174	86	259
87	0.22	0.0258851	0.23	176	87	262
88	0.22	0.0258851	0.22	178	88	265
89	0.21	0.0258851	0.22	180	89	268
90	0.21	0.0258851	0.21	182	90	271

Stationary Solver 1 in Solver 1: Solution time: 74 s. (1 minute, 14 seconds)
Parameter omega = 3.0.
Number of vertex elements: 10
Number of boundary elements: 126
Stationary Solver 1 in Solver 1 started at 30-Sep-2015 17:39:12.

Nonlinear solver
Number of degrees of freedom solved for: 36759.
Nonsymmetric matrix found.
Scales for dependent variables:
mod1.A: 1
mod1.root.mod1.mf.VCoil_1_ode: 0.19
mod1.root.mod1.mf.VCoil_2_ode: 0.19
mod1.root.mod1.mf.VCoil_3_ode: 0.19
mod1.root.mod1.mf.VCoil_4_ode: 0.19
mod1.root.mod1.mf.VCoil_5_ode: 0.19
mod1.root.mod1.mf.VCoil_6_ode: 0.19
mod1.root.mod1.mf.VCoil_7_ode: 0.19
mod1.root.mod1.mf.VCoil_8_ode: 0.19
mod1.root.mod1.mf.VCoil_9_ode: 0.19
mod1.root.mod1.mf.VCoil_10_ode: 0.19
mod1.root.mod1.mf.VCoil_11_ode: 0.19
mod1.root.mod1.mf.VCoil_12_ode: 0.19
mod1.root.mod1.mf.VCoil_13_ode: 0.19
mod1.root.mod1.mf.VCoil_14_ode: 0.19
mod1.root.mod1.mf.VCoil_15_ode: 0.19
mod1.root.mod1.mf.VCoil_16_ode: 0.19

Iter	ErrEst	Damping	Stepsize	#Res	#Jac	#Sol
1	0.049	0.1000000	0.054	3	1	3
2	0.046	0.1000000	0.051	5	2	6
3	0.048	0.0100000	0.048	8	3	10
4	0.05	0.0100000	0.05	10	4	13
5	0.052	0.0100000	0.052	12	5	16
6	0.054	0.0100000	0.055	14	6	19
7	0.056	0.0100000	0.057	16	7	22
8	0.059	0.0100000	0.059	18	8	25
9	0.061	0.0100000	0.062	20	9	28
10	0.064	0.0100000	0.065	22	10	31
11	0.067	0.0100000	0.067	24	11	34
12	0.069	0.0100000	0.07	26	12	37
13	0.072	0.0100000	0.073	28	13	40
14	0.075	0.0100000	0.076	30	14	43
15	0.079	0.0100000	0.079	32	15	46
16	0.082	0.0100000	0.083	34	16	49
17	0.086	0.0100000	0.086	36	17	52
18	0.089	0.0100000	0.09	38	18	55
19	0.093	0.0100000	0.094	40	19	58
20	0.097	0.0100000	0.098	42	20	61
21	0.1	0.0100000	0.1	44	21	64
22	0.11	0.0100000	0.11	46	22	67
23	0.11	0.0100000	0.11	48	23	70
24	0.11	0.0100000	0.12	50	24	73
25	0.12	0.0100000	0.12	52	25	76
26	0.12	0.0100000	0.13	54	26	79
27	0.13	0.0100000	0.13	56	27	82
28	0.14	0.0100000	0.14	58	28	85
29	0.14	0.0100000	0.14	60	29	88
30	0.15	0.0100000	0.15	62	30	91
31	0.15	0.0100000	0.15	64	31	94
32	0.16	0.0100000	0.16	66	32	97
33	0.17	0.0100000	0.17	68	33	100
34	0.17	0.0100000	0.17	70	34	103
35	0.18	0.0100000	0.18	72	35	106

36	0.19	0.0100000	0.19	74	36	109
37	0.18	0.1000000	0.19	75	37	111
38	0.17	0.0403578	0.18	77	38	114
39	0.18	0.0403578	0.18	79	39	117
40	0.18	0.0403578	0.19	81	40	120
41	0.18	0.0403578	0.19	83	41	123
42	0.18	0.0403578	0.19	85	42	126
43	0.18	0.0403578	0.19	87	43	129
44	0.19	0.0403578	0.19	89	44	132
45	0.19	0.0403578	0.2	91	45	135
46	0.19	0.0403578	0.2	93	46	138
47	0.19	0.0403578	0.2	95	47	141
48	0.2	0.0403578	0.2	97	48	144
49	0.2	0.0403578	0.21	99	49	147
50	0.2	0.0403578	0.21	101	50	150
51	0.2	0.0403578	0.21	103	51	153
52	0.2	0.0403578	0.21	105	52	156
53	0.2	0.0403578	0.21	107	53	159
54	0.19	0.0403578	0.2	109	54	162
55	0.19	0.0403578	0.2	111	55	165
56	0.19	0.0403578	0.19	113	56	168
57	0.18	0.0403578	0.19	115	57	171
58	0.18	0.0403578	0.18	117	58	174
59	0.17	0.0403578	0.18	119	59	177
60	0.17	0.0403578	0.17	121	60	180
61	0.16	0.0403578	0.17	123	61	183
62	0.16	0.0403578	0.16	125	62	186
63	0.16	0.0256437	0.16	127	63	189
64	0.13	0.1430420	0.15	128	64	191
65	0.12	0.1000000	0.13	130	65	194
66	0.1	0.1000000	0.12	132	66	197
67	0.093	0.1000000	0.1	134	67	200
68	0.084	0.1000000	0.093	136	68	203
69	0.075	0.1000000	0.084	138	69	206
70	0.067	0.1000000	0.075	140	70	209
71	0.06	0.1000000	0.067	142	71	212
72	0.054	0.1000000	0.06	144	72	215
73	0.049	0.1000000	0.054	146	73	218
74	0.044	0.1000000	0.049	148	74	221
75	0.04	0.1000000	0.044	150	75	224
76	0.036	0.1000000	0.04	152	76	227
77	0.032	0.1000000	0.036	154	77	230
78	0.029	0.1000000	0.032	156	78	233
79	0.026	0.1000000	0.029	158	79	236
80	0.024	0.1000000	0.026	160	80	239
81	0.021	0.1000000	0.024	162	81	242
82	0.019	0.1000000	0.022	164	82	245
83	0.018	0.1000000	0.02	166	83	248
84	0.014	0.2185642	0.018	168	84	251
85	0.013	1.0000000	0.014	169	85	253
86	0.00027	1.0000000	0.0013	170	86	255

Stationary Solver 1 in Solver 1: Solution time: 70 s. (1 minute, 10 seconds)
Parameter omega = 3.375.
Number of vertex elements: 10
Number of boundary elements: 127
Stationary Solver 1 in Solver 1 started at 30-Sep-2015 17:40:29.
Nonlinear solver
Number of degrees of freedom solved for: 36841.
Nonsymmetric matrix found.
Scales for dependent variables:
mod1.A: 1
mod1.root.mod1.mf.VCoil_1_ode: 0.19
mod1.root.mod1.mf.VCoil_2_ode: 0.19
mod1.root.mod1.mf.VCoil_3_ode: 0.19
mod1.root.mod1.mf.VCoil_4_ode: 0.19
mod1.root.mod1.mf.VCoil_5_ode: 0.19
mod1.root.mod1.mf.VCoil_6_ode: 0.19
mod1.root.mod1.mf.VCoil_7_ode: 0.19
mod1.root.mod1.mf.VCoil_8_ode: 0.19
mod1.root.mod1.mf.VCoil_9_ode: 0.19
mod1.root.mod1.mf.VCoil_10_ode: 0.19
mod1.root.mod1.mf.VCoil_11_ode: 0.19
mod1.root.mod1.mf.VCoil_12_ode: 0.19
mod1.root.mod1.mf.VCoil_13_ode: 0.19
mod1.root.mod1.mf.VCoil_14_ode: 0.19
mod1.root.mod1.mf.VCoil_15_ode: 0.19
mod1.root.mod1.mf.VCoil_16_ode: 0.19

Iter	ErrEst	Damping	Stepsize	#Res	#Jac	#Sol
1	0.05	0.1000000	0.055	3	1	3
2	0.047	0.1000000	0.052	5	2	6
3	0.049	0.0100000	0.049	8	3	10
4	0.051	0.0100000	0.051	10	4	13
5	0.053	0.0100000	0.054	12	5	16
6	0.055	0.0100000	0.056	14	6	19
7	0.058	0.0100000	0.058	16	7	22
8	0.06	0.0100000	0.061	18	8	25
9	0.063	0.0100000	0.063	20	9	28
10	0.065	0.0100000	0.066	22	10	31
11	0.068	0.0100000	0.069	24	11	34
12	0.071	0.0100000	0.072	26	12	37
13	0.074	0.0100000	0.075	28	13	40
14	0.077	0.0100000	0.078	30	14	43
15	0.081	0.0100000	0.081	32	15	46
16	0.084	0.0100000	0.085	34	16	49
17	0.088	0.0100000	0.089	36	17	52
18	0.091	0.0100000	0.092	38	18	55
19	0.095	0.0100000	0.096	40	19	58
20	0.099	0.0100000	0.1	42	20	61
21	0.1	0.0100000	0.1	44	21	64
22	0.11	0.0100000	0.11	46	22	67
23	0.11	0.0100000	0.11	48	23	70
24	0.12	0.0100000	0.12	50	24	73
25	0.12	0.0100000	0.12	52	25	76
26	0.13	0.0100000	0.13	54	26	79
27	0.13	0.0100000	0.13	56	27	82
28	0.14	0.0100000	0.14	58	28	85
29	0.14	0.0100000	0.14	60	29	88
30	0.15	0.0100000	0.15	62	30	91
31	0.15	0.0100000	0.16	64	31	94
32	0.16	0.0100000	0.16	66	32	97
33	0.17	0.0100000	0.17	68	33	100
34	0.17	0.1000000	0.17	69	34	102
35	0.16	0.0290886	0.16	71	35	105
36	0.16	0.0290886	0.17	73	36	108

37	0.17	0.0290886	0.17	75	37	111
38	0.17	0.0290886	0.18	77	38	114
39	0.17	0.0290886	0.18	79	39	117
40	0.18	0.0290886	0.18	81	40	120
41	0.18	0.0290886	0.19	83	41	123
42	0.19	0.0290886	0.19	85	42	126
43	0.19	0.0290886	0.2	87	43	129
44	0.19	0.0290886	0.2	89	44	132
45	0.2	0.0290886	0.2	91	45	135
46	0.2	0.0290886	0.21	93	46	138
47	0.21	0.0290886	0.21	95	47	141
48	0.21	0.0290886	0.22	97	48	144
49	0.22	0.0290886	0.22	99	49	147
50	0.22	0.0290886	0.23	101	50	150
51	0.23	0.0290886	0.23	103	51	153
52	0.23	0.0290886	0.24	105	52	156
53	0.23	0.0290886	0.24	107	53	159
54	0.23	0.0290886	0.24	109	54	162
55	0.23	0.0290886	0.23	111	55	165
56	0.23	0.0290886	0.23	113	56	168
57	0.22	0.0290886	0.23	115	57	171
58	0.22	0.0290886	0.23	117	58	174
59	0.22	0.0290886	0.22	119	59	177
60	0.21	0.0290886	0.22	121	60	180
61	0.21	0.0290886	0.22	123	61	183
62	0.21	0.0290886	0.21	125	62	186
63	0.2	0.0290886	0.21	127	63	189
64	0.2	0.0290886	0.2	129	64	192
65	0.19	0.0290886	0.2	131	65	195
66	0.19	0.0290886	0.2	133	66	198
67	0.19	0.0290886	0.19	135	67	201
68	0.18	0.0172647	0.18	137	68	204
69	0.16	0.1726466	0.18	138	69	206
70	0.14	0.0661292	0.15	140	70	209
71	0.13	0.0661292	0.14	142	71	212
72	0.12	0.0661292	0.13	144	72	215
73	0.11	0.0661292	0.12	146	73	218
74	0.1	0.0661292	0.11	148	74	221
75	0.096	0.0661292	0.1	150	75	224
76	0.089	0.0661292	0.095	152	76	227
77	0.082	0.0661292	0.088	154	77	230
78	0.077	0.0661292	0.082	156	78	233
79	0.071	0.0661292	0.076	158	79	236
80	0.067	0.0661292	0.071	160	80	239
81	0.062	0.0661292	0.066	162	81	242
82	0.058	0.0661292	0.062	164	82	245
83	0.055	0.0661292	0.058	166	83	248
84	0.051	0.0661292	0.055	168	84	251
85	0.048	0.0661292	0.051	170	85	254
86	0.045	0.0661292	0.048	172	86	257
87	0.042	0.0661292	0.045	174	87	260
88	0.039	0.0661292	0.042	176	88	263
89	0.037	0.0661292	0.04	178	89	266
90	0.035	0.0661292	0.037	180	90	269

Stationary Solver 1 in Solver 1: Solution time: 82 s. (1 minute, 22 seconds)
Parameter omega = 3.75.
Number of vertex elements: 10
Number of boundary elements: 128
Stationary Solver 1 in Solver 1 started at 30-Sep-2015 17:41:59.
Nonlinear solver
Number of degrees of freedom solved for: 36827.
Nonsymmetric matrix found.
Scales for dependent variables:
mod1.A: 1
mod1.root.mod1.mf.VCoil_1_ode: 0.19
mod1.root.mod1.mf.VCoil_2_ode: 0.19
mod1.root.mod1.mf.VCoil_3_ode: 0.19
mod1.root.mod1.mf.VCoil_4_ode: 0.19
mod1.root.mod1.mf.VCoil_5_ode: 0.19
mod1.root.mod1.mf.VCoil_6_ode: 0.19
mod1.root.mod1.mf.VCoil_7_ode: 0.19
mod1.root.mod1.mf.VCoil_8_ode: 0.19
mod1.root.mod1.mf.VCoil_9_ode: 0.19
mod1.root.mod1.mf.VCoil_10_ode: 0.19
mod1.root.mod1.mf.VCoil_11_ode: 0.19
mod1.root.mod1.mf.VCoil_12_ode: 0.19
mod1.root.mod1.mf.VCoil_13_ode: 0.19
mod1.root.mod1.mf.VCoil_14_ode: 0.19
mod1.root.mod1.mf.VCoil_15_ode: 0.19
mod1.root.mod1.mf.VCoil_16_ode: 0.19

Iter	ErrEst	Damping	Stepsize	#Res	#Jac	#Sol
1	0.051	0.1000000	0.056	3	1	3
2	0.048	0.1000000	0.053	5	2	6
3	0.05	0.0100000	0.05	8	3	10
4	0.052	0.0100000	0.052	10	4	13
5	0.054	0.0100000	0.055	12	5	16
6	0.056	0.0100000	0.057	14	6	19
7	0.059	0.0100000	0.059	16	7	22
8	0.061	0.0100000	0.062	18	8	25
9	0.064	0.0100000	0.065	20	9	28
10	0.067	0.0100000	0.067	22	10	31
11	0.069	0.0100000	0.07	24	11	34
12	0.072	0.0100000	0.073	26	12	37
13	0.076	0.0100000	0.076	28	13	40
14	0.079	0.0100000	0.08	30	14	43
15	0.082	0.0100000	0.083	32	15	46
16	0.086	0.0100000	0.087	34	16	49
17	0.089	0.0100000	0.09	36	17	52
18	0.093	0.0100000	0.094	38	18	55
19	0.097	0.0100000	0.098	40	19	58
20	0.1	0.0100000	0.1	42	20	61
21	0.11	0.0100000	0.11	44	21	64
22	0.11	0.0100000	0.11	46	22	67
23	0.11	0.0100000	0.12	48	23	70
24	0.12	0.0100000	0.12	50	24	73
25	0.12	0.0100000	0.13	52	25	76
26	0.13	0.0100000	0.13	54	26	79
27	0.13	0.0100000	0.14	56	27	82
28	0.14	0.0100000	0.14	58	28	85
29	0.14	0.0100000	0.15	60	29	88
30	0.15	0.0100000	0.15	62	30	91
31	0.14	0.1000000	0.16	63	31	93
32	0.15	0.0100000	0.15	66	32	97
33	0.14	0.1000000	0.15	67	33	99

34	0.15	0.1000000	0.15	69	34	102
35	0.14	0.0328079	0.14	71	35	105
36	0.14	0.0328079	0.14	73	36	108
37	0.14	0.0328079	0.14	75	37	111
38	0.14	0.0328079	0.15	77	38	114
39	0.15	0.0328079	0.15	79	39	117
40	0.15	0.0328079	0.15	81	40	120
41	0.15	0.0328079	0.16	83	41	123
42	0.15	0.0328079	0.16	85	42	126
43	0.16	0.0328079	0.16	87	43	129
44	0.16	0.0328079	0.16	89	44	132
45	0.16	0.0328079	0.16	91	45	135
46	0.16	0.0328079	0.17	93	46	138
47	0.16	0.0328079	0.17	95	47	141
48	0.16	0.0328079	0.17	97	48	144
49	0.17	0.0328079	0.17	99	49	147
50	0.17	0.0328079	0.17	101	50	150
51	0.17	0.0328079	0.18	103	51	153
52	0.17	0.0328079	0.18	105	52	156
53	0.17	0.0328079	0.18	107	53	159
54	0.17	0.0328079	0.17	109	54	162
55	0.16	0.0284580	0.17	111	55	165
56	0.16	0.0284580	0.17	113	56	168
57	0.16	0.0284580	0.17	115	57	171
58	0.16	0.0284580	0.16	117	58	174
59	0.16	0.0284580	0.16	119	59	177
60	0.15	0.0284580	0.16	121	60	180
61	0.15	0.0284580	0.16	123	61	183
62	0.15	0.0284580	0.15	125	62	186
63	0.15	0.0284580	0.15	127	63	189
64	0.14	0.0284580	0.15	129	64	192
65	0.14	0.0284580	0.14	131	65	195
66	0.14	0.0284580	0.14	133	66	198
67	0.13	0.0284580	0.14	135	67	201
68	0.13	0.0284580	0.13	137	68	204
69	0.13	0.0284580	0.13	139	69	207
70	0.12	0.0284580	0.13	141	70	210
71	0.12	0.0284580	0.13	143	71	213
72	0.12	0.0284580	0.12	145	72	216
73	0.11	0.2845801	0.11	146	73	218
74	0.072	0.0697177	0.078	148	74	221
75	0.067	0.0697177	0.072	150	75	224
76	0.062	0.0697177	0.067	152	76	227
77	0.058	0.0697177	0.062	154	77	230
78	0.054	0.0697177	0.058	156	78	233
79	0.051	0.0697177	0.054	158	79	236
80	0.047	0.0697177	0.051	160	80	239
81	0.044	0.0697177	0.048	162	81	242
82	0.041	0.0697177	0.045	164	82	245
83	0.039	0.0697177	0.042	166	83	248
84	0.036	0.0697177	0.039	168	84	251
85	0.034	0.0697177	0.036	170	85	254
86	0.032	0.0697177	0.034	172	86	257
87	0.028	0.1142599	0.032	174	87	260
88	0.026	0.1000000	0.028	176	88	263
89	0.023	0.1000000	0.026	178	89	266
90	0.019	0.1786950	0.023	180	90	269

Stationary Solver 1 in Solver 1: Solution time: 83 s. (1 minute, 23 seconds)
Parameter omega = 4.125.
Number of vertex elements: 10
Number of boundary elements: 129
Stationary Solver 1 in Solver 1 started at 30-Sep-2015 17:43:29.
Nonlinear solver
Number of degrees of freedom solved for: 36869.
Nonsymmetric matrix found.
Scales for dependent variables:
mod1.A: 1
mod1.root.mod1.mf.VCoil_1_ode: 0.19
mod1.root.mod1.mf.VCoil_2_ode: 0.19
mod1.root.mod1.mf.VCoil_3_ode: 0.19
mod1.root.mod1.mf.VCoil_4_ode: 0.19
mod1.root.mod1.mf.VCoil_5_ode: 0.19
mod1.root.mod1.mf.VCoil_6_ode: 0.19
mod1.root.mod1.mf.VCoil_7_ode: 0.19
mod1.root.mod1.mf.VCoil_8_ode: 0.19
mod1.root.mod1.mf.VCoil_9_ode: 0.19
mod1.root.mod1.mf.VCoil_10_ode: 0.19
mod1.root.mod1.mf.VCoil_11_ode: 0.19
mod1.root.mod1.mf.VCoil_12_ode: 0.19
mod1.root.mod1.mf.VCoil_13_ode: 0.19
mod1.root.mod1.mf.VCoil_14_ode: 0.19
mod1.root.mod1.mf.VCoil_15_ode: 0.19
mod1.root.mod1.mf.VCoil_16_ode: 0.19

Iter	ErrEst	Damping	Stepsize	#Res	#Jac	#Sol
1	0.051	0.1000000	0.057	3	1	3
2	0.048	0.1000000	0.054	5	2	6
3	0.05	0.0100000	0.051	8	3	10
4	0.053	0.0100000	0.053	10	4	13
5	0.055	0.0100000	0.055	12	5	16
6	0.057	0.0100000	0.058	14	6	19
7	0.06	0.0100000	0.06	16	7	22
8	0.062	0.0100000	0.063	18	8	25
9	0.065	0.0100000	0.065	20	9	28
10	0.067	0.0100000	0.068	22	10	31
11	0.07	0.0100000	0.071	24	11	34
12	0.073	0.0100000	0.074	26	12	37
13	0.077	0.0100000	0.077	28	13	40
14	0.08	0.0100000	0.081	30	14	43
15	0.083	0.0100000	0.084	32	15	46
16	0.087	0.0100000	0.088	34	16	49
17	0.091	0.0100000	0.092	36	17	52
18	0.095	0.0100000	0.096	38	18	55
19	0.098	0.0100000	0.099	40	19	58
20	0.1	0.0100000	0.1	42	20	61
21	0.11	0.0100000	0.11	44	21	64
22	0.11	0.0100000	0.11	46	22	67
23	0.12	0.0100000	0.12	48	23	70
24	0.12	0.0100000	0.12	50	24	73
25	0.12	0.0100000	0.13	52	25	76
26	0.13	0.0100000	0.13	54	26	79
27	0.13	0.0100000	0.14	56	27	82
28	0.14	0.0100000	0.14	58	28	85
29	0.13	0.1000000	0.15	59	29	87
30	0.14	0.0087288	0.14	62	30	91

31	0.13	0.0872879	0.14	63	31	93
32	0.14	0.0087288	0.14	66	32	97
33	0.13	0.0872879	0.14	67	33	99
34	0.13	0.0872879	0.14	69	34	102
35	0.13	0.0087288	0.13	72	35	106
36	0.14	0.0087288	0.14	74	36	109
37	0.14	0.0087288	0.15	76	37	112
38	0.15	0.0087288	0.15	78	38	115
39	0.16	0.0087288	0.16	80	39	118
40	0.16	0.0087288	0.17	82	40	121
41	0.17	0.0087288	0.17	84	41	124
42	0.18	0.0087288	0.18	86	42	127
43	0.19	0.0087288	0.19	88	43	130
44	0.19	0.0087288	0.2	90	44	133
45	0.2	0.0087288	0.2	92	45	136
46	0.21	0.0087288	0.21	94	46	139
47	0.22	0.0087288	0.22	96	47	142
48	0.23	0.0087288	0.23	98	48	145
49	0.23	0.0872879	0.24	99	49	147
50	0.22	0.0355868	0.23	101	50	150
51	0.22	0.0355868	0.23	103	51	153
52	0.22	0.0355868	0.23	105	52	156
53	0.22	0.0355868	0.23	107	53	159
54	0.22	0.0355868	0.22	109	54	162
55	0.21	0.0355868	0.22	111	55	165
56	0.21	0.0355868	0.22	113	56	168
57	0.21	0.0355868	0.22	115	57	171
58	0.23	0.0081895	0.23	117	58	174
59	0.23	0.0081895	0.23	119	59	177
60	0.21	0.0213455	0.21	120	60	179
61	0.21	0.0213455	0.21	122	61	182
62	0.2	0.0213455	0.21	124	62	185
63	0.2	0.0213455	0.21	126	63	188
64	0.2	0.0213455	0.2	128	64	191
65	0.2	0.0213455	0.2	130	65	194
66	0.19	0.0213455	0.2	132	66	197
67	0.19	0.0213455	0.19	134	67	200
68	0.19	0.0213455	0.19	136	68	203
69	0.18	0.0213455	0.19	138	69	206
70	0.18	0.0213455	0.19	140	70	209
71	0.18	0.0213455	0.18	142	71	212
72	0.18	0.0213455	0.18	144	72	215
73	0.17	0.0213455	0.18	146	73	218
74	0.17	0.0213455	0.17	148	74	221
75	0.17	0.0213455	0.17	150	75	224
76	0.16	0.0213455	0.17	152	76	227
77	0.16	0.0213455	0.17	154	77	230
78	0.16	0.0213455	0.16	156	78	233
79	0.16	0.0213455	0.16	158	79	236
80	0.14	0.2134550	0.15	159	80	238
81	0.1	0.0685852	0.11	161	81	241
82	0.096	0.0685852	0.1	163	82	244
83	0.088	0.0685852	0.095	165	83	247
84	0.082	0.0685852	0.088	167	84	250
85	0.076	0.0685852	0.082	169	85	253
86	0.071	0.0685852	0.076	171	86	256
87	0.066	0.0685852	0.071	173	87	259
88	0.062	0.0685852	0.066	175	88	262
89	0.058	0.0685852	0.062	177	89	265
90	0.054	0.0685852	0.058	179	90	268

Stationary Solver 1 in Solver 1: Solution time: 76 s. (1 minute, 16 seconds)

E.7 One Hundred Iterations

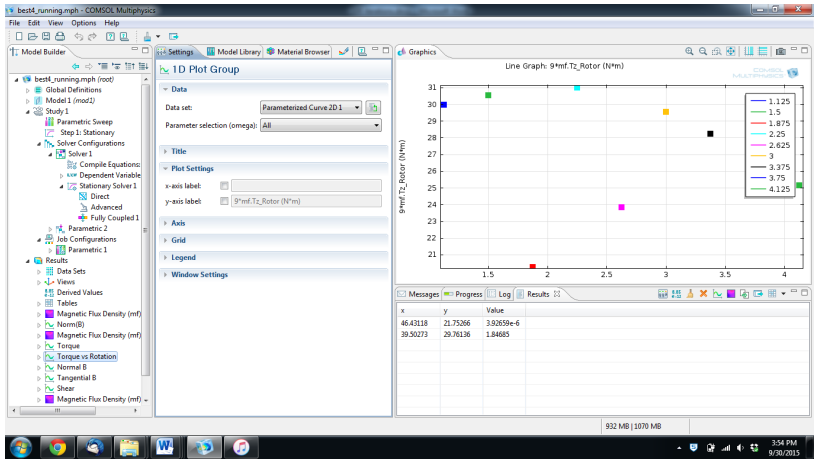

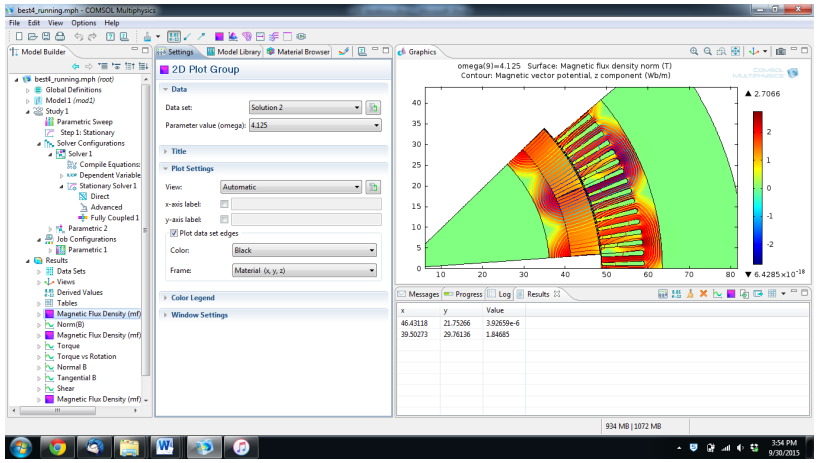


```
==========================================================
Stationary Solver 1 in Solver 1 started at 30-Sep-2015 15:34:14.
Nonlinear solver
Number of degrees of freedom solved for: 37017.
Nonsymmetric matrix found.
Scales for dependent variables:
mod1.A: 1
mod1.root.mod1.mf.VCoil_1_ode: 0.19
mod1.root.mod1.mf.VCoil_2_ode: 0.19
mod1.root.mod1.mf.VCoil_3_ode: 0.19
mod1.root.mod1.mf.VCoil_4_ode: 0.19
mod1.root.mod1.mf.VCoil_5_ode: 0.19
mod1.root.mod1.mf.VCoil_6_ode: 0.19
mod1.root.mod1.mf.VCoil_7_ode: 0.19
mod1.root.mod1.mf.VCoil_8_ode: 0.19
mod1.root.mod1.mf.VCoil_9_ode: 0.19
mod1.root.mod1.mf.VCoil_10_ode: 0.19
mod1.root.mod1.mf.VCoil_11_ode: 0.19
mod1.root.mod1.mf.VCoil_12_ode: 0.19
mod1.root.mod1.mf.VCoil_13_ode: 0.19
mod1.root.mod1.mf.VCoil_14_ode: 0.19
mod1.root.mod1.mf.VCoil_15_ode: 0.19
mod1.root.mod1.mf.VCoil_16_ode: 0.19
```

Iter	ErrEst	Damping	Stepsize	#Res	#Jac	#Sol
1	0.044	0.1000000	0.049	3	1	3
2	0.041	0.1000000	0.046	5	2	6
3	0.039	0.1000000	0.044	7	3	9
4	0.041	0.0100000	0.041	10	4	13
5	0.039	0.1000000	0.043	11	5	15
6	0.04	0.0100000	0.041	14	6	19
7	0.042	0.0100000	0.043	16	7	22
8	0.044	0.0100000	0.044	18	8	25
9	0.046	0.0100000	0.046	20	9	28
10	0.048	0.0100000	0.048	22	10	31
11	0.05	0.0100000	0.05	24	11	34
12	0.052	0.0100000	0.052	26	12	37
13	0.054	0.0100000	0.055	28	13	40
14	0.057	0.0100000	0.057	30	14	43
15	0.059	0.0100000	0.059	32	15	46
16	0.061	0.0100000	0.062	34	16	49
17	0.064	0.0100000	0.065	36	17	52
18	0.067	0.0100000	0.067	38	18	55
19	0.07	0.0100000	0.07	40	19	58
20	0.073	0.0100000	0.073	42	20	61
21	0.076	0.0100000	0.076	44	21	64
22	0.079	0.0100000	0.08	46	22	67
23	0.082	0.0100000	0.083	48	23	70
24	0.086	0.0100000	0.087	50	24	73
25	0.089	0.0100000	0.09	52	25	76
26	0.093	0.0100000	0.094	54	26	79
27	0.097	0.0100000	0.098	56	27	82
28	0.1	0.0100000	0.1	58	28	85
29	0.11	0.0100000	0.11	60	29	88
30	0.11	0.0165913	0.11	62	30	91
31	0.11	0.0165913	0.12	64	31	94
32	0.12	0.0165913	0.12	66	32	97
33	0.12	0.0165913	0.12	68	33	100
34	0.13	0.0165913	0.13	70	34	103
35	0.13	0.0165913	0.13	72	35	106
36	0.14	0.0165913	0.14	74	36	109
37	0.14	0.0165913	0.14	76	37	112
38	0.14	0.0165913	0.15	78	38	115
39	0.15	0.0165913	0.15	80	39	118
40	0.15	0.0165913	0.16	82	40	121
41	0.16	0.0165913	0.16	84	41	124

42	0.17	0.0165913	0.17	86	42	127
43	0.17	0.0165913	0.17	88	43	130
44	0.18	0.0165913	0.18	90	44	133
45	0.18	0.0165913	0.19	92	45	136
46	0.19	0.0165913	0.19	94	46	139
47	0.2	0.0165913	0.2	96	47	142
48	0.2	0.0165913	0.21	98	48	145
49	0.21	0.0165913	0.21	100	49	148
50	0.22	0.0165913	0.22	102	50	151
51	0.22	0.0165913	0.23	104	51	154
52	0.23	0.0165913	0.23	106	52	157
53	0.24	0.0165913	0.24	108	53	160
54	0.24	0.0165913	0.25	110	54	163
55	0.25	0.0165913	0.25	112	55	166
56	0.26	0.0165913	0.26	114	56	169
57	0.26	0.0165913	0.26	116	57	172
58	0.26	0.0165913	0.27	118	58	175
59	0.26	0.0165913	0.27	120	59	178
60	0.27	0.0165913	0.27	122	60	181
61	0.27	0.0165913	0.27	124	61	184
62	0.27	0.0165913	0.27	126	62	187
63	0.27	0.0165913	0.27	128	63	190
64	0.26	0.0165913	0.27	130	64	193
65	0.26	0.0165913	0.27	132	65	196
66	0.26	0.0165913	0.26	134	66	199
67	0.26	0.0165913	0.26	136	67	202
68	0.26	0.0165913	0.26	138	68	205
69	0.25	0.0165913	0.26	140	69	208
70	0.25	0.0165913	0.25	142	70	211
71	0.21	0.1659130	0.24	143	71	213
72	0.18	0.1000000	0.2	145	72	216
73	0.16	0.1000000	0.18	147	73	219
74	0.15	0.1000000	0.16	149	74	222
75	0.13	0.1000000	0.14	151	75	225
76	0.11	0.0966479	0.13	153	76	228
77	0.1	0.0966479	0.11	155	77	231
78	0.092	0.0966479	0.1	157	78	234
79	0.083	0.0966479	0.092	159	79	237
80	0.075	0.0966479	0.083	161	80	240
81	0.067	0.0966479	0.074	163	81	243
82	0.061	0.0966479	0.067	165	82	246
83	0.055	0.0966479	0.061	167	83	249
84	0.049	0.0966479	0.055	169	84	252
85	0.045	0.0966479	0.049	171	85	255
86	0.04	0.0966479	0.045	173	86	258
87	0.037	0.0966479	0.04	175	87	261
88	0.033	0.0966479	0.036	177	88	264
89	0.03	0.0966479	0.033	179	89	267
90	0.027	0.0966479	0.03	181	90	270
91	0.024	0.0966479	0.027	183	91	273
92	0.022	0.0966479	0.024	185	92	276
93	0.02	0.0966479	0.022	187	93	279
94	0.014	0.9664794	0.019	188	94	281
95	0.00021	1.0000000	0.0012	189	95	283

Stationary Solver 1 in Solver 1: Solution time: 81 s. (1 minute, 21 seconds)

==========

Parameter omega = 1.125.

Stationary Solver 1 in Solver 1 started at 30-Sep-2015 15:38:38.

Nonlinear solver

Number of degrees of freedom solved for: 37017.

Nonsymmetric matrix found.

Scales for dependent variables:

mod1.A: 1

mod1.root.mod1.mf.VCoil_1_ode: 0.19

mod1.root.mod1.mf.VCoil_2_ode: 0.19

mod1.root.mod1.mf.VCoil_3_ode: 0.19

mod1.root.mod1.mf.VCoil_4_ode: 0.19

mod1.root.mod1.mf.VCoil_5_ode: 0.19

mod1.root.mod1.mf.VCoil_6_ode: 0.19

mod1.root.mod1.mf.VCoil_7_ode: 0.19

mod1.root.mod1.mf.VCoil_8_ode: 0.19

mod1.root.mod1.mf.VCoil_9_ode: 0.19

mod1.root.mod1.mf.VCoil_10_ode: 0.19

mod1.root.mod1.mf.VCoil_11_ode: 0.19

mod1.root.mod1.mf.VCoil_12_ode: 0.19

mod1.root.mod1.mf.VCoil_13_ode: 0.19

mod1.root.mod1.mf.VCoil_14_ode: 0.19

mod1.root.mod1.mf.VCoil_15_ode: 0.19

mod1.root.mod1.mf.VCoil_16_ode: 0.19

Iter	ErrEst	Damping	Stepsize	#Res	#Jac	#Sol
1	0.044	0.1000000	0.049	3	1	3
2	0.041	0.1000000	0.046	5	2	6
3	0.039	0.1000000	0.044	7	3	9
4	0.041	0.0100000	0.041	10	4	13
5	0.039	0.1000000	0.043	11	5	15
6	0.04	0.0100000	0.041	14	6	19
7	0.042	0.0100000	0.043	16	7	22
8	0.044	0.0100000	0.044	18	8	25
9	0.046	0.0100000	0.046	20	9	28
10	0.048	0.0100000	0.048	22	10	31
11	0.05	0.0100000	0.05	24	11	34
12	0.052	0.0100000	0.052	26	12	37
13	0.054	0.0100000	0.055	28	13	40
14	0.057	0.0100000	0.057	30	14	43
15	0.059	0.0100000	0.059	32	15	46
16	0.061	0.0100000	0.062	34	16	49
17	0.064	0.0100000	0.065	36	17	52
18	0.067	0.0100000	0.067	38	18	55
19	0.07	0.0100000	0.07	40	19	58
20	0.073	0.0100000	0.073	42	20	61
21	0.076	0.0100000	0.076	44	21	64
22	0.079	0.0100000	0.08	46	22	67
23	0.082	0.0100000	0.083	48	23	70
24	0.086	0.0100000	0.087	50	24	73
25	0.089	0.0100000	0.09	52	25	76
26	0.093	0.0100000	0.094	54	26	79
27	0.097	0.0100000	0.098	56	27	82
28	0.1	0.0100000	0.1	58	28	85
29	0.11	0.0100000	0.11	60	29	88
30	0.11	0.0165913	0.11	62	30	91
31	0.11	0.0165913	0.12	64	31	94
32	0.12	0.0165913	0.12	66	32	97
33	0.12	0.0165913	0.12	68	33	100
34	0.13	0.0165913	0.13	70	34	103

35	0.13	0.0165913	0.13	72	35	106
36	0.14	0.0165913	0.14	74	36	109
37	0.14	0.0165913	0.14	76	37	112
38	0.14	0.0165913	0.15	78	38	115
39	0.15	0.0165913	0.15	80	39	118
40	0.15	0.0165913	0.16	82	40	121
41	0.16	0.0165913	0.16	84	41	124
42	0.17	0.0165913	0.17	86	42	127
43	0.17	0.0165913	0.17	88	43	130
44	0.18	0.0165913	0.18	90	44	133
45	0.18	0.0165913	0.19	92	45	136
46	0.19	0.0165913	0.19	94	46	139
47	0.2	0.0165913	0.2	96	47	142
48	0.2	0.0165913	0.21	98	48	145
49	0.21	0.0165913	0.21	100	49	148
50	0.22	0.0165913	0.22	102	50	151
51	0.22	0.0165913	0.23	104	51	154
52	0.23	0.0165913	0.23	106	52	157
53	0.24	0.0165913	0.24	108	53	160
54	0.24	0.0165913	0.25	110	54	163
55	0.25	0.0165913	0.25	112	55	166
56	0.26	0.0165913	0.26	114	56	169
57	0.26	0.0165913	0.26	116	57	172
58	0.26	0.0165913	0.27	118	58	175
59	0.26	0.0165913	0.27	120	59	178
60	0.27	0.0165913	0.27	122	60	181
61	0.27	0.0165913	0.27	124	61	184
62	0.27	0.0165913	0.27	126	62	187
63	0.27	0.0165913	0.27	128	63	190
64	0.26	0.0165913	0.27	130	64	193
65	0.26	0.0165913	0.27	132	65	196
66	0.26	0.0165913	0.26	134	66	199
67	0.26	0.0165913	0.26	136	67	202
68	0.26	0.0165913	0.26	138	68	205
69	0.25	0.0165913	0.26	140	69	208
70	0.25	0.0165913	0.25	142	70	211
71	0.21	0.1659130	0.24	143	71	213
72	0.18	0.1000000	0.2	145	72	216
73	0.16	0.1000000	0.18	147	73	219
74	0.15	0.1000000	0.16	149	74	222
75	0.13	0.1000000	0.14	151	75	225
76	0.11	0.0966479	0.13	153	76	228
77	0.1	0.0966479	0.11	155	77	231
78	0.092	0.0966479	0.1	157	78	234
79	0.083	0.0966479	0.092	159	79	237
80	0.075	0.0966479	0.083	161	80	240
81	0.067	0.0966479	0.074	163	81	243
82	0.061	0.0966479	0.067	165	82	246
83	0.055	0.0966479	0.061	167	83	249
84	0.049	0.0966479	0.055	169	84	252
85	0.045	0.0966479	0.049	171	85	255
86	0.04	0.0966479	0.045	173	86	258
87	0.037	0.0966479	0.04	175	87	261
88	0.033	0.0966479	0.036	177	88	264
89	0.03	0.0966479	0.033	179	89	267
90	0.027	0.0966479	0.03	181	90	270
91	0.024	0.0966479	0.027	183	91	273
92	0.022	0.0966479	0.024	185	92	276
93	0.02	0.0966479	0.022	187	93	279
94	0.014	0.9664794	0.019	188	94	281
95	0.00021	1.0000000	0.0012	189	95	283

Stationary Solver 1 in Solver 1: Solution time: 96 s. (1 minute, 36 seconds)
Parameter omega = 1.5.
Number of vertex elements: 10
Number of boundary elements: 122
Stationary Solver 1 in Solver 1 started at 30-Sep-2015 15:40:22.
Nonlinear solver
Number of degrees of freedom solved for: 36911.
Nonsymmetric matrix found.
Scales for dependent variables:
mod1.A: 1
mod1.root.mod1.mf.VCoil_1_ode: 0.19
mod1.root.mod1.mf.VCoil_2_ode: 0.19
mod1.root.mod1.mf.VCoil_3_ode: 0.19
mod1.root.mod1.mf.VCoil_4_ode: 0.19
mod1.root.mod1.mf.VCoil_5_ode: 0.19
mod1.root.mod1.mf.VCoil_6_ode: 0.19
mod1.root.mod1.mf.VCoil_7_ode: 0.19
mod1.root.mod1.mf.VCoil_8_ode: 0.19
mod1.root.mod1.mf.VCoil_9_ode: 0.19
mod1.root.mod1.mf.VCoil_10_ode: 0.19
mod1.root.mod1.mf.VCoil_11_ode: 0.19
mod1.root.mod1.mf.VCoil_12_ode: 0.19
mod1.root.mod1.mf.VCoil_13_ode: 0.19
mod1.root.mod1.mf.VCoil_14_ode: 0.19
mod1.root.mod1.mf.VCoil_15_ode: 0.19
mod1.root.mod1.mf.VCoil_16_ode: 0.19

Iter	ErrEst	Damping	Stepsize	#Res	#Jac	#Sol
1	0.045	0.1000000	0.05	3	1	3
2	0.042	0.1000000	0.047	5	2	6
3	0.041	0.1000000	0.044	7	3	9
4	0.039	0.1000000	0.042	9	4	12
5	0.04	0.0100000	0.04	12	5	16
6	0.041	0.0100000	0.042	14	6	19
7	0.043	0.0100000	0.044	16	7	22
8	0.045	0.0100000	0.046	18	8	25
9	0.047	0.0100000	0.047	20	9	28
10	0.049	0.0100000	0.049	22	10	31
11	0.051	0.0100000	0.052	24	11	34
12	0.053	0.0100000	0.054	26	12	37
13	0.056	0.0100000	0.056	28	13	40
14	0.058	0.0100000	0.058	30	14	43
15	0.06	0.0100000	0.061	32	15	46
16	0.063	0.0100000	0.064	34	16	49
17	0.066	0.0100000	0.066	36	17	52
18	0.068	0.0100000	0.069	38	18	55
19	0.071	0.0100000	0.072	40	19	58
20	0.074	0.0100000	0.075	42	20	61
21	0.078	0.0100000	0.078	44	21	64
22	0.081	0.0100000	0.082	46	22	67
23	0.084	0.0100000	0.085	48	23	70
24	0.088	0.0100000	0.089	50	24	73
25	0.092	0.0100000	0.093	52	25	76
26	0.096	0.0100000	0.097	54	26	79

27	0.1	0.0100000	0.1	56	27	82
28	0.1	0.0100000	0.11	58	28	85
29	0.11	0.0100000	0.11	60	29	88
30	0.11	0.0100000	0.11	62	30	91
31	0.12	0.0100000	0.12	64	31	94
32	0.12	0.0100000	0.12	66	32	97
33	0.13	0.0100000	0.13	68	33	100
34	0.13	0.0100000	0.13	70	34	103
35	0.14	0.0100000	0.14	72	35	106
36	0.14	0.0100000	0.15	74	36	109
37	0.15	0.0100000	0.15	76	37	112
38	0.16	0.0100000	0.16	78	38	115
39	0.16	0.0100000	0.16	80	39	118
40	0.17	0.0100000	0.17	82	40	121
41	0.18	0.0100000	0.18	84	41	124
42	0.18	0.0100000	0.19	86	42	127
43	0.19	0.1000000	0.19	87	43	129
44	0.17	0.0645361	0.18	89	44	132
45	0.17	0.0645361	0.18	91	45	135
46	0.16	0.0645361	0.18	93	46	138
47	0.16	0.0645361	0.17	95	47	141
48	0.16	0.0645361	0.17	97	48	144
49	0.16	0.0645361	0.17	99	49	147
50	0.15	0.0645361	0.17	101	50	150
51	0.15	0.0645361	0.16	103	51	153
52	0.15	0.0645361	0.16	105	52	156
53	0.14	0.0645361	0.15	107	53	159
54	0.14	0.0645361	0.15	109	54	162
55	0.13	0.0645361	0.14	111	55	165
56	0.13	0.0645361	0.14	113	56	168
57	0.12	0.0523015	0.13	115	57	171
58	0.12	0.0523015	0.12	117	58	174
59	0.11	0.0523015	0.12	119	59	177
60	0.11	0.0523015	0.11	121	60	180
61	0.1	0.0523015	0.11	123	61	183
62	0.098	0.0523015	0.1	125	62	186
63	0.093	0.0523015	0.099	127	63	189
64	0.089	0.0523015	0.094	129	64	192
65	0.085	0.0523015	0.09	131	65	195
66	0.081	0.0523015	0.085	133	66	198
67	0.077	0.0523015	0.081	135	67	201
68	0.074	0.0523015	0.078	137	68	204
69	0.07	0.0523015	0.074	139	69	207
70	0.067	0.0523015	0.07	141	70	210
71	0.063	0.0523015	0.067	143	71	213
72	0.064	0.5230153	0.061	144	72	215
73	0.026	0.1153894	0.029	146	73	218
74	0.015	0.4111196	0.026	148	74	221
75	0.0088	0.4439298	0.015	150	75	224
76	0.0072	0.1556226	0.0085	152	76	227
77	0.0044	1.0000000	0.0083	153	77	229
78	8.3e-005	1.0000000	0.00049	154	78	231

Stationary Solver 1 in Solver 1: Solution time: 70 s. (1 minute, 10 seconds)
Parameter omega = 1.875.
Number of vertex elements: 10
Number of boundary elements: 123
Stationary Solver 1 in Solver 1 started at 30-Sep-2015 15:41:39.

Nonlinear solver
Number of degrees of freedom solved for: 36825.
Nonsymmetric matrix found.
Scales for dependent variables:
mod1.A: 1
mod1.root.mod1.mf.VCoil_1_ode: 0.19
mod1.root.mod1.mf.VCoil_2_ode: 0.19
mod1.root.mod1.mf.VCoil_3_ode: 0.19
mod1.root.mod1.mf.VCoil_4_ode: 0.19
mod1.root.mod1.mf.VCoil_5_ode: 0.19
mod1.root.mod1.mf.VCoil_6_ode: 0.19
mod1.root.mod1.mf.VCoil_7_ode: 0.19
mod1.root.mod1.mf.VCoil_8_ode: 0.19
mod1.root.mod1.mf.VCoil_9_ode: 0.19
mod1.root.mod1.mf.VCoil_10_ode: 0.19
mod1.root.mod1.mf.VCoil_11_ode: 0.19
mod1.root.mod1.mf.VCoil_12_ode: 0.19
mod1.root.mod1.mf.VCoil_13_ode: 0.19
mod1.root.mod1.mf.VCoil_14_ode: 0.19
mod1.root.mod1.mf.VCoil_15_ode: 0.19
mod1.root.mod1.mf.VCoil_16_ode: 0.19

Iter	ErrEst	Damping	Stepsize	#Res	#Jac	#Sol
1	0.046	0.1000000	0.051	3	1	3
2	0.043	0.1000000	0.048	5	2	6
3	0.045	0.0100000	0.045	8	3	10
4	0.047	0.0100000	0.047	10	4	13
5	0.049	0.0100000	0.049	12	5	16
6	0.051	0.0100000	0.051	14	6	19
7	0.053	0.0100000	0.054	16	7	22
8	0.055	0.0100000	0.056	18	8	25
9	0.058	0.0100000	0.058	20	9	28
10	0.06	0.0100000	0.061	22	10	31
11	0.063	0.0100000	0.063	24	11	34
12	0.065	0.0100000	0.066	26	12	37
13	0.068	0.0100000	0.069	28	13	40
14	0.071	0.0100000	0.071	30	14	43
15	0.074	0.0100000	0.074	32	15	46
16	0.077	0.0100000	0.078	34	16	49
17	0.08	0.0100000	0.081	36	17	52
18	0.084	0.0100000	0.084	38	18	55
19	0.087	0.0100000	0.088	40	19	58
20	0.091	0.0100000	0.092	42	20	61
21	0.094	0.0100000	0.095	44	21	64
22	0.099	0.0100000	0.1	46	22	67
23	0.1	0.0100000	0.1	48	23	70
24	0.11	0.0100000	0.11	50	24	73
25	0.11	0.0100000	0.11	52	25	76
26	0.12	0.0100000	0.12	54	26	79
27	0.12	0.0100000	0.12	56	27	82
28	0.13	0.0100000	0.13	58	28	85
29	0.13	0.0100000	0.13	60	29	88
30	0.14	0.0100000	0.14	62	30	91
31	0.14	0.0100000	0.14	64	31	94
32	0.15	0.0100000	0.15	66	32	97
33	0.16	0.0100000	0.16	68	33	100
34	0.16	0.0100000	0.16	70	34	103
35	0.17	0.0100000	0.17	72	35	106

36	0.18	0.0100000	0.18	74	36	109
37	0.18	0.0100000	0.19	76	37	112
38	0.19	0.0100000	0.19	78	38	115
39	0.2	0.0100000	0.2	80	39	118
40	0.21	0.0100000	0.21	82	40	121
41	0.22	0.0100000	0.22	84	41	124
42	0.23	0.0100000	0.23	86	42	127
43	0.23	0.0100000	0.24	88	43	130
44	0.24	0.0100000	0.25	90	44	133
45	0.25	0.0100000	0.26	92	45	136
46	0.26	0.0100000	0.27	94	46	139
47	0.28	0.0100000	0.28	96	47	142
48	0.29	0.0100000	0.29	98	48	145
49	0.3	0.0100000	0.3	100	49	148
50	0.31	0.0100000	0.31	102	50	151
51	0.32	0.0100000	0.33	104	51	154
52	0.34	0.0100000	0.34	106	52	157
53	0.35	0.0100000	0.35	108	53	160
54	0.36	0.0100000	0.37	110	54	163
55	0.38	0.0118020	0.38	112	55	166
56	0.39	0.0118020	0.4	114	56	169
57	0.4	0.0118020	0.41	116	57	172
58	0.42	0.0118020	0.42	118	58	175
59	0.42	0.0173061	0.43	120	59	178
60	0.43	0.0173061	0.43	122	60	181
61	0.43	0.0173061	0.44	124	61	184
62	0.43	0.0173061	0.44	126	62	187
63	0.43	0.0173061	0.44	128	63	190
64	0.43	0.0173061	0.44	130	64	193
65	0.43	0.0180233	0.44	132	65	196
66	0.43	0.0180233	0.43	134	66	199
67	0.42	0.0180233	0.43	136	67	202
68	0.42	0.0180233	0.43	138	68	205
69	0.41	0.0180233	0.42	140	69	208
70	0.41	0.0180233	0.41	142	70	211
71	0.4	0.0180233	0.41	144	71	214
72	0.39	0.0180233	0.4	146	72	217
73	0.39	0.0180233	0.39	148	73	220
74	0.38	0.0180233	0.39	150	74	223
75	0.38	0.0180233	0.38	152	75	226
76	0.37	0.0180233	0.38	154	76	229
77	0.36	0.0180233	0.37	156	77	232
78	0.36	0.0180233	0.36	158	78	235
79	0.35	0.0180233	0.36	160	79	238
80	0.34	0.0180233	0.35	162	80	241
81	0.34	0.0180233	0.34	164	81	244
82	0.33	0.0180233	0.34	166	82	247
83	0.32	0.0180233	0.33	168	83	250
84	0.32	0.0180233	0.32	170	84	253
85	0.31	0.0180233	0.32	172	85	256
86	0.31	0.0180233	0.31	174	86	259
87	0.3	0.0180233	0.3	176	87	262
88	0.29	0.0180233	0.3	178	88	265
89	0.29	0.0180233	0.29	180	89	268
90	0.28	0.0180233	0.29	182	90	271
91	0.28	0.0181262	0.28	184	91	274
92	0.27	0.0229074	0.28	186	92	277
93	0.26	0.0229074	0.27	188	93	280
94	0.26	0.0229074	0.26	190	94	283
95	0.25	0.0229074	0.26	192	95	286
96	0.24	0.0229074	0.25	194	96	289
97	0.24	0.0229074	0.24	196	97	292
98	0.23	0.0229074	0.24	198	98	295
99	0.23	0.0229074	0.23	200	99	298
100	0.22	0.0229074	0.23	202	100	301

Stationary Solver 1 in Solver 1: Solution time: 92 s. (1 minute, 32 seconds)
Parameter omega = 2.25.
Number of vertex elements: 10
Number of boundary elements: 124
Stationary Solver 1 in Solver 1 started at 30-Sep-2015 15:43:18.
Nonlinear solver
Number of degrees of freedom solved for: 36647.
Nonsymmetric matrix found.
Scales for dependent variables:
mod1.A: 1
mod1.root.mod1.mf.VCoil_1_ode: 0.19
mod1.root.mod1.mf.VCoil_2_ode: 0.19
mod1.root.mod1.mf.VCoil_3_ode: 0.19
mod1.root.mod1.mf.VCoil_4_ode: 0.19
mod1.root.mod1.mf.VCoil_5_ode: 0.19
mod1.root.mod1.mf.VCoil_6_ode: 0.19
mod1.root.mod1.mf.VCoil_7_ode: 0.19
mod1.root.mod1.mf.VCoil_8_ode: 0.19
mod1.root.mod1.mf.VCoil_9_ode: 0.19
mod1.root.mod1.mf.VCoil_10_ode: 0.19
mod1.root.mod1.mf.VCoil_11_ode: 0.19
mod1.root.mod1.mf.VCoil_12_ode: 0.19
mod1.root.mod1.mf.VCoil_13_ode: 0.19
mod1.root.mod1.mf.VCoil_14_ode: 0.19
mod1.root.mod1.mf.VCoil_15_ode: 0.19
mod1.root.mod1.mf.VCoil_16_ode: 0.19

Iter	ErrEst	Damping	Stepsize	#Res	#Jac	#Sol
1	0.047	0.1000000	0.052	3	1	3
2	0.044	0.1000000	0.049	5	2	6
3	0.046	0.0100000	0.046	8	3	10
4	0.048	0.0100000	0.048	10	4	13
5	0.05	0.0100000	0.05	12	5	16
6	0.048	0.1000000	0.052	13	6	18
7	0.049	0.0100000	0.05	16	7	22
8	0.051	0.0100000	0.052	18	8	25
9	0.054	0.0100000	0.054	20	9	28
10	0.056	0.0100000	0.056	22	10	31
11	0.058	0.0100000	0.059	24	11	34
12	0.061	0.0100000	0.061	26	12	37
13	0.063	0.0100000	0.064	28	13	40
14	0.066	0.0100000	0.067	30	14	43
15	0.069	0.0100000	0.07	32	15	46
16	0.072	0.0100000	0.073	34	16	49
17	0.075	0.0100000	0.076	36	17	52
18	0.078	0.0100000	0.079	38	18	55
19	0.082	0.0100000	0.082	40	19	58
20	0.085	0.0100000	0.086	42	20	61
21	0.089	0.0100000	0.09	44	21	64
22	0.093	0.0100000	0.093	46	22	67

23	0.097	0.0100000	0.097	48	23	70
24	0.1	0.0100000	0.1	50	24	73
25	0.1	0.0100000	0.11	52	25	76
26	0.11	0.0100000	0.11	54	26	79
27	0.11	0.0100000	0.12	56	27	82
28	0.12	0.0100000	0.12	58	28	85
29	0.12	0.0100000	0.13	60	29	88
30	0.13	0.0100000	0.13	62	30	91
31	0.13	0.0100000	0.14	64	31	94
32	0.14	0.0100000	0.14	66	32	97
33	0.15	0.0100000	0.15	68	33	100
34	0.15	0.0100000	0.15	70	34	103
35	0.16	0.0100000	0.16	72	35	106
36	0.16	0.0100000	0.17	74	36	109
37	0.17	0.0100000	0.17	76	37	112
38	0.18	0.0100000	0.18	78	38	115
39	0.19	0.0100000	0.19	80	39	118
40	0.18	0.1000000	0.19	81	40	120
41	0.17	0.0625646	0.18	83	41	123
42	0.17	0.0625646	0.18	85	42	126
43	0.17	0.0625646	0.18	87	43	129
44	0.16	0.0625646	0.18	89	44	132
45	0.16	0.0625646	0.17	91	45	135
46	0.16	0.0625646	0.17	93	46	138
47	0.16	0.0625646	0.17	95	47	141
48	0.17	0.0062565	0.17	98	48	145
49	0.17	0.0625646	0.17	99	49	147
50	0.17	0.0192446	0.17	101	50	150
51	0.17	0.0192446	0.18	103	51	153
52	0.18	0.0192446	0.18	105	52	156
53	0.18	0.0192446	0.18	107	53	159
54	0.18	0.0192446	0.19	109	54	162
55	0.19	0.0192446	0.19	111	55	165
56	0.19	0.0192446	0.19	113	56	168
57	0.19	0.0192446	0.19	115	57	171
58	0.19	0.0192446	0.19	117	58	174
59	0.19	0.0192446	0.19	119	59	177
60	0.19	0.0192446	0.19	121	60	180
61	0.18	0.1924456	0.18	122	61	182
62	0.14	0.0540705	0.15	124	62	185
63	0.13	0.0461513	0.14	126	63	188
64	0.13	0.0461513	0.13	128	64	191
65	0.12	0.0461513	0.13	130	65	194
66	0.12	0.0461513	0.12	132	66	197
67	0.11	0.0461513	0.12	134	67	200
68	0.11	0.0461513	0.11	136	68	203
69	0.1	0.0461513	0.11	138	69	206
70	0.099	0.0461513	0.1	140	70	209
71	0.095	0.0461513	0.1	142	71	212
72	0.091	0.0461513	0.096	144	72	215
73	0.088	0.0461513	0.092	146	73	218
74	0.084	0.0461513	0.088	148	74	221
75	0.08	0.0461513	0.084	150	75	224
76	0.076	0.0461513	0.08	152	76	227
77	0.073	0.0461513	0.077	154	77	230
78	0.07	0.0461513	0.073	156	78	233
79	0.067	0.0461513	0.07	158	79	236
80	0.064	0.0461513	0.067	160	80	239
81	0.061	0.0461513	0.064	162	81	242
82	0.058	0.0461513	0.061	164	82	245
83	0.055	0.0461513	0.058	166	83	248
84	0.04	0.4615128	0.054	167	84	250
85	0.02	0.3214642	0.029	169	85	253
86	0.014	0.2734717	0.02	171	86	256
87	0.0081	1.0000000	0.014	172	87	258
88	0.00039	1.0000000	0.0017	173	88	260

Stationary Solver 1 in Solver 1: Solution time: 85 s. (1 minute, 25 seconds)
Parameter omega = 2.625.
Number of vertex elements: 10
Number of boundary elements: 125
Stationary Solver 1 in Solver 1 started at 30-Sep-2015 15:44:50.
Nonlinear solver
Number of degrees of freedom solved for: 36885.
Nonsymmetric matrix found.
Scales for dependent variables:
mod1.A: 1
mod1.root.mod1.mf.VCoil_1_ode: 0.19
mod1.root.mod1.mf.VCoil_2_ode: 0.19
mod1.root.mod1.mf.VCoil_3_ode: 0.19
mod1.root.mod1.mf.VCoil_4_ode: 0.19
mod1.root.mod1.mf.VCoil_5_ode: 0.19
mod1.root.mod1.mf.VCoil_6_ode: 0.19
mod1.root.mod1.mf.VCoil_7_ode: 0.19
mod1.root.mod1.mf.VCoil_8_ode: 0.19
mod1.root.mod1.mf.VCoil_9_ode: 0.19
mod1.root.mod1.mf.VCoil_10_ode: 0.19
mod1.root.mod1.mf.VCoil_11_ode: 0.19
mod1.root.mod1.mf.VCoil_12_ode: 0.19
mod1.root.mod1.mf.VCoil_13_ode: 0.19
mod1.root.mod1.mf.VCoil_14_ode: 0.19
mod1.root.mod1.mf.VCoil_15_ode: 0.19
mod1.root.mod1.mf.VCoil_16_ode: 0.19

Iter	ErrEst	Damping	Stepsize	#Res	#Jac	#Sol
1	0.048	0.1000000	0.053	3	1	3
2	0.045	0.1000000	0.05	5	2	6
3	0.047	0.0100000	0.047	8	3	10
4	0.049	0.0100000	0.049	10	4	13
5	0.051	0.0100000	0.051	12	5	16
6	0.053	0.0100000	0.054	14	6	19
7	0.055	0.0100000	0.056	16	7	22
8	0.058	0.0100000	0.058	18	8	25
9	0.06	0.0100000	0.061	20	9	28
10	0.063	0.0100000	0.063	22	10	31
11	0.065	0.0100000	0.066	24	11	34
12	0.068	0.0100000	0.069	26	12	37
13	0.071	0.0100000	0.072	28	13	40
14	0.074	0.0100000	0.075	30	14	43
15	0.077	0.0100000	0.078	32	15	46
16	0.08	0.0100000	0.081	34	16	49
17	0.084	0.0100000	0.085	36	17	52
18	0.087	0.0100000	0.088	38	18	55
19	0.091	0.0100000	0.092	40	19	58
20	0.095	0.0100000	0.096	42	20	61
21	0.099	0.0100000	0.1	44	21	64

22	0.1	0.0100000	0.1	46	22	67
23	0.11	0.0100000	0.11	48	23	70
24	0.11	0.0100000	0.11	50	24	73
25	0.12	0.0100000	0.12	52	25	76
26	0.12	0.0100000	0.12	54	26	79
27	0.13	0.0100000	0.13	56	27	82
28	0.13	0.0100000	0.13	58	28	85
29	0.14	0.0100000	0.14	60	29	88
30	0.14	0.0100000	0.15	62	30	91
31	0.15	0.0100000	0.15	64	31	94
32	0.16	0.0100000	0.16	66	32	97
33	0.16	0.0100000	0.16	68	33	100
34	0.17	0.0100000	0.17	70	34	103
35	0.18	0.0100000	0.18	72	35	106
36	0.18	0.0100000	0.19	74	36	109
37	0.19	0.0100000	0.19	76	37	112
38	0.2	0.0100000	0.2	78	38	115
39	0.21	0.0100000	0.21	80	39	118
40	0.22	0.0100000	0.22	82	40	121
41	0.22	0.0100000	0.23	84	41	124
42	0.23	0.0114514	0.23	86	42	127
43	0.24	0.0130367	0.24	88	43	130
44	0.25	0.0130367	0.25	90	44	133
45	0.26	0.0130367	0.26	92	45	136
46	0.26	0.0213471	0.27	94	46	139
47	0.27	0.0213471	0.28	96	47	142
48	0.28	0.0213471	0.28	98	48	145
49	0.29	0.0213471	0.29	100	49	148
50	0.29	0.0213471	0.3	102	50	151
51	0.3	0.0213471	0.31	104	51	154
52	0.31	0.0213471	0.32	106	52	157
53	0.32	0.0213471	0.33	108	53	160
54	0.33	0.0213471	0.34	110	54	163
55	0.34	0.0213471	0.34	112	55	166
56	0.34	0.0213471	0.35	114	56	169
57	0.35	0.0213471	0.36	116	57	172
58	0.35	0.0213471	0.36	118	58	175
59	0.35	0.0213471	0.36	120	59	178
60	0.36	0.0213471	0.36	122	60	181
61	0.35	0.0213471	0.36	124	61	184
62	0.35	0.0213471	0.36	126	62	187
63	0.35	0.0213471	0.36	128	63	190
64	0.35	0.0213471	0.36	130	64	193
65	0.34	0.0213471	0.35	132	65	196
66	0.34	0.0213471	0.35	134	66	199
67	0.33	0.0213471	0.34	136	67	202
68	0.33	0.0213471	0.34	138	68	205
69	0.32	0.0213471	0.33	140	69	208
70	0.32	0.0213471	0.32	142	70	211
71	0.31	0.0213471	0.32	144	71	214
72	0.3	0.0213471	0.31	146	72	217
73	0.3	0.0213471	0.31	148	73	220
74	0.29	0.0213471	0.3	150	74	223
75	0.29	0.0213471	0.29	152	75	226
76	0.28	0.0213471	0.29	154	76	229
77	0.27	0.0213471	0.28	156	77	232
78	0.27	0.0213471	0.28	158	78	235
79	0.26	0.0213471	0.27	160	79	238
80	0.26	0.0213471	0.26	162	80	241
81	0.25	0.0213471	0.26	164	81	244
82	0.25	0.0213471	0.25	166	82	247
83	0.24	0.0213471	0.25	168	83	250
84	0.24	0.0213471	0.24	170	84	253
85	0.23	0.0213471	0.24	172	85	256
86	0.23	0.0213471	0.23	174	86	259
87	0.22	0.0258851	0.23	176	87	262
88	0.22	0.0258851	0.22	178	88	265
89	0.21	0.0258851	0.22	180	89	268
90	0.21	0.0258851	0.21	182	90	271
91	0.2	0.0258851	0.21	184	91	274
92	0.2	0.0258851	0.2	186	92	277
93	0.2	0.0258851	0.2	188	93	280
94	0.19	0.1152239	0.2	189	94	282
95	0.16	0.0332688	0.17	191	95	285
96	0.15	0.0332688	0.16	193	96	288
97	0.15	0.0332688	0.15	195	97	291
98	0.14	0.0332688	0.15	197	98	294
99	0.14	0.0332688	0.14	199	99	297
100	0.13	0.0332688	0.14	201	100	300

Stationary Solver 1 in Solver 1: Solution time: 92 s. (1 minute, 32 seconds)
Parameter omega = 3.0.
Number of vertex elements: 10
Number of boundary elements: 126
Stationary Solver 1 in Solver 1 started at 30-Sep-2015 15:46:30.
Nonlinear solver
Number of degrees of freedom solved for: 36759.
Nonsymmetric matrix found.
Scales for dependent variables:
mod1.A: 1
mod1.root.mod1.mf.VCoil_1_ode: 0.19
mod1.root.mod1.mf.VCoil_2_ode: 0.19
mod1.root.mod1.mf.VCoil_3_ode: 0.19
mod1.root.mod1.mf.VCoil_4_ode: 0.19
mod1.root.mod1.mf.VCoil_5_ode: 0.19
mod1.root.mod1.mf.VCoil_6_ode: 0.19
mod1.root.mod1.mf.VCoil_7_ode: 0.19
mod1.root.mod1.mf.VCoil_8_ode: 0.19
mod1.root.mod1.mf.VCoil_9_ode: 0.19
mod1.root.mod1.mf.VCoil_10_ode: 0.19
mod1.root.mod1.mf.VCoil_11_ode: 0.19
mod1.root.mod1.mf.VCoil_12_ode: 0.19
mod1.root.mod1.mf.VCoil_13_ode: 0.19
mod1.root.mod1.mf.VCoil_14_ode: 0.19
mod1.root.mod1.mf.VCoil_15_ode: 0.19
mod1.root.mod1.mf.VCoil_16_ode: 0.19

Iter	ErrEst	Damping	Stepsize	#Res	#Jac	#Sol
1	0.049	0.1000000	0.054	3	1	3
2	0.046	0.1000000	0.051	5	2	6
3	0.048	0.0100000	0.048	8	3	10
4	0.05	0.0100000	0.05	10	4	13
5	0.052	0.0100000	0.052	12	5	16
6	0.054	0.0100000	0.055	14	6	19
7	0.056	0.0100000	0.057	16	7	22
8	0.059	0.0100000	0.059	18	8	25

9	0.061	0.0100000	0.062	20	9	28
10	0.064	0.0100000	0.065	22	10	31
11	0.067	0.0100000	0.067	24	11	34
12	0.069	0.0100000	0.07	26	12	37
13	0.072	0.0100000	0.073	28	13	40
14	0.075	0.0100000	0.076	30	14	43
15	0.079	0.0100000	0.079	32	15	46
16	0.082	0.0100000	0.083	34	16	49
17	0.086	0.0100000	0.086	36	17	52
18	0.089	0.0100000	0.09	38	18	55
19	0.093	0.0100000	0.094	40	19	58
20	0.097	0.0100000	0.098	42	20	61
21	0.1	0.0100000	0.1	44	21	64
22	0.11	0.0100000	0.11	46	22	67
23	0.11	0.0100000	0.11	48	23	70
24	0.11	0.0100000	0.12	50	24	73
25	0.12	0.0100000	0.12	52	25	76
26	0.12	0.0100000	0.13	54	26	79
27	0.13	0.0100000	0.13	56	27	82
28	0.14	0.0100000	0.14	58	28	85
29	0.14	0.0100000	0.14	60	29	88
30	0.15	0.0100000	0.15	62	30	91
31	0.15	0.0100000	0.15	64	31	94
32	0.16	0.0100000	0.16	66	32	97
33	0.17	0.0100000	0.17	68	33	100
34	0.17	0.0100000	0.17	70	34	103
35	0.18	0.0100000	0.18	72	35	106
36	0.19	0.0100000	0.19	74	36	109
37	0.18	0.1000000	0.19	75	37	111
38	0.17	0.0403578	0.18	77	38	114
39	0.18	0.0403578	0.18	79	39	117
40	0.18	0.0403578	0.19	81	40	120
41	0.18	0.0403578	0.19	83	41	123
42	0.18	0.0403578	0.19	85	42	126
43	0.18	0.0403578	0.19	87	43	129
44	0.19	0.0403578	0.19	89	44	132
45	0.19	0.0403578	0.2	91	45	135
46	0.19	0.0403578	0.2	93	46	138
47	0.19	0.0403578	0.2	95	47	141
48	0.2	0.0403578	0.2	97	48	144
49	0.2	0.0403578	0.21	99	49	147
50	0.2	0.0403578	0.21	101	50	150
51	0.2	0.0403578	0.21	103	51	153
52	0.2	0.0403578	0.21	105	52	156
53	0.2	0.0403578	0.21	107	53	159
54	0.19	0.0403578	0.2	109	54	162
55	0.19	0.0403578	0.2	111	55	165
56	0.19	0.0403578	0.19	113	56	168
57	0.18	0.0403578	0.19	115	57	171
58	0.18	0.0403578	0.18	117	58	174
59	0.17	0.0403578	0.18	119	59	177
60	0.17	0.0403578	0.17	121	60	180
61	0.16	0.0403578	0.17	123	61	183
62	0.16	0.0403578	0.16	125	62	186
63	0.16	0.0256437	0.16	127	63	189
64	0.13	0.1430420	0.15	128	64	191
65	0.12	0.1000000	0.13	130	65	194
66	0.1	0.1000000	0.12	132	66	197
67	0.093	0.1000000	0.1	134	67	200
68	0.084	0.1000000	0.093	136	68	203
69	0.075	0.1000000	0.084	138	69	206
70	0.067	0.1000000	0.075	140	70	209
71	0.06	0.1000000	0.067	142	71	212
72	0.054	0.1000000	0.06	144	72	215
73	0.049	0.1000000	0.054	146	73	218
74	0.044	0.1000000	0.049	148	74	221
75	0.04	0.1000000	0.044	150	75	224
76	0.036	0.1000000	0.04	152	76	227
77	0.032	0.1000000	0.036	154	77	230
78	0.029	0.1000000	0.032	156	78	233
79	0.026	0.1000000	0.029	158	79	236
80	0.024	0.1000000	0.026	160	80	239
81	0.021	0.1000000	0.024	162	81	242
82	0.019	0.1000000	0.022	164	82	245
83	0.018	0.1000000	0.02	166	83	248
84	0.014	0.2185642	0.018	168	84	251
85	0.013	1.0000000	0.014	169	85	253
86	0.00027	1.0000000	0.0013	170	86	255

Stationary Solver 1 in Solver 1: Solution time: 77 s. (1 minute, 17 seconds)
Parameter omega = 3.375.
Number of vertex elements: 10
Number of boundary elements: 127
Stationary Solver 1 in Solver 1 started at 30-Sep-2015 15:47:55.
Nonlinear solver
Number of degrees of freedom solved for: 36841.
Nonsymmetric matrix found.
Scales for dependent variables:
mod1.A: 1
mod1.root.mod1.mf.VCoil_1_ode: 0.19
mod1.root.mod1.mf.VCoil_2_ode: 0.19
mod1.root.mod1.mf.VCoil_3_ode: 0.19
mod1.root.mod1.mf.VCoil_4_ode: 0.19
mod1.root.mod1.mf.VCoil_5_ode: 0.19
mod1.root.mod1.mf.VCoil_6_ode: 0.19
mod1.root.mod1.mf.VCoil_7_ode: 0.19
mod1.root.mod1.mf.VCoil_8_ode: 0.19
mod1.root.mod1.mf.VCoil_9_ode: 0.19
mod1.root.mod1.mf.VCoil_10_ode: 0.19
mod1.root.mod1.mf.VCoil_11_ode: 0.19
mod1.root.mod1.mf.VCoil_12_ode: 0.19
mod1.root.mod1.mf.VCoil_13_ode: 0.19
mod1.root.mod1.mf.VCoil_14_ode: 0.19
mod1.root.mod1.mf.VCoil_15_ode: 0.19
mod1.root.mod1.mf.VCoil_16_ode: 0.19

Iter	ErrEst	Damping	Stepsize	#Res	#Jac	#Sol
1	0.05	0.1000000	0.055	3	1	3
2	0.047	0.1000000	0.052	5	2	6
3	0.049	0.0100000	0.049	8	3	10
4	0.051	0.0100000	0.051	10	4	13
5	0.053	0.0100000	0.054	12	5	16
6	0.055	0.0100000	0.056	14	6	19
7	0.058	0.0100000	0.058	16	7	22
8	0.06	0.0100000	0.061	18	8	25
9	0.063	0.0100000	0.063	20	9	28

10	0.065	0.0100000	0.066	22	10	31
11	0.068	0.0100000	0.069	24	11	34
12	0.071	0.0100000	0.072	26	12	37
13	0.074	0.0100000	0.075	28	13	40
14	0.077	0.0100000	0.078	30	14	43
15	0.081	0.0100000	0.081	32	15	46
16	0.084	0.0100000	0.085	34	16	49
17	0.088	0.0100000	0.089	36	17	52
18	0.091	0.0100000	0.092	38	18	55
19	0.095	0.0100000	0.096	40	19	58
20	0.099	0.0100000	0.1	42	20	61
21	0.1	0.0100000	0.1	44	21	64
22	0.11	0.0100000	0.11	46	22	67
23	0.11	0.0100000	0.11	48	23	70
24	0.12	0.0100000	0.12	50	24	73
25	0.12	0.0100000	0.12	52	25	76
26	0.13	0.0100000	0.13	54	26	79
27	0.13	0.0100000	0.13	56	27	82
28	0.14	0.0100000	0.14	58	28	85
29	0.14	0.0100000	0.14	60	29	88
30	0.15	0.0100000	0.15	62	30	91
31	0.15	0.0100000	0.16	64	31	94
32	0.16	0.0100000	0.16	66	32	97
33	0.17	0.0100000	0.17	68	33	100
34	0.17	0.1000000	0.17	69	34	102
35	0.16	0.0290886	0.16	71	35	105
36	0.16	0.0290886	0.17	73	36	108
37	0.17	0.0290886	0.17	75	37	111
38	0.17	0.0290886	0.18	77	38	114
39	0.17	0.0290886	0.18	79	39	117
40	0.18	0.0290886	0.18	81	40	120
41	0.18	0.0290886	0.19	83	41	123
42	0.19	0.0290886	0.19	85	42	126
43	0.19	0.0290886	0.2	87	43	129
44	0.19	0.0290886	0.2	89	44	132
45	0.2	0.0290886	0.2	91	45	135
46	0.2	0.0290886	0.21	93	46	138
47	0.21	0.0290886	0.21	95	47	141
48	0.21	0.0290886	0.22	97	48	144
49	0.22	0.0290886	0.22	99	49	147
50	0.22	0.0290886	0.23	101	50	150
51	0.23	0.0290886	0.23	103	51	153
52	0.23	0.0290886	0.24	105	52	156
53	0.23	0.0290886	0.24	107	53	159
54	0.23	0.0290886	0.24	109	54	162
55	0.23	0.0290886	0.23	111	55	165
56	0.23	0.0290886	0.23	113	56	168
57	0.22	0.0290886	0.23	115	57	171
58	0.22	0.0290886	0.23	117	58	174
59	0.22	0.0290886	0.22	119	59	177
60	0.21	0.0290886	0.22	121	60	180
61	0.21	0.0290886	0.22	123	61	183
62	0.21	0.0290886	0.21	125	62	186
63	0.2	0.0290886	0.21	127	63	189
64	0.2	0.0290886	0.2	129	64	192
65	0.19	0.0290886	0.2	131	65	195
66	0.19	0.0290886	0.2	133	66	198
67	0.19	0.0290886	0.19	135	67	201
68	0.18	0.0172647	0.18	137	68	204
69	0.16	0.1726466	0.18	138	69	206
70	0.14	0.0661292	0.15	140	70	209
71	0.13	0.0661292	0.14	142	71	212
72	0.12	0.0661292	0.13	144	72	215
73	0.11	0.0661292	0.12	146	73	218
74	0.1	0.0661292	0.11	148	74	221
75	0.096	0.0661292	0.1	150	75	224
76	0.089	0.0661292	0.095	152	76	227
77	0.082	0.0661292	0.088	154	77	230
78	0.077	0.0661292	0.082	156	78	233
79	0.071	0.0661292	0.076	158	79	236
80	0.067	0.0661292	0.071	160	80	239
81	0.062	0.0661292	0.066	162	81	242
82	0.058	0.0661292	0.062	164	82	245
83	0.055	0.0661292	0.058	166	83	248
84	0.051	0.0661292	0.055	168	84	251
85	0.048	0.0661292	0.051	170	85	254
86	0.045	0.0661292	0.048	172	86	257
87	0.042	0.0661292	0.045	174	87	260
88	0.039	0.0661292	0.042	176	88	263
89	0.037	0.0661292	0.04	178	89	266
90	0.035	0.0661292	0.037	180	90	269
91	0.033	0.0661292	0.035	182	91	272
92	0.031	0.0661292	0.033	184	92	275
93	0.028	0.0983500	0.031	186	93	278
94	0.025	0.0983500	0.028	188	94	281
95	0.023	0.0983500	0.026	190	95	284
96	0.017	0.2773202	0.023	192	96	287
97	0.012	1.0000000	0.017	193	97	289
98	0.00016	1.0000000	0.00089	194	98	291

Stationary Solver 1 in Solver 1: Solution time: 90 s. (1 minute, 30 seconds)
Parameter omega = 3.75.
Number of vertex elements: 10
Number of boundary elements: 128
Stationary Solver 1 in Solver 1 started at 30-Sep-2015 15:49:31.
Nonlinear solver
Number of degrees of freedom solved for: 36827.
Nonsymmetric matrix found.
Scales for dependent variables:
mod1.A: 1
mod1.root.mod1.mf.VCoil_1_ode: 0.19
mod1.root.mod1.mf.VCoil_2_ode: 0.19
mod1.root.mod1.mf.VCoil_3_ode: 0.19
mod1.root.mod1.mf.VCoil_4_ode: 0.19
mod1.root.mod1.mf.VCoil_5_ode: 0.19
mod1.root.mod1.mf.VCoil_6_ode: 0.19
mod1.root.mod1.mf.VCoil_7_ode: 0.19
mod1.root.mod1.mf.VCoil_8_ode: 0.19
mod1.root.mod1.mf.VCoil_9_ode: 0.19
mod1.root.mod1.mf.VCoil_10_ode: 0.19
mod1.root.mod1.mf.VCoil_11_ode: 0.19
mod1.root.mod1.mf.VCoil_12_ode: 0.19
mod1.root.mod1.mf.VCoil_13_ode: 0.19
mod1.root.mod1.mf.VCoil_14_ode: 0.19
mod1.root.mod1.mf.VCoil_15_ode: 0.19

```
mod1.root.mod1.mf.VCoil_16_ode: 0.19
Iter       ErrEst     Damping    Stepsize #Res #Jac #Sol
   1        0.051   0.1000000       0.056    3    1    3
   2        0.048   0.1000000       0.053    5    2    6
   3         0.05   0.0100000        0.05    8    3   10
   4        0.052   0.0100000       0.052   10    4   13
   5        0.054   0.0100000       0.055   12    5   16
   6        0.056   0.0100000       0.057   14    6   19
   7        0.059   0.0100000       0.059   16    7   22
   8        0.061   0.0100000       0.062   18    8   25
   9        0.064   0.0100000       0.065   20    9   28
  10        0.067   0.0100000       0.067   22   10   31
  11        0.069   0.0100000        0.07   24   11   34
  12        0.072   0.0100000       0.073   26   12   37
  13        0.076   0.0100000       0.076   28   13   40
  14        0.079   0.0100000        0.08   30   14   43
  15        0.082   0.0100000       0.083   32   15   46
  16        0.086   0.0100000       0.087   34   16   49
  17        0.089   0.0100000        0.09   36   17   52
  18        0.093   0.0100000       0.094   38   18   55
  19        0.097   0.0100000       0.098   40   19   58
  20          0.1   0.0100000         0.1   42   20   61
  21         0.11   0.0100000        0.11   44   21   64
  22         0.11   0.0100000        0.11   46   22   67
  23         0.11   0.0100000        0.12   48   23   70
  24         0.12   0.0100000        0.12   50   24   73
  25         0.12   0.0100000        0.13   52   25   76
  26         0.13   0.0100000        0.13   54   26   79
  27         0.13   0.0100000        0.14   56   27   82
  28         0.14   0.0100000        0.14   58   28   85
  29         0.14   0.0100000        0.15   60   29   88
  30         0.15   0.0100000        0.15   62   30   91
  31         0.14   0.1000000        0.16   63   31   93
  32         0.15   0.0100000        0.15   66   32   97
  33         0.14   0.1000000        0.15   67   33   99
  34         0.15   0.1000000        0.15   69   34  102
  35         0.14   0.0328079        0.14   71   35  105
  36         0.14   0.0328079        0.14   73   36  108
  37         0.14   0.0328079        0.14   75   37  111
  38         0.14   0.0328079        0.15   77   38  114
  39         0.15   0.0328079        0.15   79   39  117
  40         0.15   0.0328079        0.15   81   40  120
  41         0.15   0.0328079        0.16   83   41  123
  42         0.15   0.0328079        0.16   85   42  126
  43         0.16   0.0328079        0.16   87   43  129
  44         0.16   0.0328079        0.16   89   44  132
  45         0.16   0.0328079        0.16   91   45  135
  46         0.16   0.0328079        0.17   93   46  138
  47         0.16   0.0328079        0.17   95   47  141
  48         0.16   0.0328079        0.17   97   48  144
  49         0.17   0.0328079        0.17   99   49  147
  50         0.17   0.0328079        0.17  101   50  150
  51         0.17   0.0328079        0.18  103   51  153
  52         0.17   0.0328079        0.18  105   52  156
  53         0.17   0.0328079        0.18  107   53  159
  54         0.17   0.0328079        0.17  109   54  162
  55         0.16   0.0284580        0.17  111   55  165
  56         0.16   0.0284580        0.17  113   56  168
  57         0.16   0.0284580        0.17  115   57  171
  58         0.16   0.0284580        0.16  117   58  174
  59         0.16   0.0284580        0.16  119   59  177
  60         0.15   0.0284580        0.16  121   60  180
  61         0.15   0.0284580        0.16  123   61  183
  62         0.15   0.0284580        0.15  125   62  186
  63         0.15   0.0284580        0.15  127   63  189
  64         0.14   0.0284580        0.15  129   64  192
  65         0.14   0.0284580        0.14  131   65  195
  66         0.14   0.0284580        0.14  133   66  198
  67         0.13   0.0284580        0.14  135   67  201
  68         0.13   0.0284580        0.13  137   68  204
  69         0.13   0.0284580        0.13  139   69  207
  70         0.12   0.0284580        0.13  141   70  210
  71         0.12   0.0284580        0.13  143   71  213
  72         0.12   0.0284580        0.12  145   72  216
  73         0.11   0.2845800        0.11  146   73  218
  74        0.072   0.0697177       0.078  148   74  221
  75        0.067   0.0697177       0.072  150   75  224
  76        0.062   0.0697177       0.067  152   76  227
  77        0.058   0.0697177       0.062  154   77  230
  78        0.054   0.0697177       0.058  156   78  233
  79        0.051   0.0697177       0.054  158   79  236
  80        0.047   0.0697177       0.051  160   80  239
  81        0.044   0.0697177       0.048  162   81  242
  82        0.041   0.0697177       0.045  164   82  245
  83        0.039   0.0697177       0.042  166   83  248
  84        0.036   0.0697177       0.039  168   84  251
  85        0.034   0.0697177       0.036  170   85  254
  86        0.032   0.0697177       0.034  172   86  257
  87        0.028   0.1142597       0.032  174   87  260
  88        0.026   0.1000000       0.028  176   88  263
  89        0.023   0.1000000       0.026  178   89  266
  90        0.019   0.1786949       0.023  180   90  269
  91        0.015   0.2280769       0.019  182   91  272
  92       0.0083   0.4415360       0.015  184   92  275
  93       0.0028   1.0000000      0.0082  185   93  277
  94    4.1e-005   1.0000000      0.0011  186   94  279
Stationary Solver 1 in Solver 1: Solution time: 97 s. (1 minute, 37 seconds)
Parameter omega = 4.125.
Number of vertex elements: 10
Number of boundary elements: 129
Stationary Solver 1 in Solver 1 started at 30-Sep-2015 15:51:19.
Nonlinear solver
Number of degrees of freedom solved for: 36869.
Nonsymmetric matrix found.
Scales for dependent variables:
mod1.A: 1
mod1.root.mod1.mf.VCoil_1_ode: 0.19
mod1.root.mod1.mf.VCoil_2_ode: 0.19
mod1.root.mod1.mf.VCoil_3_ode: 0.19
mod1.root.mod1.mf.VCoil_4_ode: 0.19
mod1.root.mod1.mf.VCoil_5_ode: 0.19
mod1.root.mod1.mf.VCoil_6_ode: 0.19
mod1.root.mod1.mf.VCoil_7_ode: 0.19
mod1.root.mod1.mf.VCoil_8_ode: 0.19
```

```
mod1.root.mod1.mf.VCoil_9_ode: 0.19
mod1.root.mod1.mf.VCoil_10_ode: 0.19
mod1.root.mod1.mf.VCoil_11_ode: 0.19
mod1.root.mod1.mf.VCoil_12_ode: 0.19
mod1.root.mod1.mf.VCoil_13_ode: 0.19
mod1.root.mod1.mf.VCoil_14_ode: 0.19
mod1.root.mod1.mf.VCoil_15_ode: 0.19
mod1.root.mod1.mf.VCoil_16_ode: 0.19
```

Iter	ErrEst	Damping	Stepsize	#Res	#Jac	#Sol
1	0.051	0.1000000	0.057	3	1	3
2	0.048	0.1000000	0.054	5	2	6
3	0.05	0.0100000	0.051	8	3	10
4	0.053	0.0100000	0.053	10	4	13
5	0.055	0.0100000	0.055	12	5	16
6	0.057	0.0100000	0.058	14	6	19
7	0.06	0.0100000	0.06	16	7	22
8	0.062	0.0100000	0.063	18	8	25
9	0.065	0.0100000	0.065	20	9	28
10	0.067	0.0100000	0.068	22	10	31
11	0.07	0.0100000	0.071	24	11	34
12	0.073	0.0100000	0.074	26	12	37
13	0.077	0.0100000	0.077	28	13	40
14	0.08	0.0100000	0.081	30	14	43
15	0.083	0.0100000	0.084	32	15	46
16	0.087	0.0100000	0.088	34	16	49
17	0.091	0.0100000	0.092	36	17	52
18	0.095	0.0100000	0.096	38	18	55
19	0.098	0.0100000	0.099	40	19	58
20	0.1	0.0100000	0.1	42	20	61
21	0.11	0.0100000	0.11	44	21	64
22	0.11	0.0100000	0.11	46	22	67
23	0.12	0.0100000	0.12	48	23	70
24	0.12	0.0100000	0.12	50	24	73
25	0.12	0.0100000	0.13	52	25	76
26	0.13	0.0100000	0.13	54	26	79
27	0.13	0.0100000	0.14	56	27	82
28	0.14	0.0100000	0.14	58	28	85
29	0.13	0.1000000	0.15	59	29	87
30	0.14	0.0087288	0.14	62	30	91
31	0.13	0.0872879	0.14	63	31	93
32	0.14	0.0087288	0.14	66	32	97
33	0.13	0.0872879	0.14	67	33	99
34	0.13	0.0872879	0.14	69	34	102
35	0.13	0.0087288	0.13	72	35	106
36	0.14	0.0087288	0.14	74	36	109
37	0.14	0.0087288	0.15	76	37	112
38	0.15	0.0087288	0.15	78	38	115
39	0.16	0.0087288	0.16	80	39	118
40	0.16	0.0087288	0.17	82	40	121
41	0.17	0.0087288	0.17	84	41	124
42	0.18	0.0087288	0.18	86	42	127
43	0.19	0.0087288	0.19	88	43	130
44	0.19	0.0087288	0.2	90	44	133
45	0.2	0.0087288	0.2	92	45	136
46	0.21	0.0087288	0.21	94	46	139
47	0.22	0.0087288	0.22	96	47	142
48	0.23	0.0087288	0.23	98	48	145
49	0.23	0.0872879	0.24	99	49	147
50	0.22	0.0355868	0.23	101	50	150
51	0.22	0.0355868	0.23	103	51	153
52	0.22	0.0355868	0.23	105	52	156
53	0.22	0.0355868	0.23	107	53	159
54	0.22	0.0355868	0.22	109	54	162
55	0.21	0.0355868	0.22	111	55	165
56	0.21	0.0355868	0.22	113	56	168
57	0.21	0.0355868	0.22	115	57	171
58	0.23	0.0081895	0.23	117	58	174
59	0.23	0.0081895	0.23	119	59	177
60	0.21	0.0213455	0.21	120	60	179
61	0.21	0.0213455	0.21	122	61	182
62	0.2	0.0213455	0.21	124	62	185
63	0.2	0.0213455	0.21	126	63	188
64	0.2	0.0213455	0.2	128	64	191
65	0.2	0.0213455	0.2	130	65	194
66	0.19	0.0213455	0.2	132	66	197
67	0.19	0.0213455	0.19	134	67	200
68	0.19	0.0213455	0.19	136	68	203
69	0.18	0.0213455	0.19	138	69	206
70	0.18	0.0213455	0.19	140	70	209
71	0.18	0.0213455	0.18	142	71	212
72	0.18	0.0213455	0.18	144	72	215
73	0.17	0.0213455	0.18	146	73	218
74	0.17	0.0213455	0.17	148	74	221
75	0.17	0.0213455	0.17	150	75	224
76	0.16	0.0213455	0.17	152	76	227
77	0.16	0.0213455	0.17	154	77	230
78	0.16	0.0213455	0.16	156	78	233
79	0.16	0.0213455	0.16	158	79	236
80	0.14	0.2134550	0.15	159	80	238
81	0.1	0.0685852	0.11	161	81	241
82	0.096	0.0685852	0.1	163	82	244
83	0.088	0.0685852	0.095	165	83	247
84	0.082	0.0685852	0.088	167	84	250
85	0.076	0.0685852	0.082	169	85	253
86	0.071	0.0685852	0.076	171	86	256
87	0.066	0.0685852	0.071	173	87	259
88	0.062	0.0685852	0.066	175	88	262
89	0.058	0.0685852	0.062	177	89	265
90	0.054	0.0685852	0.058	179	90	268
91	0.05	0.0685852	0.054	181	91	271
92	0.047	0.0685852	0.051	183	92	274
93	0.044	0.0685852	0.047	185	93	277
94	0.041	0.0685852	0.044	187	94	280
95	0.039	0.0685852	0.042	189	95	283
96	0.036	0.0685852	0.039	191	96	286
97	0.034	0.0685852	0.036	193	97	289
98	0.032	0.0685852	0.034	195	98	292
99	0.029	0.0716483	0.032	197	99	295
100	0.024	0.7164834	0.029	198	100	297

```
Stationary Solver 1 in Solver 1: Solution time: 112 s. (1 minute, 52 seconds)
```

Appendix F

Drawings

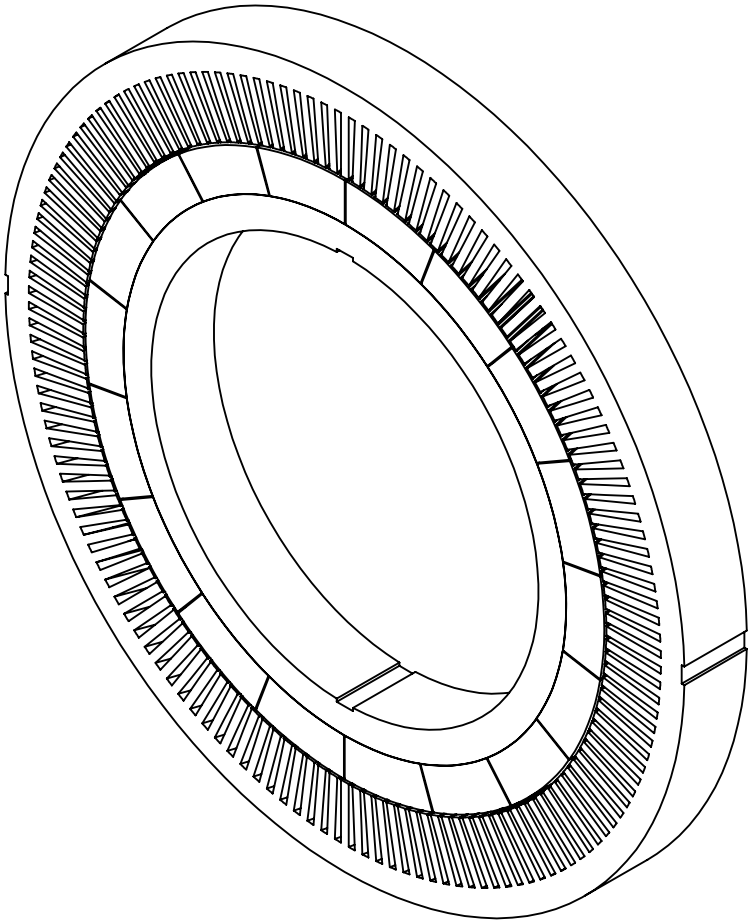

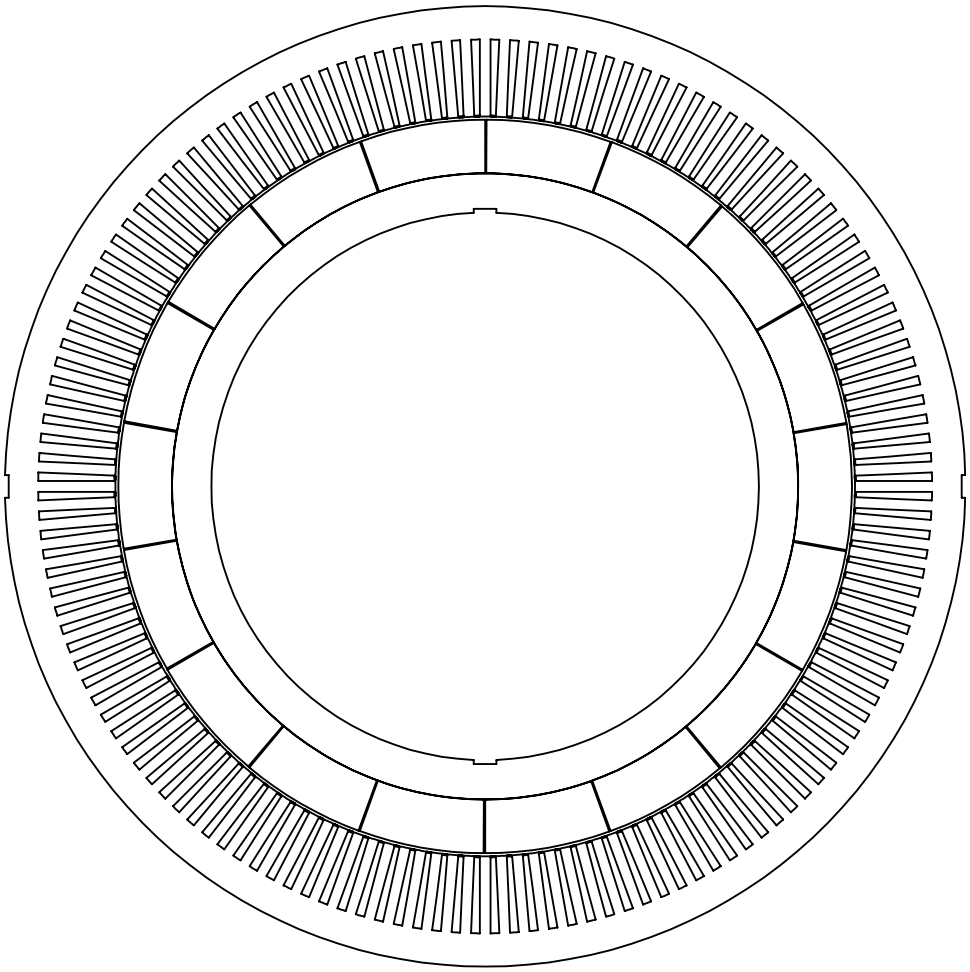

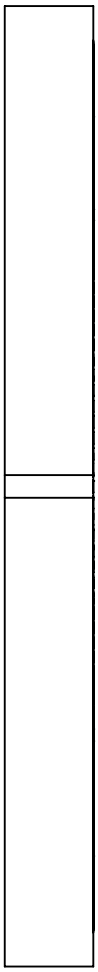

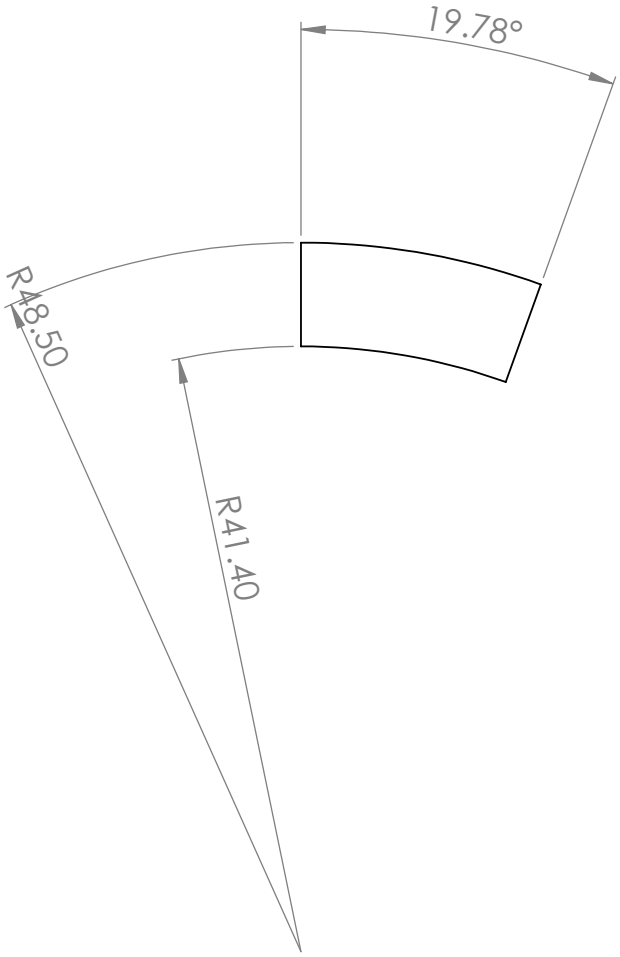
19.78°
R48.50
R41.40

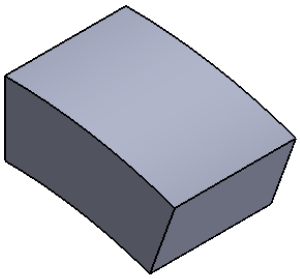

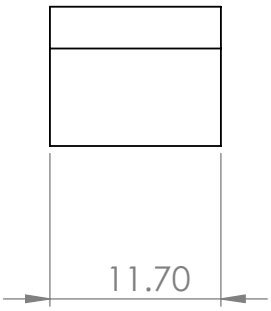
11.70

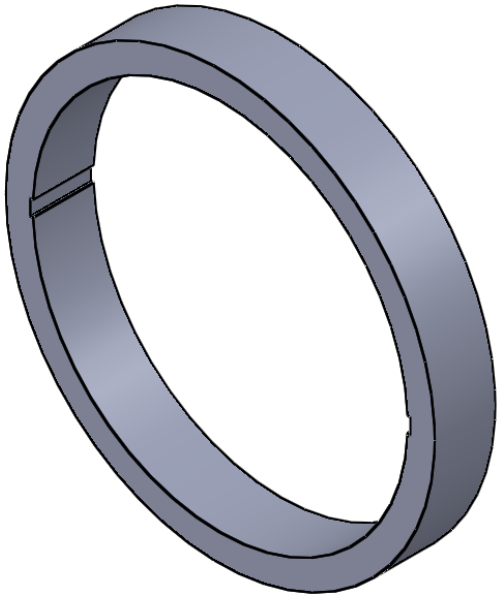

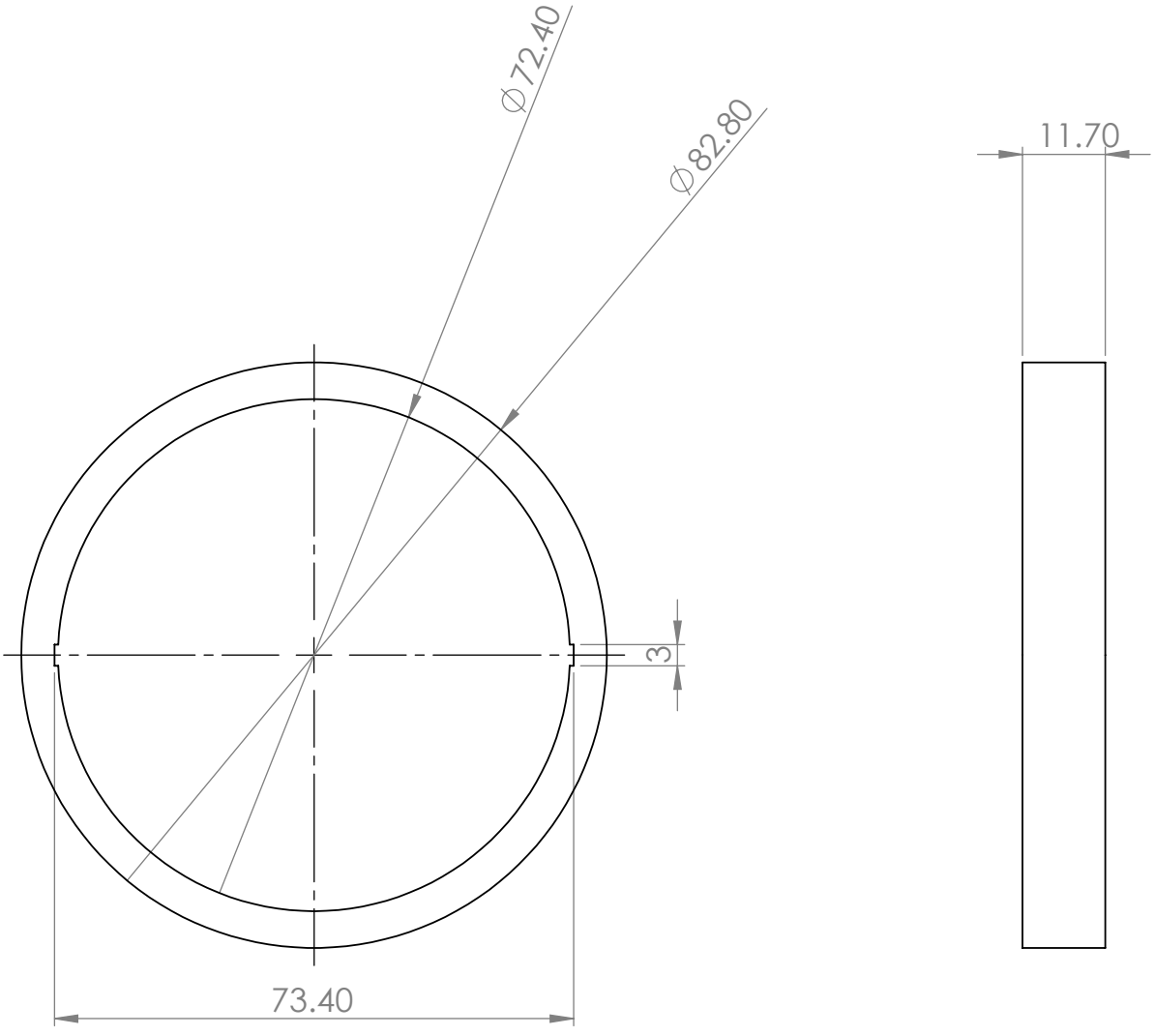
Ø72.40
Ø82.80
11.70
3
73.40

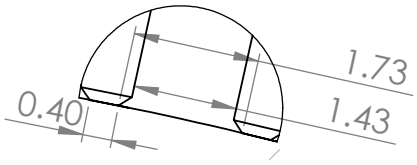

DETAIL A
SCALE 10 : 1

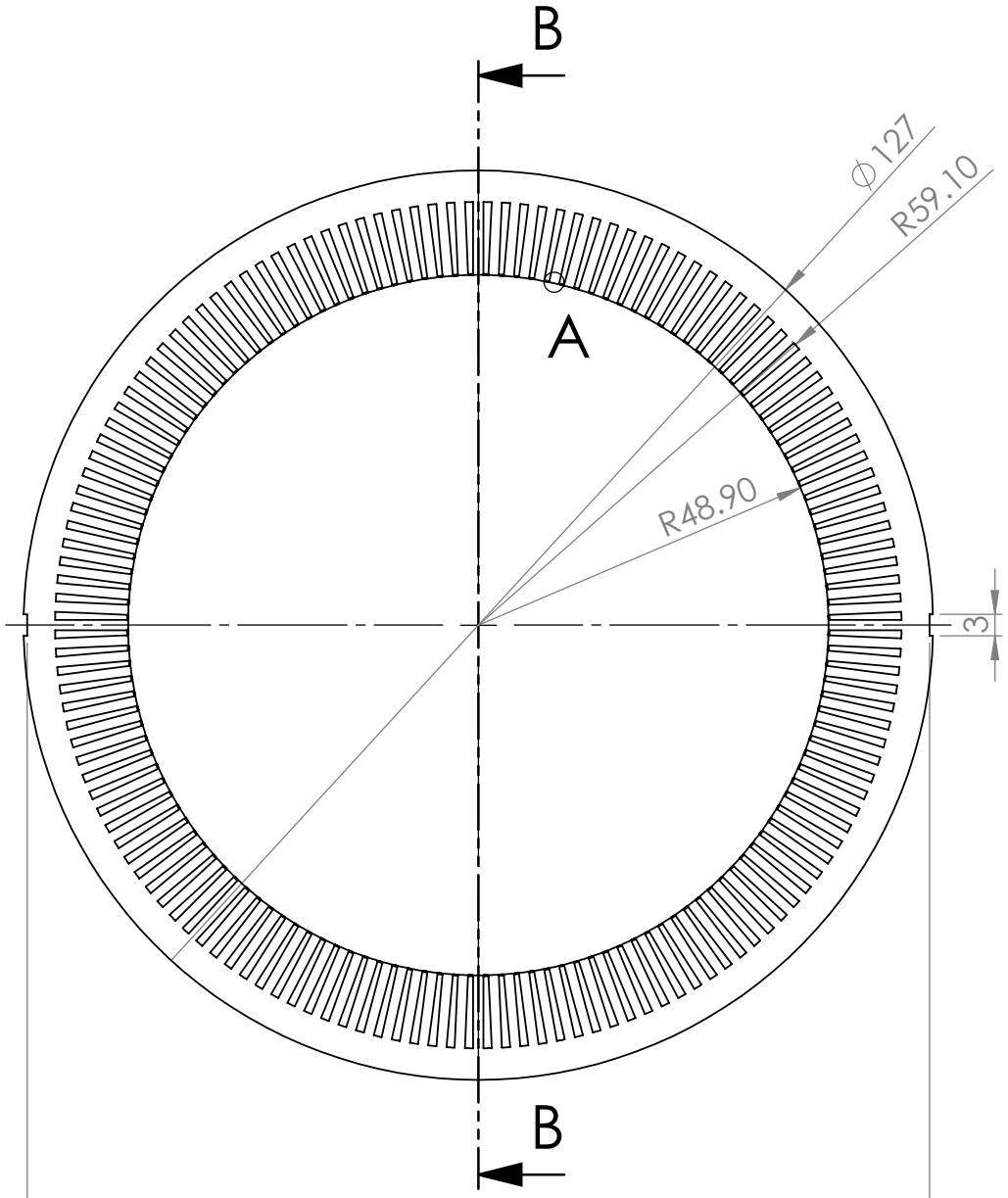

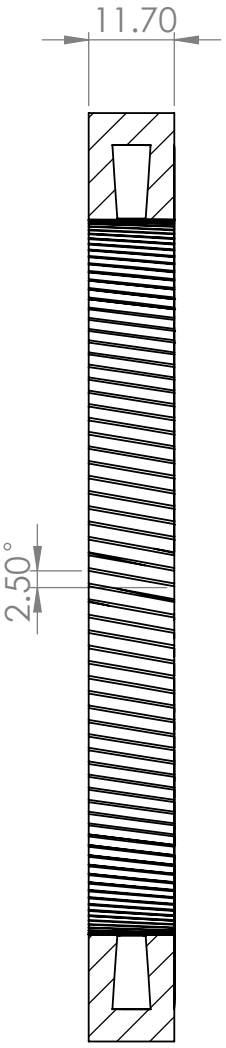

SECTION B-B

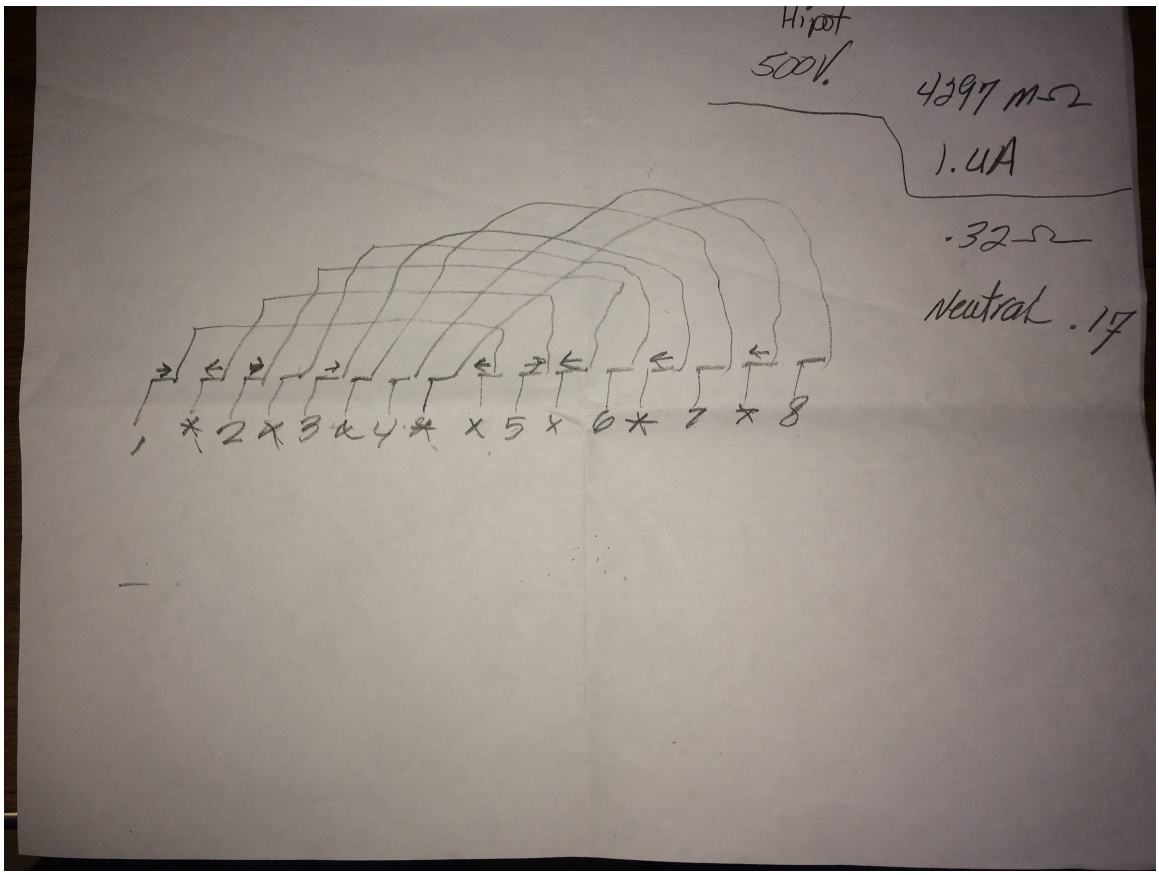

Figure F-1: Winding diagram delivered with motor

Bibliography

[1] Sangok Seok, Albert Wang, Meng Yee (Michael) Chuah, Dong Jin Hyun, Jongwoo Lee, David M. Otten, Jeffrey H. Lang, and Sangbae Kim. Design principles for energy efficient legged locomotion and implementation on the mit cheetah robot. *IEEE/ASME Transactions on Mechatronics*, 20(3):1117–1129, June 2015.

[2] Hiroyuki Mikami, Kazumasa Ide, Yukiaki Shimizu, Masaharu Senoo, and Hideaki Seki. Historical evolution of motor technology. *Hitachi Review*, 60(1), 2011.

[3] Peter P. Silvester and Ronald L. Ferrari. *Finite Elements for Electrical Engineers*. Cambridge University Press, 1996.

[4] A. E. Fitzgerald, Charles Kingsley Jr., and Stephen D. Umans. *Electric Machinery*. McGraw-Hill, 2003.

[5] David G. Dorrell, Min-Fu Hseih, Mircea Popescu, Lyndon Evans, David A. Staton, and Vic Grout. A review of the design issues and techniques for radial-flux brushless surface and internal rare-earth permanent-magnet motors. *IEEE Transactions on Industrial Electronics*, 58(9):3741–3757, September 2011.

[6] C. Rasmussen and E. Ritchie. A magnetic equivalent circuit approach for predicting pm motor performance. *IEEE Transactions on Magnetics*, 34(5), September 1998.

[7] S.P Lim. and K.J. Tseng. Dynamic model of interior permanent magnet motor with skewed stator slots. IEEE Industrial Electronics Conference (IECON99), pages 1471–1477, San Jose, USA, November 1999.

[8] H. Roisse, M. Hecquet, and P. Brochet. Simulations of synchronous machines using a electric-magnetic coupled network model. *IEEE Transactions on Magnetics*, 34(5), September 1998.

[9] W. Soong, D. Staton, and T. Miller. Design of a new axially-laminated interior permanent magnet motor. *IEEE Transactions on Industry Applications*, 31(2):358–367, 1995.

[10] A. Wijenayake and P. Schmidt. Modeling and analysis of permanent magnet synchronous motor by taking saturation and core loss into account. Proc. of International Conference on Power Electronics and Drive Systems, pages 530–534, Singapore, 2007.

[11] A. Gebregergis, M. Chowdhury, M. Islam, and T. Sebastian. Modeling of permanent-magnet synchronous machine including torque ripple effects. *IEEE Transactions on Industry Applications*, 51(1), January.

[12] C. Koechli and Y. Perriard. Analytical model for slotless permanent magnet axial flux motors. 2013 IEEE International Electric Machines & Drives Conference (IEMDC), pages 788–792, 2013.

[13] F. Dubas and C. Espanet. Analytical solution of the magnetic field in permanent-magnet motors taking into account slotting effect: No-load vector potential and flux density calculation. *IEEE Transactions on Magnetics*, 45(5):2097–2109, May 2009.

[14] F. Deng. Improved analytical modeling of commutation losses including space harmonic effects in permanent magnet brushless dc motors. In *The 1998 IEEE Industry Applications Conference*, Thirty-Third IAS Annual Meeting, pages 380–386, 1998.

[15] A.Sari, F. Dubas, J-M. Kauffmann, and C. Espanet. Cogging torque evaluation through a magnetic field analytical computation in permanent magnet motors. International Conference on Electrical Machines and Systems, pages 1–5, 2009.

[16] D. Zarko, D. Ban, and T. Lipo. Analytical solution for cogging torque in surface permanent-magnet motors using conformal mapping. *IEEE Transactions on Magnetics*, 44(1):52–65, January 2008.

[17] D. Zarko, D. Ban, and T. Lipo. Analytical calculation of magnetic field distribution in the slotted air gap of a surface permanent-magnet motor using complex relative air-gap permeance. *IEEE Transactions on Magnetics*, 42(7):1828–1837, 2006.

[18] Md Azizur Rahman. History of interior permanent magnet motors. *IEEE Industry Applications Magazine*, 2013.

[19] Niaja Farve. Design of a low-mass high-torque brushless motor for application in quadruped robotics. Master's thesis, Massachusetts Institute of Technology, 2012.

[20] A. Bannerjee, J. H. Lang, and J. L. Kirtley. Fine grain commutation: Integrated design of permanent-magnet synchronous machine drives with highest torque density. In *Proceedings of 2012 XXth International Conference on Electrical Machines (ICEM)*, pages 671–677, 2012.

[21] Allied Motion. Ht series high torque brushless torque motors.

[22] Hermann A. Haus and James R. Melcher. *Electromagnetic Fields and Energy*. Prentice-Hall, 1988.

[23] James R. Melcher. *Continuum Electromechanics*. The MIT Press, 1981.

[24] Herbert H. Woodson and James R. Melcher. *Electromechanical Dynamics*. John Wiley and Sons, 1968.

[25] James L. Kirtley. *Electric Power Principles*. John Wiley & Sons, 2010.

[26] Lyman Taylor. *Metals Handbook*, volume 1 of *Metals Handbook*. American Society for Metals, Reading, Massachusetts, eighth edition, 1961.

[27] Joseph R. Davis. *Metals Handbook*, volume 2 of *Metals Handbook*. American Society for Metals, Reading, Massachusetts, tenth edition, 1990.

[28] John Ofori-Tenkorang. *Permanent-magnet synchronous motors and associated power electronics for direct-drive vehicle propulsion*. PhD dissertation, Massachusetts Institute of Technology, Department of Electrical Engineering and Computer Science, 1997.

[29] Luke Dosiek and Pragasen Pillay. Cogging torque reduction in permanent magnet machines. *IEEE Transactions on Industry Applications*, 43(6):1565–1571, July 2007.

[30] E. Muljadi and J. Green. Cogging torque reduction in a permanent magnet wind turbine generator. In *21st American Society of Mechanical Engineers Wind Energy Symposium*, 2002.

[31] Humberto L Raposo. Magnetization curves for supermendur and hiperco 50. email, hraposo@cartech.com, June 2013.